DETECTION OF SIGNALS CORRUPTED BY THE COMBINATION OF GAUSSIAN AND NON-GAUSSIAN NOISE

THESIS

BY

SURYAKANT BABUBHAI PATEL

PRESENTED TO THE DEPARTMENT OF ELECTRICAL ENGINEERING OF UNIVERSITY OF ASTON IN BIRMINGHAM FOR THE DEGREE OF DOCTOR OF PHILOSOPHY

BIRMINGHAM

DECEMBER 1975

SUMMARY

The detection of signals in the presence of noise is one of the most basic and important problems encountered by communication engineers. Although the literature abounds with analyses of communications in Gaussian noise, relatively little work has appeared dealing with communications in non-Gaussian noise. In this thesis several digital communication systems disturbed by non-Gaussian noise are analysed. The thesis is divided into two main parts.

In the first part, a filtered-Poisson impulse noise model is utilized to calulate error probability characteristics of a linear receiver operating in additive impulsive noise. Firstly the effect that non-Gaussian interference has on the performance of a receiver that has been optimized for Gaussian noise is determined. The factors affecting the choice of modulation scheme so as to minimize the deterimental effects of non-Gaussian noise are then discussed.

In the second part, a new theoretical model of impulsive noise that fits well with the observed statistics of noise in radio channels below 100 MHz has been developed. This empirical noise model is applied to the detection of known signals in the presence of noise to determine the optimal receiver structure. The performance of such a detector has been assessed and is found to depend on the signal shape, the time-bandwidth product, as well as the signal-to-noise ratio. The optimal signal to minimize the probability of error of the detector is determined. Attention is then turned to the problem of threshold detection. Detector structure, large sample performance and robustness against errors in the detector parameters are examined.

Finally, estimators of such parameters as the occurrence of an impulse and the parameters in an empirical noise model are developed for the case of an adaptive system with slowly varying conditions.

ACKNOWLEDGEMENT

The author wishes to express his sincere appreciation and gratitude to his supervisor, Dr. R. L. Brewster, for his valuable assistance, constant guidance, and encouragement throughout the period spent on this research. The author is also grateful to Professor J. E. Flood, Head of Department of the Electrical Engineering, for the encouragement and helpful guidance he has given throughout the project in his capacity as project advisor. Thanks are also due to colleagues for their helpful discussions and to Miss H. Robson for her patient typing of the manuscript.

Finally, the financial support provided by the U. K. Science Research Council in support of this work is gratefully appreciated.

CONTENTS

LIST OF SYMBOLS

a_i	ith impulse amplitude
a	constant $(=6\sigma_o^2)$
a_2	constant $(=B/4\sigma_o^2)$
$A(t)$	broad-band random process modulating $G'(t)$
α	common parameter for generalised Gaussian and chi-distribution
α_{kn}	phase (Chapter 4)
B	system bandwidth
$B(\alpha,\beta\|Z)$	incomplete beta function $(=\int_o^Z \zeta^{\alpha-1}(1-\zeta)^{\beta-1}d\zeta)$
β	chi-distribution parameter (degrees of freedom)
β_{kn}	phase (Chapter 4)
$\hat{C}$	capacitor parameter
C	normalised filter time constant (Chapter 3)
C_{2k}	coefficients (k=2,3..) $\{=(-1)^k k!<{}_1F_1(-k;1;a^2/<a^2>)>\}$
${}^kC_\ell$	binomial coefficient$\{=k!/\ell!(k-\ell)!\}$
$\vec{\chi}$	(chi) set of random parameters
χ	phase parameter
D	decision variable
$\delta(t)$	Kronecker delta
Δ	integration constant
Δ_ϕ	function of $\phi\{=\sqrt{\gamma}/\cos\phi\}$
$e^{\hat{x}}$	constant$(=\frac{1}{\sqrt{2\pi}}\exp\{-\hat{x}^2/2\}$
E	signal energy
$E(t)$	envelope of interfering process in the receiver (PART B)
$E_s(t)$	envelope of the signal
$E_n(t)$	envelope of the noise

ε	fraction of time the noise contains non-Gaussian noise
ε_1	apriori probability of having H_o
f_c	oscillator frequency ($\omega_c=2\pi f_c$)
$f_{\hat{x}}$	constant $[=\{1+(\hat{x}/\sqrt{R})^{\alpha}\}^{}]$
${}_1F_1(\ )$	confluent hypergeometric function
$g(t)$	complex envelope of a Gaussian process
$g_{opt}[\cdot]$	nonlinear element for optimum detectors (base-band)
$g_{NB,opt}[\cdot]$	nonlinear element for optimum detectors (narrow-band)
$g_{a\ell}[\cdot]$	nonlinear element defined by aℓ(amplifier limiter)
g_M	likelihood equation (M=no. of samples)
$G'(t)$	zero-mean generalised Gaussian process
$G_1'(t)$	in phase component corresponding to G'(t)
$G_2'(t)$	quadrature component corresponding to G'(t)
$G(t_k)$	constant$\{=\sqrt{2}\int_o^T \tilde{h}_{CR}(t-t_k)dt\}$ (PART A)
γ	(gamma) number of impulses in the bit interval (PART A) or chi-distribution parameter (PART B)
$\Gamma(x)$	gamma function
$h_R(t)$	linear receiving filter
$h_{CR}(t)$	R.F. linear filter
$\tilde{h}_{CR}(t)$	complex envelope of the impulse response
H_o, H_1	hypotheses in decision problem
$H(j\omega)$	transfer function
j	$(-1)^{\frac{1}{2}}$
J_o	Bessel function of the first kind of zero order
$J(\ )$	jacobian of the transformation

$K(\alpha,\beta)$	parameter of the generalised hyperbolic distribution $\{=\alpha\Gamma(\beta+1/\alpha)/2\Gamma(\beta)\Gamma(1/\alpha)\}$
$K_\beta(\cdot)$	modified Bessel function of the second kind
$K_\ell[e(t)]$	coefficients of Fourier series expansion
$L_k(k=0,1...)$	threshold levels in decision problem
$\hat{L}_1$	normalized threshold level $(=L_1/\sigma_g)$
λ_{2k}	2kth cumulant (semi-invariants)
$\hat{\lambda}_n$	standardized cumulants $\{=\nu\int_t h_R^2(t)dt\}^{\frac{1}{2}}$
λ,λ_o	constants used to calculate the Chernoff bound
λ,λ_2	Lagrange multipliers
$\Lambda(\vec{r})$	likelihood ratio
Λ	likelihood equation
M	number of independent samples
M	dimension in M-ary system (Chapter 4)
μ	constant $(=-\lambda_1/\lambda_2)$ {Chapter 6}
μ	maximum ARE (base-band)
μ_{NB}	maximum ARE (narrow-band)
$n(t)$	impulse noise process
$n_G(t)$	Gaussian noise process
N_o	white Gaussian noise spectral height (joules)
N	number of pulses occurring within the observation interval
ν	(nu) impulses arrival rate at the receiver (PART A)
$p_Y(.)$	probability density of Y
$p_{X_1,X_2}(.,.)$	joint probability density of X_1,X_2
$p_r(r/H_i)$	condition probability density on H_i
p_i	a priori probabilities
P	signal power

$P_Y(.)$	cumulative distribution
$P_o(.)$	$\{=1-P_E(\cdot)\}$
Pe_{max}	upper bound (Chernoff) on probability of error
Pe_I	probability of error in unfiltered Poisson process
Pe_G	probability of error in unfiltered Poisson plus Gaussian process
Pe_{FI}	probability of error in filtered Poisson process
Pe_{FI+G}	probability of error in filtered Poisson plus Gaussian process and multiplicative noise
ϕ	(ph) random phase
$\Phi_Z(j\xi)$	characteristic function of random variable Z
ψ	(psi) random phase
$\psi_\Lambda(r)$	Ξ_o/Ξ_1
$Q(t)$	random process specified by $\|A(t)\|^{-1}$ (scaling process)
$r(t)$	slowly varying complex envelope of $R(t)$
$\hat{r}, r^1$	quadrature and in-phase component of r
$R(t)$	received signal plus noise over the symbol period
R	impulse noise variance to Gaussian noise various ratio
ρ	constant $(=2/\lambda_2)$
$s_i(t)$	complex envelope of $S_i(t)$
$S_i(t)$	signal on hypotheses H_i (i=0,1)
$\hat{S}_i(t)$	low-pass signal
$\hat{S}_{op}(t)$	optimal low-pass signal
S_F^2	variance of fading process
$\vec{S}$	signal vector
σ_q	parameter of Gaussian process

σ'	parameter of generalised Gaussian process
σ_o	$\{=(\sqrt{2}\sigma')^{\alpha}/\gamma\}$
σ_2	σ_o^2
t	time variable
T	bit interval (signal duration)
T_o	observation interval
$\upsilon(t)$	(upsilon) $\{=s^2(t)/4\sigma_o^2\}$
$V_i(t)$	typical waveform from the ith source
W^2	mean-square bandwidth
ω_c	carrier frequency (rad/sec)
$x(t)$	complex envelope of $X(t)$
$X(t)$	interference process in the receiver
$X'(t)$	in-phase component corresponding to $X(t)$
$\hat{X}(t)$	quadrature component corresponding to $X(t)$
$\vec{X}$	random vector
ξ	dummy variable used in characteristic function
Ξ_i	$\{=\sigma_o^2+\lvert r-s_i\rvert^2\}$
$y(t)$	received unfiltered Poisson noise process
$Y(j\omega)$	transfer function of transmitting filter
$Z(t)$	received filtered Poisson process
Z_I	SNR $\{=(E/\lambda_2)^{\frac{1}{2}}\}$
Z_{I+G}	SNR $\{=(E/\sigma_g+\lambda_2)^{\frac{1}{2}}\}$
Z_{FI}	SNR $\{=[E/\langle a^2\rangle\gamma(1-CK)]^{\frac{1}{2}}\}$
Z_{FI+G}	SNR $\{=S_F/(\sigma_g^2+\lambda_2)^{\frac{1}{2}}\}$

ABBREVIATIONS

A.P.K.	amplitude and phase keying
ARE	asymptotic relative efficiency
ARE_{NB}	asymptotic relative efficiency for narrow-band system
$ARE_{a\ell}$	asymptotic relative efficiency when amplifier-limiter used
$a\ell$	amplifier-limiter (nonlinearity)
$b\ell$	blanker (hole puncher)nonlinearity
CF	characteristic function
erf(x)	error function $\{= \frac{1}{\sqrt{2\pi}} \int_{-\infty}^{x} \exp(-\zeta^2/2)\,d\zeta\}$
erfc(x)	1-erf(x)
Ei(x)	integral exponential function $\{\int_{x}^{\infty} \exp(-\zeta)\,d\zeta/\zeta\}$
$g\ell$	general nonlinearity
He_n	Hermite polynomials
HF	high frequency
$h\ell$	hard-limiter with dead zone
IN	impulse noise
Im{•}	imaginary part of {•}
LF	low frequency
ML	maximum likelihood
pdf	probability density function
P.S.K.	phase shift keying
Pr(.)	probability of event in brackets
Pe	probability of error
R.F.	radio frequency
Re{•}	real part of {•}
SNR	signal-to-noise ratio
$s\ell$	semi-optimum nonlinearity
UHF	ultra high frequency

VLF	very low frequency
VHF	very high frequency
var(.)	variance of (.)
$\langle \cdot \rangle_a$	statistical average with respect to variable a.
$\dot{h}(t)$	derivative of h(t) with respect to t
$\vec{g}$	vector
$\vec{g}_t$	transpose of a vector
$\int_{\vec{\Omega}} d\vec{t}$	integral over the set $\vec{\Omega}$
$\approx$	approximately equal to

CHAPTER 1

INTRODUCTION

1.1. INTRODUCTION

In the past decade, we have witnessed an enormous growth of computer usage and of the computer industry itself. Advances in solid-state techniques, large scale memory units, speed of computations in arithmetic units and in programming contributed to this overwhelming success of digital computing machines, and resulted in their application to industry, business and military data processing and control. Scientific and engineering computations also can be carried out at speeds hitherto unattainable.

It was found out rather early in this development that, due to their bulkiness and strict environmental requirements, large scale digital computers do not lend themselves very well to transportation. In a large number of cases, however, the physical locations of data acquisition, usage, distribution and processing are not the same. Means had to be developed for transporting the data at speeds comparable in magnitude with those of computer's peripheral equipment, sometimes even at speeds equal to its arithmetic calculations.

Moreover, in certain cases it is mandatory that the computer be used on a time-shared basis, due mostly to economic considerations. All these problems brought forward the question of digital data transmission over some kind of communication channel. In any communication system, mobile or otherwise, electrical noise within the receiver is the limiting factor that determines satisfactory reception. As a consequence, the type of signal transmitted, the transmission medium, the

quality of reception all hinge on quantitative and qualitative knowledge of such noise.

In radio communication systems, the noise external to the receiving antenna of a communication system is composed of emission from natural sources and electromagnetic pollution of man-made origin. In addition to the thermal radiation from the local environment, natural noise consists of atmospheric radio noise, galactic radio noise, and solar noise. On the other hand, the causes of man-made electromagnetic pollution are automotive ignition systems, power lines and radiated interference from a variety of electrical equipment. Clearly, the contribution of each class of sources depends on the radiation spectrum and the number of sources of that class present in the specific environment.

The characteristics of the noise generated by various types of sources have been studied extensively [1] - [3] and the relative field strengths, statistical characteristics, frequency and distance dependence of these noise fields have been reported comprehensively in several papers [4] - [16]. There is therefore no need to describe them in detail here.

What needs to be emphasized, however, is the fact that the atmospheric radio noise and the man-made noise are constituted by nondeterministic impulsive waveforms of frequent occurrence: to be precise, the area of the impulses and their arrival times can be considered as random variables.

The levels of the impulsive noise (IN) (either atmospheric or man-made noise) are often much larger than that of the usual Gaussian noise, as can be seen from Fig. 1.1 , where the median operating noise power F_{am} is shown in dB above kT_0B (k is the Boltmann's constant, T_0 is 288.0K and B is the effective noise bandwidth of the receiving system in Hz).

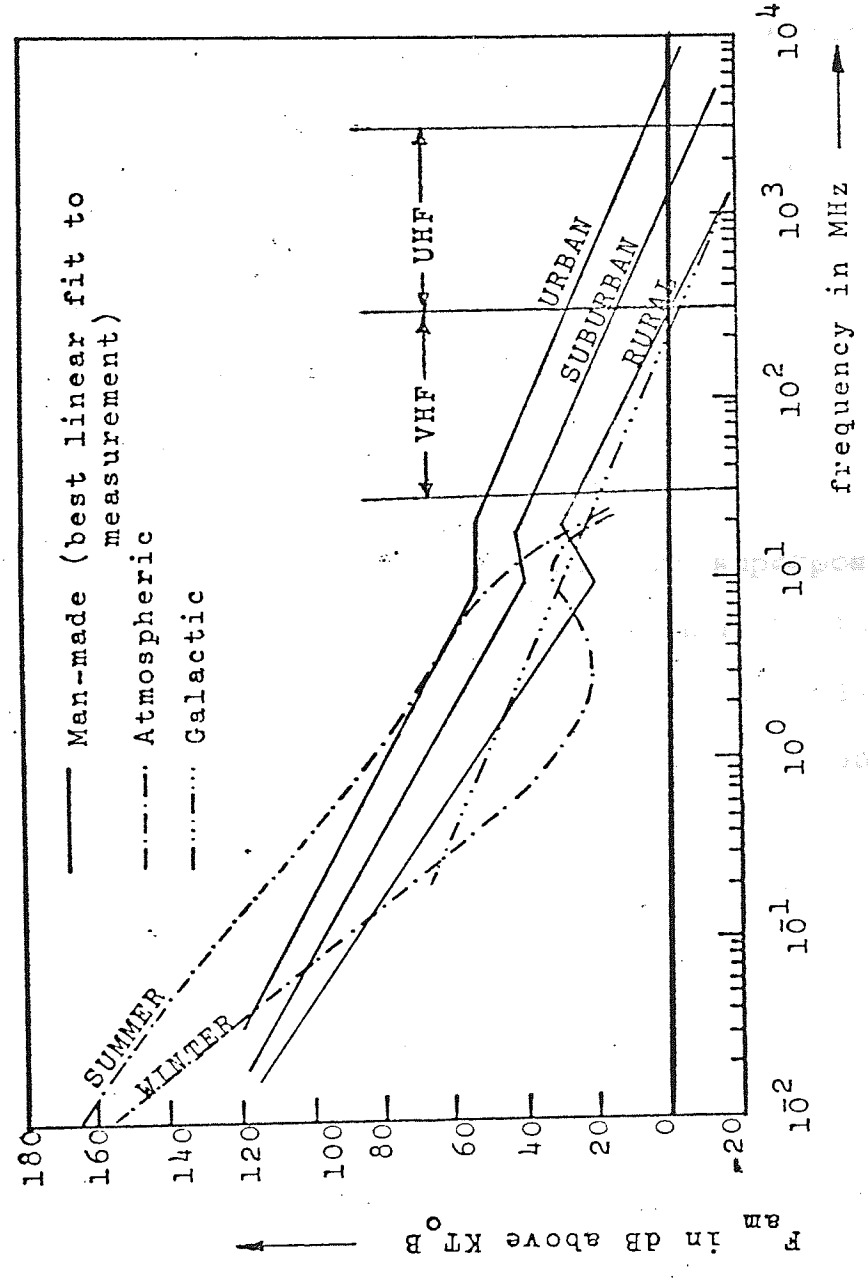

Fig. 1.1
Median operating noise Power F_{am}, measured by receivers with bandwidth B, VS. frequency.

Fig. 1.1 shows man-made noise sources together with natural noise sources, and these values are the levels expected from an omnidirectional, short, loss-less, vertical antenna near the surface [17].

From the figure one can see that in the VHF and UHF regions the man-made IN is generally predominant while on the other hand at low frequencies both the atmospheric and the man-made noise are significant.

The transmission of digital information over the switched telephone network has also been the subject of many investigations in recent years [18]-[26]. In general, the noise on the switched network consists of background thermal noise, crosstalk, hum, impulses due to switching, multifrequency pulsing tones and other miscellaneous disturbances. As such it can broadly be described as the independent superposition of 'burst noise' (bursts of high amplitude) and the lower amplitude 'background noise' (Gaussian noise). The independence of the two processes is due to the independence of the sources which generate them. It has also been determined that bursts occur at random considerably more often than is predicted by the rms values of the Gaussian background noise. When one of these bursts is viewed on an oscilloscope, it appears somewhat like an impulse response of a narrowband channel. In the work to follow, no mention is made of the capabilities of the switched telephone network for data transmission. For a complete discussion of this subject, see Alexander, Gryb and Nast [27].

The use of the above channels for data transmssion, with the possibility of data impairment, has made the problem of detection of digital signals in non-Gaussian noise of increasing relevance and importance.

Studies of digital communication system performance in

impulsive background noise, in contrast with studies of their performance in Gaussian noise, are comparatively few. Perhaps the main reason for this is that even the simpler models of IN lead to mathematical difficulties when applied to the problem of communication system analysis. The output statistics of any system, even a linear system, are difficult to calculate if the input contains non-Gaussian noise. A few of the more recent studies of digital system performance in impulsive interference are summarized in the following section.

1.2. BACKGROUND

The various IN models proposed in the literature differ from each other in several respects. All IN, however, is characterized by brief periods of large amplitude excursions, separated by intervals of quiescent conditions. The relatively new area of IN analysis suffers from the problems of non-standardization and incompletness. It is difficult to compare the results of two authors, and impossible to obtain comparison of the major binary signalling techniques, because of the multitude of noise models, signal sets, analytical methods and simplifying assumptions. The problem of immunizing a communication system against IN has been examined by many authors and has almost as many 'solutions', each depending on the initial assumptions made.

Two different approaches are available for detection in non-Gaussian noise. The first approach assumes the non-Gaussian noise probability density function (pdf) is of a certain form with all known parameters. Using an appropriate criterion, the 'best' or 'optimum' receiver is derived. Usually the receiver is rather complicated and thus difficult to implement. However,

suboptimum detectors are used to counteract either the large amplitude or the aperiodic nature of the non-Gaussian noise and will be classified as either a time or an amplitude based modification to existing receivers.

The second approach involves using a nonparametric detector. This type of detector is robust, that is, the detector is, in most cases, not very sensitive to the pdf form. However, the false alarm probability, i.e., the probability of deciding the signal is present when it is not, is constant regardless of the noise distribution. Since most of the proposed detectors in this category are of rank type, which require complicated ordering, these procedures are not practicable in real-time communication systems.

The time-based modifications exploit the aperiodic and frequency spectrum properties of the IN. Examples of this technique are smearing-desmearing and swept-frequency modulation systems. The communication system based on this technique is illustrated in Fig. 1.2. The smear-desmear system consists of shaping $Y(\omega)$ in such a way that the transmitted waveform looks quite different from the IN. The receiver filter $H(\omega)$ will, therefore, discriminate readily between signal and noise. No loss of signalling rate occurs so long as the total response, $Y(\omega)H(\omega)$, is satisfactory. This technique is used by Sussman [28], Wainwright [29] and Lerner [30]. Winkler [31] and J. C. Dute and C. A. Hine [32] accomplish a similar result with a swept frequency system using a chirp radar technique [33], which was analysized for a simplified case by Engle [34]. His signalling rate is slower than the bandwidth permits; but some further overlapping of signals appears to be possible and could correct this. The

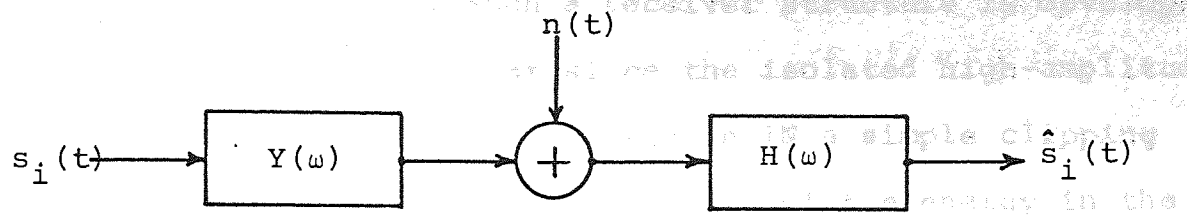

Fig. 1.2
A model of communication system using smear-desmear technique

smear-desmear technique arrives at the filter shapes rather intuitively, with little attention given to the procedure for determining the shapes. Richter [35] evaluates the use of this technique of filtering, which is shown to be helpful at high signal-to-noise ratios (SNRS) and hurtful at low SNRs. However, this technique has not been employed extensively because of its poor performance [36], [37]. One possible explanation for poor performance is that the true characteristics of IN are not represented by a model where amplitude peaks are caused by a phase relationship of noise components. Another time-based modification, used by Black [38], Brillant [39], and Baghdady [40], uses the property that a noise impulse will produce the same response in several adjacent channels having the same impulse response. An impulse response from a channel adjacent to the channel of interest can then be subtracted from the desired signal-plus-impulse noise, leaving only the signal. This assumes that there are no signals in the adjacent channel, which would produce worse effects, or that a spare channel is made available to cancel IN in several other channels.

The amplitude-based modifications act to suppress the large amplitude excursions of the IN by including a nonlinear

device in the receiver. A schematic diagram of such a system is shown in Fig. 1.3. Such a receiver structure is developed on the intuitive notion that since the isolated high-amplitude impulses contain much of the energy in IN a simple clipping circuit in the receiver can remove most of the energy in the noise without significantly reducing the signal energy [41] [48]. If the limiter is set to a value just above the peak value of the signal, bursts of very high amplitude noise are clipped and, after spreading, will not cause as many errors as they would have without limiting. A precise analysis of the effect of limiting prior to spreading is not practicable.

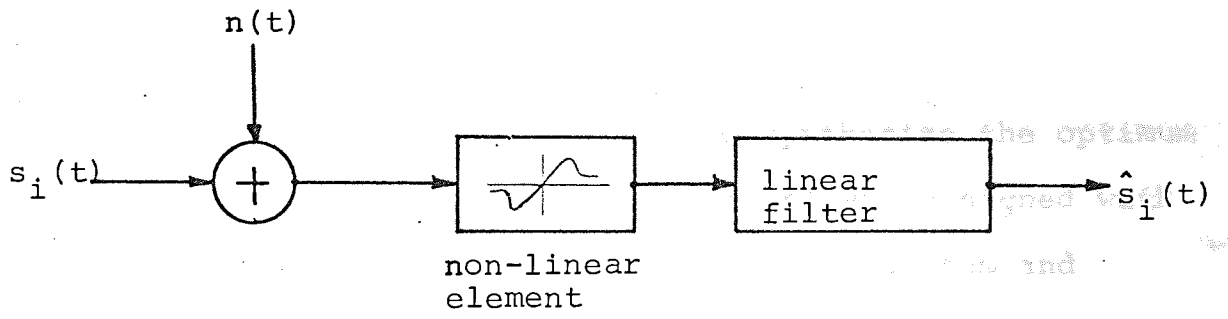

Fig. 1.3.
A model of communication system using amplitude-based modification

The process is nonlinear, and the response of the combined limiter-filter depends strongly on the noise burst amplitude and its time of occurrence. The exact evaluation of the improvement by analytical means does not appear feasible. However, an upper bound on the improvement can be found, as a result of the following reasoning.

When a noise burst occurs with polarity opposite to that of the data signal at the time of its occurence, and is of sufficient amplitude to cause an error in the bit during which it occurs, the limiting will not prevent the error. Limiting cannot reduce the effect of the noise on the bit during which

it occurs. The most that the limiting can do is to prevent the burst from causing errors in other bits, even after spreading, and this is an upper bound on its effectiveness.

Experiments with various nonlinearities have indicated that clippers like the hard limiter are effective and practical [49][51]. An important aspect of such nonlinear processing is the preclipping filtering. For maximum processing efficiency, the impulsive nature of the noise must be maintained despite the dispersive effects of the transmitting channel. The processing bandwidth must therefore be considerably wider than the signal bandwidth. An entirely different and more complex approach is taken by Rappaport and Kurz [52], Hall [4], Modestino [53], and Snyder [54]. They assume an approximate conditional Gaussian pdf for the IN in the presence of each signalling element, and then use decision theory to synthesize the optimum receiving system. Hall's [4] 'log-correlator' was designed with the same parameters as an existing conventional system and showed an error-rate considerably better, but he reduced the data signalling rate below what the bandwidth will permit. He claims advantages over other methods of combating IN. His basis for claiming superior performance over the smear-desmear system (Hall [4]) is that the smear-desmear system attempts to make the non-Gaussian noise appear Gaussian and then uses the optimum receiver for Gaussian noise. However, his technique optimizes directly the non-Gaussian noise. Because Gaussian noise gives the lowest channel capacity for a given noise variance (or highest entropy) [55], his system is therefore capable of giving better performance. Since he does not prove that he has actually attained the optimum receiver, it is not really clear where his receiver stands in relation to smear-desmear. Rappaport and Kurz [52] and also

Snyder [54] derive nonlinear receivers similar to Hall's, but they also signal at a rate slower than the bandwidth permits and/or do not take into account the bandwidth of the channel at the nonlinear element. These approaches do not take into account the nature of IN defined above, and hence tend to be insensitive to the impulse response of the receiving filter.

1.3. OUTLINE OF WORK

The thesis is divided into two main parts. In Part A (Chapters 2-4) we utilize a filtered Poisson impulse noise (FPIN) model to calculate error probability characteristics of a linear receiver operating in an additive combination of impulsive and Gaussian noise. Naturally, this method of data processing is no longer optimum if the noise is non-Gaussian. Two questions which might be asked in this event are:

(1) What effect does non-Gaussian interference have on the performance of a receiver that has been optimized for Gaussian noise (matched filter)?

(2) Can the choice of modulation scheme be judiciously made so as to minimize the detrimental effects of the non-Gaussian noise?

The first question is dealt with in Chapter 3 and the latter question in Chapter 4. No attempt is made here to introduce a non-linear device in the receiver to improve its characteristics.

Chapter 2 gives the derivation of the pdf for the linearly filtered narrowband Poisson process. Here we confine our attention to the first-order case only. The approach is canonical, in that the results are, in form, independent of

the particular emitted waveform, propagation condition, source distributions and beam patterns, as long as the interference is narrow-band following the RF stages of a typical receiver. This is by far the most common case in application.

The performance analysis for a band-limited channel using a linear receiver in the presence of FPIN is presented in Chapter 3. Only the binary signal set is considered in this chapter. At the end of the chapter we look at the case of a fading channel, which one frequently encounters in data transmission over HF radio links [56], [57].

In Chapter 4 a method of modulation is described which gives a particularly good error-rate performance, in comparison to the conventional M-ary P.S.K. system, in the presence of IN. The modulation scheme is an hybrid arrangement of phase and amplitude-modulation techniques.

Part B (Chapters 5-9) briefly describes the development of a new model of IN that fits well with observed probability distributions of noise. The main object of this part is to apply this new model to the detection of known signals in the presence of noise. It will be seen from the analysis that the linear matched filter alone is a rather poor receiver choice for IN. It is shown that the use of nonlinear transformation combined with the linear matched filter leads to the design of a superior receiving system in IN.

In Chapter 5 a semiempirical, but more analytically tractable, model is constructed similar to that introduced by Hall [4] for impulsive atmospheric noise, but used here for independent sources. This model is represented by $X(t) = A(t)G'(t)$, where A, G' are independent processes, both zero mean, and G'(t) is regarded as generalized Gaussian. The

first-order probability density of X(t) is determined empirically for large X, which in turn specifies the parameters of the first-order probability density of A. At the end of the chapter, the model is justified by comparison with observed probability distributions.

In Chapter 6 this noise model is applied to the detection of known signals in the presence of noise to determine the optimal receiver structure (Likelihood receiver) and its performance. We can observe, from the upper band on the probability of error, that the receiver performance depends on the SNR, the time-bandwidth product, and the particular signal used. Consequently, a solution for an optimal signal to achieve the minimum probability of error is derived from the solution of the nonlinear differential equations.

Chapter 7 formulates the threshold detection problem for channels with additive impulsive and Gaussian noise. Following this, the case of coherent, completely known, signals is analyzed. The assumptions made lead us to a relatively simple detector structure consisting of a zero-memory nonlinearity followed by a linear filter whose output is then compared with some threshold. To illustrate the form these nonlinearities can take, plots are given for a mixture noise. It is shown that a fairly simple nonlinearity can give good performance without being over sensitive to parameter error (robustness of the detectors).

In Chapter 8, maximum likelihood estimators are developed for various noise parameters of the impulse distribution. A robust procedure is presented and evaluated for estimating the occurrence of an impulse.

Finally, in Chapter 9, some conclusions are given. The reader is reminded of the limitation of the present work

and topics are suggested for future research, aimed at removing some of these limitations.

It should be noted at this point that, for simplicity, attention is confined to the discrete-time case. Moreover, as in most other treatments of detection of signals in non-Gaussian noise, such as references [58] through [68], we assume that the received samples are statistically independent. Some work has been done with dependent samples, for example that in references [4], [54], [69], [70], and should be kept in mind since our assumption of independent samples does not always hold true. For example, Watt and Maxwell [11] have shown experimentally that the statistics of received VLF atmospheric noise pulses are usually dependent on the values of the preceding pulses. However, the specification of a physically meaningful multivariate non-Gaussian noise distribution is not simple, and no results on dependent samples are included here.

PART A

CHAPTER 2

POISSON IMPULSE NOISE MODEL

This chapter defines filtered Poisson-plus-Gaussian and unfiltered Poisson-plus-Gaussian noise processes at the receiver input. Asymptotic expressions for the probability density functions of the decision variable at the linear receiver output are derived for the limiting cases when the input noise is very impulsive and quasi-Gaussian.

2.1. INTRODUCTION

In this chapter we construct an analytically tractable, statistical model of the very broad class of non-Gaussian channels based on the Poisson postulate of independent events occurring in time. If we let $V_i(t)$ be a typical waveform from the i^{th} source, after processing by the receiver's aperture, then

$$n(t) = \sum_i V_i(t ; \vec{\chi})$$

is the total received disturbance, and

$$\{n\} = \sum_i \{V_i(t ; \vec{\chi})\}$$

is the total received Poisson process, where $\vec{\chi}$ represents a set of (time-invariant) random parameters descriptive of waveform level and structure.

The waveform description of IN depends on the noise source, the coupling media, and the characteristics of the channel under observation. For example, capacitive and inductive coupling of switching transients between adjacent channels comprises the major cause by which IN is introduced

in a wire system. The determination of the noise waveforms can be a time-consuming and expensive process. The number of different waveforms encountered can be very large, and normally the measuring equipment must have large bandwidth and a capability for handling aperiodic waveforms [18]. Kurland and Molony [19] experimentally determined and ranked the error performance for 15 different noise waveforms at various SNRs. No pattern appears to exist in the relative standing of the various waveforms as the SNR was changed. Fennick [20], [21] has reported on specific switched telephone lines where 2000 distinct waveforms have been analyzed. The result was widely varying amplitude and phase spectra characteristics. However, when a subset of approximately 200 of the waveforms were added together, the composite noise spectrum appears to approximate the channel transfer characteristic. This would suggest that a weighted unit-impulse response of the channel could be used as a typical noise waveform.

The model chosen therefore is the Poisson IN model by Rice [71], for which the times of arrival of individual noise pulses are determined by the Poisson distribution, and the random amplitude are independently determined by a selectable distribution, [72]. The filtered IN output then is the sum of impulse responses of the channel filter or RF filter, appropriately weighted by amplitude and time of arrival. This noise model has been used by Richter [35], Ziemer [58] and Huynh [59] in studies of digital communications systems. However, the analyses presented in the above references assumed an unfiltered Poisson noise process at the receiver's input (i.e. the effect of RF filter is neglected).

The work in this chapter is an extension of the theory of Bello and Esposito [41], [42], and Moor [60] to perturbing noise modelled as the mixture of FPIN and a white Gaussian process of known spectral density. This model is a more realistic representation of ambient and reverberant acoustic fields in under-water sound [1 pt. 1], man-made interference phenomena generally [5], atmospheric noise [7] and clutter (in radar) [73].

2.2 NOISE MODEL

The noise process at the input of a narrowband receiver is considered to be a time sequence of amplitude distributed impulses that occur within an observation interval of duration T_o. If t represents the instant of observation and if the interval commences at time $(t-T_o)$, the input-noise process, n(t), can be expressed as

$$n(t) = \sum_{i=1}^{N} a_i \, \delta(t-t_i) \tag{2.1}$$

where a_i is the amplitude of the i^{th} impulse, t_i is the occurrence time of the i^{th} impulse, N is the number of pulses occurring within the observation interval T_o, and $\delta(t)$ is a unit-impulse function. If the impulses arrive at the receiver with a rate ν, then N can be taken to be a Poisson-distributed random variable of which the distribution parameter is νT_o, i.e.,

$$P_{T_o}(N) = \frac{(\nu T_o)^N}{N!} \exp(-\nu T_o) \tag{2.2}$$

The assertion of a Poisson process then implies that the individual pulses are independent and that the arrival times,

t_i, are uniformally distributed in $(t-T_o, t)$. The amplitudes a_i are assumed to be statistically independent of each other and of the occurrence times, and to have identical pdf $p_A(a)$.

Given a filter transfer function $H_R(j\omega)$, the response of such a filter to IN (2.1) is simply

$$Y(t) = \sum_i a_i h_R(t-t_i). \tag{2.3}$$

Note, however, that if n(t) is the input to a filter with complex response envelope $h_{CR}(t)$, the complex output envelope will be

$$Z(t) = \sum_i a_i h_{CR}(t-t_i) \exp(j\psi_i) \tag{2.4}$$

i.e., an additional random phase ψ_i will have to be introduced to measure the phase difference between the excitation due to a random phase and a reference phase. This situation arises when the detector is preceeded by a frequency selective network which passes only a band of frequencies, narrow compared to the centre frequency of the band. This is not only desirable in order to discriminate against unwanted signals in other frequency bands, but is simultaneously more or less inescapable because of the inherent characteristics of the elements of which the receiver is built. Thus, although the noise at the input of the receiver may be, and usually is, of relatively constant strength over a wide band of frequencies, the noise presented to the detector is narrow-band because of its passage through the frequency selective parts of the receiver.

2.3 pdf DERIVATION OF THE DECISION VARIABLE AT THE OUTPUT OF A LINEAR FILTER AT THE END OF EVERY SIGNALLING PERIOD.

The first - (and higher) order pdf's for the Poisson random variables,

$$Y = \sum_i a_i h_R(T-t_i) \tag{2.5a}$$

and

$$Z = \sum_i a_i G(t_i) \cos\psi_i \tag{2.5b}$$

where

$$G(t_i) = \int_{-\infty}^{T} h_{CR}(t-t_i)\, dt,$$

at the output of the detector (derived in the next chapter i.e., (3.23a)) at the end of every signalling period of duration T, are obtained by starting with the corresponding characteristic functions (CFs). Here we shall confine our attention to the first-order cases only. Accordingly, we begin with the well known relation [71], [72]

$$\Phi_Y(j\xi) = \exp\{\nu \int_t dt \langle \exp(j\xi a h_R(t)) - 1 \rangle_a\} \tag{2.6}$$

for the CF of the random variable Y, where $\langle . \rangle_a$ denotes the statistical average with respect to variable a, and the integration is carried over the observation time. The above equation can be rewritten in a closed form as

$$\Phi_Y(j\xi) = \exp\{\nu \int_t dt \left[\Phi_A(j\xi h_R(t)) - 1 \right]\}$$

where

$$\Phi_A(j\xi) = \langle \exp(j\xi a) \rangle_a .$$

Extending the analysis further we obtain the CF of the random variable Z as (see(a.7) of Appendix A)

$$\Phi_Z(j\xi) = \exp\{\nu \int_t dt \langle J_0(\xi a G(t)) - 1 \rangle_a\} \tag{2.7}$$

where $J_0(.)$ is the Bessel function of the first kind of zero order. The desired pdfs are then formally obtained by the appropriate Fourier transforms:

$$p_Y(y) = \int_{-\infty}^{\infty} \frac{d\xi}{2\pi} \exp\{-j\xi y + \nu \int_t dt \langle \exp(j\xi a h_R(t)) - 1 \rangle_a\} \tag{2.8a}$$

and

$$p_Z(z) = \int_{-\infty}^{\infty} \frac{d\xi}{2\pi} \exp\{-j\xi z + \nu \int_t dt \langle J_0(\xi a G(t)) - 1 \rangle_a\} . \tag{2.8b}$$

2.4 MOMENTS

The various moments $\langle y^k \rangle$, $\langle z^k \rangle$ $(k>1)$ are of practical interest: from measurements of these moments we can obtain estimates of the basic parameters $\nu, \langle a^2 \rangle_a$ ..... etc. needed for the description of the pdf. First, it is readily shown that all even moments of Y and Z exist, e.g., $\langle y^{2k} \rangle, \langle z^{2k} \rangle < \infty$ and that odd moments $\langle y^{2k+1} \rangle, \langle z^{2k+1} \rangle = 0$.

The $2k^{th}$ cumulant λ_{2k} (semi-invariants) [71] of Y are readily obtained by expanding the inner exponential of (2.8a), yielding

$$\lambda_{2k} = \nu \langle a^{2k} \rangle_a \int_t h_R^{2k}(t)\, dt. \qquad (2.9)$$

In order to deduce the relation between the moments $\langle y^{2k} \rangle$ and the semi-invariants λ_{2k}, we use the identity [74]

$$1 + \sum_{k=1}^{\infty} \frac{\langle y^{2k} \rangle}{(2k)!} (j\xi)^{2k} = \exp\left[\sum_{k=1}^{\infty} \frac{\lambda_{2k}}{(2k)!} (j\xi)^{2k} \right] \qquad (2.10)$$

in a purely formal way, without paying any attention to the questions of existence of moments or convergence of series. It is seen that λ_{2k} is a polynomial in $\langle y^2 \rangle$, $\langle y^4 \rangle$, ... $\langle y^{2k} \rangle$ and conversely $\langle y^{2k} \rangle$ is a polynomial in λ_2, λ_4, ... λ_{2k}. In particular we have

$$\langle y^2 \rangle = \lambda_2, \langle y^4 \rangle = \lambda_4 + 3\lambda_2^2, \ldots\ldots\text{etc.} \qquad (2.11)$$

(where we have used the fact $\langle y^{2k+1} \rangle = 0$ for $k = 0, 1, 2, \ldots$ ...). The general recursion relation between moments and cumulants is [75],

$$\langle y^k \rangle = \sum_{\ell=1}^{k} \binom{k-1}{\ell-1} \lambda_{k-\ell+1} \langle y^{\ell-1} \rangle \qquad (2.12)$$

where

$$\binom{k-1}{\ell-1} = \frac{(k-1)!}{(\ell-1)!\,(k-\ell)!} \qquad \text{(Binomial coefficient).}$$

Moments of Z are readily obtained, most easily by expressing the CF (2.7) as the power series

$$\Phi_Z(j\xi) = \sum_{\ell=0}^{\infty} \frac{1}{\ell!} \{ \sum_{k=1}^{\infty} \left(\frac{(-1)^k \lambda_{2k} \xi^{2k}}{(k!)^2 2^{2k}} \right) \}^{\ell} \qquad (2.13)$$

(this form is obtained be expanding the exponential and the Bessel function in a series form). Using the well-known relation between the CF and its moments [72]

$$\langle z^{2k} \rangle = (-1)^k \frac{d^{2k}}{d\xi^{2k}} \Phi_Z(j\xi) \Big|_{\xi=0}$$

we have

$$\langle z^2 \rangle = \frac{\lambda_2}{2}, \quad \langle z^4 \rangle = \frac{3}{2}\frac{\lambda_4}{4} + \frac{3\lambda_2^2}{4},$$

$$\langle z^6 \rangle = \frac{5}{2}\frac{\lambda_6}{8} + \frac{45}{2}\frac{\lambda_2\lambda_4}{8} + \frac{15\lambda_2^3}{8}, \ldots \text{etc.} \qquad (2.14)$$

where

λ_{2k} (k=1,2 .....) is defined by (2.9).

2.5 ASYMPTOTIC BEHAVIOURS OF CFs (2.6) AND (2.7)

The parameter of the Poisson ensemble which has most influence in determining the general features of the noise is the density ν. As the noise density increases, the noise distribution tends towards the Gaussian. When the density is small, the noise pulses overlap only slightly so that the noise has the attributes of a deterministic, interfering signal, whose time-structure is essentially that of a single typical impulse. These two limiting regions are important, since the exact distributions are usually too complex to be used analytically, and must be approximated differently in

each of the two cases.

In accordance with the statistical features of 'impulsive' noise; the 'tails' ($|y|\to\infty$, $|z|\to\infty$) of the pdfs $p_Y(y)$, $p_Z(z)$ fall off less rapidly than Gaussian. Conversely, for small amplitudes ($|y|,|z|\to 0$) or, equivalently, large $|\xi|$, the CFs (2.6) and (2.7) accordingly reduces to $\exp(-2\nu T)$, so that the Fourier transform yields $p_Y(y) = \exp(-2\nu T)\delta(y-0)$ and $p_Z(z) = \exp(-2\nu T)\delta(z-0)$: these show the expected 'gaps-in-time', typical of impulsive interference. T defines the period of observation (or bit interval). To see how the CF for $|\xi|\to 0$ is obtained for $\Phi_Y(y)$, we demonstrate this with the case where $p_A(a)$ is Gaussian. Using $\Phi_A(j\xi) = \exp(-\langle a^2\rangle_a \xi^2/2)$ in (2.6) and assuming $h_R(t) \approx 0$ for $|t|>T$ yields

$$\Phi_Y(y) = \exp\{\nu \int_{-T}^{T} dt\ [\exp(-\xi^2 \langle a^2\rangle_a h_R^2(t)/2) - 1]\}.$$

For large ξ , the method of Laplace may be applied to the integral [76]. Subdivide the interval (-T,T) such that one zero crossing occurs at t_i in each subdivision. Redefine $h_{R_i}(t)$ outside each subinterval such that

$$\exp(-\xi^2 \langle a^2\rangle_a\ h_{R_i}^2(t)/2) = 0 .$$

Then, making use of the property that for large ξ, the exponential is approximately zero except for $h_{R_i}(t) \approx 0$

$$\Phi_Y(y) = \exp\ [\nu\{-2T + \sum_{i=-n}^{n} \int_{-T+t_i}^{-T+t_{i+1}} dt \exp\ (-\xi^2 \langle a^2\rangle_a \cdot h_{R_i}^2\ (t)/2)\}]$$

$$= \exp\left[\nu\{-2T + \sum_{i=-n}^{n} \int_{-\infty}^{\infty} dt \exp(-\xi^2 \langle a^2 \rangle_a h_{R_i}^2 (t)/2)\}\right].$$

Using Taylor series expansion about t_i and using the fact at $t=t_i$, $h_{R_i}(t) = 0$ we obtain after integrating

$$\Phi_Y(y) = \exp\{\nu(-2T + \frac{1}{|\xi|} \sum_{i=-n}^{n} \frac{\sqrt{2\pi}}{\langle a^2 \rangle_a^{\frac{1}{2}} |\dot{h}_R(t_i)|})\}$$

where $\dot{h}_R(t_i)$ is the first derivative of $h_R(t_i)$. This summation in the exponent is a constant, say U, therefore for large ξ,

$$\Phi_Y(y) = \exp\{\nu\ (-2T + U/\ |\xi|)\}.$$

For $\xi \to \infty$, as expected $\Phi_Y(y) \to \exp(-2\nu T)$.
The pdf then always contains 'dc component', a delta function at the origin of area $\exp(-2\nu T)$.

2.5.1 SERIES EXPANSION OF THE pdfs (2.8)

Many authors have treated the series expansion of the pdf $p_Y(y)$ (2.8a). Among them are Richter [35], Ziemer [58], Rice [71], Middleton [77] andMullen and Middleton [78]. The series expansion usually used is the Gram Charlier Type A or rearranged as an Edgeworth expansion [74], [79]. This is useful for representing a non-Gaussian, but near Gaussian, noise probability density. These series have been obtained as follows: assume

$$p(x) = \sum_{\ell=0}^{\infty} c_\ell \frac{\theta^\ell (x)}{\ell!} \qquad (2.15)$$

with

$$\theta^n(x) = \frac{1}{\sqrt{2\pi}} \frac{d^n}{dx^n} \exp(-x^2/2) = (-1)^n He_n(x)\theta^0(x),$$

c_ℓ's are constants and He_n are Hermite polynomials. To find the coefficients c_ℓ we make use of the orthogonality relation

$$\int_{-\infty}^{\infty} \theta^0(x)\ He_n(x) He_m(x)\ dx = \delta_{nm} n!\ .$$

Multiplying both sides of (2.15) by $He_n(x)$ and integrating over $(-\infty,\infty)$ to obtain

$$c_n = (-1)^n \int_{-\infty}^{\infty} p(x)\ He_n(x)\ dx. \qquad (2.16)$$

The low-order relation in terms of cumulants (2.9) are [74],[79]

$$c_0=1,\ c_1=c_2=0,\ c_3=\lambda_3,\ c_4=\lambda_4,\ c_5=-\lambda_5,$$

$$c_6=\lambda_6 + 10\lambda_3^2\ ,\ \ldots\ldots\ldots\ldots\text{etc.}, \qquad (2.17)$$

Since it is desired to vary ν while keeping λ_2 constant (=1), it is necessary to scale the rms value of the random variable a. i.e.,

$$\langle \check{a}^2 \rangle_a = 1/\hat{\nu}^2$$

where

$$\hat{\nu} = \{\nu \int_t h_R^2(t)\ dt\}^{\frac{1}{2}}\ .$$

This can always be obtained by making a transformation in pdf of a, i.e.,

$$p_A(a\nu) = \frac{\hat{\nu}}{\langle a^2 \rangle_a} p_A(a\hat{\nu}).$$

The standardized cumulants are

$$\hat{\lambda}_n = \frac{\lambda_n}{\hat{\nu}^{\frac{n}{2}} \langle a^2 \rangle_a} \quad . \tag{2.18}$$

Using (2.17) and (2.18) in (2.15) yields

$$p(x) = \theta^0(x) + \frac{\lambda_3 \theta^3(x)}{3! \langle a^2 \rangle_a \hat{\nu}^{\frac{3}{2}}} + \frac{\lambda_4 \theta^4(x)}{4! \langle a^2 \rangle_a \hat{\nu}^2} - \frac{\lambda_5 \theta^5(x)}{5! \langle a^2 \rangle_a \hat{\nu}^{\frac{5}{2}}} +$$

$$+ \frac{\theta^6(x)}{6! \langle a^2 \rangle_a} \left\{ \frac{\lambda_6}{\hat{\nu}^3} + \frac{10 \lambda_3^2}{\hat{\nu}^3} \right\} + O(\theta^7(x)) . \tag{2.19}$$

By rearranging the terms so that they are monotonic in $\hat{\nu}^{n/2}$ instead of monotonic with $\theta^n(x)$, the Edgeworth series results. This series has a remainder with ever-decreasing order as the number of terms is increased:

$$p(x) = \theta^0(x) + \frac{\lambda_3 \theta^3(x)}{3! \langle a^2 \rangle_a \hat{\nu}^{\frac{3}{2}}} + \left\{ \frac{\lambda_4 \theta^4(x)}{4! \langle a^2 \rangle_a \hat{\nu}^2} + \frac{10 \lambda_3^2 \theta^6(x)}{6! \langle a^2 \rangle_a \hat{\nu}^3} \right\} +$$

$$+ O(\hat{\nu}^{\frac{3}{2}}) . \tag{2.20}$$

Note: each λ contains $\hat{\nu}$ as a factor. Clearly as $\hat{\nu} \to \infty$, (2.19) and (2.20) tend towards Gaussian, as anticipated. The non-Gaussian noise model which results by considering the first few terms of (2.20) was studied recently by Bodharamik et al [61]. This series approach therefore will not be studied in this thesis.

2.5.2 LOW ν-CASE (VERY IMPULSIVE)

The low ν-case is that for which essentially no overlap in impulse response occurs. A natural approach in this case is the consideration of the expansion of (2.8a) and (2.8b) as a series in powers of ν:

$$p_Y(y) = \frac{1}{2\pi}\int_{-\infty}^{\infty} d\xi \exp(-j\xi y)\{1+\nu\int_t dt[\Phi_A(j\xi h_R(t))-1]+O(\nu^2)\} \tag{2.21a}$$

and

$$p_Z(z) = \frac{1}{2\pi}\int_{-\infty}^{\infty} d\xi \exp(-j\xi z)\{1+\nu\int_t dt\langle J_0(\xi aG(t))-1\rangle_a +O(\nu^2)\} \tag{2.21b}$$

2.6 ADDITIVE COMBINATION OF POISSON AND GAUSSIAN NOISE

The situation of greatest interest includes a Gaussian background noise, attributable usually to a very large number of effectively weak, comparable interfering sources, in addition to the relatively few large sources (ν small). The desired CFs (2.6) and (2.7) are readily extended, to give

$$\Phi_{Y_1(P+G)}(j\xi) = \exp\{-\frac{\sigma_g^2\xi^2}{2} + \nu\int_t dt\langle\exp(-j\xi a h_R(t))-1\rangle_a\} \tag{2.22a}$$

and

$$\Phi_{Z_1(P+G)}(j\xi) = \exp\{-\frac{\sigma_g^2\xi^2}{2} + \nu\int_t dt\langle J_0(\xi aG(t))-1\rangle_a\} \tag{2.22b}$$

where σ_g^2 is the variance of the Gaussian noise with zero mean.

Now, of course, there are no 'gaps-in-time' : $p_{Y_1}(y) \neq \delta(y-0)$, etc., for any $\nu>0$. For large ν the asymptotic normal forms are obtained from the usual expansion of $\langle J_0(.)\rangle_a$ and the method suggested in the previous section. The associated pdfs are then found, as noted above, by Fourier inversion similar to (2.8).

MOMENTS

Using similar arguments to those used before in section (2.4) we can readily show that all even moments $\langle y_1^{2k}\rangle$, $\langle z_1^{2k}\rangle$ exist ($<\infty$) and that all odd moments $\langle y_1^{2k+1}\rangle$ and $\langle z_1^{2k+1}\rangle=0$. The cumulants λ'_{2k} $(=\lambda_{2k})$ of Y_1 can easily be obtained from (2.9) for k=2,3..... For k=1 the cumulant is given by

$$\lambda'_2 = \sigma_g^2 + \nu\langle a^2\rangle_a \int_t h_R^2(t)\, dt. \qquad (2.23)$$

Defining $R_n = (1+ \frac{2\sigma_q^2}{\lambda_2})$, various moments of Z_1 are

$$\langle z_1^2\rangle = \frac{\lambda_2}{2} R_n,\ \langle z_1^4\rangle = \frac{3}{4}\left(\frac{\lambda_4}{2} + \lambda_2^2 R_n^2\right),$$

$$\langle z_1^6\rangle = \frac{1}{8}\left(\frac{5\lambda_6}{2} + \frac{45}{2}\lambda_2\lambda_4 R_n + 15\lambda_2^3 R_n^3\right), \ldots\text{.etc.} \qquad (2.24)$$

where λ_{2k} are defined by (2.9). In the next chapter this noise model is applied to detection of known signals in the presence of Poisson IN.

CHAPTER 3

PERFORMANCE OF LINEAR RECEIVERS IN POISSON IMPULSIVE NOISE CHANNEL [131]

This chapter studies the influence of generalized stationary Poisson IN on the receiver, optimized for white Gaussian noise (matched filters). No attempt is made to introduce a limiter in order to improve its characteristics. Approximate results for the error probability of a P.S.K. system are obtained by taking the noise parameter ν to be either very large or very small (i.e., quasi-Gaussian or impulsive noise cases).

3.1 INTRODUCTION

In this chapter the effects of the IN on communication receivers are analysed in a way which separates the effects of the noise parameters from those of the parameters of the receiver. Measurements of the IN statistical characteristics can thus be made and applied to the study of any receiver performance and, conversely, a receiver characteristic can be obtained and used to determine its performance for any IN.

Much of the work in the literature is somewhat heuristic in nature, since a distribution is often assumed for the amplitude of the detected IN quite independently of the specific system configuration. Thus, for example, no explicit dependence is generally found between the probability of error and the shape of the bandwidth of the RF filter used in radio receivers or the channeling filters used in wire links. Bello and Esposito

[41],[42] and Conti et al [62] however, defined for the receiver a hierarchy of functions called the Receiver Impulse Characteristics (RICs) and for the noise a hierarchy of time-amplitude distribution. Under rather broad conditions the RICs can be computed a priori, i.e., without reference to any IN, and the noise distribution functions can be measured without reference to any particular receiver. It is important to point out that Bello and Esposito [41] did not make any specific assumption on the RF filter, but they analyzed the effects on the shape and the bandwidth of the RF filter on the RIC and consequently the error probability of the communication system.

Another interesting paper by Valfbein et al [80] deals with the problem of finding the error probability as an average of an appropriate function, which depends on the modulation system used, over the normalized maximum value of the IN voltage. However, they assumed an ideal RF filter and therefore their results did not take into account the shape of the RF filter.

The model of IN studied in this chapter consists of considering the perturbing additive noise as a mixture of

a) a train of Dirac functions with an appropriate amplitude-time probability structure,

b) a white Gaussian noise with known spectral density

and multiplicative noise introduced by the random channel. Calculations of error probability of digital data systems operating over fading channels have generally assumed that the additive noise is normally distributed. Exceptions to this occurs in two papers by Bello [56],[57] where he uses an empirical noise model for the atmospheric noise. More

general calculations are needed, however, because the additive interference in fading channels can be of a more general nature. Here we treat in detail the case of the P.S.K. binary system, but the method is applicable to any digital modulation system.

3.2 PROBLEM FORMULATION

A block diagram of the communication system studied is shown in Fig. 3.1. This is the well-known coherent receiver of P.S.K.signals, except for the appearance of the RF filter. The receiver is optimum for a purely Gaussian interference and presupposes a knowledge of the carrier phase of the incoming signal (since the fading considered here is assumed to be slow, it should be possible to derive a suitable, and essentially noiseless phase reference for an ideal P.S.K.system[81]).At the input to the RF filter we are assuming the presence of two types of noise, namely, Gaussian noise $n_G(t)$ and Poisson IN $n(t)$.

The Gaussian noise $n_G(t)$ is modelled in the usual fashion as a zero-mean Gaussian process having flat power-spectrum density over the RF filter bandwidth

$$S_G(j\omega) = \frac{N_o}{2} \qquad (3.1)$$

where N_o is the spectral height in joules.

The IN (defined by (2.1)) fed into the RF filter has an essentially flat spectrum over the RF bandwidth B, and thus each noise pulse produces an output of the same shape as the impulse response of that filter. However, since the energies in the noise pulses are random and the occurrence times of the pulses bear no relation to the phase of the centre frequency

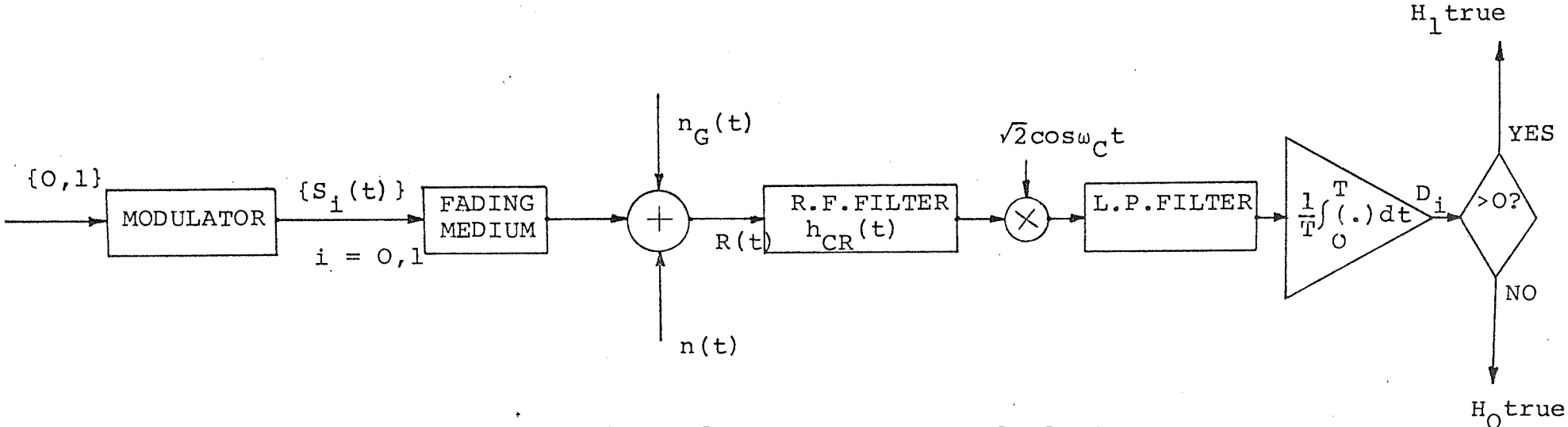

Fig. 3.1 Linear receiver under impulse and Gaussian noise calculations.

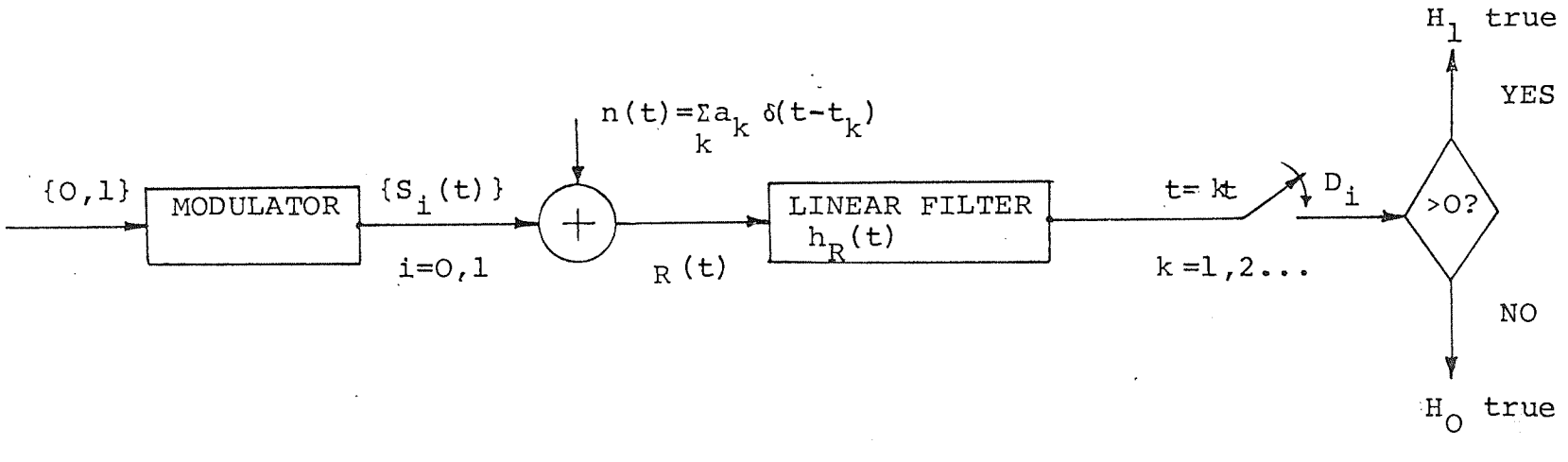

Fig. 3.2 Linear time-invariant detector.

of the RF filter, the complex envelope of the RF filter response to an impulse must be modelled as the product of a complex random gain by the complex envelope of the filter impulse response. Thus if the complex envelope of the RF filter impulse response is $h_{CR}(t)$, the output of the RF filter $Z(t)$ due to the IN can be characterized as

$$Z(t) = \sum_k a_k h_{CR}(t-t_k) \exp(j\psi_k) \qquad (2.4)$$

where a_k is a random amplitude, ψ_k is a random phase and $\{t_k\}$ are the occurrence times of the input noise pulses.

We assume that the data to be transmitted is presented to the transmitter in a sequence of binary digits which can be denoted by zeros and ones appearing at a rate of every T seconds. If the m^{th} position of the sequence is one, the system transmits the signal waveform $S_1(t)$ during the interval $mT \leq t \leq (m+1)T$; if it is a zero, the transmitted signal is $S_0(t)$. We also assume these signals representing the elements of the binary sequence are statistically independent, and each signal will be assumed to be restricted to a duration of T seconds. Having observed the received waveform $R(t) (= S_i(t, S_F) + n_G(t) + n(t))$ during the signal duration T, the receiver is to choose between two hypotheses. H_1 (signal $S_1(t)$ was sent) and H_0 (signal $S_0(t)$ was sent). S_F is the random gain due to the multiplicative noise. We are mainly concerned with the evaluation of the probability of an error occurring in the receiver estimate.

Before beginning the detailed discussion of the problem formulated above, it is profitable to have an overview of the performance of the linear detector operating in unfiltered

Poisson IN (without RF filter in Fig. 3.1) and without any multiplicative noise [35],[58]. This case is considered in the next section.

3.3. PERFORMANCE OF LINEAR DETECTORS IN UNFILTERED POISSON NOISE CHANNEL

3.3.1 ADDITIVE POISSON IMPULSE NOISE

In this section we do not consider the effect of the RF filter and multiplicative noise. The block diagram of the system studied in this section is shown in Fig. 3.2. The composite signal plus noise at the input to the linear filter may be written as

$$R(t) = S_i(t) + n(t) \quad , \quad i = 0,1. \tag{3.2}$$

The noise n(t)is the Poisson IN model described in Chapter 2 (2.1). Since the processing channel is linear, we shall be justified in dealing with signal and noise separately. When no signal is present the pdf of the noise variable X for a high IN ($\gamma<<1$), at time t=kT(k=1,2.....), at the output of the filter was obtained in the last chapter (2.21a) as

$$p_X(x)=\frac{1}{2\pi}\int_{-\infty}^{\infty} d\xi \exp(-j\xi x)\{1+\nu\int_t dt[\Phi_A(j\xi h_R(t))-1]+O(\nu^2)\}. \tag{3.3}$$

Evaluating the above integral with respect to ξ and using the fact

$$p_A(a) = \frac{1}{2\pi}\int_{-\infty}^{\infty}\exp(-j\xi a)\Phi_A(j\xi)\,d\xi$$

we obtain

$$p_X(x) = (1-\gamma)\delta(x) + \frac{\gamma}{T}\int_{-T/2}^{T/2} \frac{dt}{h_R(t)}\, p_A\left\{\frac{x}{h_R(t)}\right\} \qquad (3.4)$$

where we have assumed

$$h_R(t) = 0 \text{ for } |t| > T/2 \text{ and } \int_{-\infty}^{\infty} |h_R(t)|\,dt < \infty$$

as the physical realization and stability constraints on the filter, $\gamma = \nu T$ is the number of impulses in time T and $\delta(x)$ the Kronecker delta. For $p_A(a)$ symmetrical the mean can be shown to be zero.

With antipodal signals, i.e., $S_0(t) = -S_1(t)$ the output at the end of a bit interval under no noise condition is simply

$$D_{S_i} = \int_{-\infty}^{T} (-1)^{i+1} S_i(\tau) h_R(T-\tau)\,d\tau, \quad i=0,1 . \qquad (3.5)$$

If $S_1(t)$ was sent, the filtered output variable at time T, due to the noise plus signal, is $D = D_{S_1} + X$ while if $S_0(t)$ was transmitted it is $D = -D_{S_0} + X$. The decision variable D has the same statistics as X, fluctuating about D_{S_i} rather than zero. Its pdf is given by (3.4). If $D<0$ (>0) the decision is that $S_0(t)\{S_1(t)\}$ was sent. Thus it follows that an error would be made when $-D_{S_0} + X > 0$ and $D_{S_1} + X < 0$ i.e.,

$$Pe_1 = Pr(-D_{S_0} + X > 0); \quad Pe_2 = Pr(D_{S_1} + X < 0) \qquad (3.6)$$

where Pr(.) denotes the probability of the event inside the parenthesis taking place. For symmetrical noise distributions the two kinds of errors are equal, i.e., $Pe_1 = Pe_2$. The

average probability of error Pe_I is then

$$Pe_I = \int_{D_{S_1}}^{\infty} p_X(x). \tag{3.7}$$

Since it is of interest to calculate the performance of the system in the presence of an IN burst only, the average probability of error Pe_I using (3.4) in (3.7) yields

$$Pe_I = \frac{\gamma}{T} \int_{D_{S_1}}^{\infty} dx \int_0^T \frac{dt}{|h_R(t)|} \; p_A\{\frac{x}{|h_R(t)|}\}. \tag{3.8}$$

Absolute values occur since only symmetrical distributions for $p_A(a)$ are considered.

Further simplification of the error probability requires a knowledge of the filter characteristics. By way of illustration, we shall now apply the results obtained to the evaluation of Pe_I when $h_R(t)$ is a matched filter. For P.S.K. signalling, the i^{th} transmitted signal, which occurs with a priori probability 0.5, is of the form

$$S_i(t) = \begin{cases} (-1)^i (\frac{2E}{T})^{\frac{1}{2}} \cos \omega_c t, & 0 \leq t \leq T \\ 0 \quad \text{Otherwise} & i = 0,1 \end{cases} \tag{3.9}$$

where E is energy of the signal, $\omega_c = 2\pi n_o/T$ (n_o is an integer). The matched filter then has impulse response

$$h_R(t) = \begin{cases} (\frac{2}{T})^{\frac{1}{2}} \cos\omega_c (T-t), & 0 \leq t \leq T \\ 0 \qquad\qquad \text{Otherwise.} \end{cases} \tag{3.10}$$

Using (3.9), (3.10) in (3.8) and making a change in variable $\theta = 2\pi(T-t)/T$ we obtain

$$Pe_I = \frac{2\gamma}{\pi} \int_0^{\pi/2} d\theta \int_{(\frac{ET}{2})^{\frac{1}{2}} \frac{1}{\cos\theta}}^{\infty} p_A(a)\, da \tag{3.11}$$

$p_A(a)$, $-\infty<a<\infty$	Pe_I - Linear Filter	Pe_I - Matched Filter
1 GAUSSIAN $\frac{1}{\sqrt{2\pi\langle a^2\rangle}} \exp(-\frac{a^2}{2\langle a^2\rangle})$	$\frac{\gamma}{T}\int_0^T \mathrm{erfc}\{\frac{\sqrt{D_S}}{\sqrt{\langle a^2\rangle}h_R(t)}\}\,dt$	$\frac{2\gamma}{\pi}\int_0^{\pi/2} \mathrm{erfc}(Z_I\Delta_\phi/\sqrt{2})\,d\phi$
2 EXPONENTIAL $\frac{1}{\sqrt{2\langle a^2\rangle}} \exp(\sqrt{\frac{2}{\langle a^2\rangle}}\,\lvert a\rvert)$	$\frac{\gamma}{2T}\int_0^T \exp\{-\sqrt{\frac{2D_S}{\langle a^2\rangle}}\frac{1}{h_R(t)}\}dt$	$\frac{\gamma}{\pi}\int_0^{\pi/2}\exp(-Z_I\Delta_\phi)\,d\phi$
3 RAYLEIGH $\frac{\lvert a\rvert}{\langle a^2\rangle}\exp(-\frac{a^2}{\langle a^2\rangle})$	$\frac{\gamma}{2T}\int_0^T \exp\{-\frac{D_S}{\langle a^2\rangle}\frac{1}{h_R^2(t)}\}dt$	$\frac{\gamma}{\pi}\int_0^{\pi/2}\exp(-Z_I^2\Delta_\phi^2/2)\,d\phi$
4 GENERALIZED HYPERBOLIC* $\frac{\Gamma(\beta+\frac{1}{2})}{\sqrt{2\pi\langle a^2\rangle(\beta-1)}\,\Gamma(\beta)}\frac{1}{\left[\left(\frac{a}{\sqrt{2\langle a^2\rangle(\beta-1)}}\right)^2+1\right]^{\beta+\frac{1}{2}}}$	$\frac{\gamma}{2T}\int_0^T dt\frac{\Gamma(\beta+\frac{1}{2})}{\sqrt{\pi}\Gamma(\beta)}B(\beta,\frac{1}{2}\lvert\frac{1}{1+\frac{D_S}{2\langle a^2\rangle(\beta-1)h_R^2(t)}})$	$\frac{\gamma}{\pi}\frac{\Gamma(\beta+\frac{1}{2})}{2\Gamma(\beta)}\int_0^{\pi/2}B(\beta,\frac{1}{2}\lvert\frac{1}{1+\frac{Z_I\Delta_\phi^2}{4(\beta-1)}})d\phi$

where $\Delta_\phi = \sqrt{\gamma}/\cos\phi$

$\Gamma(x)$ = Gamma fx. [82]

$B(\ )$ = Incomplete Beta function [83]

$\mathrm{erfc}\,(x)$ = Complement of error fx. $= \frac{1}{\sqrt{2\pi}}\int_x^\infty \exp(-t^2/2)dt$.

* This pdf is derived in Part B of the thesis

Fig. 3.3 Probability of bit error expressions for linear receivers for various amplitude pdfs $p_A(a)$.

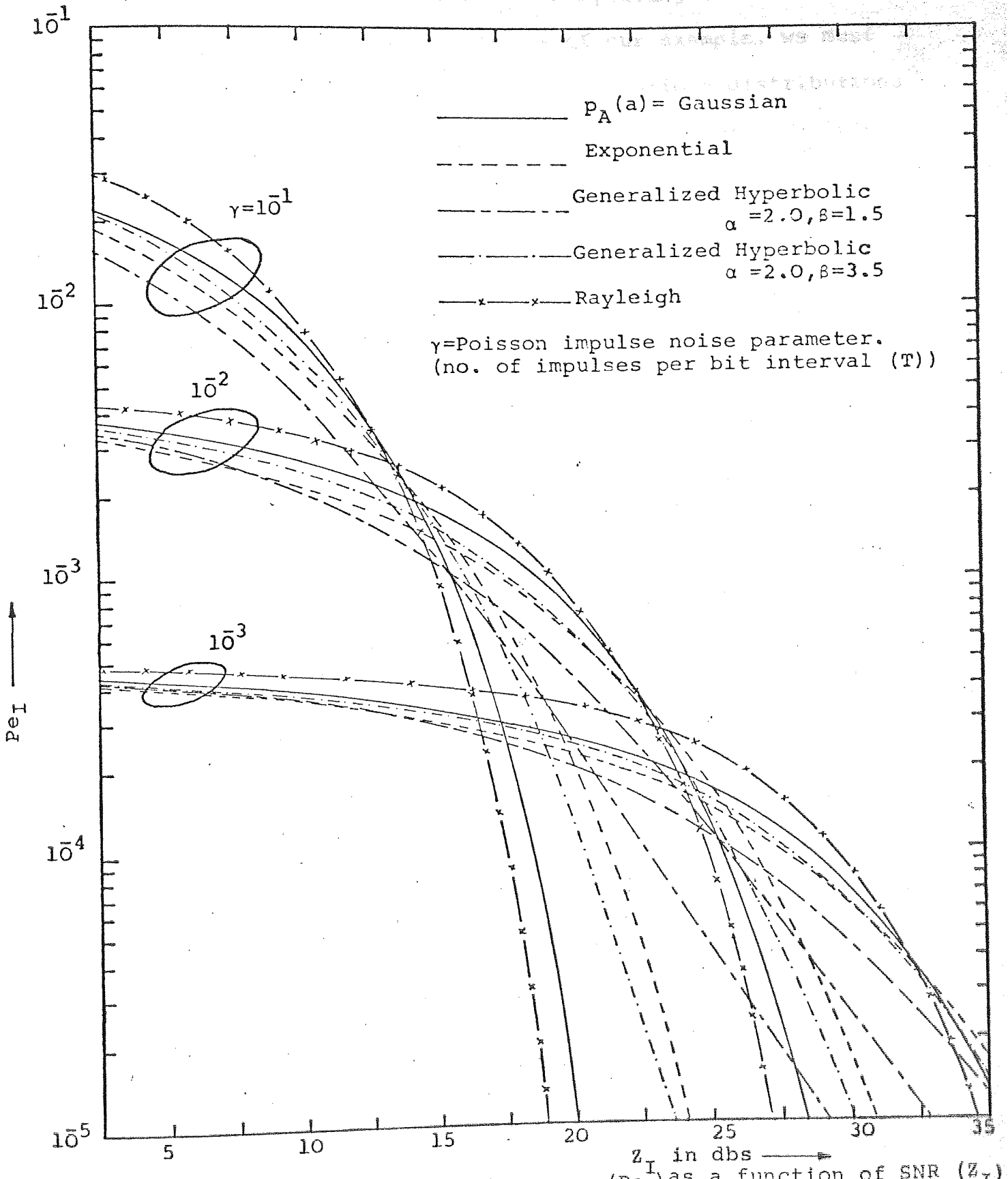

Fig.3.4 Average probability of bit error (Pe_I) as a function of SNR (Z_I) for P.S.K. system operating in additive unfiltered Poisson impulse noise ($\gamma << 1$) with various amplitude pdfs ($p_A(a)$)

where we have substituted for $D_{S_1} = \sqrt{E}$ by using (3.9) and (3.10) in (3.5). To complete the analysis of our example, we must assign the pdf of the noise amplitude. Various distributions are considered and the final error expressions are tabulated in Fig. 3.3. The SNR Z_I used in Fig. 3.3 is defined as

$$Z_I = \sqrt{E/\lambda_2} \tag{3.12}$$

where λ_2 is defined by (2.9).

At this point it might be asked what is the optimum filter that minimizes the error expression of (3.8) under constraint of transmitted power? Using calculus of variation techniques [112], a complicated integral equation can be derived whose solution produces the optimum filter. The solution depends on the Lagrange multiplier, SNRs and signal shape. Solution of these equations appears to be a substantial problem and beyond the scope of the work covered in this thesis.

DISCUSSION

Using the expressions given in Fig.3.3 the numerical results for probability of error Pe_I against SNR Z_I defined by (3.12), with γ as a parameter, for various amplitude pdf $p_A(a)$ have been calculated and are plotted in Fig. 3.4. The results show an interesting behaviour. For low SNR, the mean error probability tends towards a limit 0.5γ, for which the following explanation can be offered. The pulses being much larger in amplitude than the signal, the detector will decide that $S_1(t)$ will have been transmitted whenever a noise pulse has occurred in the transmission interval. For 0.5 of the time, the decision will be wrong and, as the mean number of noise pulses is γ, the error probability must tend towards

0.5γ. So, as γ becomes smaller (which increases the noise pulse amplitude), the error probability becomes less sensitive to the SNR over a wide range. It can also be observed that Pe_I is larger for large SNR's if $p_A(a)$ is exponential than if it is Gaussian, the probability for large noise impulses being greater for the former pdf than for the latter.

In practice, the measured values of Pe_I for small SNR's are much larger than the theory predicts, a possible explanation for this being that the generated noise for these conditions is actually better modelled by an additive combination of Gaussian and IN because of the thermal noise added by amplification [58]. We now modify the theory to take this into account.

3.3.2 ADDITIVE COMBINATION OF GAUSSIAN AND UNFILTERED POISSON NOISE

For an input consisting of additive signal and noise, i.e., $R(t) = S_i(t) + n_G(t) + n(t)$, where $n(t)$ and $n_G(t)$ are sample functions from zero mean white impulsive (2.1), and white Gaussian noise processes, respectively , it follows that the linear filter output at time t=T may be written as

$$R = D_{S_i} + n_G + X \tag{3.13}$$

where D_{S_i} is defined by (3.5), X and n_G are the noise components of the output. The pdf of the decision variable $D = n_G + X$ at the ouptut may be obtained by convolving $p_X(\zeta)$ with the pdf of $p_G(\zeta)$ (Gaussian), i.e.,

$$p_D(x) = \int_{-\infty}^{\infty} p_X(\zeta)\, p_G(x-\zeta)\, d\zeta \tag{3.14}$$

Using $p_X(\zeta)$ from (3.4) and

$$p_G(\zeta) = \frac{1}{(2\pi\sigma_g^2)^{\frac{1}{2}}} \exp\left(-\frac{\zeta^2}{2\sigma_g^2}\right)$$

in (3.14) yields

a) for $p_A(a) = \frac{1}{(2\langle a^2\rangle)^{\frac{1}{2}}} \exp\left[-\left(\frac{2}{\langle a^2\rangle}\right)^{\frac{1}{2}}|a|\right]$ (exponential)

$$p_D(x) = \frac{(1-\gamma)}{(2\pi\sigma_g^2)^{\frac{1}{2}}} \exp\left(-\frac{x^2}{2\sigma_g^2}\right) + \frac{\gamma}{T(2\langle a^2\rangle)^{\frac{1}{2}}}\int_0^T \frac{dt}{h_R(t)} \cdot$$

$$\cdot \exp\left\{\frac{\sigma_g^2}{\langle a^2\rangle h_R^2(t)}\right\} \left[\exp\left\{-\left(\frac{2}{\langle a^2\rangle}\right)^{\frac{1}{2}} \frac{x}{h_R(t)}\right\} \operatorname{erf}\left\{\frac{x}{\sigma_g} - \left(\frac{2}{\langle a^2\rangle}\right)^{\frac{1}{2}} \frac{\sigma_g}{h_R(t)}\right\} + \exp\left\{\left(\frac{2}{\langle a^2\rangle}\right)^{\frac{1}{2}} \frac{x}{h_R(t)}\right\} \operatorname{erfc}\left\{\frac{x}{\sigma_g} + \left(\frac{2}{\langle a^2\rangle}\right)^{\frac{1}{2}} \frac{\sigma_g}{h_R(t)}\right\}\right] \qquad (3.15a)$$

and

b) $p_A(a) = \frac{1}{(2\pi\langle a^2\rangle)^{\frac{1}{2}}} \exp\left(-\frac{a^2}{2\langle a^2\rangle}\right)$ (Gaussian):

$$p_D(x) = \frac{(1-\gamma)}{(2\pi\sigma_g^2)^{\frac{1}{2}}} \exp\left(-\frac{x^2}{2\sigma_g^2}\right) + \frac{\gamma}{T(2\pi)^{\frac{1}{2}}} \int_0^T dt \cdot$$

$$\cdot \left[\frac{\exp\left\{\frac{-x^2}{2(\sigma_g^2 + h_R^2(t)\langle a^2\rangle)}\right\}}{\{\sigma_g^2 + h_R^2(t)\langle a^2\rangle\}^{\frac{1}{2}}}\right] \qquad (3.15b)$$

For P.S.K. signals and matched filter described by (3.9) and (3.10), respectively, and using (3.15), the probability error expressions become

a) $p_A(a)$ exponential

$$Pe_E = (1-\gamma)\operatorname{erfc}(Z_{I+G}R_1) + \frac{\gamma R_1}{\pi\sqrt{R}}\int_0^{\pi/2} d\phi\, \Delta_\phi \exp\left(\frac{\Delta_\phi^2}{2R}\right) \cdot$$

$$\cdot \int_{Z_{I+G}}^{\infty} \{\exp(-\frac{\Delta_\phi \xi R_1}{\sqrt{R}}) \operatorname{erf}(\xi R_1 - \frac{\Delta_\phi}{R}) + \exp(\Delta_\phi \frac{\xi R_1}{\sqrt{R}}) \cdot$$

$$\cdot \operatorname{erfc}(\xi R_1 + \frac{\Delta_\phi}{R})\} \, d\xi \qquad (3.16a)$$

b) $p_A(a)$ Gaussian

$$Pe_G = (1-\gamma)\operatorname{erfc}(Z_{I+G} + R_1) + \frac{2\gamma}{\pi} \int_0^{\pi/2} \operatorname{erfc}\left(\frac{R_1 Z_{I+G}}{\{1 + 2R/\Delta_\phi^2\}^{\frac{1}{2}}}\right) d\phi$$

(3.16b)

where

$$Z_{I+G} = \text{SNR} = \sqrt{E/(\sigma_g^2 + \lambda_2)} \; ; \; (\lambda_2 = \langle a^2 \rangle \gamma / T \; (2.9)),$$

$$\Delta_\phi = \sqrt{\gamma}/\cos\phi \, ,$$

$$R_1 = \sqrt{1+R}$$

and

$$R = \text{IN variance to Gaussian noise variance ratio} = \lambda_2/\sigma_g^2$$

DISCUSSION

The probability of error expression of (3.16b) Pe_G is plotted in Fig. 3.5 against SNR Z_{I+G} (3.17) with R and γ as parameters. The most striking feature of the results is that even a small amount of Gaussian noise has a considerable effect on the probability of error at low SNR while on the other hand at high SNR the effect of Gaussian noise is negligiably small. In practice the Gaussian noise is always present due to the thermal noise added by the amplification. The effect of each noise component, therefore, on the probability of error Pe_G may

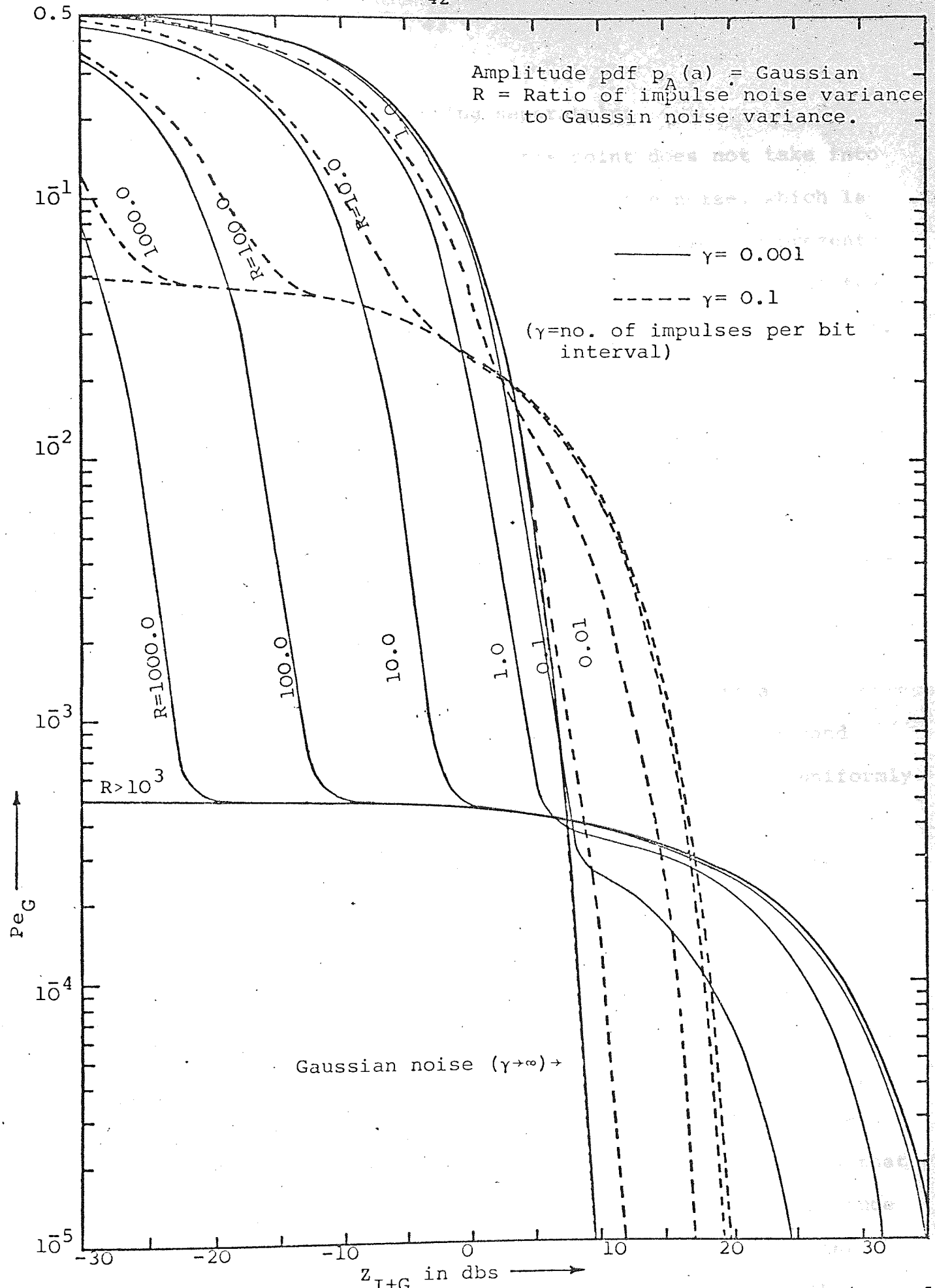

Fig.3.5 Average probability of error (Pe_G) as a function of SNR(Z_{I+G}) fo P.S.K. system operating in additive unfiltered IN ($\gamma<<1$) and Gaussian noise.

roughly be considered as acting seperately.

The analysis presented upto this point does not take into account any effect of the bandlimiting of the noise, which is usually the case in practice. In the next section we present the analysis which includes the effects of bandlimiting of the noise by placing a bandpass filter prior to the matched filter. We also consider the case when the multiplicative noise is present.

3.4 ERROR PROBABILITY DUE TO FLAT FADING AND FILTERED IMPULSIVE PLUS GAUSSIAN NOISE

Analysis of the detection of an incoming radio signal that is subject to fading requires an extension of the theory used in the last section. The transmitted signal, in this case, first passes through a linear medium which fades in a frequency-nonselective way. That is to say, the whole band of frequencies occupied by the two signals is acted on uniformly by the medium; there is no possibility of simultaneous constructive interference at one frequency and destructive interference at another. Put another way, if there is more than one transmission path, the difference of delays of any pair of paths must be much less than the reciprocal of the width of the band of frequencies occupied by the quantity. In this section, the assumption of 'slow fading' is made, i.e., the fading bandwidth is assumed to be small compared to the signal information bandwidth. The same assumption implies that while the signal may still be regarded as a constant amplitude sinusoid in formulating and solving detection problems, the amplitude must now be regarded as a random variable at the receiver. To calculate error probabilities with fading signals,

we must know the amplitude pdf associated with fading. The error probabilities calculated in the above section, which appear as functions of SNR, must now be averaged over the possible range of SNR's using the fading amplitude pdf in the averaging process. Because of the 'slow fading', we need not consider the change in the processing filters, only in the calculation of error probabilities, assuming the same processing filters as would have been used in the nonfading case.

After passing through the fading medium, the transmitted signal is further perturbed by additive noise, which we assume is white Gaussian, plus impulsive, and statistically independent of fading medium. The resultant signal R(t)is the received signal. Thus if $S_i(t,S_F)$ represents the signal of duration T received in the time interval $0<t<T$ for a unity gain channel and no additive noise, the above channel assumptions amount to a statement that the received signalling element R(t), including fading and additive noises, is given by

$$R(t)=S_i(t,S_F) +n(t) + n_G(t),\ i=0,1;\ 0<t<T \qquad (3.17)$$

where $S_i(t,S_F) = (-1)^{i+1}\sqrt{2}S_F\cos\omega_c t$, S_F is the random path - transmission factor, essentially a non-negative quantity which remains constant in the interval (0,T). Note: we have assumed for simplicity $\sqrt{E}/T = 1$ in (3.9) and adjust the received signal energy by changing the characteristics of the fading process, i.e., its variance (S_F).

If $h_{CR}(t)$ is the impulse response of the RF filter, which is assumed to be physically realizable, the signal $r(t)$ at the output of the RF filter is simply

$$r(t) = \int_0^T h_{CR}(\zeta)\ S_i(t-\zeta, S_F)\ d\zeta + \int_0^\infty h_{CR}(\zeta) n_G(t-\zeta) d\zeta +$$

$$+ \sum_k a_k h_{CR}(t-t_k)\ \exp\ (j\psi_k). \qquad (3.18)$$

Assuming the bandwidth of the RF filter is large compared to the signal, the signal $S_i(t,S_F)$ comes out of the RF filter undistorted.

The second term is still Gaussian signal $\hat{n}_G(t)$ with zero mean and variance:

$$\hat{\sigma}_g^2 = \frac{N_o}{2} \int_t h_{CR}^2(t)\ dt. \qquad (3.19)$$

The third term is due to the IN, which was discussed in the previous chapter. Multiplying (3.18) by $\sqrt{2}\ \cos\omega_c t$ and integrating with respect to t between O and T gives the decision random variable at time T as (neglecting all higher-order frequency terms)

$$D = D_{S_i} + Z + D_G, \qquad i = O,1 \qquad (3.20)$$

where D_{S_i}, Z and D_G are due to the signal fading with pdf $p_F(x)$, filtered Poisson IN with pdf $p_Z(x)$, and Gaussian noise with pdf $p_G(x)$ respectively.

The process Z(t), which occurs before the integrator as a result of the filtered IN, is obtained by using the complex notation for the impulse response of the RF filter [84] i.e.,

$$h_{CR}(t-t_k) = 2Re\{\tilde{h}_{CR}(t-t_k)\ \exp(-j\psi_k + j\omega_c t)\}$$

$$= 2\tilde{h}_{CR}(t-t_k)\ \cos\ (\omega_c t - \psi_k) \qquad (3.21)$$

where

$$\psi_k = \omega_c t_k - \left[\frac{\omega_c t_k}{2}\right]_I 2\pi$$

$[\ ]_I$ = integer part of $[\ ]$,

$\tilde{h}_{CR}(.)$ = complex envelope of the impulse response

in $\sum_k a_k h_{CR}(t-t_k)$ so that

$$Z(t) = \sum_k 2a_k \tilde{h}_{CR}(t-t_k)\cos(\omega_c t-\psi_k). \qquad (3.22)$$

Multiplying the above equation by $\sqrt{2}\cos\omega_c t$ and integrating with respect to t between 0 and T yields the random variable (neglecting the higher frequency terms)

$$Z = \sum_k A_k G(t_k)\cos\psi_k \qquad (3.23)$$

at time T where

$$G(t_k)=\sqrt{2}\int_0^T \tilde{h}_{CR}(t-t_k)\,dt \quad \text{and} \quad A_k=a_k/T. \qquad (3.23a)$$

D_G is the Gaussian random variable with zero mean and variance

$$\sigma_g^2 = \frac{N_o}{2T}\int_{-\infty}^{\infty} G^2(\zeta)\,d\zeta. \qquad (3.24)$$

The random variable D_{S_i}, Z, D_G are all independent with pdfs $p_F(x)$ $p_Z(x)$, $p_G(x)$ and CFs $\Phi_F(j\xi)$, $\Phi_Z(j\xi)$ and $\Phi_G(j\xi)$ respectively.

3.4.1 PROBABILITY OF ERROR

The decision variable D can be written as

$$D = W_i + U, \qquad i = 0,1 \tag{3.25}$$

where W_i is the component due to the wanted signal, with the pdf $p_F(x)$ and U is the component due to the 'unwanted' signal (additive noise), characterised by the pdf $p_U(x)$, assumed to be an even function. Because of the uniform distribution of the phase ψ , binary symmetric operation will exist, and therefore we can assume that $S_1 = 1$ was transmitted without any loss in generality. An error would be made if D<0. Since the fading process does not change the sign of the signal, the probability of error can be written as

$$Pe_{FI+G} = \int_0^{\infty} p_F(x) \int_{-\infty}^{-x} p_U(u)\, du\, dx. \tag{3.26}$$

The above equation can easily be rewritten in terms of the CFs as

$$Pe_{FI+G} = \frac{1}{2} - \frac{1}{2\pi} \int_{-\infty}^{\infty} \Phi_U(j\xi)\, Im\{\Phi_F(j\xi)\}\, \frac{d\xi}{\xi} \tag{3.27}$$

where Im{.} is the imaginary part of {.} .

Since U is the sum of two independent random variables Z and D_G we have

$$\Phi_U(j\xi) = \Phi_Z(j\xi)\, \Phi_G(j\xi) = \Phi_Z(j\xi) \exp(-\xi^2\sigma_g^2/2). \tag{3.28}$$

Substituting the above equation in (3.27) for Pe_{FI+G} we obtain

$$Pe_{FI+G} = \frac{1}{2} - \frac{1}{2\pi} \int_{-\infty}^{\infty} \Phi_Z(j\xi)\, \mathrm{Im}\{\Phi_F(j\xi)\} \exp\left(-\frac{\xi^2\sigma_q^2}{2}\right) \frac{d\xi}{\xi} . \tag{3.29}$$

For a_i statistically independent of one another it was shown in the previous chapter that the C_F of IN can be written as (2.7)

$$\Phi_Z(j\xi) = \exp\{\nu \int_t \langle J_o(\xi AG(t)) - 1\rangle_a \, dt\}.$$

Introducing the normalizing time $\tau = t/T$ the above equation becomes

$$\Phi_Z(j\xi) = \exp\{\gamma \int_{-\infty}^{1} d\tau \langle J_o(\xi AG(\tau)) - 1\rangle_a\}. \tag{3.30}$$

QUASI-GAUSSIAN NOISE ($\gamma >> 1$)

As the number of impulses γ in the interval T becomes large ($\gamma >> 1$) the noise tends to become Gaussian. By virtue of the relation [82]

$$J_o(x) = \sum_{k=0}^{\infty} \frac{(-1)^k x^{2k}}{(k!)^2\, 2^{2k}}$$

(3.30) takes the form

$$\Phi_Z(j\xi) = \exp\{\gamma \sum_{k=1}^{\infty} \int_{-\infty}^{1} \frac{(-1)^k}{(k!)^2} \langle A^{2k}\rangle_a \left(\frac{\xi G(\tau)}{2}\right)^{2k} d\tau\}. \tag{3.31}$$

Introducing the normalized variables

$$\hat{A} = \frac{A}{(\langle A^2\rangle_a)^{\frac{1}{2}}}, \qquad \hat{G}(\tau) = \frac{G(\tau)}{\{\int_{-\infty}^{1} G^2(\tau)\, d\tau\}^{\frac{1}{2}}}$$

and using

$$\langle z^2 \rangle = \frac{\gamma \langle A^2 \rangle_a}{2T} \int_{-\infty}^{T} G^2(t)\,dt$$

from (2.14),(3.31) becomes

$$\Phi_Z(j\xi) = \exp\{\sum_{k=1}^{\infty} \frac{(-1)^k}{(k!)^2} \frac{\langle \hat{A}^{2k} \rangle_a}{\gamma^{k-1}} \left(\frac{\xi^2 \langle z^2 \rangle}{2}\right)^k \int_{-\infty}^{1} \hat{G}^{2k}(\tau)\,d\tau\}. \tag{3.32}$$

In order to specialize the analysis to a specific filter, where a compact analytical expression for Pe_{FI+G} can be obtained, we shall assume the RF filter to be an RCL filter whose equivalent low-pass impulse response has an envelope of the form (Figs. 3.8 and 3.9) [41]

$$\hat{h}_{RC}(t) = \frac{1}{C}\exp(-t/C) \tag{3.33}$$

where C is the normalised filter time constant. Similar results of increasing analytical complexity can also be obtained, for instance,for Butterworth filters. The function $G(\tau)$ of (3.23a) is in this case

$$G(\tau) = \begin{cases} \int_0^1 \frac{1}{C}\exp\{\frac{-(t-\tau)}{C}\}dt = \exp(\frac{\tau}{C})\{1-\exp(-1/C)\}, & \tau<0 \\ \int_\tau^1 \frac{1}{C}\exp\{\frac{-(t-\tau)}{C}\}dt = 1-\exp(-\frac{1}{C}+\frac{\tau}{C}), & 0<\tau<1 \\ 0, & \tau>1 \end{cases} \tag{3.34}$$

C in terms of bandwidth B and the signal duration T is given by

$$C = \frac{1}{\pi TB}. \tag{3.35}$$

Substituting (3.32) and (3.34) in (3.29) and assuming $p_F(x)$ to be Rayleigh distributed with pdf

$$p_F(x) = \frac{2x}{S_F^2} \exp\left(-\frac{x^2}{S_F^2}\right) \tag{3.36}$$

and CF

$$\Phi_F(j\xi) = {}_1F_1\left(1;\tfrac{1}{2};-\frac{\xi^2 S_F^2}{2}\right) + j\left(\frac{\pi}{2}\right)^{\frac{1}{2}} \xi S_F \exp\left(\frac{-\xi^2 S_F^2}{2}\right)$$

where ${}_1F_1(\,)$ is confluent hypergeometric function [85], we obtain

$$Pe_{FI+G} = \frac{1}{2} - \frac{Z_{FI+G}}{\sqrt{2\pi}} \int_0^\infty \exp\left[\left\{-\frac{x^2}{2}\left(Z_{FI+G}^2 + \frac{1}{1+R}\right)\right\} + \right.$$

$$\left. + \sum_{k=1}^{\infty} \frac{(-1)^k}{k!} \frac{F_{2k}}{\hat{F}_2^k} \frac{1}{\gamma^{k-1}} \left(\frac{x^2 R}{2(1+R)}\right)^k\right] dx \tag{3.37}$$

where

$$Z_{FI+G} = SNR = \frac{S_F}{\sqrt{\sigma_g^2 + \langle z^2 \rangle}} \quad ; \qquad R = \frac{\langle z^2 \rangle}{\sigma_g^2},$$

$$F_{2k} = C \sum_{\ell=0}^{2(k-1)} \frac{(2k-1)!\,(-1)^\ell}{\Gamma(2k-\ell)\,\ell!\,(2k-1-\ell)} \left\{\exp\left(-\frac{2k-1-\ell}{C}\right) - 1\right\}^{-1}$$

and

$$\hat{F}_2 = 1 - C + C\exp(-1/C). \tag{3.37a}$$

For $\gamma \to \infty$ the probability of error expression tends towards

$$Pe_{FI+G(\gamma\to\infty)} = \tfrac{1}{2}\left[1 - \left\{1 + \frac{1}{Z_{FI+G}^2}\right\}^{-\frac{1}{2}}\right] \tag{3.38}$$

which is the well-known expression for the coherent P.S.K. system operating in Gaussian noise with Rayleigh fading [86].

IMPULSIVE NOISE ($\gamma<<1$)

For low γ case, expanding the CF expression of (3.30) and neglecting all higher terms in γ except linear, yields

$$\Phi_Z(j\xi) = 1+\gamma\int_{-\infty}^{1}\langle J_o\{\xi AG(\tau)\}-1\rangle_a d\tau+O(\gamma^2). \qquad (3.39)$$

Substituting above equation in (3.29) we obtain, after integrating the first term, as

$$Pe_{FI+G}=Pe_{FI+G(\gamma\to\infty)}+\frac{\gamma S_F}{\sqrt{2\pi}}\int_0^{\infty}d\xi\exp\{-\frac{\xi^2}{2}(\sigma_g^2+S_F^2)\}\cdot$$

$$\cdot\int_{-\infty}^{1}\langle 1-J_o\{\xi AG(\tau)\}\rangle_a d\tau \qquad (3.40)$$

where

$Pe_{FI+G(\gamma\to\infty)}$ is defined by (3.38).

To achieve the desired form, we use a steepest-descent approximation of $J_o\{\xi AG(\tau)\}$, and write $\langle J_o\{\xi AG(\tau)\}\rangle_a$ as [8] :

$$\langle J_o\{\xi AG(\tau)\}\rangle_a = \exp\{-\xi^2G^2(\tau)\langle A^2\rangle_a/4\}\cdot$$

$$\cdot\{1+\sum_{k=2}^{\infty}\frac{(-1)^k}{(k!)^2 2^{2k}}\langle A^2\rangle_a^k(\xi G(\tau))^{2k}C_{2k}\} \qquad (3.41)$$

where

$C_{2k}=(-1)^k k!\ \langle {}_1F_1(-k;1;a^2/\langle a^2\rangle_a)\rangle_a$, $(k=2,3.....)$ and $A=a/T$.

The first few coefficients C_{2k} are

$$C_4=\{\langle a^4\rangle_a-2\langle a^2\rangle_a^2\}/\langle a^2\rangle_a^2$$

$$C_6=\{\langle a^6\rangle_a-9\langle a^4\rangle_a\langle a^2\rangle_a+12\langle a^2\rangle_a^3\}/\langle a^2\rangle_a^3$$

$$C_8=\{\langle a^8\rangle_a-16\langle a^6\rangle_a\langle a^2\rangle_a+72\langle a^4\rangle_a\langle a^2\rangle_a^2-72\langle a^2\rangle_a^4\}/\langle a^2\rangle_a^4$$

$$\vdots$$

etc.

These coefficients, involving the higher moments of the envelope a, are progressively critical in determining the shape of the distributions at the higher amplitudes, e.g. for the 'rare' event waveforms away from the zero magnitudes.

It is now a straightforward matter to determine the desired probability of error expression. We shall present here only the dominant terms in (3.41), viz. we omit terms $O(\xi^4)$:

$$\langle J_o\{\xi AG(\tau)\}\rangle_a \tilde{=} \exp\{-\xi^2G^2(\tau)\langle A^2\rangle_a/4\}. \qquad (3.42)$$

Note: the above equation is still exact provided the amplitude pdf $p_A(a)$ obeys the Rayleigh distribution

$$p_A(a) = \frac{2a}{\langle a^2\rangle} \exp\left(-\frac{a^2}{\langle a^2\rangle}\right).$$

The k^{th} moment then becomes

$$\langle a^k\rangle_a=\langle a^2\rangle_a^{k/2}\,\Gamma\left(\frac{k}{2}+1\right).$$

The coefficients C_k ($k=4,6,\ldots$) in (3.41) become zero.

Substituting (3.42) in (3.29) for Pe_{FI+G} and integrating with respect to ξ and τ yields

$$Pe_{FI+G} = \tfrac{1}{2}\{1 - \frac{1}{\hat{Z}}\} + \frac{\gamma}{2\hat{Z}} \int_{-\infty}^{1} \{1 - \frac{1}{[\Gamma_z G^2(\tau)+1]^{\frac{1}{2}}}\} d\tau \qquad (3.43)$$

where

$$\hat{Z} = \{1 + \frac{1}{(1+R)Z^2_{FI+G}}\}^{\frac{1}{2}}$$

and

$$\Gamma_z = \frac{R}{2\gamma(1-CK\{\{1+(1+R)Z^2_{FI+G}\}}$$.

The second term in (3.43) can now be integrated to obtain

$$\int_{-\infty}^{1} \{1 - \frac{1}{[\Gamma_z G^2(\tau)+1]^{\frac{1}{2}}}\} d\tau = C\Big[\log\{\tfrac{1}{2}+\tfrac{1}{2}(1+\Gamma_z K^2)^{\frac{1}{2}}\} + \frac{1}{C}\{1-(1+\Gamma_z)^{-\frac{1}{2}}\} + (1+\Gamma_z)^{-\frac{1}{2}} \log \frac{1+(1+\Gamma_z)^{\frac{1}{2}}}{1+\Gamma_z K+(1+\Gamma_z)^{\frac{1}{2}}(1+\Gamma_z K^2)^{\frac{1}{2}}}\Big] \qquad (3.44)$$

where Z_{FI+G} and R are defined by (3.37a), and $K=1-\exp(-1/C)$.

In order to compare the results obtained here with the nonfading case, we next obtain the error probability expression for the system shown in Fig. 3.1 when the multiplicative noise is absent. To simplify the analysis we also assume the Gaussian noise to be absent. The analysis can, however, be extended by using the arguments used in sec. (3.3.2) when the Gaussian noise is present.

Starting with (2.8b) and using the arguments of sec. (3.3.1) the error probability expression can be written as

$$Pe_{FI} = \frac{1}{2\pi} \int_{\sqrt{E}}^{\infty} dx \int_{-\infty}^{\infty} d\xi \exp\{-j\xi x + \gamma \int_{t} \langle J_o(\xi a G(t)) - 1 \rangle_a dt\}.$$

Since the expression (2.8b) is even in x, integrating the above equation with respect to x yields

$$Pe_{FI}=\frac{1}{2}-\frac{1}{2\pi}\int_{-\infty}^{\infty}\frac{\sin\xi\sqrt{E}}{\xi}\exp\{\gamma\int_t(<J_o(\xi aG(t))>_a-1)dt\}d\xi. \tag{3.45}$$

For $p_A(a)$ Rayleigh distributed, using (3.42), (3.45) reduces to

$$Pe_{FI}=\frac{1}{2}-\frac{1}{2\pi}\int_{-\infty}^{\infty}\frac{\sin\xi\sqrt{E}}{\xi}\exp\{\gamma\int_t dt[\exp(-\xi^2<a^2>_a G^2(t)/4)-1]\}d\xi. \tag{3.46}$$

For γ sufficiently small, the approximation $\exp(\gamma)=1+\gamma$ can be applied, and the integrals in the exponent of the CF can become an algebric function, letting (3.46) become

$$Pe_{FI}=\frac{1}{2}-\frac{1}{2\pi}\int_{-\infty}^{\infty}\frac{\sin\xi\sqrt{E}}{\xi}d\xi+\frac{\gamma}{2\pi}\int_t dt\int_{-\infty}^{\infty}\frac{\sin\xi\sqrt{E}}{\xi}d\xi-$$

$$-\frac{\gamma}{2\pi}\int_t dt\int_{-\infty}^{\infty}\frac{\sin\xi\sqrt{E}}{\xi}\exp(-\xi^2<a^2>_a G^2(t)/4)d\xi.$$

The final expression for Pe_{FI} after integrating the above equation with respect to ξ reduces to

$$Pe_{FI}=\gamma\int_t erfc\{\left(\frac{2E}{<a^2>_a}\right)^{\frac{1}{2}}\frac{1}{G(t)}\}dt. \tag{3.47}$$

For the high Q RLC filter described by (3.33), using (3.34) and (2.14) in the probability of error expression (3.47) and changing the variable $\xi = 1/t$ reduces to

$$Pe_{FI}=C\gamma\int_{1/K}^{\infty}\frac{erfc\left[\zeta Z_{FI}\{2\gamma(1-CK)\}^{\frac{1}{2}}\right]}{\zeta-1}d\zeta \tag{3.48}$$

where

$$Z_{FI} = SNR = \left[\frac{E}{\langle a^2 \rangle_a \gamma (1-CK)} \right]^{\frac{1}{2}} \qquad (3.49)$$

and

$$K = 1 - \exp(-1/C).$$

DISCUSSIONS

Equation (3.48) for Pe_{FI} is plotted in Fig. 3.6 as a function of SNR Z_{FI} defined by (3.49) with γ, C, R as parameters. Comparing these results with the unfiltered Poisson process of Fig. 3.4 we note that, due to the RF filter, the probability of error for filtered Poisson noise, for all γ, at same SNR, has increased. At unity SNR, the probability of error for the unfiltered Poisson process Pe_I for $\gamma = 0.1$ is 0.027, while for the filtered Poisson process Pe_{FI} is 0.15. At high SNR's, the difference is small. A possible explanation for this is that not only impulses falling within (0,T) are responsible for an error in that bit (as is the case for the unfiltered process) but also impulses that are sufficiently near (0,T) and sufficiently large that the tails of the RF filter impulse response overlaps (0,T) with sufficient strength.

Using (3.44) in (3.43), Pe_{FI+G} is plotted in Fig. 3.7 as a function of SNR Z_{FI+G} defined by (3.37a) with $\gamma = 0.1$, C and R as parameters. From Figs 3.6 and 3.7 we can observe that by increasing C, normalized filter time constant, the error probability becomes smaller. This should be the case since C is inversely proportional to the bandwidth of the receiver (see (3.35)). In practice the maximum value of C is determined by the bandwidth required for the signal to pass through without

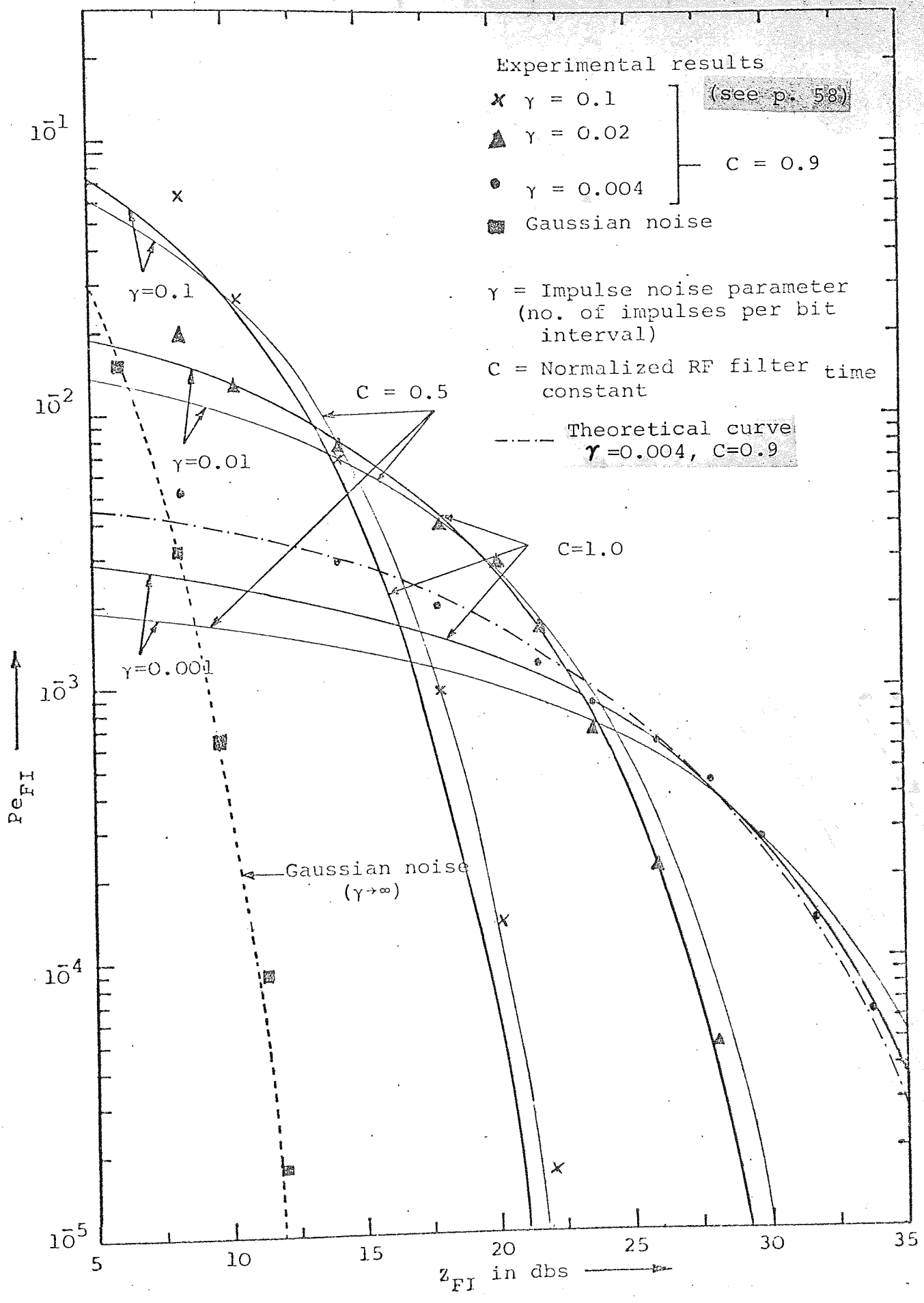

Fig. 3.6 Average probability of error (Pe_{FI}) as a function of SNR (Z_{FI}) for P.S.K. system operating in additive filtered Poisson IN($\gamma<<1$) with Rayleigh distributed amplitudes.

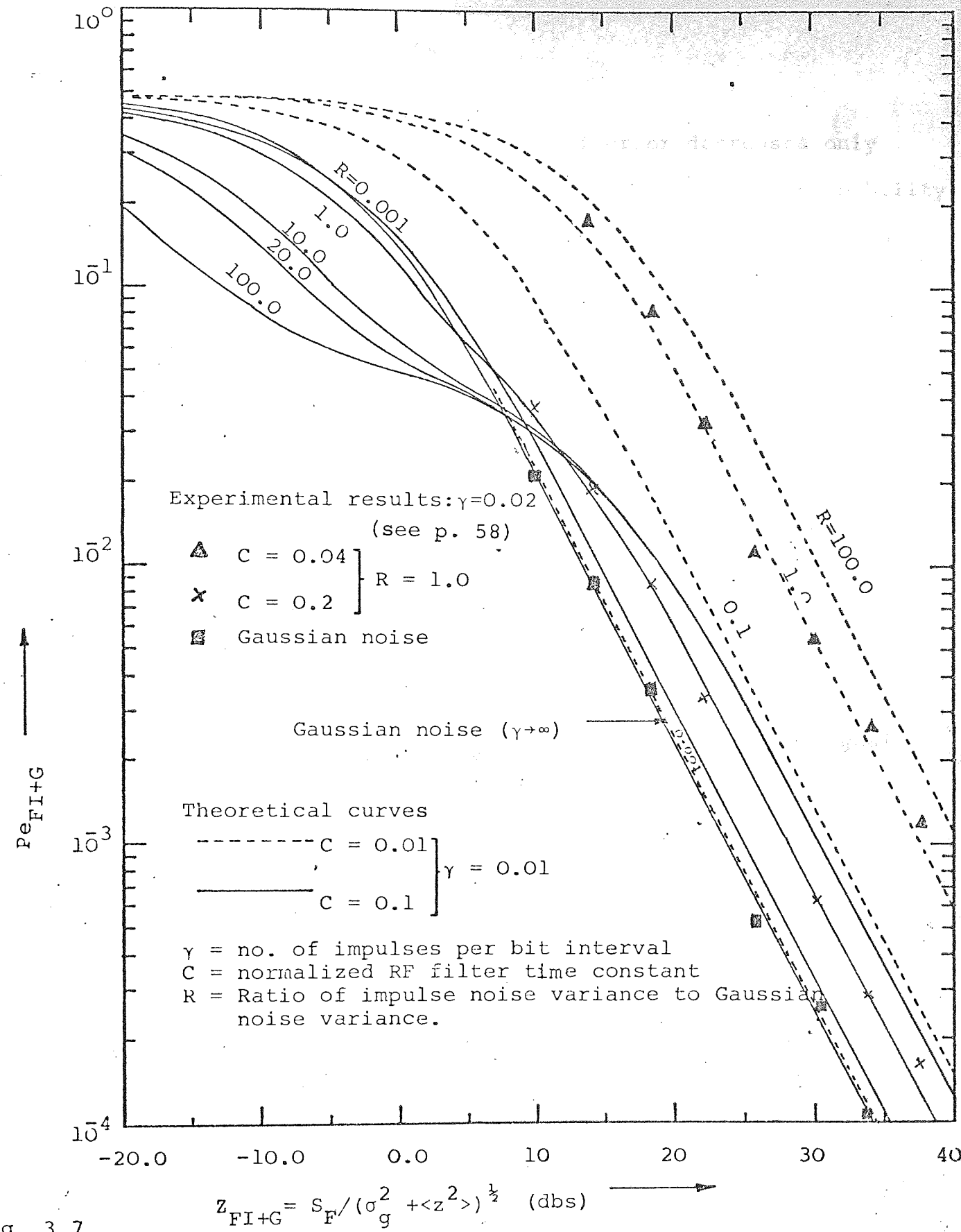

Fig. 3.7
Error rate for P.S.K. system in additive filtered Poisson IN ($\gamma \ll 1$) with Rayleigh distributed amplitude plus Gaussian noise and multiplicative noise (Rayleigh distributed)

any distortion.

For fading cases, the probability of error decreases only linearly for large SNR's while for non-fading cases the probability of error decreases exponentially. This is logical. Regardless of how large the average received signal becomes, during a deep fade the probability of error is equal or nearly equal to 0.5. Even though this does not occur often, its occurrence keeps the Pe_{FI+G} from improving exponentially.

Finally the reader is reminded that all the results presented above (for fading cases) are premised upon the assumption of slow, non-selective and purely Rayleigh fading. This model is useful in that it covers (to first-order) a practically meaningful regime for HF communications. The theoretical and experimental investigations [57],[87] reveal that by using time or space diversity (e.g., sending the signal over several independent Rayleigh channels in parallel), or feedback communication schemes [88] and the linear filter detector, we can achieve a probability of error which exponentially decreases with increasing SNR Z_{FI+G}.

3.5 EXPERIMENTAL MEASUREMENTS OF PROBABILITY OF ERROR Pe_{FI} AND Pe_{FI+G}

The motivation for carrying out experimental measurements of Pe_{FI} and Pe_{FI+G} on a simulated system as discussed in this section was to check the validity of the approximations made in the theoretical analysis.

Fig.3.7 shows a block diagram of the experimental setup, the receiver being simulated by multipliers and gated integrators. The output of the integrators was sampled at the end of the signalling intervals and the samples fed into a threshold device

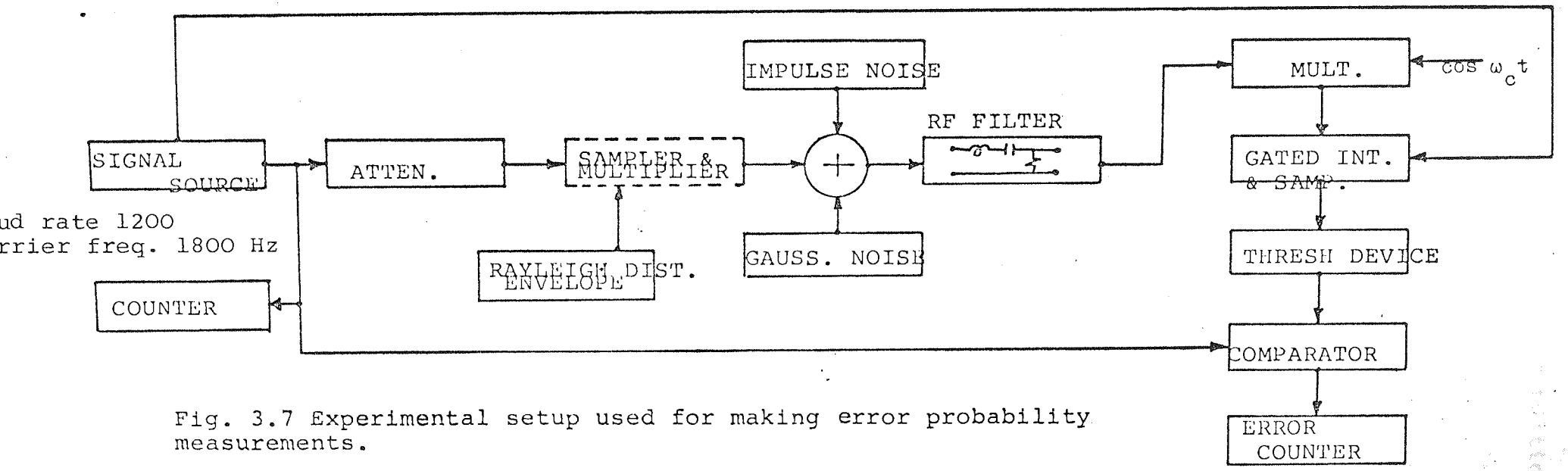

Fig. 3.7 Experimental setup used for making error probability measurements.

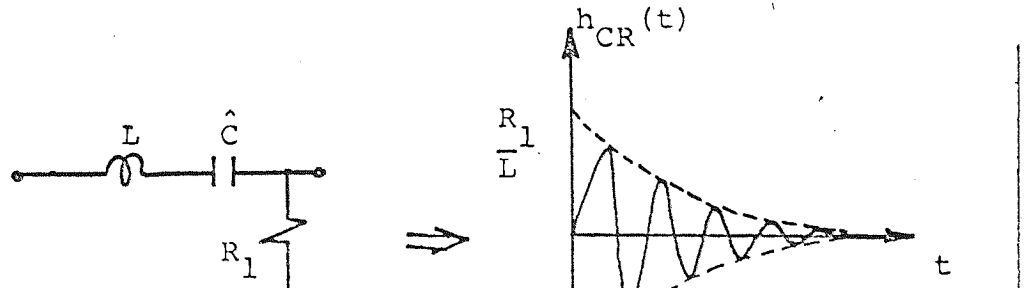

Fig 3.8 Bandpass RLC network showing the unit impulse response.

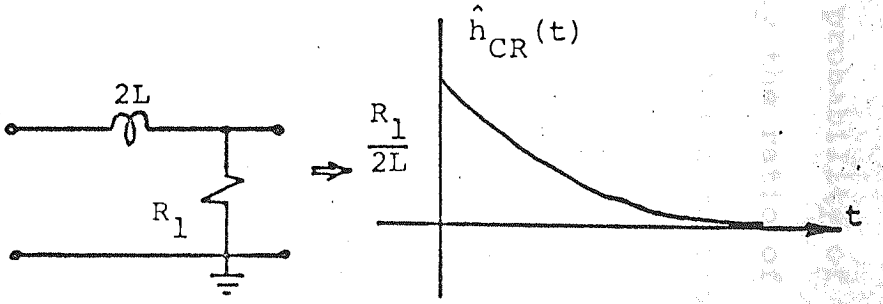

Fig. 3.9 Equivalent low-pass system showing the unit impulse response.

followed by a counter. The conditional probability of wrong reception was then given approximately by the ratio of the number of counts on this counter to the total number of transmitted signals. The accuracy of this approximation was improved by increasing the measurement time so that many errors occured.

RCL (high Q) FILTER [81]

The bandpass RLC network is shown in Fig. 3.8. The open-circuit voltage transfer function for this circuit can be shown to be

$$H_{CR}(j\omega) = \frac{j\omega R_{1/L}}{(j\omega)^2+j\omega R_{1/L}+1/L\hat{C}} \qquad (3.50)$$

By factoring the denominator of (3.50), $H_{CR}(j\omega)$ can be expressed in the form of a partial-fraction expansion

$$H_{CR}(j\omega) = \frac{A_1}{j\omega+R_{1/2L}-j\Delta_L} + \frac{A_1^*}{j\omega+R_{1/2L}+j\Delta_L} \qquad (3.51)$$

where

$$\Delta_L = \left[1/L\hat{C} - (R_{1/2L})^2\right]^{\frac{1}{2}} \quad , \quad A_1 = \frac{(-R_{1/2L}+j\Delta_L)R_1}{j2L\Delta_L}$$

and A^* denotes the complex conjugate. The band-centre frequency ω_c of this bandpass filter is given exactly by $\omega_c=\Delta_L$. For the narrow-band condition $1/\sqrt{L\hat{C}} >> R_{1/2L}$ (i.e., for a high 'Q' circuit) ω_c is closely given by $\omega_c=1/\sqrt{L\hat{C}}$. Applying the narrow-band condition, the constant A_1 reduces to $A_1 = R_{1/2L}$. Using the definition for the positive frequency lobe of $H_{CR}(j\omega)$, we have

$$H_{CR}(j\omega-j\omega_c) = \frac{R_{1/2L}}{R_{1/2L} + j(\omega-\omega_c)}$$

and the transfer function of the equivalent lowpass system is given by

$$\hat{H}_{CR}(j\omega) = \frac{R_1}{R_1 + j\omega 2L} \quad .$$

The equivalent lowpass system function $\hat{H}_{CR}(j\omega)$ can be recognized easily in this case as an R_1L network composed of a resistor R_1 and an inductance 2L, as shown in Fig. 3.9. The unit impulse response $\hat{h}_{RC}(t)$ of the equivalent lowpass system is therefore

$$\hat{h}_{RC}(t) = \frac{R_1}{2L} \exp\ (-R_1 t/2L) \ , \quad t > 0. \qquad (3.52)$$

POISSON SOURCE WITH AMPLITUDES GAUSSIANLY DISTRIBUTED

This type of Poisson IN was derived from Gaussian generators. The block diagram is shown in Fig. 3.10. Each time the noise crosses a preset level in the positive direction, an impulse was obtained. It was found that as the level was increased, away from the mean of the noise,

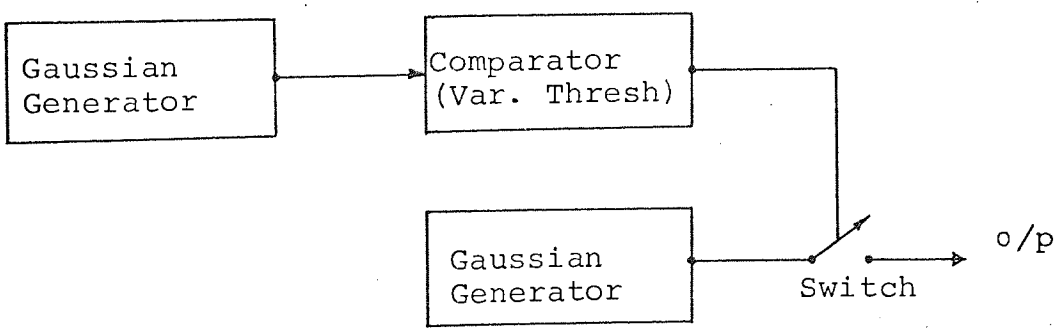

Fig.3.10. Poisson IN generator with amplitude Gaussianly distributed.

the impulses became less correlated, eventually approaching a Poisson process. To obtain the low impulse rates desired,

the 10 KHz Gaussian noise generator was filtered by a simple lowpass filter. The impulses obtained were then used to sample the output of another Gaussian noise generator. The sample durations were very short in comparison to the signal durations and were therefore good approximations to ideal delta functions. It should be stressed here that no theory was developed concerning this source.

DISCUSSIONS

Figures 3.6 and 3.7 show measured probability of error as a function of the SNR for steady and fading channels respectively. On both the figures the performance of the system in Gaussian noise is also given. The purpose of this test was to check the performance of the system before obtaining the results in IN. The experimental data shown in Fig. 3.6 correspond to values of γ ranging from 4×10^{-3} to 10^{-1} while in Fig. 3.7 only $\gamma = 2 \times 10^{-2}$ is used. For steady channel (no multiplicative noise), the simulated results for large SNR's and small γ's agrees with the theoretical results. The main reason why the simulated results for large $\gamma (\simeq 0.1)$ do not agree with the theoretical one is because the noise pulses (at this rate) do not obey the Poisson distribution. For small SNRs the measured values of Pe_{FI} are much larger than the theory predicts, a possible explanation for this being that the generated noise for these conditions was actually modelled by an additive combination of Gaussian and IN because of the thermal noise added by amplification. For the fading channel, a close agreement between the simulated and the theoretical results is obtained (this is because only high SNRs and small values of γ are considered).

CHAPTER 4

PERFORMANCE OF HYBRID MODULATION SYSTEM [128], [129]

Signal sets employing a combination of amplitude and phase keying (A.P.K.) are useful for large alphabet systems because they are economical in the use of bandwidth and do not require as high a SNR as the equivalent P.S.K. system to give the same probability of error. In this chapter a method of selection of the signal coordinates is described which minimises the probability of error in an unfiltered Poisson IN channel for a given average signal power constraint. Selected sets are compared on the basis of a symbol-error probability for average SNR.

4.1 INTRODUCTION

In the search for improved modulation formats for high-speed data transmission, attention has recently been turned to the family of suppressed carrier two-dimensional signal sets, of which quadrature amplitude modulation is an example. If the channel is Gaussian, it has been shown [89]-[97] that a hybrid modulation A.P.K. requires less power than P.S.K. for the same error probability and alphabet size.

In the early work, the authors were primarily concerned with specific regular types of A.P.K. signal structure, i.e., the signals were constrained to lie on a grid [89] or a triangular configuration [90] or concentric circles with [91] or without [92], [93] constraining the signals on each circle to lie on a ray from the origin. The more general question of what is optimum (in the sense of minimum error probability for a given

average SNR) relation between phase and amplitude among the members of signal set is still open to answer. The difficulty in finding an optimum constellation is partly that of integrating conditional pdfs over the complements of mathematically inconvenient decision regions, and partly that of minimizing the sum of these integrals.

To assist in signal-set design and performance evaluation in Poisson IN channel, an asymptotic expression is obtained for the probability of symbol error at high SNRs for signal sets with unequal energies and any dimensionality. While this expression for error probability has not yet led to a solution of the theoretically optimum design for A.P.K. signal sets, it does permit an accurate comparison of candidate designs. In this study only an unfiltered Poisson IN process is considered. The analysis can, however, be extended to the filtered Poisson noise case using the results of Chapter 3.

In the following sections the candidate signal designs are described. Curves of symbol error probability versus average SNR with γ as a parameter are shown for the 8-ary designs. The technique can, however, be extended to any signal-set size or dimension. Finally, we answer the question: How close can these theoretical results be realised in the laboratory with actual hardware? The two-dimensional nature of A.P.K. leads to modem implementations that are significantly different from P.S.K. or A.S.K. In selecting a signal-set, there are many other factors that are important other than just minimizing error probability. The cost and ease of implementation, the efficiency of symbol to bit encoding and the dynamic range of amplitudes required of the transmitter are but a few of these factors. We present

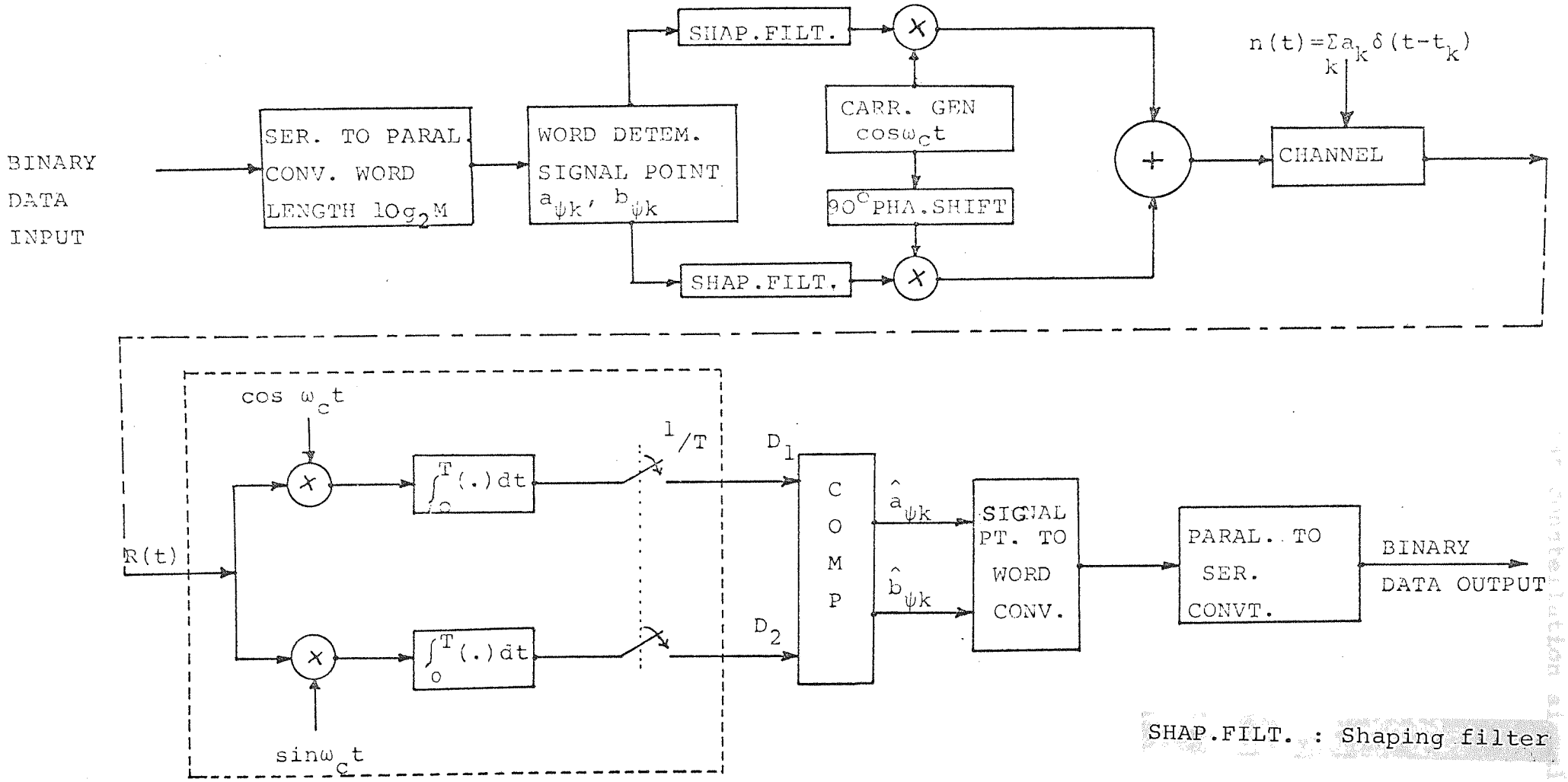

Fig.4.1 Simplified in-phase and quadrature data transmission system.

experimental results for a circular constellation signal set as an example.

4.2 SYSTEM MODEL

An A.P.K. signal set of alphabet size M can be viewed mathematically as M two-dimensional signal vectors. Binary data are mapped into one of M two-tuples ($a_{\psi k}$, $b_{\psi k}$). The numbers of each pair amplitude modulate in-phase and quadrature carriers respectively to generate the transmitted signal

$$S_k(t) = a_{\psi k}\Psi_c(t) + b_{\psi k}\Psi_s(t), \quad k=1,2,.....M \qquad (4.1)$$
$$0<t<T$$

where

$$\Psi_c(t) = (\frac{2}{T})^{\frac{1}{2}}\cos \omega_c t, \quad \Psi_s(t) = (\frac{2}{T})^{\frac{1}{2}}\sin\omega_c t \qquad (4.2)$$

over the symbol period T. It will be assumed that the two tuples are equiprobable. The simplified two-dimensional M-ary synchronous data communication system is shown in Fig.4.1.

The received signal plus Poisson IN over the symbol period, assuming no channel distortion is given by

$$R(t) = a_{\psi k}\Psi_c(t) + b_{\psi k}\Psi_s(t) + n(t) \qquad (4.3)$$

where n(t) is Poisson IN defined by (2.1). The noise can be defined as

$$n(t) = n_1(t)\Psi_c(t) + n_2(t)\Psi_s(t), \qquad 0<t<T. \qquad (4.4)$$

Using the results of Ziemer [58] it can be shown (Appendix B) that the joint pdf at time T of the normalized unfiltered Poisson IN components at the output of the matched filters

$$\hat{X}_i = X_i/\lambda_2, \qquad i = 1,2 \tag{4.5}$$

where λ_2 (defined by (2.9) $= \gamma\langle a^2\rangle\delta_{12}/T$ for matched filters defined by (3.10)) is the variance of X_i is given by (b.1) i.e.,

$$p_{\hat{X}_1,\hat{X}_2}(x_1,x_2) = (1-\gamma)\delta(x_1)\delta(x_2) + \frac{\gamma}{\pi}\left[\frac{T\lambda_2}{2(x_1^2 + x_2^2)}\right]^{\frac{1}{2}} \cdot$$

$$\cdot\, p_A\{[\frac{T\lambda_2}{2}(x_1^2 + x_2^2)]^{\frac{1}{2}}\} \tag{4.6}$$

where $\delta_i(x)$ are Kronecker deltas and $p_A(a)$ is the pdf of the impulse amplitudes. It can be observed from the above equation that for $\gamma<<1$ the joint pdf of two-dimensional unfiltered Poisson IN is approximately radial. At high SNR, the 'sphere-packing' arguments from Gaussian noise therefore will hold (approximately for $\gamma<<1$) for IN also. For example, contours of constant error are circles, and system performance can be upper bounded simply by how well the system 'packs' circular decision regions around the origin [94],[95].

In what follows we suppress the time index k, and the problem can then be reduced to the simple two-dimensional model. Since it is of interest to calculate the performance of the system only in the presence of an impulse noise burst, the joint density may be taken to be given by the second term on the right hand side of (4.6). The sampled receiver output at time T is the point $D = (D_1, D_2)$, where $D_1 = a_{\psi k} + X_1$ and $D_2 = b_{\psi k} + X_2$, and the random variables X_1 and X_2 are uncorrelated, zero means and equal variances λ_2. The average SNR is defined as

$$SNR_{av} = \frac{1}{2M\lambda_2}\sum_{k=1}^{M}(a_{\psi k}^2 + b_{\psi k}^2). \tag{4.7}$$

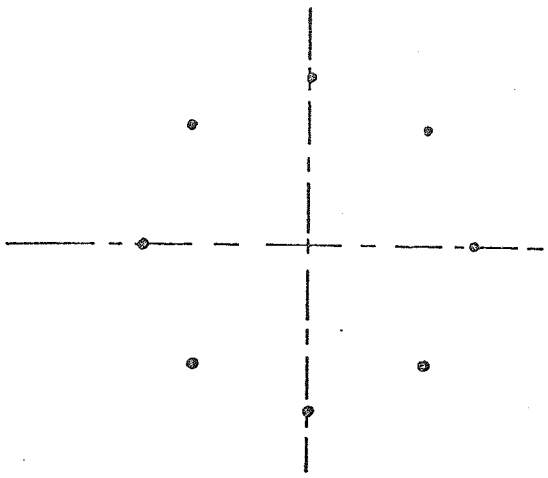

Conventional 8-phase system
$r_1=2.0$

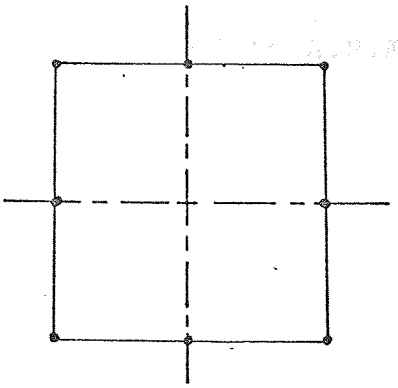

a) Square $r_1=1.155$, $r_2=1.633$

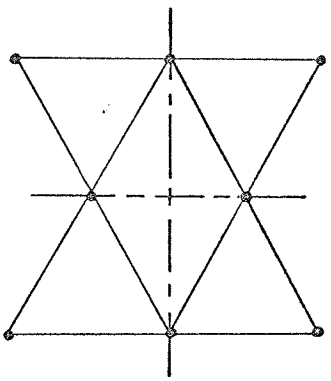

b) Triangular $r_1=0.333$, $r_2=0.577$
$r_3=0.882$

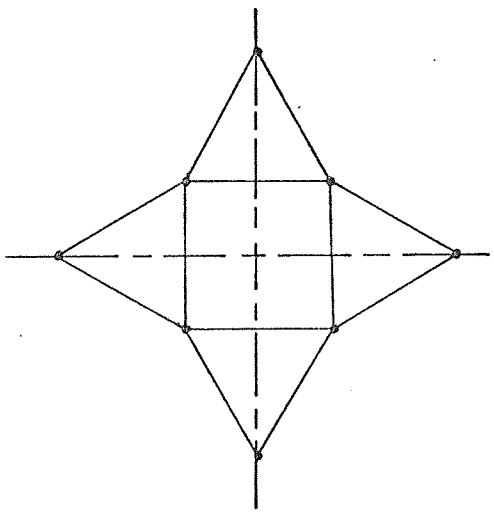

c) Circular (4,4) $r_1=0.896$,
$r_2=1.73$

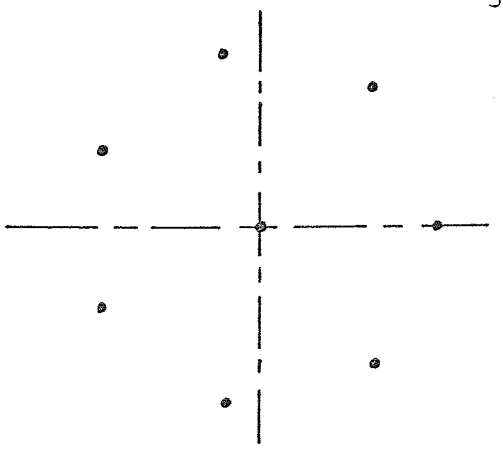

d) Circular (1,7) $r_1=1.512$

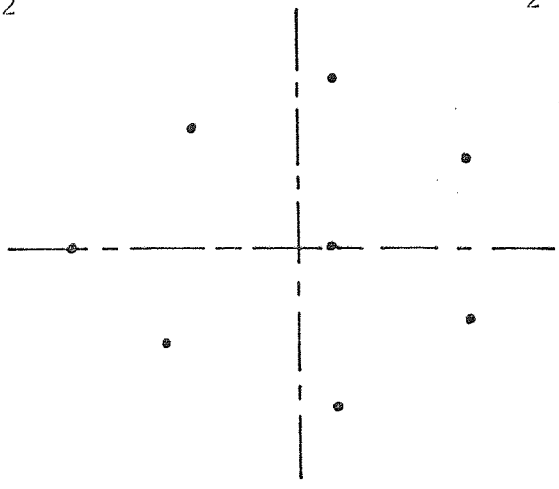

e) Minimum error signal constellation (Gaussian noise)

Fig. 4.2 Well known 8-point signal constellations
(r_ℓ - radius of ℓ^{th} circle)

4.3 A.P.K. SIGNAL SETS

Theoretical work in signal design related to A.P.K. was performed by a number of authors [89]-[97], as they extended the work of Weber [91] and Balakrishnan [96]. The authors were primarily concerned with the performance of A.P.K. modulation systems in Gaussian channels. The question of what is the optimum relation between phase and amplitude among the members of the signal set is still open to answer.

The approach employed in this investigation has been to use the above results as guidelines in an empirical search for good designs in IN channels. The optimum performance should not be greatly superior to that of the best candidate considered, if a large class of designs is tested. Most signal sets fall into four basic categories: those with signals arranged on concentric circles, and those with triangular, rectangular or hexagonal grid patterns. We consider here 8-ary signal sets only. The analysis can, however, be extended to all alphabet sizes that are powers of two. The 8-ary signal sets considered are shown in Fig. 4.2. The sets are scaled such that the average signal power is unity.

The first design is a quadrature A.S.K. where the signal array is a rectangular grid. This is an obvious candidate for selection because it combines good sphere-packing with ease of implementation. The second is a triangular set which has a structure based on concentric triangles around the origin. The third is a double circle with four signals per circle (4,4) which Lucky and Hancock [92] calculate to be the optimum 8-ary design in Gaussian noise under an average power constraint. The ratio of outer to inner circle is 1.935. In order to avoid complexity and implement the data transmission system in simpler form, the

power in the outer signals can be expanded slightly [90] giving the ratio of outer to the inner circle of 2.0. The fourth design is a circle set (1,7) consisting of a seven-signal circle surrounding a signal at the origin. The signal at the origin implies that for certain bit sequences, the transmitter must be turned off. Attempting to turn a transmitter on and off at the data rate could pose problems in certain applications. Additionally, receiver automatic-gain-control design will be complicated by this factor. The remaining candidate is a modification of (1,7). The co-ordinates of the signal points are

x	0.88	-0.48	1.44	-0.28	-1.36	0.037	-0.85	0.61
y	1.34	1.53	0.092	-1.98	0.49	0.26	-0.76	-0.97

The extra point in this case is placed outside the circle of 6 points, and the centre of mass of the whole constellation is placed at the origin. Using the gradient-search algoritm this signal array is shown [97ii] to minimize the probability of error in Gaussian noise under the average power constraint and phase jitter.

4.4 ERROR PROBABILITY PERFORMANCE

In order to assess the applicability of A.P.K. signal sets inthe design of practical communication systems, it is essential to compute their average symbol error probability performance. After this has been done, one can then weigh the savings in error probability performance over the conventional 8-phase signal set (or other A.P.K. signal sets) against other cost

effective considerations and thereby arrive at a final signal design.

Consider the arbitrary signal constellation shown in Fig. 4.3, where the decision regions are denoted by d_k. The detector, which is specified by the decision regions, will declare that signal S_k has been transmitted if and only if the demodulated vector D falls inside d_k. Because of various practical considerations, principally ease of implementation, the mathematically optimum detector will not always be the one which is built.

The probability of error is given by

$$Pe_{APK} = \sum_{k=1}^{M} p_k Pe_k \qquad (4.8)$$

where the p_k s are the (taken to be equal) a priori probabilities and Pe_k is the conditional error rate. The conditional error rate is just the probability that D falls outside d_k when S_k is transmitted, i.e.,

$$Pe_k = Pr(D \notin d_k / S_k). \qquad (4.9)$$

Since the decision regions are polygon in shape then, in mathematical terms, we are required to evaluate a double integral of a two-dimensional pdf (4.6) where the region of integration is the area outside a given polygon. This problem is, in general, mathematically intractable: hence, closed form expressions for the average probability performance of A.P.K. signal sets are not likely. We desire, however, to compute the exact error probability performance, since different upper bounds (e.g., the union bound [94] or the Gilbert bound [98],[99]) on average symbol error probability performance, when applied to a variety of other

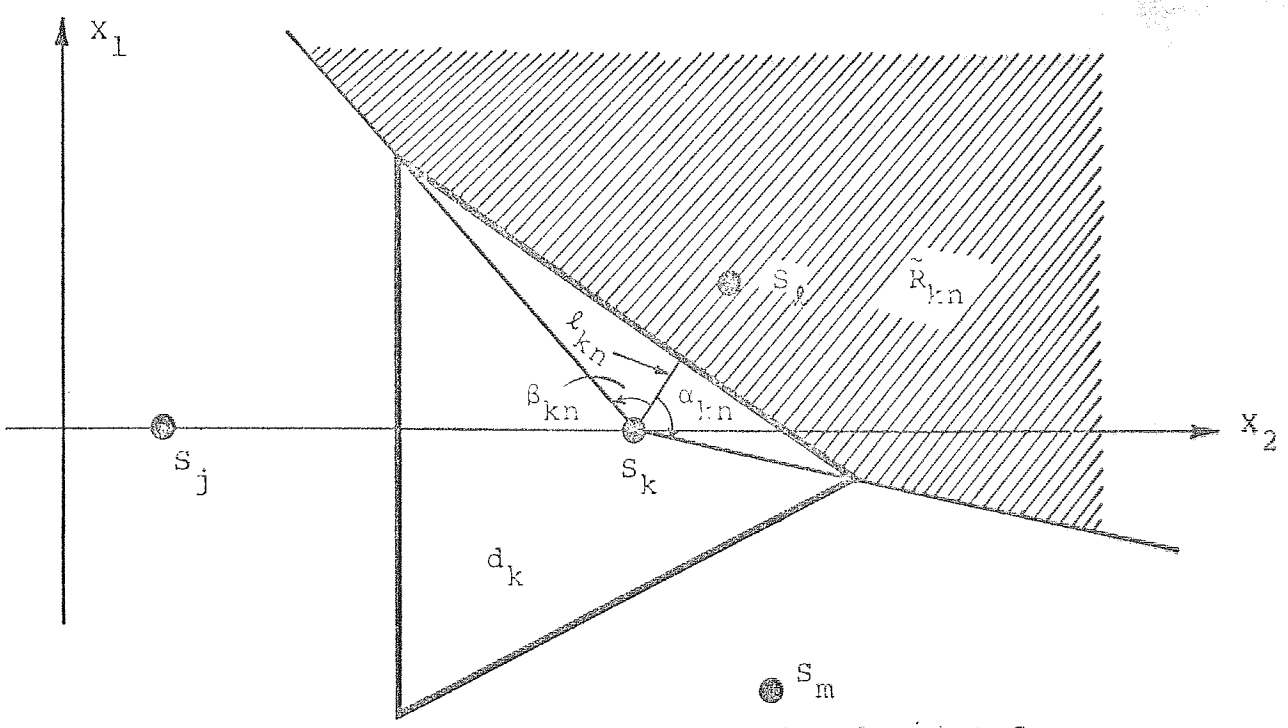

Fig.4.3 Typical decision region about signal point S_k

Noise parameter γ	APK Signal Set	Symbol SNR db	Penalty with respect to best set, db
0.1	Minimum error constellations	27.25	0.0
	Circular (1,7)	27.5	0.25
	Triangular	28.25	1.0
	Circular(4,4) $(r_2/r_1=2)$	28.4	1.15
	Square	29.8	2.55
0.01	Minimum error constellations	36.4	0.0
	Circular (1,7)	36.6	0.2
	Triangular	36.9	0.5
	Circular(4,4) $(r_2/r_1=2)$	37.3	0.9
	Square	38.4	2.0

Fig.4.5 Comparison of A.P.K. sets with minimum error constellations (Gaussian noise) for average SNR at 10^{-6} symbol error probability and Poisson IN parameter γ.

signal sets, yields different results with regard to the relative ranking of these sets.

The conditional error probability may be calculated numerically as follows. The signal space (see Fig. 4.3) can be subdivided into nonoverlapping regions R_{kn}, n=1,.....N_k where N_k is the number of sides in the polygon R_k and $\tilde{R}_{kn}$ denotes the region outside the n^{th} side. Thus the conditional error rate can be written as

$$Pe_k = \sum_{n=1}^{N_k} Pe_{kn} \tag{4.10}$$

where

$$Pe_{kn} = \iint_{\tilde{R}_{kn}} p_{\hat{X}_1,\hat{X}_2}(x_1,x_2)dx_1dx_2 \tag{4.11}$$

and $p_{\hat{X}_1,\hat{X}_2}(x_1,x_2)$ is defined by (4.6). Transforming the joint pdf (4.6) into polar coordinates and using Fig. 4.3 the above equation becomes

$$Pe_{kn} = \frac{\gamma}{\pi}\left(\frac{\lambda_2 T}{2}\right)^{\frac{1}{2}}\left[2\int_0^{\alpha_{kn}}\int_{\frac{\ell_{kn}}{\sqrt{\lambda_2}\cos\phi}}^{\infty} p_A\{r\left(\frac{\lambda_2 T}{2}\right)^{\frac{1}{2}}\}dr\,d\phi + \right.$$

$$\left. + \int_{\alpha_{kn}}^{\beta_{kn}}\int_{\frac{\ell_{kn}}{\sqrt{\lambda_2}\cos\phi}}^{\infty} p_A\{r\left(\frac{\lambda_2 T}{2}\right)^{\frac{1}{2}}\}dr d\phi\right]. \tag{4.12}$$

Using (4.12) in (4.10), the final error probability can be obtained from (4.8) by using (4.10).

In what follows we assume that the pdf of IN amplitude $p_A(a)$ is normally distributed with zero mean and variance

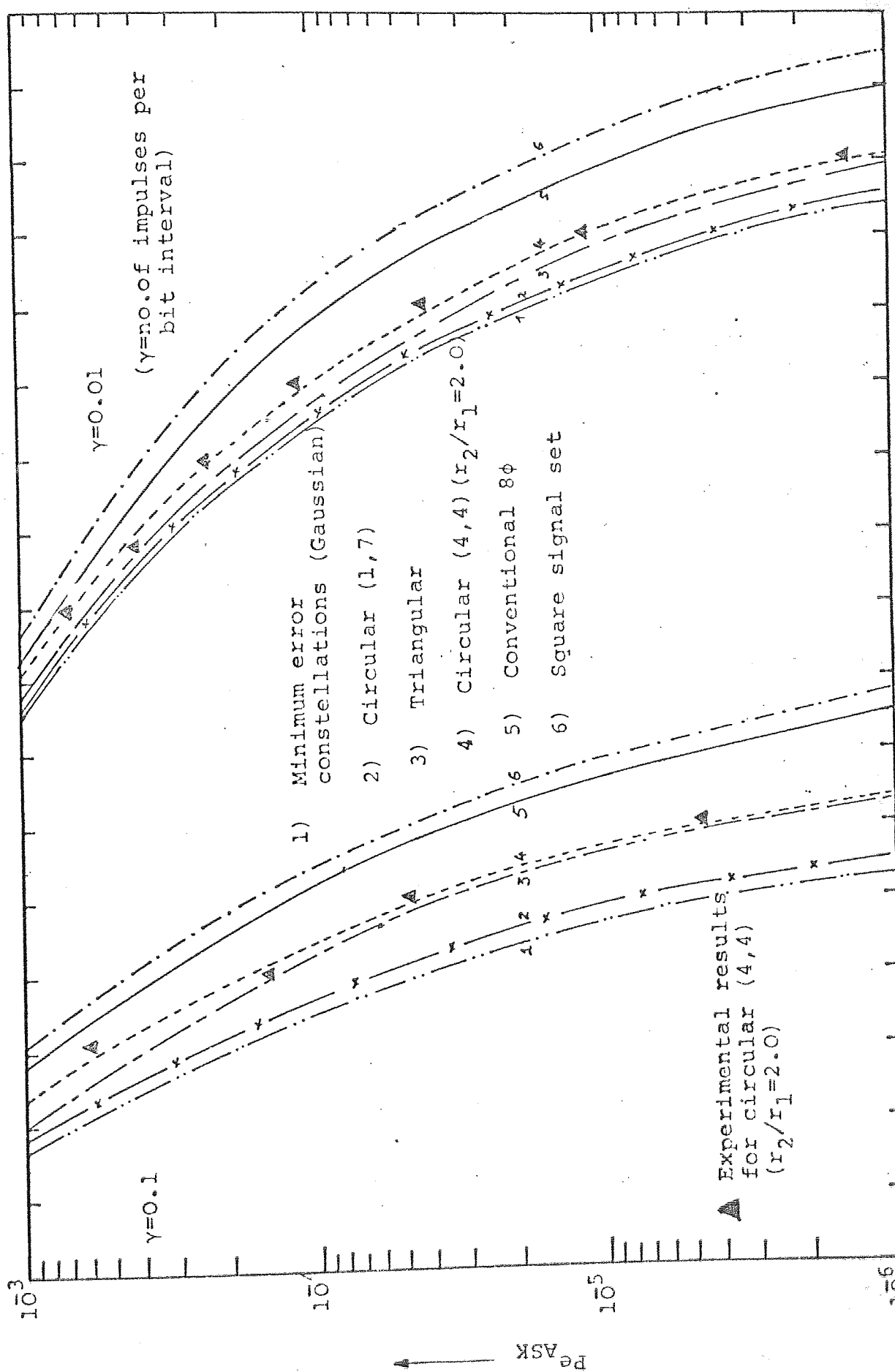

Fig.4.4 Relative performance of 8-point constellations in additive unfiltered Poisson IN ($\gamma<1$) under average power constraints for various values of noise parameter γ.

σ_a^2 i.e.,

$$p_A(a) = \frac{1}{(2\pi\sigma_a^2)^{\frac{1}{2}}} \exp\left(-\frac{a^2}{2\sigma_a^2}\right) . \qquad (4.13)$$

In principle, any choice for $p_A(a)$ may be made (i.e. see Fig. 3.3) which is consistent with experimental measurements of the statistical properties of IN occurring in nature.

4.4.1 SIGNAL SET COMPARISON WITH M=8

For M=8, the performance of each signal set in Fig. 4.2 has been evaluated by means of (4.8). The results are shown in Fig. 4.4 as a function of average SNR defined by (4.7) and γ as a parameter. The minimum error signal constellation (for Gaussian noise plus phase jitter [97]) is the best of the five A.P.K. designs for average SNR in Poisson IN. It offers an advantage of 2.2 dbs and 1.6 dbs over P.S.K. at $Pe_{APK}=10^{-6}$ for γ=0.1 and 0.01 respectively. The relative performance of candidate designs from the curves is summarized in Fig.4.5 which gives the average symbol SNR required to achieve a symbol error probability of 10^{-6}.

Finally, it remains to verify the theoretical analysis with experimental results. For convenience a basic signalling rate of 800 bauds was used, operating over an ideal linear channel in the frequency range of 600-3000 Hz. Due to the ease of implementation the circular $(4,4;r_2/r_1 = 2.0)$ signal set shown in Fig. 4.2c was implemented. Details of the circuitry are given in reference [100] . The configuration shown in Fig. 4.1 was used to evaluate the error performance of the signal format in the presence of additive IN.

(a)

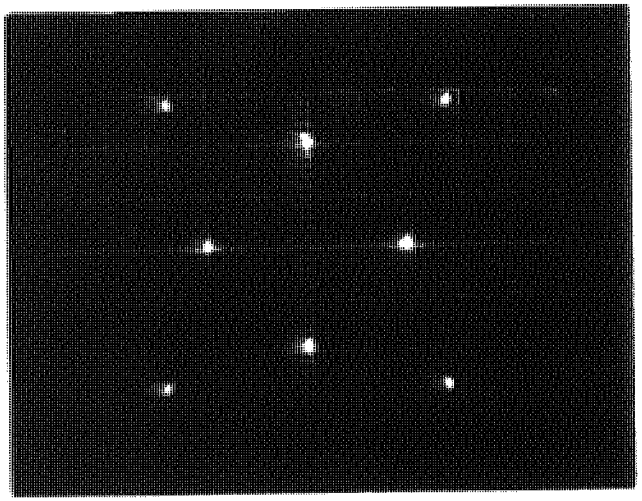

(c)

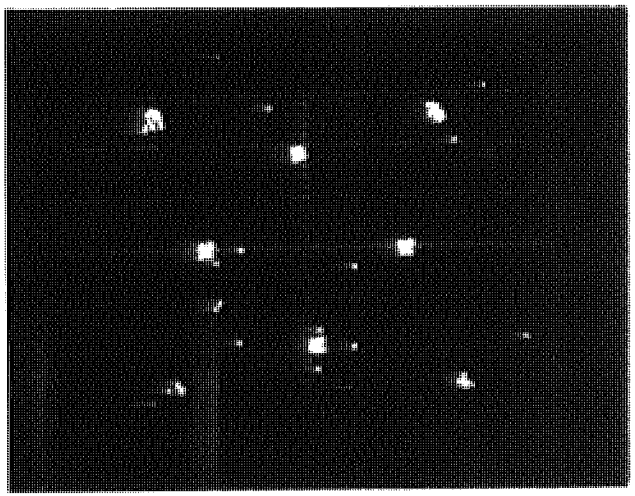

(b)

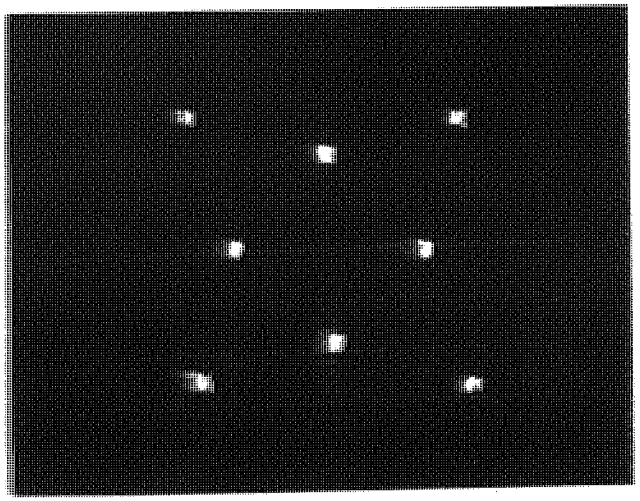

(a) Transmitted signal set (see Fig. 4.2c).

(b) Received signal set without IN (Gaussian noise is introduced due to amplification).

(c) Received signal set with unfiltered Poisson IN.

Fig. 4.6 Circular (4,4) r_2/r_1=2.0, Polar plots.

Fig. 4.6 shows the polar plots, generated by attaching the $\hat{a}_{\psi k}$ and $\hat{b}_{\psi k}$ (see Fig. 4.1) to the horizontal and vertical inputs of an oscilloscope. Z-axis intensification at the sampling instant produced the point in signal space. Fig. 4.6 b is obtained when the IN is absent. The displacement of the signal points is due to the thermal noise added by amplification. Fig.4.6c shows the spread of signal points when Poisson IN is present.

Since timing jitter and phase offset are not included in the theory, timing phase and coherent carrier phase were adjusted manually at the receiver.

The experimental results are shown in Fig. 4.4. Correspondence between predicted and measured performance is seen to be quite good.

4.5 CONCLUSION

A.P.K. with M-ary alphabets is an attractive method of reducing the bandwidth required for transmission of digital information. The bandwidth is exchanged for power but A.P.K. achieves a much more efficient exchange than M-ary P.S.K.. Performance of A,P.K. signal sets in an IN channel is analysed. The A.P.K. sets studied in this investigation were empirically generated but included the regular grid, triangular, and hexagonal lattice designs, as well as various circular configurations.

An important conclusion about A.P.K. signal selection and performance which can be drawn for the comparison of signal sets summarized in Fig. 4.5 is, on an average SNR basis, the circular sets are best for M=8.

The technique employed to obtain the performance of 8-point signal constellations is amenable for use in higher order signal design problems.

PART B

CHAPTER 5

SEMIEMPIRICAL IMPULSE NOISE MODEL [130]

This chapter formulates and justifies a class of non-Gaussian random processes that can serve as a noise model for impulsive phenomena observed in radio communication channels below 100 MHz. The model is applied, in the rest of the thesis, to the detection of known signals in the presence of additive noise.

5.1 INTRODUCTION

The empirical models differ fundamentally in their concept from the filtered-impulse models in that they result from an attempt to construct a mathematical expression that fits the observed data without regard for the physics of the noise source. In every case, these empirical models consist of mathematical expressions constructed in an attempt to fit the measured data of the first-order statistics of the envelope of the received noise.

In view of the great influx of large amplitude pulses, Omura and others [63],[64] formulated log-normal models of noise. One of the models includes Rayleigh distributed atmospheric radio noise at low levels and log-normal distribution at high levels. Beckmann [9] has given a physical argument which supports this empirical noise model, particularly in the situation where there is little thunder-storm activity. It is noted that several workers have proposed models similar to that considered by Beckmann, although they differ in regard to how the two distributions should be combined to give the best resultant

model. Recently, Hall [4] postulated a descriptive mathematical model for atmospheric noise as a narrow-band Gaussian process which is modulated by a slowly varying stochastic process. This postulation leads to the so called 't' noise model for which the pdf of the atmospheric noise is a modified Student's 't' distribution. This model explains some of the observed properties of the noise. A model of similar form has also been found by Giordano and Haber [7] from different considerations. A recent summary of the various empirical models that have been proposed is presented by Ibuken [10].

In view of the shortcomings of the models menticned above, a new model has been derived taking into consideration the known properties of the burst form of atmospheric radio noise. This model is then compared with the atmospheric data for verification.

5.2 IMPULSE NOISE MCDEL

In order to incorporate the impulse nature of the noise with large dynamic range in the model it is proposed to predict the clustering of atmospheric pulses by

$$X(t) = A(t)\ G'(t) \tag{5.1}$$

where A(t) is a comparatively broad-band random process, slowly varying vis-à-vis G'(t), and which effectively sets the unit, or scale of G'(t).

The statistical properties of A(t) are to be determined empirically. This is done to begin with by choosing $p_A(a)$, the first-order pdf of X(t) for large amplitudes, as is observed empirically. G'(t) is a zero mean generalised Gaussian process

$$p_{G'}(x) = \frac{\alpha}{2\sqrt{2}\,\Gamma(\frac{1}{\alpha})\,\sigma'} \exp\{-(\frac{x}{\sqrt{2}\sigma'})^{\alpha}\}$$

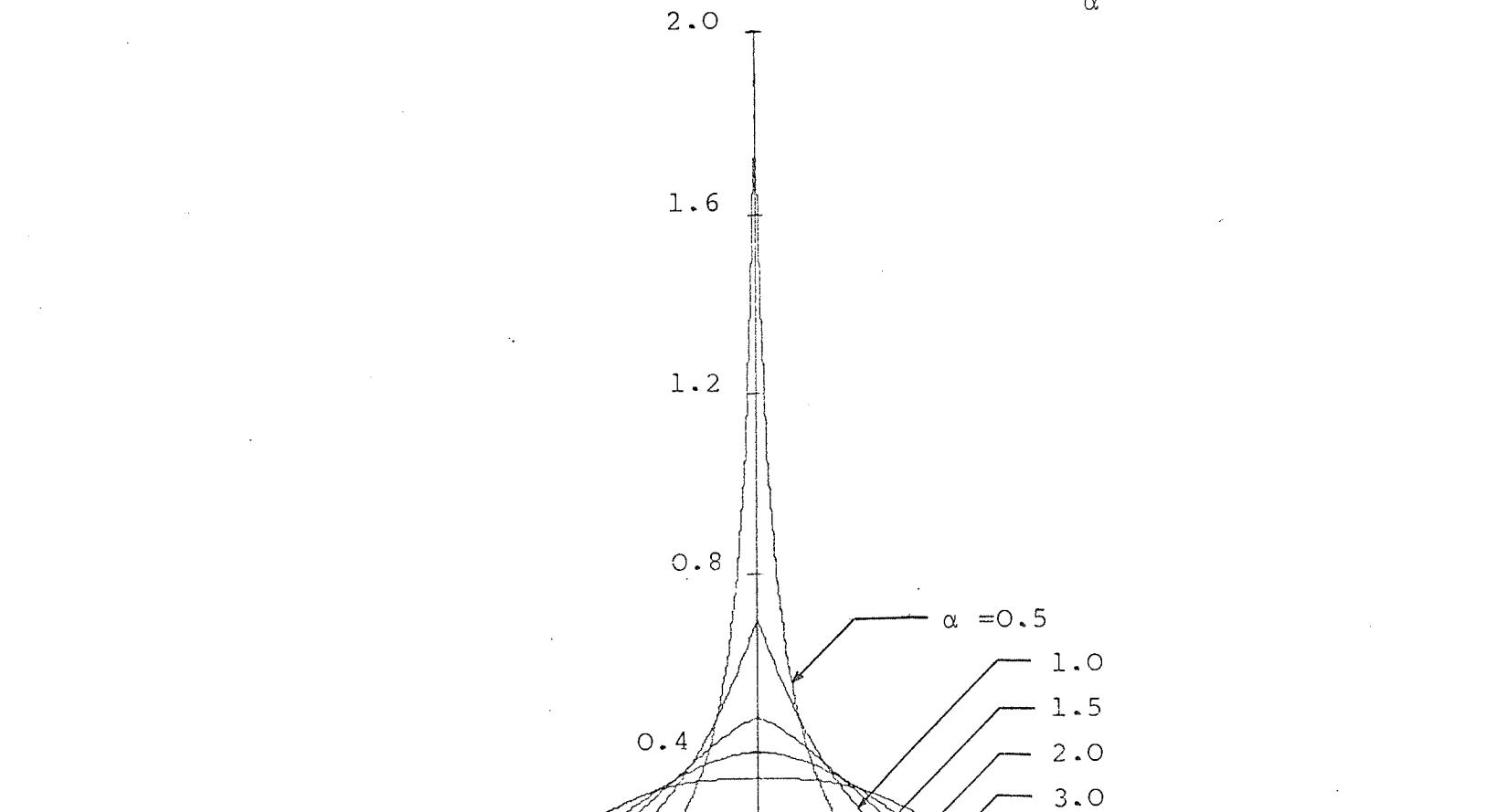

Fig. 5.1 Generalised Gaussian probability density function $\left(\sigma' = \left[\frac{\Gamma(\frac{1}{\alpha})}{2\,\Gamma(\frac{3}{\alpha})} \right]^{\frac{1}{2}} \right)$

[65], independent of A(t), with pdf

$$p_{G'}(g) = \frac{\alpha}{2\sqrt{2}\Gamma(\frac{1}{\alpha})\sigma'} \exp\{-(\frac{g}{\sqrt{2}\sigma'})^{\alpha}\} \qquad (5.2)$$

where

$$\sigma' = \left(\frac{\sigma^2 \Gamma(\frac{1}{\alpha})}{2\Gamma(\frac{3}{\alpha})} \right)^{\frac{1}{2}},$$

σ, α are distribution constants and $\Gamma(x)$ is a gamma function of x. For $\alpha=2$ this density reduces to the Gaussian density, whereas for $\alpha=1$ it becomes the Laplace density. Furthermore, according to Algazi and Lerner [66], densities representative of certain atmospheric IN can be obtained by picking $0.1<\alpha<0.6$. This distribution is plotted in Fig. 5.1 for different values of α.

For large amplitudes of X(t) it is known empirically that the $p_X(x)$, the pdf of X(t) at t_i (i=1,2...), falls off much more slowly than it would if X(t) were Gaussian only. This is because of the more or less discrete large impulsive transients that greatly exceed the background noise and tend to take on the amplitude distributions of the transients themselves. To generate a class of first-order pdf in A(t) that yields the proper behaviour at large amplitudes in X(t), we follow the procedure suggested by Hall [4] for his 't' model. Accordingly, we consider the reciprocal non-Gaussian random process

$$Q(t) = |A(t)|^{-1}. \qquad (5.3)$$

The first order pdf of Q(t) is assumed to be

$$p_Q(q) = \frac{\alpha}{2\gamma^{\beta}\Gamma(\beta)} |q|^{\alpha\beta-1} \exp(-\frac{|q|^{\alpha}}{\gamma}), \quad -\infty<q<\infty \qquad (5.4)$$

$$p_Q(q) = \frac{\alpha}{2\Gamma(\beta)\gamma^{\beta}} |q|^{\alpha\beta-1} \exp\left[-\frac{|q|^{\alpha}}{\gamma}\right]$$

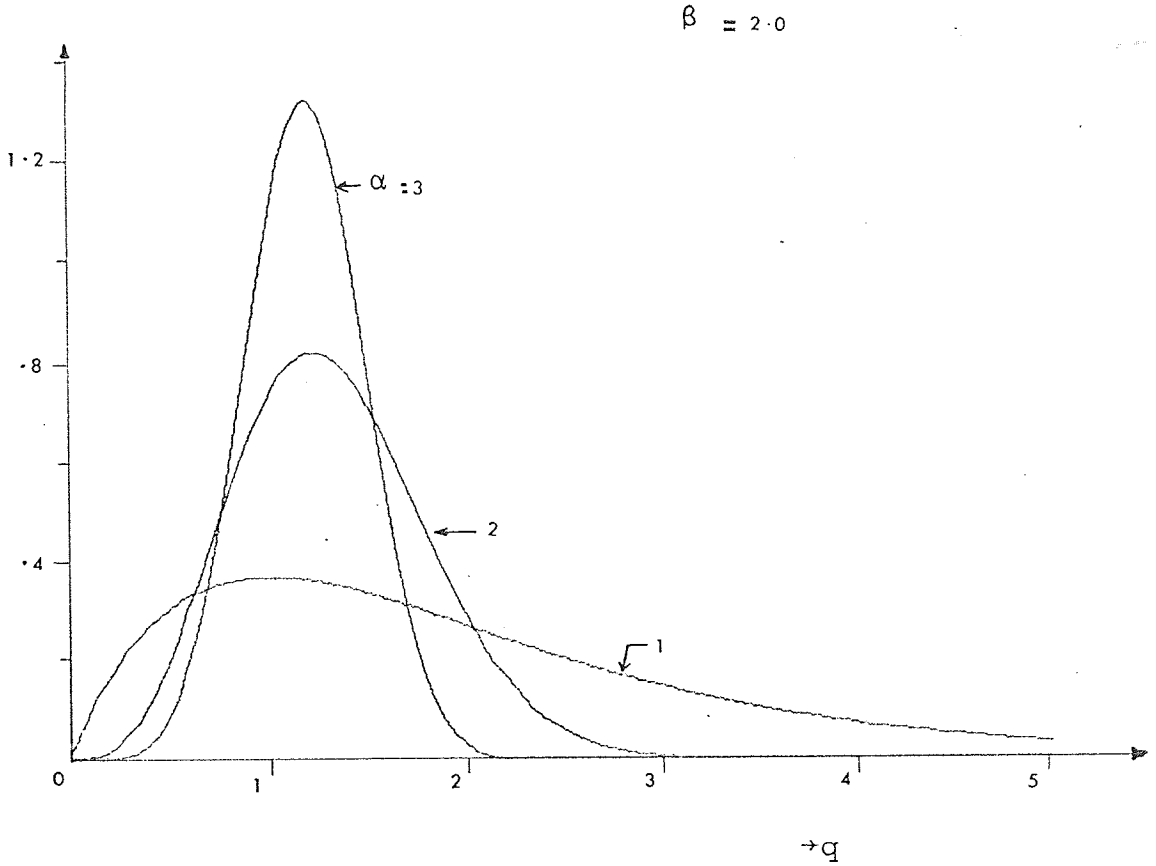

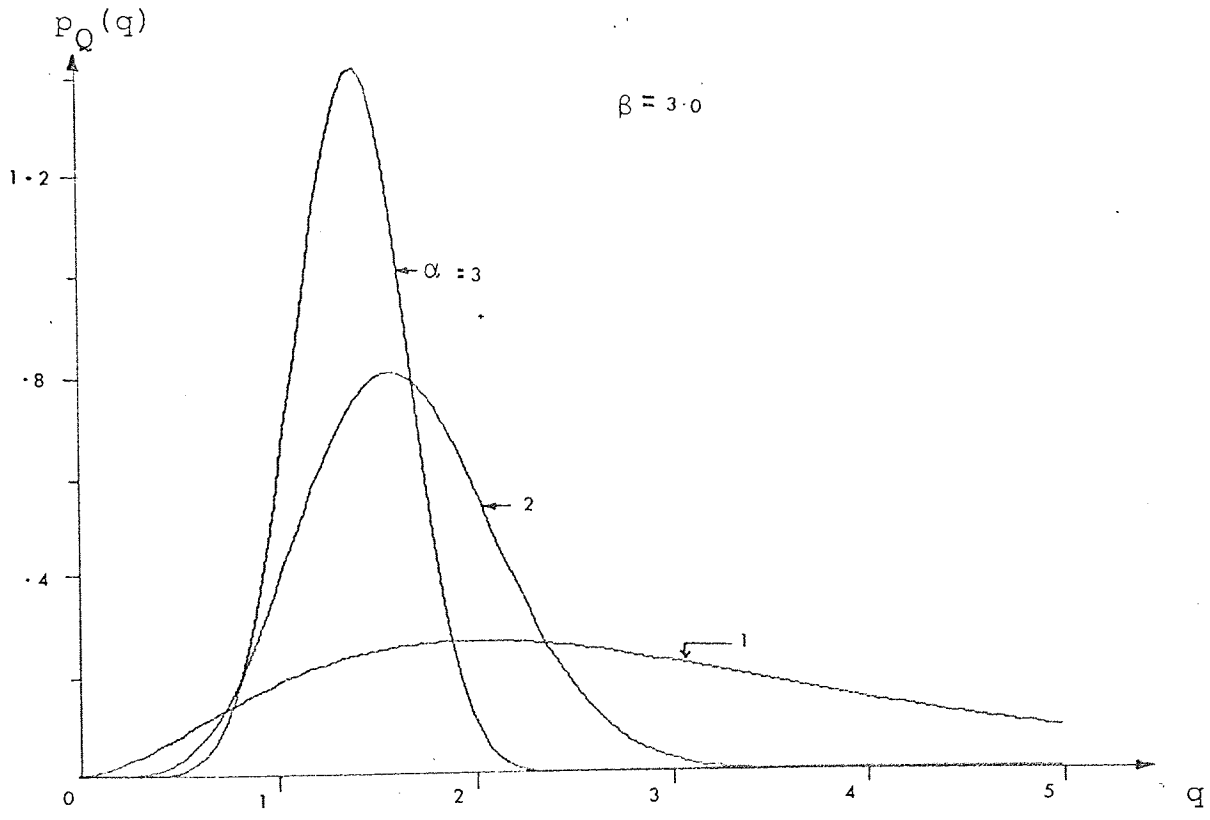

Fig. 5.2 Generalized chi-probability density function (γ=1.0) only +ve values of q are shown.

with parameters α, β, γ. For $\alpha=2$; $p_Q(q)$ is a chi-squared distribution with 2β degrees of freedom. Using (5.4) in (5.3) one can readily show that the pdf of A(t) is

$$p_A(a) = \frac{\alpha}{2\gamma^{\beta}\Gamma(\beta)} |a|^{1-\alpha\beta} \exp\left(-\frac{1}{\gamma|a|^{\alpha}}\right), \quad -\infty<a<\infty. \tag{5.5}$$

For large values of a, the distribution behaves as

$$\lim_{a\to\infty} p_A(a) = \lim_{a\to\infty} |a|^{1-\alpha\beta} \quad \text{for } \gamma>0, \tag{5.5a}$$

which is the desired form of large amplitude dependence for X(t), since $|a|\to\infty$ implies $x\to\infty$. It is seen that the hyperbolic distribution specified by the above equation is asymptotically identical in form to perhaps the simplest of the empirical models [22],[66] proposed from observation of measured data on the envelope of received atmospheric noise [10]. Thus it is concluded that the above equation gives a reasonable specification of the asymptotic behaviour of the first-order statistics of A(t). Dependence of parameters α and β on the distribution, specified by (5.4), is shown in Fig.5.2 for $\gamma=1.0$.

To obtain the pdf of $X(t) = A(t)G'(t)$ we make use of [101]

$$p_X(x) = \int_{-\infty}^{\infty} \zeta p_Q(\zeta) p_{G'}(x\zeta)\, d\zeta, \quad -\infty<x<\infty. \tag{5.6}$$

Substituting values of $p_{G'}(x\zeta)$ and $p_Q(\zeta)$ from (5.2) and (5.4) respectively in the above equation and making a change in variable $\S=\zeta^{\alpha}$ yields

$$p_X(x) = \frac{\alpha}{2\sqrt{2}\sigma'\gamma^{\beta}\Gamma(\beta)\Gamma(\frac{1}{\alpha})} \int_0^{\infty} \S^{(\alpha\beta+1)/\alpha-1} \exp\left(-\frac{\S}{K(x)}\right) d\S$$

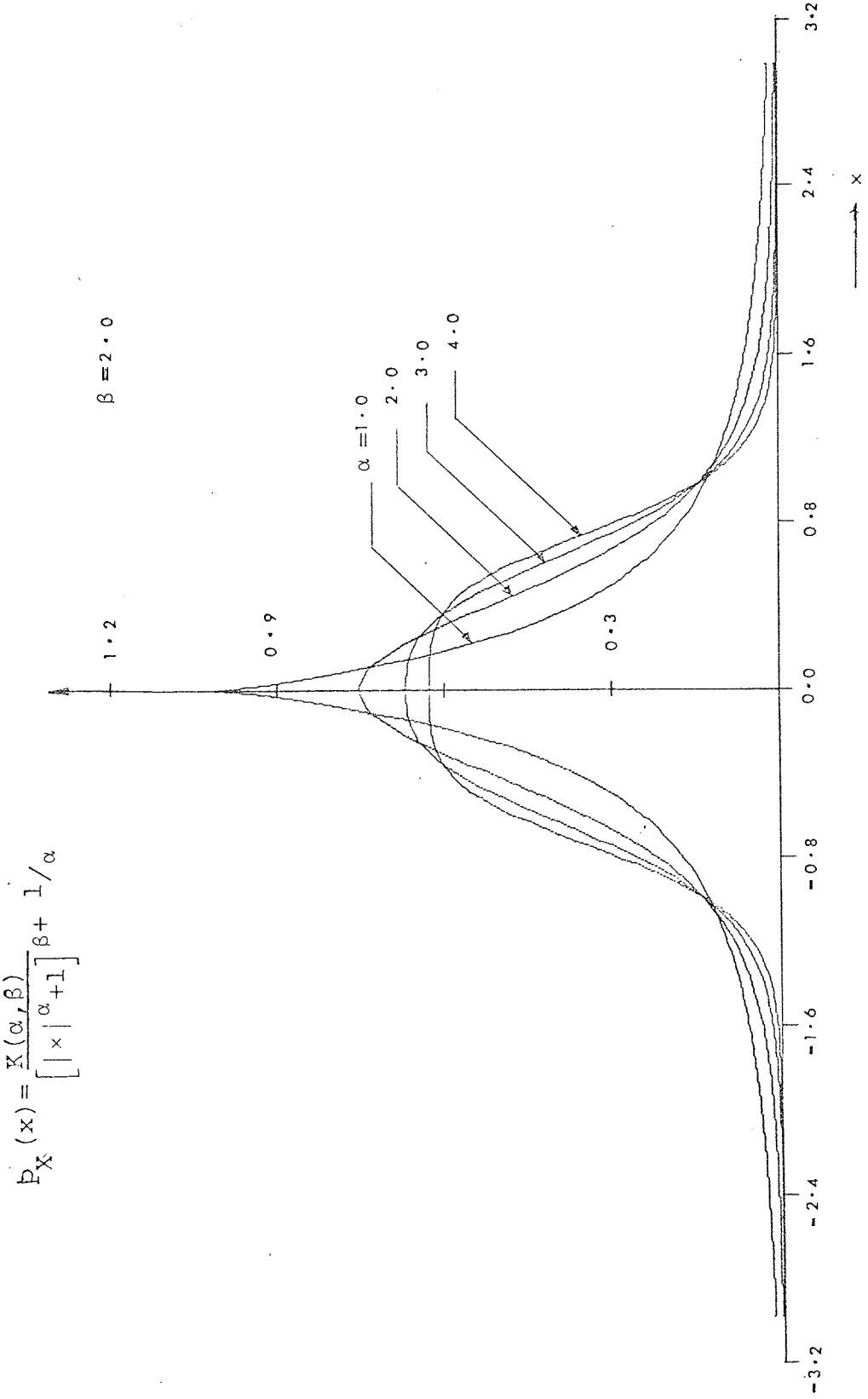

Fig.5.3 Probability density function of Interference process in the receiver (Generalised hyperbolic pdf)

$$p_X(x) = \frac{K(\alpha,\beta)}{\left[|x|^{\alpha}+1\right]^{\beta+\frac{1}{\alpha}}}$$

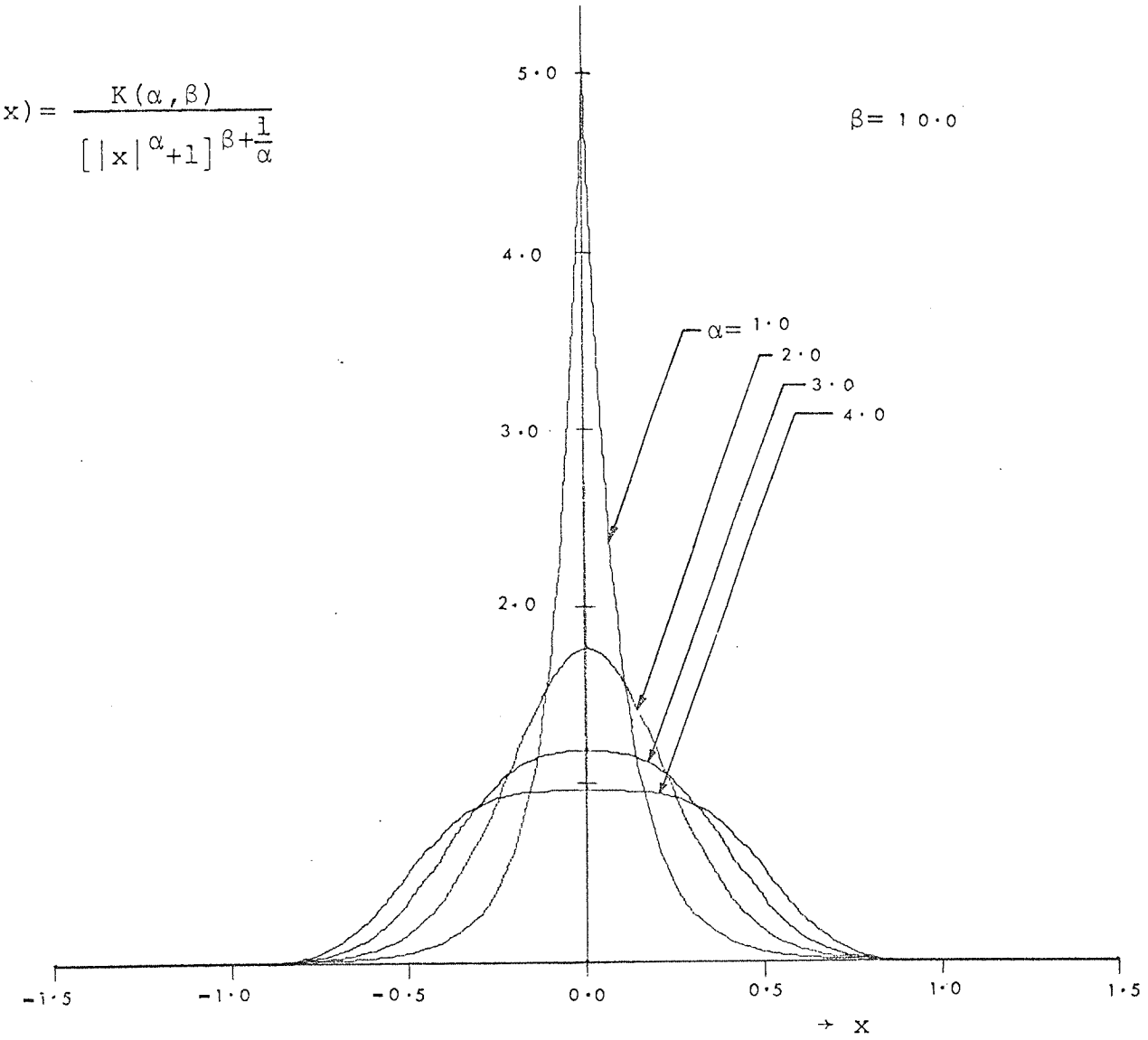

Fig. 5.4 Probability density function of interference process in the receiver (Generalised hyperbolic pdf)

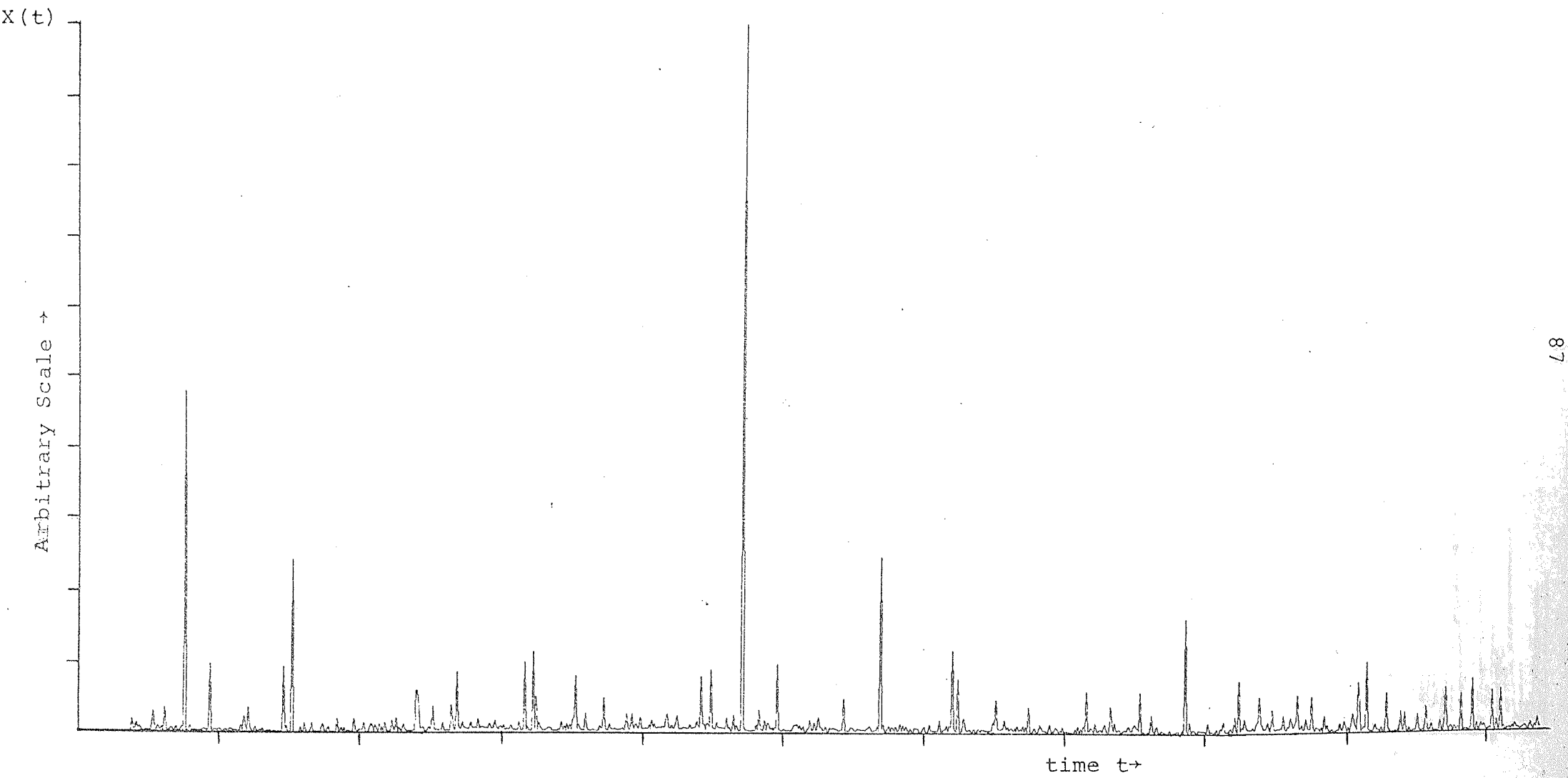

Fig. 5.5 IN process specified by the random variable with pdf $p_X(x) = \frac{K(\alpha,\beta)}{[1+x^2]^{3/2}}$

(only +ve values are shown)

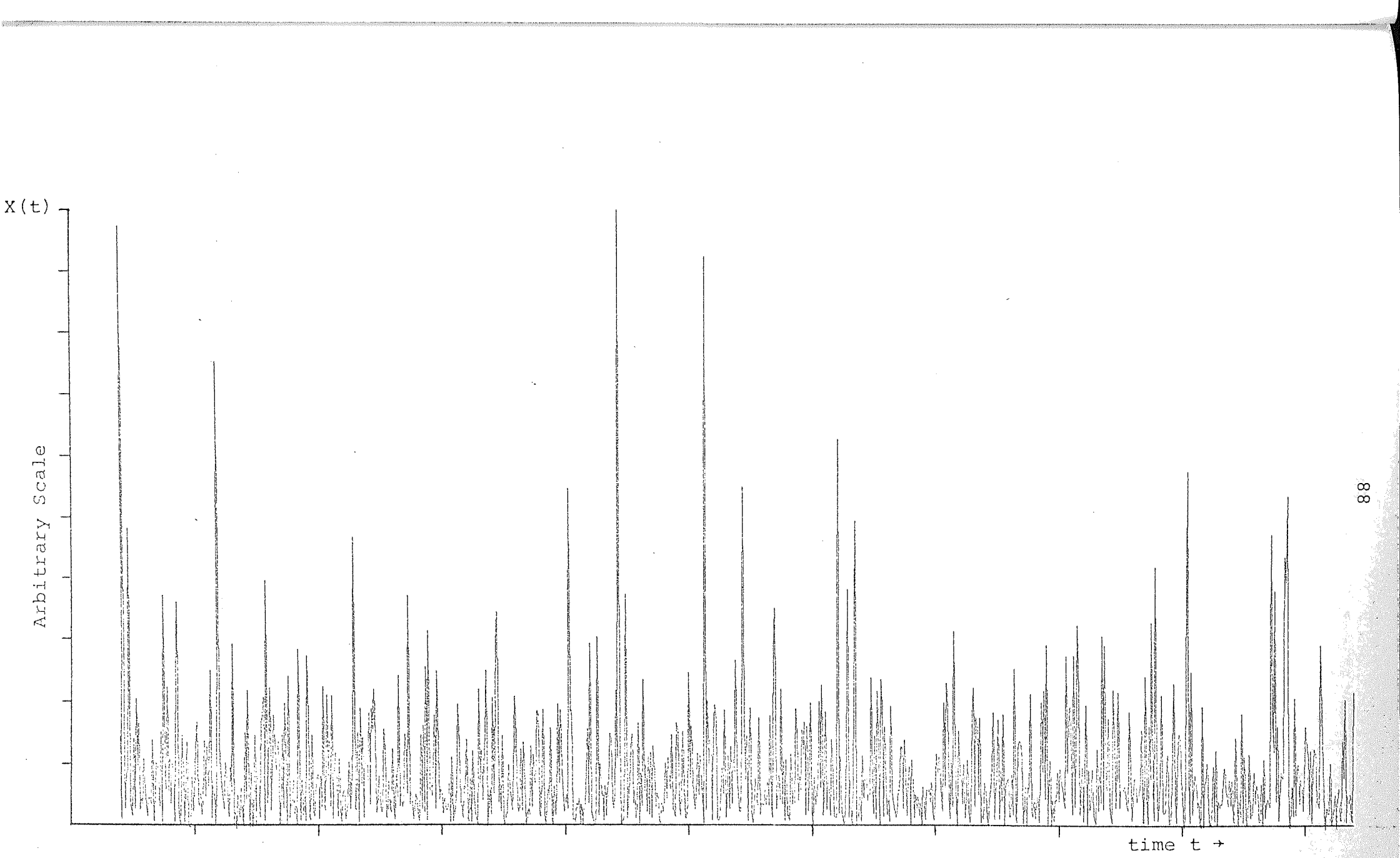

Fig. 5.6 IN process specified by the random variable with pdf $p_X(x) = \frac{K(\alpha,\beta)}{[1+|x|]^6}$

(only +ve values are shown)

where

$$K(x) = \{(\frac{x}{\sqrt{2}\sigma'})^{\alpha} + \frac{1}{\gamma}\}^{-1}.$$

Referring to standard integral tables [82] i.e.,

$$\int_0^{\infty} \omega^c \exp(-\omega/d)\, d\omega = d^{c+1}\Gamma(c+1)$$

the pdf of process X(t) becomes

$$p_X(x) = K(\alpha,\beta)\,\sigma_o^{\alpha\beta}\{|x|^{\alpha}+\sigma_o^{\alpha}\}^{-(\beta+\frac{1}{\alpha})}, \quad -\infty<x<\infty \qquad (5.7)$$

where we have defined

$$\sigma_o^{\alpha} = \frac{(\sqrt{2}\sigma')^{\alpha}}{\gamma} \quad \text{and} \quad K(\alpha,\beta) = \frac{\alpha\Gamma(\beta+\frac{1}{\alpha})}{2\Gamma(\beta)\Gamma(\frac{1}{\alpha})}. \qquad (5.8)$$

Equation (5.7) describe the pdf of IN component of the atmospheric noise below 100 MHz. This density function will be called generalised hyperbolic distribution. To illustrate the density of (5.7), a set of curves is given in Figs 5.3 and 5.4 for $\beta=2$ and $\beta=10$ respectively and $\sigma_o=1.0$, $\alpha=1.0,2.0,3.0,4.0$. Random numbers were generated on the digital computer for $\alpha=1,2$; $\beta=1,5$; $\sigma_o=1.0$ and are plotted in Figs.5.5 and 5.6. The impulsive nature of the noise can be observed from these plots.

Evidence that the generalised density of (5.7) is a reasonable one to consider in communication problems is provided by the densities proposed by Hall [4] and Mertz [22] for the amplitude distribution of IN. Mertz assumed that the noise amplitude is given by

$$p_M(x) = \frac{\beta h^{\beta}}{2}\,(|x|+h)^{-(\beta+1)}, \quad -\infty<x<\infty$$

where h is a small constant and β ranges from just over 2 to about 5. This equation is precisely the pdf of (5.7) with $\alpha=1$ and $\sigma_o=h$. For $\alpha=2$ and $\beta=0.5$ we have a Cauchy density. This density function has been used in several previous papers, such as Rappaport and Kurz [52], to represent severe noise.

5.2.1 MOMENTS OF GENERALISED HYPERBOLIC DISTRIBUTION

Since the pdf of X(t) is an even function, all odd moments are zero. The various even moments, when they exist, are found most easily from

$$\langle x^k \rangle = \int_{-\infty}^{\infty} x^k p_X(x)\,dx.$$

Using (5.7) in the above equation yields

$$\langle x^k \rangle = \frac{2}{\sigma_o} K(\alpha,\beta) \int_o^{\infty} x^k \{ (\frac{x}{\sigma_o})^{\alpha} + 1 \}^{-(\beta+\frac{1}{\alpha})} dx.$$

Changing the variable $\S=\{1+(x/\sigma_o)^{\alpha}\}^{-1}$ and using [85]

$$\int_o^1 \S^{p-1}(1-\S)^{q-1} d\S = \frac{\Gamma(p)\Gamma(q)}{\Gamma(p+q)} \qquad \text{(Beta function)}$$

in the above equation yields

$$\langle x^k \rangle = \frac{\sigma_o^k \Gamma(\beta-\frac{k}{\alpha})\Gamma(\frac{k+1}{\alpha})}{\Gamma(\beta)\Gamma(\frac{1}{\alpha})} . \qquad (5.9)$$

The validity of the integral is if $\alpha\beta>k$. For k=2 the above equation reduces to

$$\langle x^2 \rangle = \frac{\sigma_o^2 \Gamma(\beta-\frac{2}{\alpha})\Gamma(\frac{3}{\alpha})}{\Gamma(\beta)\Gamma(\frac{1}{\alpha})} , \qquad \alpha\beta>2 \qquad (5.9a)$$

In practice it usually happens that the model fits the data very closely for $\alpha\beta \leq 2$, which indicates that the noise has very large average power. This agrees in principle with the results of Mandelbrot [102] in which he notes that intermittent phenomena often appear to have barely convergent, or even divergent, second moments, dependent strongly on sample size.

5.2.2 CUMULATIVE DISTRIBUTION

The cumulative distribution $P_X(x)$ can easily be obtained from

$$P_X(x) = \int_{-\infty}^{x} p_X(\zeta)d\zeta \ .$$

Utilizing (5.7) and performing the integration yields

$$P_X(x) = \frac{1}{2}\left[1 \pm \left\{1 - \frac{2}{\alpha}K(\alpha,\beta)B\left(\beta,\frac{1}{\alpha}\middle| \frac{1}{1+(\frac{x}{\sigma_o})^{\alpha}}\right)\right\}\right] \qquad (5.10)$$

where $\pm$ refers to $x \gtrless 0$; $B(\ )$ is an incomplete Beta function [85] and $K(\alpha,\beta)$ is defined by (5.8).

5.2.3 CHARACTERISTIC FUNCTION

The CF is given by

$$\Phi_X(j\xi) = K(\alpha,\beta)\int_{-\infty}^{\infty} \exp(j\xi x)\{|x|^{\alpha}+\sigma_o^{\alpha}\}^{-(\beta+\frac{1}{\alpha})}\,\sigma_o^{\alpha\beta}\,dx$$

which, since $\sin(x\xi)$ is an odd function, reduces to

$$\Phi_X(j\xi) = K(\alpha,\beta)\int_{-\infty}^{\infty}\cos(\xi x)\{|x|^{\alpha}+\sigma_o^{\alpha}\}^{-(\beta+\frac{1}{\alpha})}\,\sigma_o^{\alpha\beta}\,dx \qquad (5.11)$$

The above integral can be evaluated in a series form by using

the complex integral method. A closed form can, however, be obtained when $\alpha=2.0$: Using [85]

$$K_\nu(xZ) = \frac{\Gamma(\nu+\frac{1}{2})}{\sqrt{\pi}x^\nu} (2Z)^\nu \int_0^\infty \cos(x\zeta)\{\zeta^2+Z^2\}^{-(\nu+\frac{1}{2})} d\zeta$$

in (5.11) yields

$$\Phi_X(j\xi) = \sigma_o^\beta K_\beta(\xi\sigma_o)\xi^\beta/\Gamma(\beta)2^{\beta-1}. \qquad (5.12)$$

$K_\beta(.)$ is the modified Bessel function of the second kind.

5.3 FIRST-ORDER DISTRIBUTION OF ENVELOPE

Since the noise is always observed through the passband of some receiver filter, we now develop the first-order distribution of the envelope of the noise. If the receiver is sufficiently narrow-band, the noise at the receiver output can reasonably be assumed to be modelled well as a Gaussian process. This follows from the fact that narrow-band filtered noise is the sum of contributions from many independent lightning discharges, none of which is dominant at the filter output. Experimental data indicate, however, that the bandwidth required to achieve this condition at VLF is less than 50 Hz, so a Gaussian assumption is not always physically viable at VLF. The modelling problem can be simplified by noting that for communication applications the receiver bandwidth is substantially smaller than the band centre frequency. This fact enables the received atmospheric noise to be regarded as a narrow-band random process. This assumption is always satisfied for communication problems and is not nearly as strong as a Gaussian assumption. Almost all the available experimental data [10]-[14] have been obtained in narrow-band conditions.

The statistical independence of A(t) and G'(t) requires, at least, that their spectra do not noticeably overlap. As mentioned before, A(t) will be of quite low frequency, while G'(t) is comparatively narrow-band, centred about some carrier frequency ω_c, even when a radio frequency stage which is broad compared to usual communication practice is used in the receiver.

The resulting process X(t) is, therefore, narrow-band and can be expressed as

$$\begin{aligned} X(t) &= G_1'(t)A(t)\cos\omega_c t + G_2'(t)A(t)\sin\omega_c t \\ &= X'(t)\cos\omega_c t + \hat{X}(t)\sin\omega_c t \\ &= |A(t)|G(t)\cos(\omega_c t+\phi) \\ &= E(t)\cos(\omega_c t+\phi) \end{aligned} \tag{5.13}$$

where

$\hat{X}(t)$ and $G_2'(t)$ = quadrature component corresponding to X(t) and G'(t) respectively

X'(t) and $G_1'(t)$ = in phase component corresponding to X(t) and G'(t) respectively

$G^2(t) = G_1'^2(t) + G_2'^2(t)$ is the envelope of process G'(t) (≥ 0)

$E(t) = G(t)|A(t)|$ (≥ 0) is the envelope of X(t)

$\phi = \tan^{-1}(G_2'(t)/G_1'(t))$ is the phase

$\omega_c = 2\pi f_c$ carrier frequency in rad/sec.

X'(t) and $\hat{X}(t)$ at the instant t are independent and identically distributed random variables.

For general integer values of α it is impossible to obtain

a closed form expression for the pdf of the envelope. However, for $\alpha=2$ a closed form can be obtained. In what follows we assume that $\alpha=2$: $Q(t)$ reduces to chi-density and $G'(t)$ to Gaussian density. Since $G'(t)$ is Gaussian, $G_1'(t)$ and $G_2'(t)$ are also Gaussian processes, the phase ϕ must in the first-order be uniformly distributed over 2π. The envelope $G(t)$ will likewise have a Rayleigh distribution in the first-order, but the envelope $E(t)$ will, in general, not. For $A(t) = \{Q(t)\}^{-1}$ the pdf of $A(t)$ is [103]

$$p_A(a) = \frac{1}{a^2}\, p_Q(1/a).$$

Using (5.4) and $\alpha=2$ in the above equation yields

$$p_A(a) = \frac{1}{\Gamma(\beta)\gamma^{\beta}} \left(\frac{1}{a}\right)^{2\beta+1} \exp\left(\frac{-1}{\gamma a^2}\right). \tag{5.14}$$

The joint pdf of $X'(t)$ and $\hat{X}(t)$ is easily obtained by using

$$p_{X',\hat{X}}(x',\hat{x}) = p_{AG_1',AG_2'}(x',\hat{x})$$

$$= \int_{-\infty}^{\infty} \frac{1}{\zeta^2}\, p_A(\zeta)\, p_{G_1'}(x'/\zeta)\, p_{G_2'}(\hat{x}/\zeta)\, d\zeta. \tag{5.15}$$

Substituting

$$p_{G_1'}(x'/\zeta) = \frac{1}{\sqrt{2}\sigma'\Gamma(\tfrac{1}{2})} \exp\{-(\frac{x'}{\sqrt{2}\sigma'\zeta})^2\};$$

$$p_{G_2'}(\hat{x}/\zeta) = \frac{1}{\sqrt{2}\sigma'\Gamma(\tfrac{1}{2})} \exp\{-(\frac{\hat{x}}{\sqrt{2}\sigma'\zeta})^2\}$$

and $p_A(x')$ from (5.14) and defining $e^2 = x'^2 + \hat{x}^2$, we get

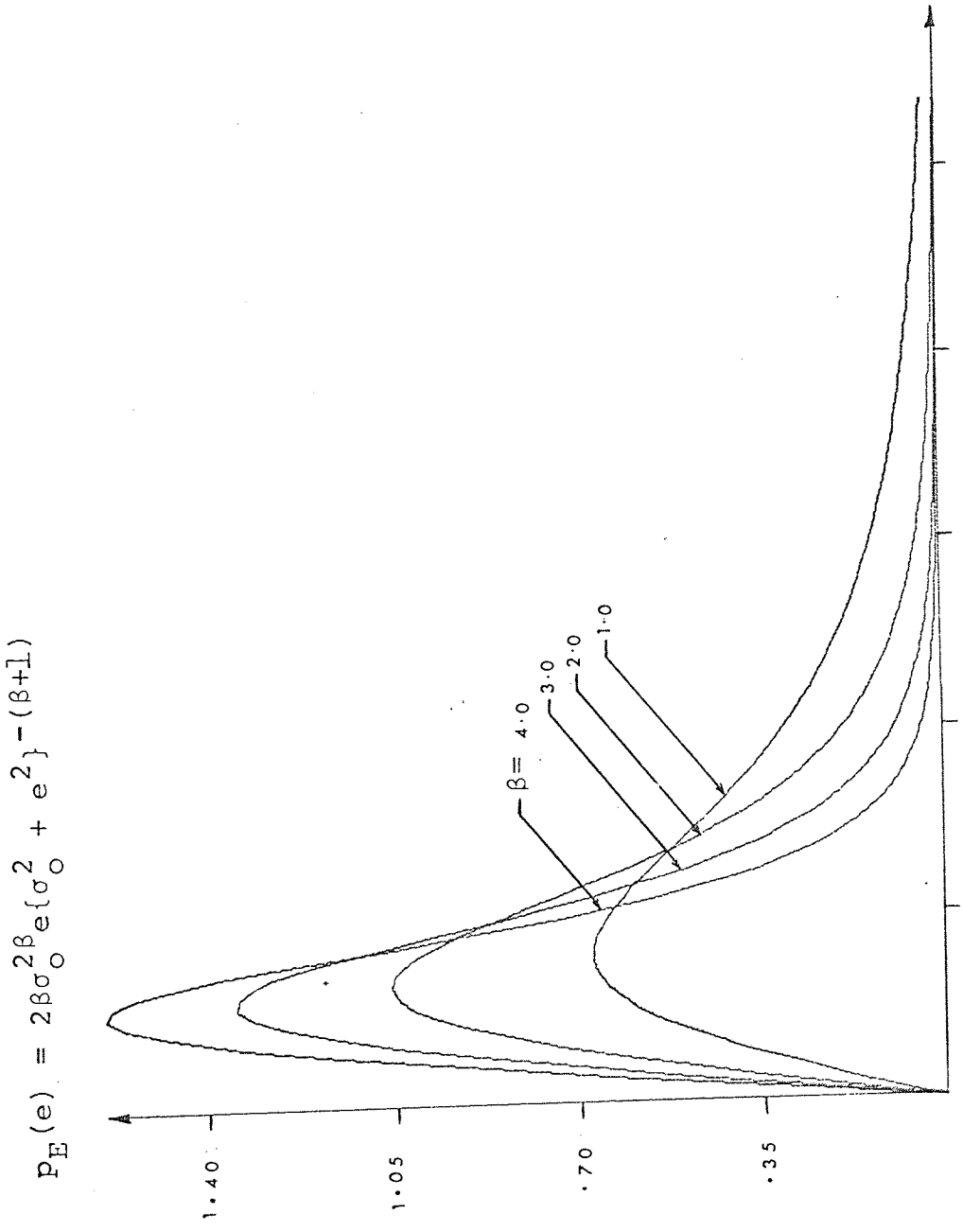

Fig. 5.7 Envelope density function of the interfering process in the receiver (σ_o=1.0)

$$p_{X',\hat{X}}(x',\hat{x}) = \frac{(\Gamma(\tfrac{1}{2})\sigma')^{-2}}{2\Gamma(\beta)\gamma^{\beta}} \int_{o}^{\infty} \zeta^{\beta} \exp\left(\frac{-\zeta}{K(e)}\right) d\zeta$$

where

$$K(e) = (e^2+2\sigma'^2/\gamma)^{-1}2\sigma'^2$$

Using (5.8) and evaluating the integral yields

$$p_{X',\hat{X}}(x',\hat{x}) = \frac{\Gamma(\beta+1)\sigma_o^{2\beta}}{\Gamma^2(\tfrac{1}{2})\Gamma(\beta)}\{\sigma_o^2 + e^2\}^{-(\beta+1)}. \qquad (5.16)$$

The joint probability density of envelope and phase of the narrow-band received noise is given by

$$p_{E,\phi}(e,\phi) = e p_{X',\hat{X}}(x',\hat{x}).$$

Using (5.16) in the above equation to obtain

$$p_{E,\phi}(e,\phi) = \frac{\Gamma(\beta+1)\sigma_o^{2\beta}}{\Gamma^2(\tfrac{1}{2})\Gamma(\beta)} e\{\sigma_o^2 + e^2\}^{-(\beta+1)}.$$

Since the phase is uniformly distributed over 2π, the pdf of the envelope $E(t)$ is

$$p_E(e) = 2\beta\sigma_o^{2\beta} e\{\sigma_o^2+e^2\}^{-(\beta+1)}, \quad 0<e<\infty. \qquad (5.17)$$

Equation (5.17) is plotted in Fig. 5.7 for various values of β and $\sigma_o = 1.0$. It is important to note, in support of the model derived, the asymptotic forms of $p_E(e)$:

$$\lim_{e\to\infty} \; p_E(e) = 2\beta\sigma_o^{2\beta} \; e^{-(2\beta+1)}$$

which has precisely the desired behaviour specified by (5.5a). For $e \tilde{} o$ the distribution behaves as:

$$\lim_{e\to o} \; p_E(e) = \frac{2\beta e}{\sigma_o^2} = \lim_{e\to o} \; \frac{e}{\sigma_e^2} \exp\left(\frac{-e^2}{2\sigma_e^2}\right)$$

where $\sigma_e^2 = \sigma_o^2 / 2\beta$. This is of course in agreement with both experimental results and intuition, since the noise at low levels is expected to be the resultant contributions from a large number of independent noise sources, and hence behaves as if it were Rayleigh distributed. The noise model recently proposed by Shinde et al [104] for HF atmospheric noise can be obtained from (5.17) by substituting $\beta=1.5$ and $\sigma_o^2=1.0$.

The various first-order moments of the envelope are easily obtained directly from

$$\langle e^k \rangle = 2\beta\sigma_o^{2\beta} \int_o^\infty e^{k+1} \{\sigma_o^2+e^2\}^{-(\beta+1)} de$$

$$= \beta\sigma_o^k \Gamma(\beta-\tfrac{k}{2}) \Gamma(\tfrac{k}{2}+1) / \Gamma(\beta+1) \quad \text{for} \quad \alpha\beta>k. \qquad (5.18)$$

The probability $P_o(e)$ that the envelope intensity exceeds level e is given by

$$P_o(e) = 1-P_E(e) = \int_e^\infty p_E(\zeta) \, d\zeta$$

$$= \sigma_o^{2\beta} \{\sigma_o^2+e^2\}^{-\beta}. \qquad (5.19)$$

5.4 COMPARISON OF THE NOISE MODEL WITH MEASURED DATA

Since we are attempting to develop a model for a random

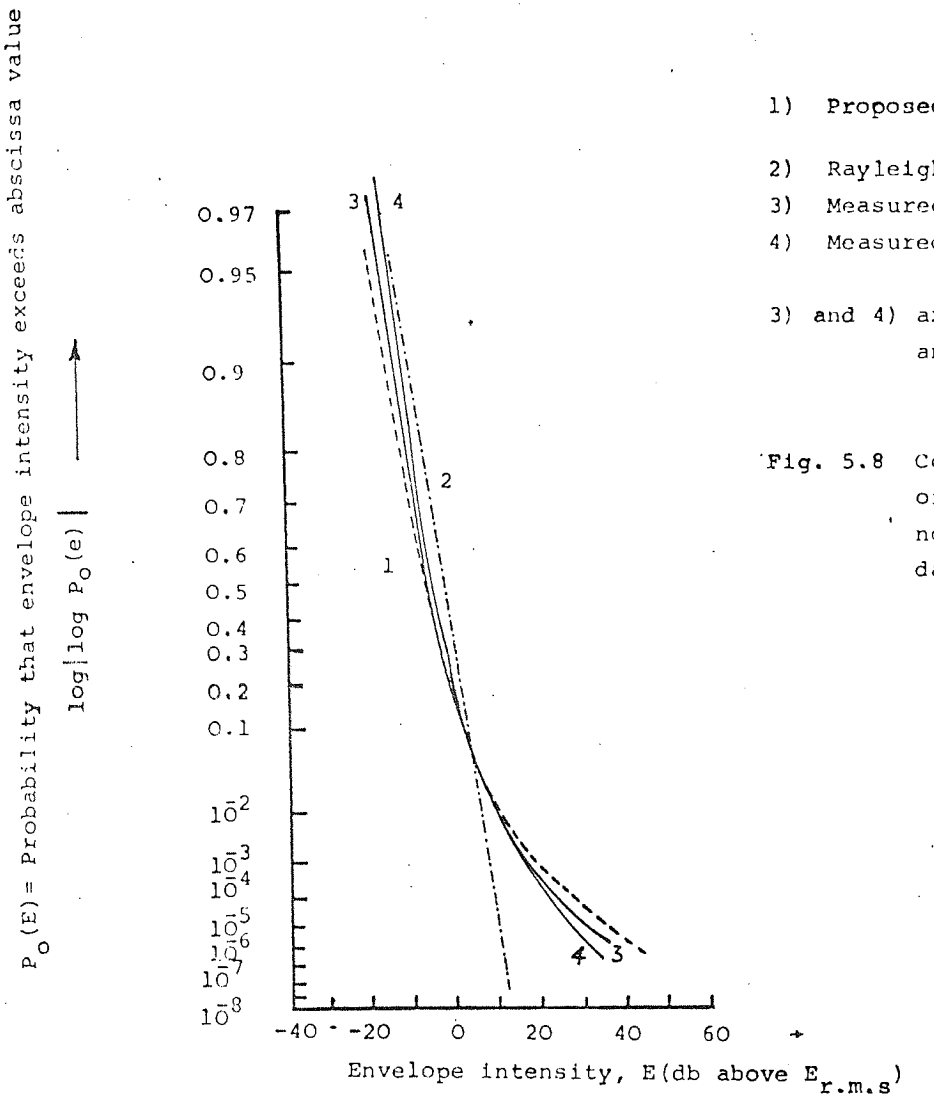

1) Proposed model with $\beta=1.5, \sigma_o=0.07\langle E^2\rangle$ $\langle E^2\rangle$= 10 db below $E^2_{r.m.s.}$
2) Rayleigh-distributed envelope $\langle E^2\rangle = E^2_{r.m.s.}$
3) Measured data, Singapore
4) Measured data, Slough, England.

3) and 4) are measured with centre frequency f_c=20 MHz and bandwidth B=425 Hz

Fig. 5.8 Composite probability distribution function of the envelope of received HF atmospheric noise. Comparison of 'model' results with data measured at Singapore and Slough, England

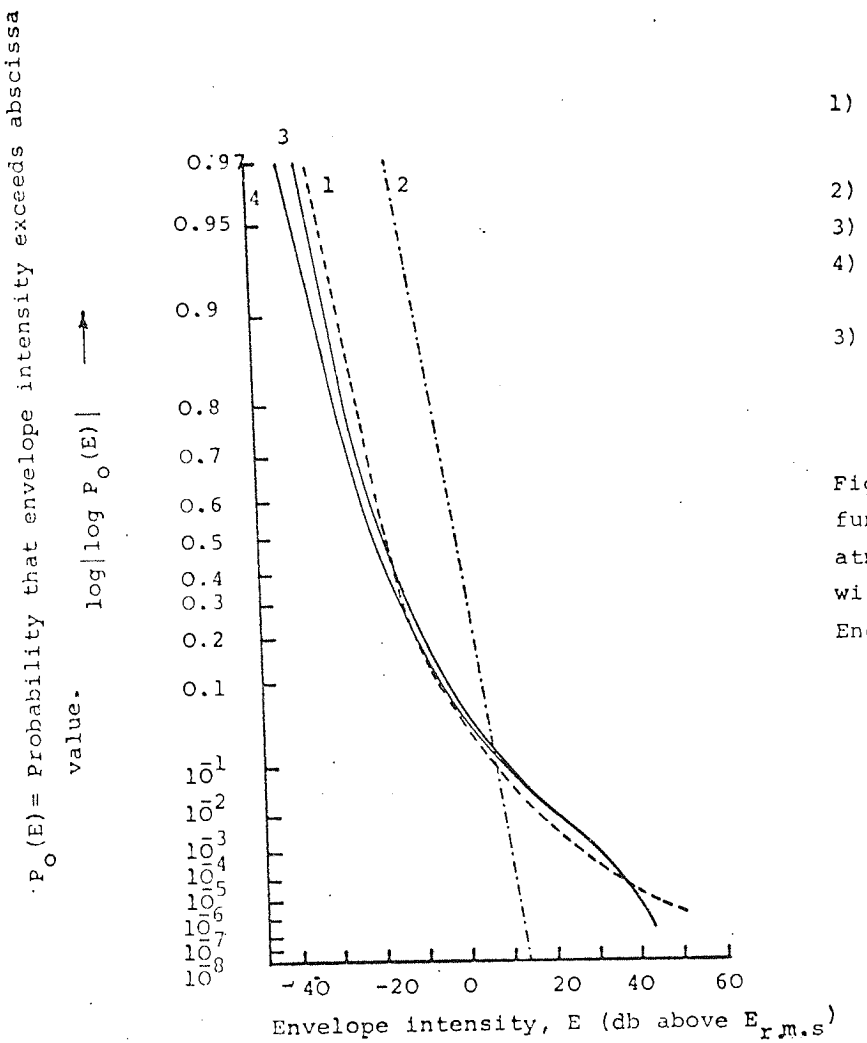

1) Proposed model with $\beta=1.0, \sigma_o=0.64\langle E\rangle$ {$\langle E\rangle$=13 db below $E_{r.m.s}$}
2) Rayleigh-distributed envelope $\langle E^2\rangle = E^2_{r.m.s.}$
3) Measured data, Slough, England
4) Measured data, Singapore

3) and 4) are measured with centre frequency f_c=24KHz and bandwidth B=425 Hz

Fig. 5.9 Composite probability distribution function of the envelope of received VLF atmospheric noise. Comparison of 'model'results with data measured at Singapore and Slough, England.

process, the measurements required to check the validity of the model fall into two categories:

a) measurements of probability of the envelope of the received noise (since all measured data are obtained on a narrow-band channel)

b) measurements of the average number of level crossings per unit time of a fixed level by the envelope of the received noise.

The second measurement is of interest, because it bears out the experimental fact that the average number of level crossings per unit time for the case of non-Gaussian noise is not given by the product of the pdf of the envelope with a suitable bandwidth product, as it would be if the noise were a Gaussian process [71].

The probability $P_o(e)$ that the envelope intensity exceeds level e was derived in the last section and is given by (5.19). This model is compared with experimental results [4], [12], [104] in Figs. 5.8 and 5.9 (note that in these figures $\log|\log P_o(e)|$ is plotted vs. log e. This choice of scale has the interesting property that the Rayleigh-distributed envelope plots as a straight line). The figures show that by using suitable values of β and σ_o in the noise model (5.17) a close agreement with the observed values can be obtained.

As for the distribution of envelope level crossings, we assume that the observed non-Gaussian noise is bandlimited by the receiver to an RF bandwidth 2B, it follows that the envelope of the received noise is bandlimited to a frequency band of width 2B centred about zero frequency [105]. Thus it can be shown [106] that this bandlimited envelope E(t) is approximately described in the time interval $[0,T_o]$ by its

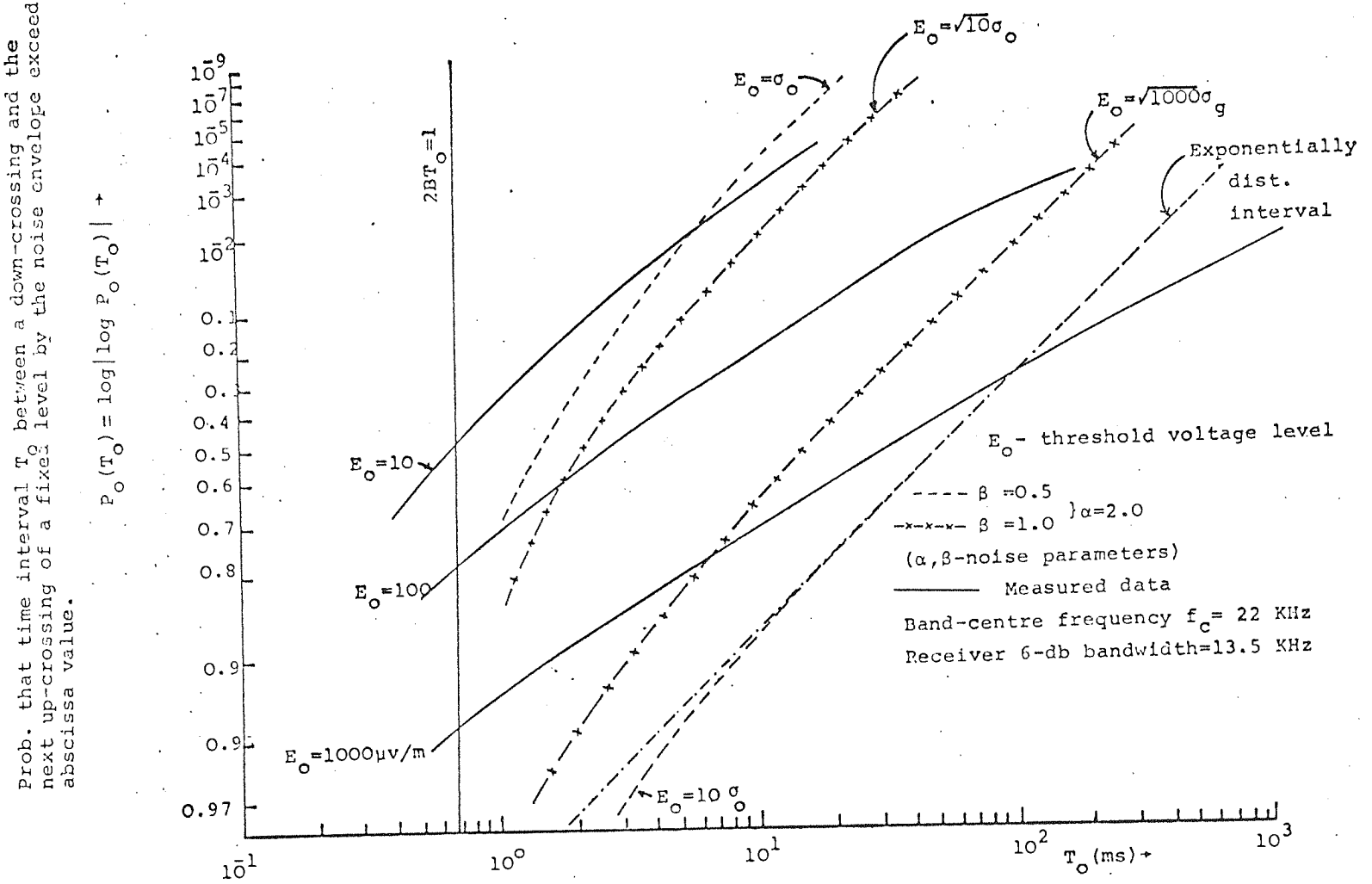

Fig. 5.10 Probability distribution of the time interval between envelope level crossings.

$2BT_o$ independent equidistant samples provided $2BT_o >> 1$.

Let T_1 be defined as the interval between a down-crossing of the level E_o by the envelope of the received noise, and the next up-crossing of the same level. (This is the quantity whose statistics have been measured by Watt and Maxwell [11]). The probability that T_1 exceeds T_o is given by [107]

$$P_o(T_o) = \Pr\{E(t) < E_o\}^{2BT_o - 1}. \tag{5.20}$$

Using (5.17) in the above equation yields

$$P_o(T_o) = \left[1 - \left\{\left(\frac{E_o}{\sigma_o}\right)^2 + 1\right\}^{-\beta}\right]^{2T_oB - 1}. \tag{5.21}$$

Special cases of this result corresponding to $\beta = 0.5$ and 1.0 are plotted in Fig. 5.10 along with experimental results [4], [11]. The pdf of spacing between successive envelope crossings is given by the derivative of $P_o(T_o)$ as

$$p_o(T_o) = 2\beta E_o (2BT_o - 1)\sigma_o^{-2}\left\{\left(\frac{E_o}{\sigma_o}\right)^2 + 1\right\}^{-(\beta+1)} \cdot$$

$$\cdot \left[1 - \left\{\left(\frac{E_o^2}{\sigma_o}\right) + 1\right\}^{-\beta}\right]^{2BT_o - 2}. \tag{5.22}$$

The maximum value of $p_o(T_o)$ occurs when T_o is

$$T_o = \frac{1}{2B}\left[1 - \frac{1}{\log\left(1 - \left\{\left(\frac{E_o}{\sigma_o}\right)^2 + 1\right\}^{-\beta}\right)}\right]. \tag{5.23}$$

Thus the occurrence of maximum value of $p_o(T_o)$ indicates that the noise pulses are dependent and they have a tendency to cluster. This result is in agreement with the observed correlation between pulses [11].

5.5 DISCUSSION

In this chapter we were mainly concerned with the development of an analytical model for 'impulsive' phenomena and with verification of the applicability of this model as a description of received non-Gaussian noise. The model proposed here takes the received IN X(t) to be given by $X(t)=A(t)G'(t)$ where G'(t) is a zero-mean generalised Gaussian process independent of A(t), and A(t) is a stationary slowly varying random process, independent of G'(t), which modulates X(t). This modulating process is further described as $A(t)=1/Q(t)$ where the first-order statistics of Q(t) are specified by the generalised 'two-sided' chi-distribution with parameters α,β,γ. The probability distribution of the envelope of the noise model ($\alpha=2.0$) is in good agreement with experimental results, with this agreement being particularly good at VLF and HF. This is demonstrated in Figs. 5.8 and 5.9.

Even though it is established empirically that $\beta=1.0$ (or less), and consequently the power of the process A(t) and $X(t)\rightarrow\infty$, the model may still be used. Physically of course, $\langle x^2\rangle$ must be finite. What probably occurs in reality is that not one, but at least two laws for A(t) are required at large amplitudes, up to some very high but finite level, at and above which there is not only possible saturation at the front end of the receiver, but also a modification of β, now larger than 1.0, to ensure the necessary finiteness of $\langle x^2\rangle$.

The higher order statistics of the noise are given by (5.21) and (5.22) for $P_o(T_o)$ and $p_o(T_o)$ respectively, which is verified for LF and VLF radio channels.

Finally, the parameters σ_o and β are to be determined empirically. We expect that they will show secular variations

with the time of day, week, etc. They may also vary with the urban region chosen for study. They will certainly depend on the bandwidth and frequency allocation of the receiver used. In any case, they are a part of the experimental data to be investigated in any overall study. This problem is considered further in Chapter 8.

CHAPTER 6

OPTIMUM DETECTION AND SIGNAL DESIGN FOR NON-GAUSSIAN CHANNELS [130]

In this chapter, explicit receiver structure for the optimum detection of binary signals in non-Gaussian noise environments is determined. The resulting optimum structure, while shown to bear some resemblance to that which would have been obtained in the presence of Gaussian noise alone, exhibits an interesting nonlinear behaviour. The performance of the detector, specified by the upper bound on the probability of error, is assessed and is seen to depend on the signal shape, the time-bandwidth product, and SNR. Consequently, a solution for an optimal signal to achieve the minimum probability of error is derived.

6.1 SIGNAL DETECTION

6.1.1 INTRODUCTION

In order to optimize the detection process a knowledge of all higher order pdfs of the interference is required. If the interference is Gaussian, a second-order statistic implies all the higher order statistics, so that solutions for optimal detection are quite simple. This is not always true for non-Gaussian noise. Moreover, in practice when one meets non-Gaussian noise it is in general non-stationary, for example its statistics may depend on many factors including geography and the time of day [15].

In order to circumvent this difficulty we assume:

1) the samples of the input process are statistically independent,

i.e., the correlation time of the noise is small compared to the duration of a signal to be detected (the noise bandwidth is large compared to the signal bandwidth)

2) The noise is considered to be quasi-stationary with statistics which remain constant over a period which is long compared to the signal interval.

With these two assumptions made, the multi-variate probability density of the noise samples can be represented by the product of univariate probability densities, i.e.,

$$p_{\vec{X}}(\vec{x}) = \prod_{i=1}^{M} p_{X_i}(x_i)$$

where

$$\vec{X} = \begin{bmatrix} X_1 \\ X_2 \\ \vdots \\ X_M \end{bmatrix} \quad \text{(a vector).}$$

This representation is fully justified if the interference is a Markov-type process and if the samples of the input process are separated in time by an interval longer than the correlation time of the noise [108]. It it also known that any stationary random process can be approximated by a Markov-process (univariate or multi-variate) with an arbitrary degree of accuracy.

Consider the binary communication system shown in Fig.6.1. $S_i(t)$ (i=0,1) are deterministic signals of duration T seconds; and X(t) is assumed to be a sample function from a non-Gaussian random process whose pdf is specified by a generalised hyperbolic distribution. In each signalling interval the encoder selects either $S_o(t)$ or $S_1(t)$. The apriori probability of achieving signal $S_o(t)$ or $S_1(t)$ is assumed to be equally probable; and

each element of the transmitted sequence is independent of all other elements. At the end of each signalling interval, the receiver, which is in perfect synchronization

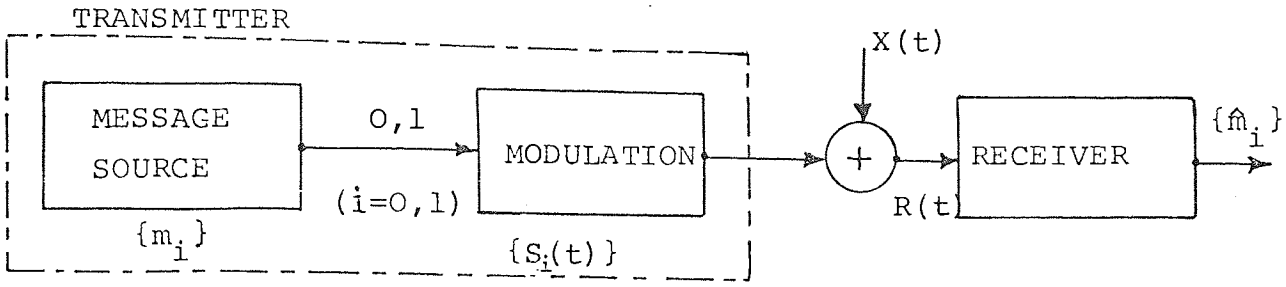

Fig. 6.1 System model

with the transmitter, must decide on the basis of the received data which of the two signals was transmitted. In this case the decision problem reduces to choosing between the two hypotheses:

$$H_o : R(t)=S_o(t) + X(t)$$

$$H_1 : R(t)=S_1(t) + X(t), \qquad 0<t<T.$$

We recall from the discussion in section 5.3 that in practice attention can be restricted to the situation in which the receiver bandwidth is substantially less than the band centre frequency. Thus the decision problem can be written directly in term of the slowly varying complex envelopes of R(t) and X(t). In terms of these complex envelopes, the decision problem becomes that of choosing between the two hypotheses

$$H_o : r(t) = s_o(t) + x(t)$$

$$H_1 : r(t) = s_1(t) + x(t), \qquad 0<t<T \qquad (6.1)$$

where $R(t) = \mathrm{Re}\{r(t)\exp(j\omega_c t)\}$. (r(t) = slowly varying complex envelope of R(t)).

To simplify the analysis, assume that there is a discrete representation of the problem, whether obtained from sampling or orthonormal expansions. Although this is a severe restriction, it still leads to useful results. Therefore, with M the dimension of the discrete representation space, the receiver observes

$$H_o : \vec{r} = \vec{s}_o + \vec{x}$$

$$H_1 : \vec{r} = \vec{s}_1 + \vec{x} \,. \qquad (6.2)$$

The number of samples M is dependent on the bandwidth in which signal of duration T is observed.

6.1.2 LIKELIHOOD RATIO

Since $A(t)=1/Q(t)$ is a slowly varying random process, we can write $x(t) = A(t)g(t)$ {see (5.1) }, where $g(t)$ is the complex envelope of $G'(t)$. Since $g(t)$ is the complex envelope of a Gaussian process, it follows that it is a complex Gaussian process with pdf

$$p_{\vec{g}}(\vec{g}) = \frac{1}{(2\pi\sigma'^2)^M} \exp\left[\frac{-\vec{g}_t^* \vec{g}}{2\sigma'^2}\right] \qquad (6.3)$$

where $\vec{g}_t = [g_1, g_2, \ldots . g_M]$ and * denotes the complex conjugate. The conditional pdf $p_{\vec{r}}(\vec{r}|Q)$ can now be obtained from

$$p_{\vec{r}}(\vec{r}|\vec{Q}) = \prod_{k=1}^{M} Q_k^2 \; p_{\vec{g}}(g_i = Q_i r_i ;\; i=1, \ldots . . . M) ,$$

where use has been made of the fact that in terms of real variables

$$p_{g_i}(g_i) = p_{G_1'}(G_1') \cdot p_{G_2'}(G_2')$$

so that the Jacobian of the transformation is $J(g \to r) = Q^2$. Using (6.3) the joint pdf becomes

$$p_{\vec{r}}(\vec{r}|\vec{Q}) = \frac{1}{(2\pi\sigma'^2)^M} \exp\{-\frac{1}{2\sigma'^2} \sum_{k=1}^{M} Q_k^2 |r_k|^2\} \prod_{\ell=1}^{M} Q^2. \tag{6.4}$$

The pdf of $\vec{r}$ can now be obtained by using

$$p_{\vec{r}}(\vec{r}) = \int_{\vec{Q}} p_{\vec{r}}(\vec{r}\,|\,\vec{Q}\,)\ p_{\vec{Q}}(\vec{Q})\ d\vec{Q}.$$

Using (5.4), (6.4) and [82]

$$\int_0^\infty \zeta^M \exp(-p^2\zeta^2) d\zeta = \Gamma(\tfrac{M+1}{2})/2p^{M+1}$$

in the above equation and performing the M fold integration yields

$$p_{\vec{r}}(\vec{r}) = \{\frac{\beta}{\pi}\sigma_o^{2\beta}\}^M \prod_{\ell=1}^{M} \frac{1}{[|r_\ell|^2+\sigma_o^2]^{\beta+1}} \tag{6.5}$$

where σ_o is defined by (5.8).

The conditional pdf of the received signal under hypotheses $H_i\{i=0,1\}$ is given by

$$p_{\vec{r}}(\vec{r}/H_i) = p_{\vec{r}}(\vec{r}-\vec{s}_i).$$

The likelihood ratio $\Lambda(\vec{r})$ is given by

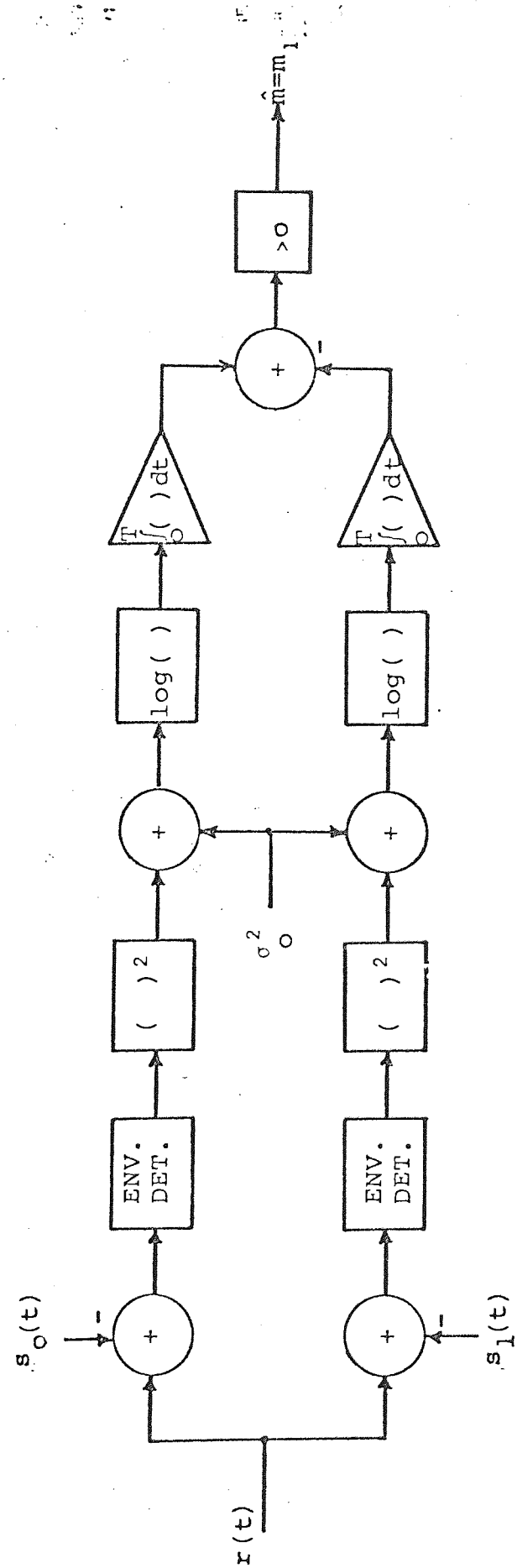

Fig. 6.2 Optimum receiver for VLF channels

$$\Lambda(\vec{r}) = \frac{p_{\vec{r}}(\vec{r}/H_1)}{p_{\vec{r}}(\vec{r}/H_o)} = \prod_{\ell=1}^{M} \psi_\Lambda^{\beta+1}(r_\ell) \qquad (6.6)$$

where

$$\Xi_{ik} = \sigma_o^2 + |r_k - s_{ik}|^2, \quad i=1,2 \; ; \; k=1,.....M \qquad (6.7)$$

and

$$\psi_\Lambda(r_\ell) = \Xi_{o\ell}/\Xi_{1\ell} \; .$$

Thus by Bayes rule we choose $\hat{m}=s_1(t) = m_1$ if

$$\sum_{\ell=1}^{M} \log[\sigma_o^2 + |r_\ell - s_{1\ell}|^2] \geq \sum_{\ell=1}^{M} \log[\sigma_o^2 + |r_\ell - s_{o\ell}|^2] \qquad (6.8)$$

where $\hat{m}$ is the estimate of the transmitted signal. When the sample size M is large enough (6.8) can be approximately represented in integral form as follows:

$$\int_o^T \log[\sigma_o^2 + |r(t)-s_1(t)|^2]dt \geq \int_o^T \log[\sigma_o^2 + |r(t)-s_o(t)|^2]dt \qquad (6.9)$$

where T is the signalling interval. The receiver structure which implements this rule is shown in Fig.6.2 . It is seen that the non-linear receiver agrees with intuition, since it suppresses the received signal at those times when the received signal is predominantly due to a pulse of noise, and bases its decision strongly on the received signal at those times when the noise sample is small. Thus, the receiver ignores the received signal when it is largely the result of a pulse of noise and bases its decision on the relatively quiet periods between the occurrence of these noise pulses.

6.2 PERFORMANCE OF OPTIMUM COHERENT DETECTOR

In many cases of interest, the test likelihood ratio can be derived, but an exact performance calculation is sometimes impossible. For our noise model we encounter this difficulty. Therefore, it is useful to search for another measure that may be weaker than the probability of error, but that is easier to evaluate. We shall use the upper bound given by Chernoff [109]. The probability of error for equally likely signals is

$$Pe = Pr\{\log\Lambda(\vec{r}) = \sum_{k=1}^{M} \psi_\Lambda(r_k) \gtrless 0/H_1\}.$$

To simplify the analysis we assume, in what follows, that $\beta=1.0$ in the noise model (6.5) and $s_o(t)=0$, $s_1(t)= \hat{S}(t)\cos\omega_c t$. The analysis can, however, be extended to any value of β using a similar argument.

The quantities $\psi_\Lambda(r_\ell)$ are statistically independent. Using the Chernoff bound the Pe expression becomes

$$Pe \leqslant Pe_{max} = \prod_{\ell=1}^{M} \langle \psi_\Lambda^{\lambda_o}(r_\ell)\rangle \qquad (6.10)$$

where λ_o is a constant which is chosen to make the upper bound exponentially tight. To find λ_o we solve the equation

$$\sum_{\ell=1}^{M} \frac{1}{\langle \psi_\Lambda^{\lambda}(r_\ell)\rangle} \left\langle \frac{d}{d\lambda} \psi_\Lambda^{\lambda}(r_\ell) \right\rangle \Big|_{\lambda=\lambda_o} = 0 . \qquad (6.11)$$

Using (6.5) and (6.7) when $\beta=1$ yields

$$\langle \psi_\Lambda^{\lambda}(r_\ell)\rangle = \frac{\sigma_o^2}{\pi} \int_{-\infty}^{\infty} \int dr' d\hat{r} \{ \Xi_{o\ell}^{\lambda-2} \Xi_{1\ell}^{-\lambda} \} \qquad (6.12)$$

where $\Xi_{i\ell}$ are defined by (6.7). Using (6.12) and $s_o=0$ in (6.11) it is seen that the solution is obtained when the numerator of the resulting equation is zero. (The denominator is always positive for all values of λ). The only way the numerator can be zero is by having $\lambda_o=1.0$; since then the numerator becomes an odd function of r' and hence when integrated becomes zero. It can also be shown, by differentiating the numerator of the resulting equation with respect to λ and showing that it has always a positive gradient for all λ, that the solution obtained is unique.

Utilizing $\lambda_o=1.0$, (6.10) becomes

$$Pe_{max} = \prod_{\ell=1}^{M} \frac{\sigma_o^2}{\pi} \int_{-\infty}^{\infty} d\hat{r}_\ell \int_{-\infty}^{\infty} dr'_\ell \{1/\Xi_{o\ell}\Xi_{1\ell}\}.$$

Solving the inner integral by contour integration techniques and introducing new variables

$$\zeta_\ell = \hat{r}_\ell^2/\{\hat{r}_\ell^2+\sigma_o^2\}, \quad \upsilon_\ell = s_{1\ell}^2/4\sigma_o^2$$

yields

$$Pe_{max} = \prod_{\ell=1}^{M} \frac{1}{\upsilon_\ell+1} \int_o^1 \frac{1}{2\sqrt{\zeta_\ell}} \{1-\frac{\zeta_\ell\upsilon_\ell}{1+\upsilon_\ell}\} d\zeta_\ell .$$

Using standard integral tables [85] the above equation can be expressed in series form:

$$Pe_{max} = \prod_{\ell=1}^{M} \frac{1}{\upsilon_\ell+1} \sum_{k=0}^{\infty} \frac{1}{2k+1} \{\frac{\upsilon_\ell}{1+\upsilon_\ell}\}^k . \qquad (6.13)$$

For M>>1 (6.13) can be expressed in the following integral form

$$\frac{\log Pe_{max}}{2BT} = \frac{1}{T}\int_{-T/2}^{T/2}\left[\log\left\{\sum_{k=0}^{\infty}\frac{1}{2k+1}\left(\frac{\upsilon(t)}{1+\upsilon(t)}\right)^k\right\}-\log\{\upsilon(t)+1\}\right]dt, \tag{6.14}$$

For small values of $\upsilon(t)$ (<1) the above equation can be simplified to

$$\log\,(Pe_{max}) \approx a_2 F(s) \tag{6.15}$$

where

$$F(s) = \int_{-T/2}^{T/2}\{s_1^4(t)-as_1^2(t)\}dt, \tag{6.15a}$$

$$a = 6\sigma_o^2 \quad \text{and} \quad a_2 = B/18\sigma_o^4 .$$

From the error probability expressions it is seen that the performance depends not only on the signal power, as in the case of Gaussian noise, but also on the particular signal as well as the time-bandwidth product 2BT. These bounds have obvious significance in assessing detector performance. Perhaps less obvious is the fact that, since it is known that the particular signal which minimizes the upper bound on the probability of error is also the signal which minimizes the actual probability of error [61],[110], the formula for error bound may be used to determine an optimal signal. Since the transmitted signal must generally have finite energy, an average energy constraint

$$P^2T = \int_{-T/2}^{T/2}\hat{s}^2(t)\cos^2\omega_c t\,dt$$

will be required. For any chosen signalling waveform, a plot of the normalized parameter on the right hand side (R.H.S.) of (6.14) as a function of $(P/\sigma_o)^2$ can therefore be obtained. For given $(P/\sigma_o)^2$, the signalling waveform that maximizes the R.H.S. of (6.14) is optimal. In order to obtain an idea of the effect of the signalling waveform on system performance, several basic waveforms will be considered. The details for the signal optimization will then be presented in section 6.3.

1) SQUARE SIGNALS

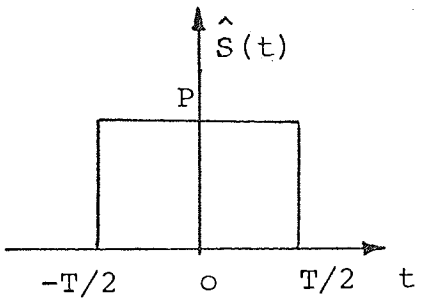

$$\hat{S}(t) = \begin{cases} P, & |t| \leq T/2 \\ 0, & |t| > T/2 \end{cases} \qquad (6.16)$$

Substituting (6.16) in (6.14) yields

$$-\frac{\log Pe}{2BT}\Big|_{max} = \log(\hat{P}+1) - \log\left[\sum_{\ell=0}^{\infty} \frac{1}{2\ell+1}\left(\frac{\hat{P}}{1+\hat{P}}\right)^{\ell}\right] \qquad (6.17)$$

where

$$\hat{P} = P^2/4\sigma_o^2.$$

2) TRIANGULAR SIGNALS

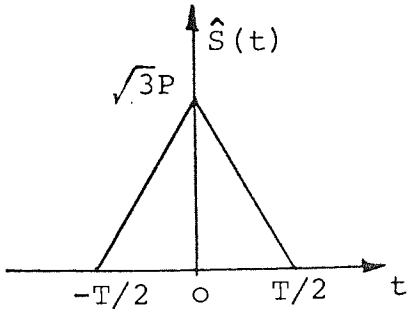

$$\hat{S}(t) = \begin{cases} \sqrt{3}P(1-2|t|/T), & |t| \leq T/2 \\ 0, & |t| > T/2 \end{cases} \qquad (6.18)$$

Using (6.18) in (6.14) and using a substitution $\zeta = 2t/T$ yields

$$-\frac{\log Pe_{max}}{2BT} = \int_0^1 [\log\{\hat{P}_1(\zeta)+1\} - \log\{\sum_{k=0}^{\infty} \frac{1}{2k+1}(\frac{\hat{P}_1(\zeta)}{1+\hat{P}_1(\zeta)})^k\}]d\zeta \qquad (6.19)$$

where

$$\hat{P}_1(\zeta) = 3P^2(1-\zeta^2)^2/4\sigma_o^2 .$$

3) HALF-WAVE SINUSOIDAL SIGNALS

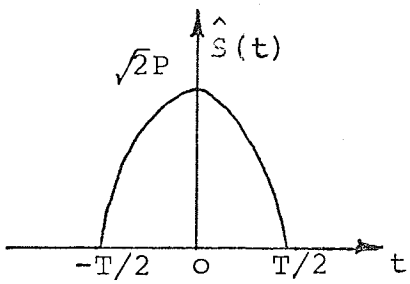

$$\hat{S}(t) = \begin{cases} \sqrt{2}P\cos(\frac{\pi t}{T}), & |t| \leq T/2 \\ 0, & |t| > T/2 \end{cases} \qquad (6.20)$$

Using (6.20) in (6.14) and using a substitution $\zeta=2t/T$ yields

$$-\frac{\log Pe_{max}}{2BT} = \int_0^1 [\log\{\hat{P}_2(\zeta)+1\} - \log\{\sum_{k=0}^{\infty} \frac{1}{2k+1}(\frac{\hat{P}_2(\zeta)}{1+\hat{P}_2(\zeta)})^k\}]\, d\zeta \qquad (6.21)$$

where

$$\hat{P}_2(\zeta) = P^2\cos^2(\pi\zeta/2)/2\sigma_o^2 .$$

Equation (6.17), (6.19) and (6.21) are plotted in Fig. 6.3 which shows the uniformly superior performance of square signals for systems of equal time-bandwidth products. The advantage is most pronounced for large SNR $(P/\sigma_o)^2$. It should be realized, however, that square signals generally require more bandwidth than other signals. This point will be discussed further in developing an optimal signal in the next section.

From (6.14) and Fig. 6.3 it is seen that for large 2BT, the optimum receiver performance is significantly superior to

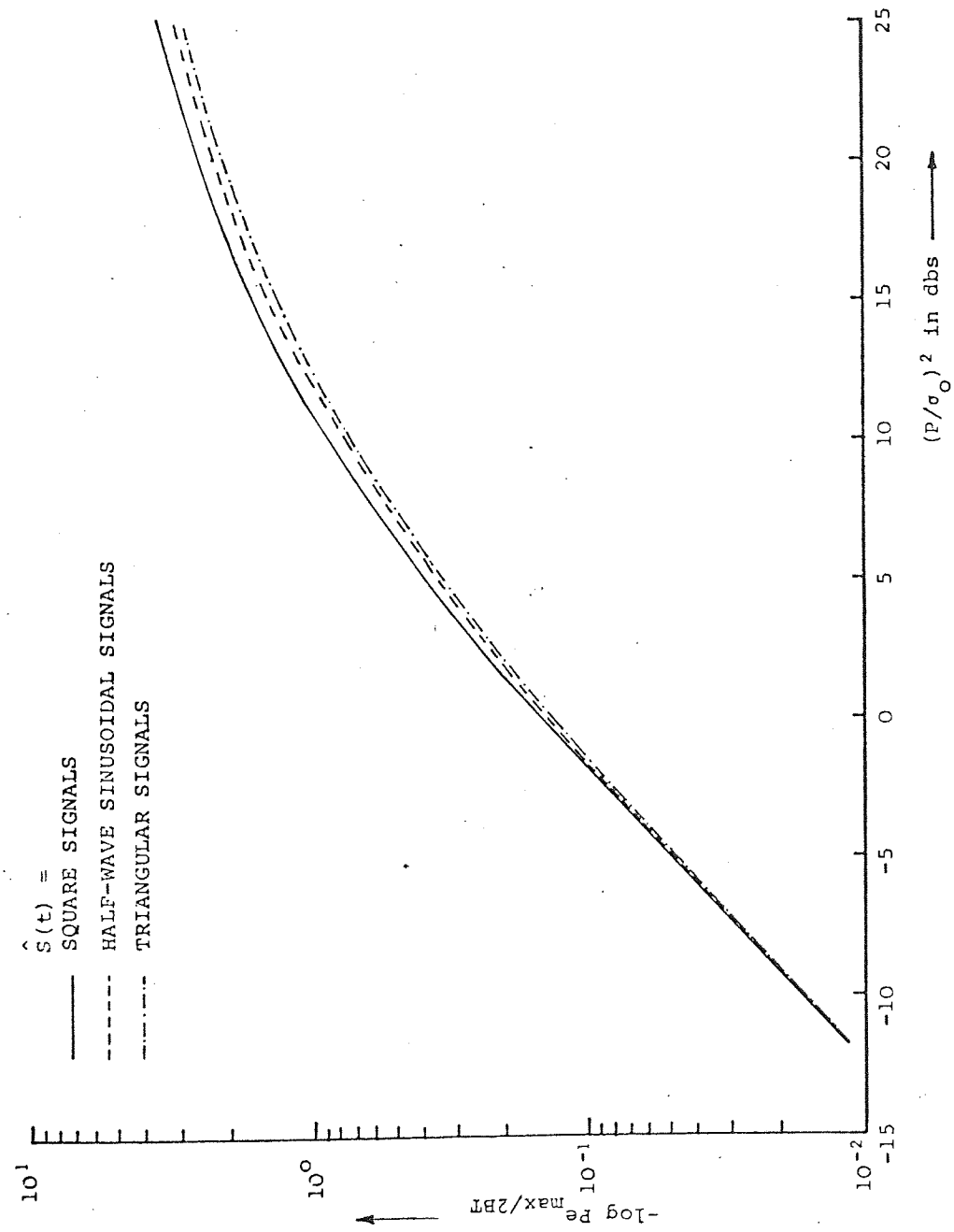

Fig. 6.3 Performance of optimum receiver for various transmitted signal shapes.

the performance of an optimal matched-filter receiver in the presence of additive Gaussian noise with the same average noise power. This superiority is consistent with the notion that a channel perturbed by additive atmospheric noise has a higher capacity than an otherwise similar channel perturbed by additive Gaussian noise having the same average power.

6.2.1 UPPER BOUNDS FOR INCOHERENT DETECTION

A straightforward method to evaluate the upper bound on the probability of error when the carrier phase of the received signal is unknown seems to be unavailable. However, the difficulty can be avoided if one realises that for fixed random phase θ the problem actually reduces to that of the problem of finding Pe_{max} for the case of coherent reception; then the results obtained above can be utilized.

Let $Pe_{max/\theta}$ be the upper bound on the probability of error when θ is fixed. For the transmitting system the solution of $Pe_{max/\theta}$ is readily obtained by using (6.15) of which the signal $s_1(t)$ is replaced by $s_1(t,\theta)$ i.e.,

$$Pe_{max/\theta} = \exp\left[a_2 \int_{-T/2}^{T/2} \{ s_1^4,(t,\theta) - a s_1^2(t,\theta) \}\, dt\right].$$

To obtain Pe_{max} one has to average $Pe_{max/\theta}$ over the entire range of $\theta\,[o, 2\pi]$. Thus

$$Pe_{max} = \frac{1}{2\pi} \int_o^{2\pi} Pe_{max/\theta}\, d\theta$$

where we have assumed the phase is uniformly distributed. We observe the $Pe_{max/\theta}$ is a function of $\int_o^T s_1^2(t;\theta)dt$ as well as $\int_o^T s_1^4(t, \theta)dt$. Therefore, it is necessary to evaluate these

two terms. Using $s_1=\hat{S}(t)\cos\{\omega_c t+\theta(t)\}$ we get

$$\int_o^T \hat{S}^2(t)\cos^2\{\omega_c t+\theta(t)\}dt=\frac{1}{2}\int_o^T \hat{S}^2(t)dt$$

and

$$\int_o^T \hat{S}^4(t)\cos^4\{\omega_c t+\theta(t)\}dt= \frac{3}{8}\int_o^T \hat{S}^4(t)dt.$$

Here we assume the integral of the double frequency terms is negligible.

The results from the above equation indicate that $Pe_{max/\theta}$ is independent of θ. Consequently, the error bounds for coherent and incoherent detectors appears to be the same. However, it is important to note that the probability of error for both cases are different; obviously, due to the completely known received signal, the coherent system should have better performance than the incoherent system. The optimum signal derived in the next section applies to this case also.

6.3 SIGNAL DESIGN

In this section we consider the problem of minimizing the upper bound on the probability of error by a choice of transmitting signal. We shall develop the optimal signal design, subject to some physically meaningful constraints. In the first case we minimize the Pe_{max} with only an energy constraint. The second case considered is to minimize Pe_{max} subject to energy and the mean-square bandwidth.

Here we define the energy and the mean-square bandwidth of the envelope signals as

$$E = \int_{-T/2}^{T/2} \hat{S}^2(t)dt \qquad (6.22)$$

and

$$W^2 = \int_{-T/2}^{T/2} \left[\frac{d\hat{S}(t)}{dt} \right]^2 dt \qquad (6.23)$$

respectively. As shown by Abramson [111], the mean-square bandwidth is the bandwidth that contains the major part of the signal energy. Since the optimal signal is difficult to obtain using the actual probability of error bound (6.14), we consider an asymptotic expression of error bound for small $s(t)/\sigma_o$ (6.15). This is justified since optimality is usually no longer the primary concern at stronger input signal levels.

From (6.15), it is obvious that to minimize Pe_{max} we need to minimize the performance index $F(S)$. We first consider the simpler case when the mean-square bandwidth W^2 is allowed to take any value and the signal energy is required to be finite.

To carry out the minimization, using the calculus of variation technique [112], we let

$$\hat{S}(t) = \hat{S}_{op}(t) + \varepsilon \hat{S}_A(t) \qquad (6.24)$$

where $\hat{S}_{op}(t)$ is the optimal signal envelope and $\hat{S}_A(t)$ is an arbitrary function. We impose the energy constraint (6.22). From (6.15) the index that we have to minimize becomes

$$F_1(S) = \int_{-T/2}^{T/2} \hat{S}^4(t)dt. \qquad (6.25)$$

Using the standard technique in constrained minimization theory [112], we define the function

$$I(S) = F_1(S) + \lambda_1 \left[\int_{-T/2}^{T/2} \hat{S}^2(t)dt - E \right], \qquad (6.26)$$

where λ_1 is a Lagrange multiplier, and E is the energy. Then on substituting (6.24) in (6.26) and carrying out

$$\left.\frac{dI(S)}{d\varepsilon}\right|_{\varepsilon=0} = 0 \qquad (6.27)$$

the final result becomes

$$\int_{-T/2}^{T/2} \hat{S}_A(t)\left[\lambda_1 \hat{S}_{op}(t) + 2\hat{S}^3_{op}(t)\right]dt = 0 \; . \qquad (6.28)$$

Since $\hat{S}_A(t)$ is arbitrary, the terms in the brackets must be identically zero, in which case

$$\lambda_1 \hat{S}_{op}(t) + 2\hat{S}^3_{op}(t) = 0, \qquad -T/2 < t < T/2. \qquad (6.29)$$

We use the given constraint on E of (6.22) to evaluate the constraint λ_1 as $-2\hat{S}^2_{op}(t)$. Finally the solution for optimal signal, found by integrating $\lambda_1 = -2E/T$ and substituting for λ_1 into (6.29), becomes

$$\hat{S}_{op}(t) = (E/T)^{\frac{1}{2}} \; , \qquad -T/2 < t < T/2 \; . \qquad (6.30)$$

The optimal signal, for this case, is a rectangular signal with given energy E and W^2 of (6.23) $= \infty$. This is shown in Fig. 6.4. Note that the signals considered in the last section agree with the results obtained here. However, it is obvious that the rectangular signal never exists in practice at the receiver, owing to the band limited nature of any phyisical communication channel. Actually, the transmitting signal appears distorted due to loss of high frequency components.

The problem of signal optimization is more meaningful if we

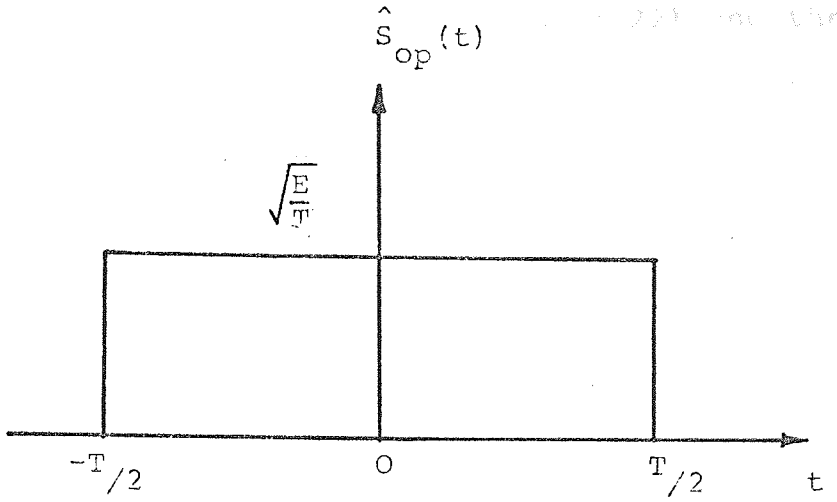

Fig. 6.4 Optimal signal with energy constraint

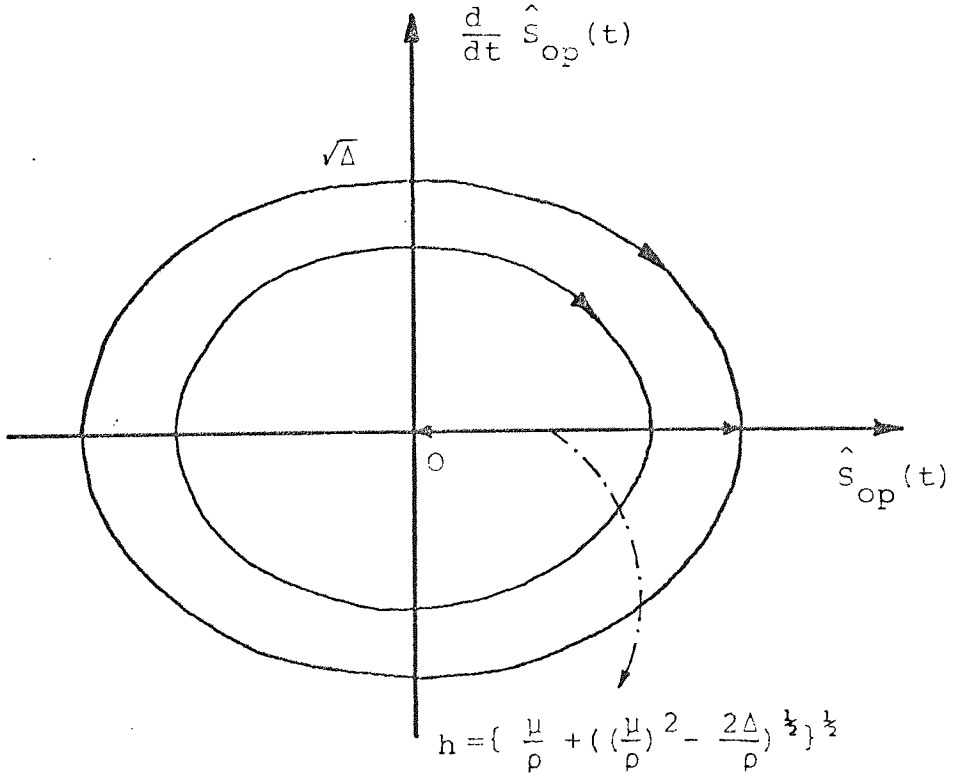

Fig. 6.5 Phase-plane trajectories.

constrain both the energy and bandwidth of $\hat{S}(t)$. We define the bandwidth as in (6.23) and the energy as in (6.22) and then assume that both are bounded by fixed finite values. We require, in addition, the end point assumption

$$\hat{S}_{op}(\pm T/2) = 0 \tag{6.31}$$

in order to avoid discontinuities at the end points. Then, for this case, the index I(S) for minimization is

$$I(S)=F(s)+\lambda_1\left[\int_{-T/2}^{T/2} \hat{S}^2(t)dt-E\right]+$$

$$+\lambda_2\left[\int_{-T/2}^{T/2} \left\{\frac{d\hat{S}(t)}{dt}\right\}^2 dt-W^2\right] \tag{6.32}$$

Wnere λ_1,λ_2 are Lagrange multipliers and F(s) is defined by (6.15a).

The details of the minimization process are similar to the first case. Using the calculus of variations with the boundary condition (6.31) we obtain the equation that specifies $\hat{S}_{op}(t)$ in the following form

$$\frac{d^2}{dt^2}\hat{S}_{op}(t)+\mu\hat{S}_{op}(t)=\rho\hat{S}^3_{op}(t) \tag{6.33}$$

where

$$\mu=-\lambda_1/\lambda_2 \quad \text{and} \quad \rho=2/\lambda_2 .$$

This is the non-linear differential equation that is known as Duffing's equation [113]. Integrating the above equation with respect to t yields

$$\{\frac{d}{dt}\hat{S}_{op}(t)\}^2+\mu\hat{S}^2_{op}(t)=\Delta+\frac{\rho}{2}\hat{S}^4_{op}(t) \qquad (6.34)$$

where Δ is an integration constant. For $\lambda<0$, real solutions exist only for $\Delta \geq 0$ and these are illustrated in Fig. 6.5 .

The origin is a singular trajectory (a centre), while the nontrival solutions are represented by a family of concentric closed paths. The latter represents the periodic solution of (6.33). From the phase-plane trajectories in Fig. 6.5 and (6.34), it is clear that $\hat{S}_{op}(t)$ is an even function, with maximum value h (see Fig. 6.5). The absolute value of the slope $\hat{S}_{op}(t)$ takes the maximum value at the end points ($t=\pm T/2$) and monotonically decreases reaching the minimum value of zero at $t=0$. If the slope at the end points $\sqrt{\Delta}$ increases, h increases regardless of μ and ρ and vice versa. This implies that the trajectory is unique for given T,E and W^2.

Using (6.34), (6.33) can be expressed in the following form

$$dt=\pm\frac{d\{\hat{S}_{op}(t)\}}{\left[\Delta-\mu\hat{S}^2_{op}(t)+\frac{\rho}{2}\hat{S}^4_{op}(t)\right]^{\frac{1}{2}}}, \quad \rho<0. \qquad (6.35)$$

In general, the above equation will involve elliptic integrals and elliptic functions. Reduction to a standard form can be easily carried out with the help of Appendix C. As seen from the Appendix, the solution depends on the values of μ and ρ. Since an analytical solution to yield μ and ρ in terms of the constraint parameters E and W^2 seems impossible, in practice μ and ρ are chosen to meet the required energy E and bandwidth W^2 using trial and error.

For $|\rho|$ small we could use the method of perturbation to

obtain an approximate solution of (6.33). For $\rho=0$, (6.33) possesses the periodic solution;

$$\hat{S}_{op}(t) = A\cos\sqrt{\mu}t \tag{6.36}$$

where the constants A and μ can be determined from the constraint equations (6.22) and (6.23). Let us characterize (6.36) as the solution of the initial-value problem

$$\hat{S}_{op}(t) = A, \qquad \frac{d}{dt}\hat{S}_{op}(t) = 0 \tag{6.37}$$

for $t=0$. If we apply the Poincare theorem [114], we know that for sufficiently small $|\rho|$, the solution of (6.33) satisfying (6.37) may be expressed as a power series in ρ. Let

$$\hat{S}_{op}(\tau) = S_a(\omega t) + \rho S_b(\omega t) + \rho^2 S_c(\omega t) + \ldots\ldots \tag{6.38}$$

be the expansion, where S_a, S_b..... is to be a periodic function of $\tau=\omega t$ of period 2π. The quantity ω is introduced as the true fundamental frequency and will be an analytic function of ρ. To determine ω, we introduce an expansion of the form

$$\omega = 1+\omega_1\rho + \omega_2\rho^2 + \ldots\ldots\ldots \tag{6.39}$$

where the first term is unity since the fundamental frequency reduces to unity for $\rho=0$. In terms of the new variable $\tau=\omega t$, (6.33) becomes

$$\omega^2 \frac{d^2}{d\tau^2}\hat{S}_{op}(\tau) + \mu\hat{S}_{op}(\tau) = \rho S^3_{op}(\tau). \tag{6.40}$$

If we substitute (6.38) and (6.39) in (6.40) and equate coefficients of corresponding powers of ρ, we obtain a sequence of nested differential equations in $S_a(t)$, $S_b(t)$,..... The first three are

$$\frac{d^2}{d\tau^2} S_a(\tau) + \mu S_a(\tau) = 0 \tag{6.41}$$

$$\frac{d^2}{d\tau^2} S_b(\tau) + \mu S_b(\tau) = S_a^3(\tau) - 2\omega_1 \frac{d^2 S_a(\tau)}{d\tau^2} \tag{6.42}$$

$$\frac{d^2}{d\tau^2} S_c(\tau) + \mu S_c(\tau) = 3S_a^2(\tau) S_b(\tau) - (\omega_1^2 + 2\omega_2) \frac{d^2 S_a(\tau)}{d\tau^2} -$$

$$\vdots \qquad - 2\omega_1 \frac{d^2}{d\tau^2} S_b(\tau) \tag{6.43}$$

etc.

Solutions of the above differential equations are

$$S_a(\tau) = A \cos\sqrt{\mu}\tau \tag{6.44}$$

$$S_b(\tau) = \frac{A^3}{32\mu} \{\cos\sqrt{\mu}\tau - \cos 3\sqrt{\mu}\tau\} \tag{6.45}$$

$$S_c(\tau) = \frac{3A^5}{128\mu^2} \left[\frac{23}{24}\cos\sqrt{\mu}\tau - \cos 3\sqrt{\mu}\tau + \frac{1}{24} \cos 5\sqrt{\mu}\tau\right]. \tag{6.46}$$

In obtaining the above solutions we have eliminated all the secular terms by imposing

$$\omega_1 = \frac{3A^2}{8\mu} \quad ; \qquad \omega_2 = -\frac{21A^4}{256\mu^2} \quad . \tag{6.47}$$

In a similar manner, the remaining terms of the two expansions (6.38) and (6.39) are determined by the initial conditions and

W_T^2 = Mean square bandwidth of a signal of duration T.

T = Signal duration in 10^{-2} Secs

W^2 = Mean square bandwidth in $10^4 (HZ)^2$

E = Energy in $Volt^2$

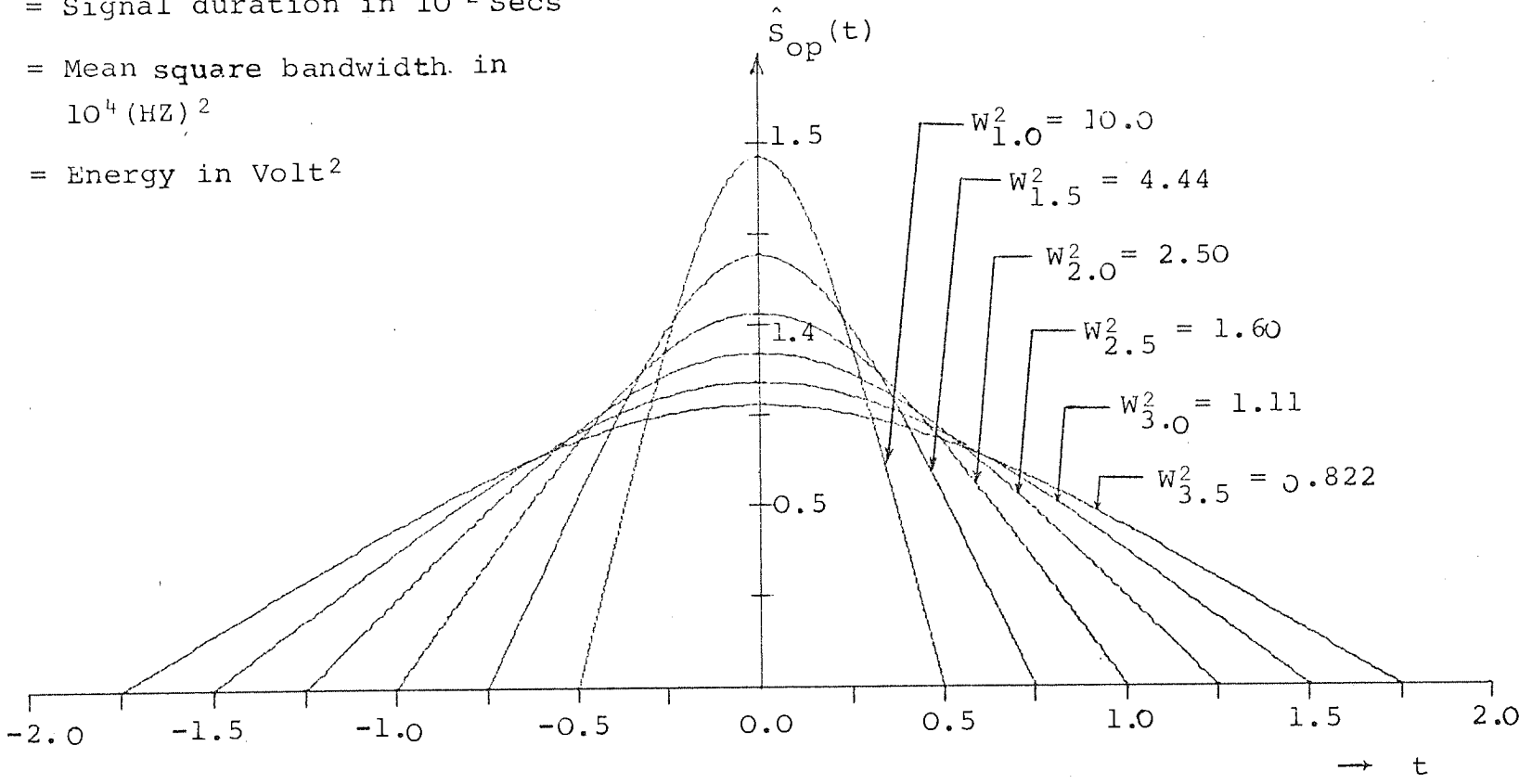

Fig. 6.6 Optimal signals with equal energy E=1.0

E_T = Energy of a signal of duration T.

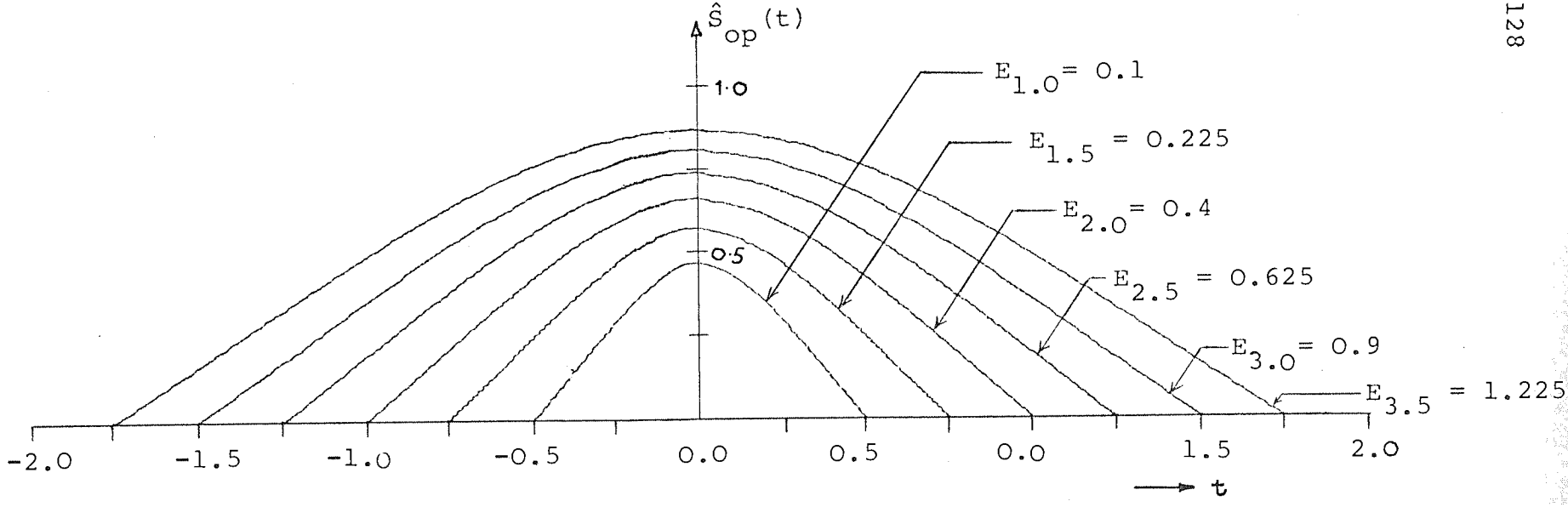

Fig. 6.7 Optimal signals with mean-square bandwidth 1.0 X 10^4 $(HZ)^2$

W_E^2 = Mean square bandwidth of a signal of energy E.

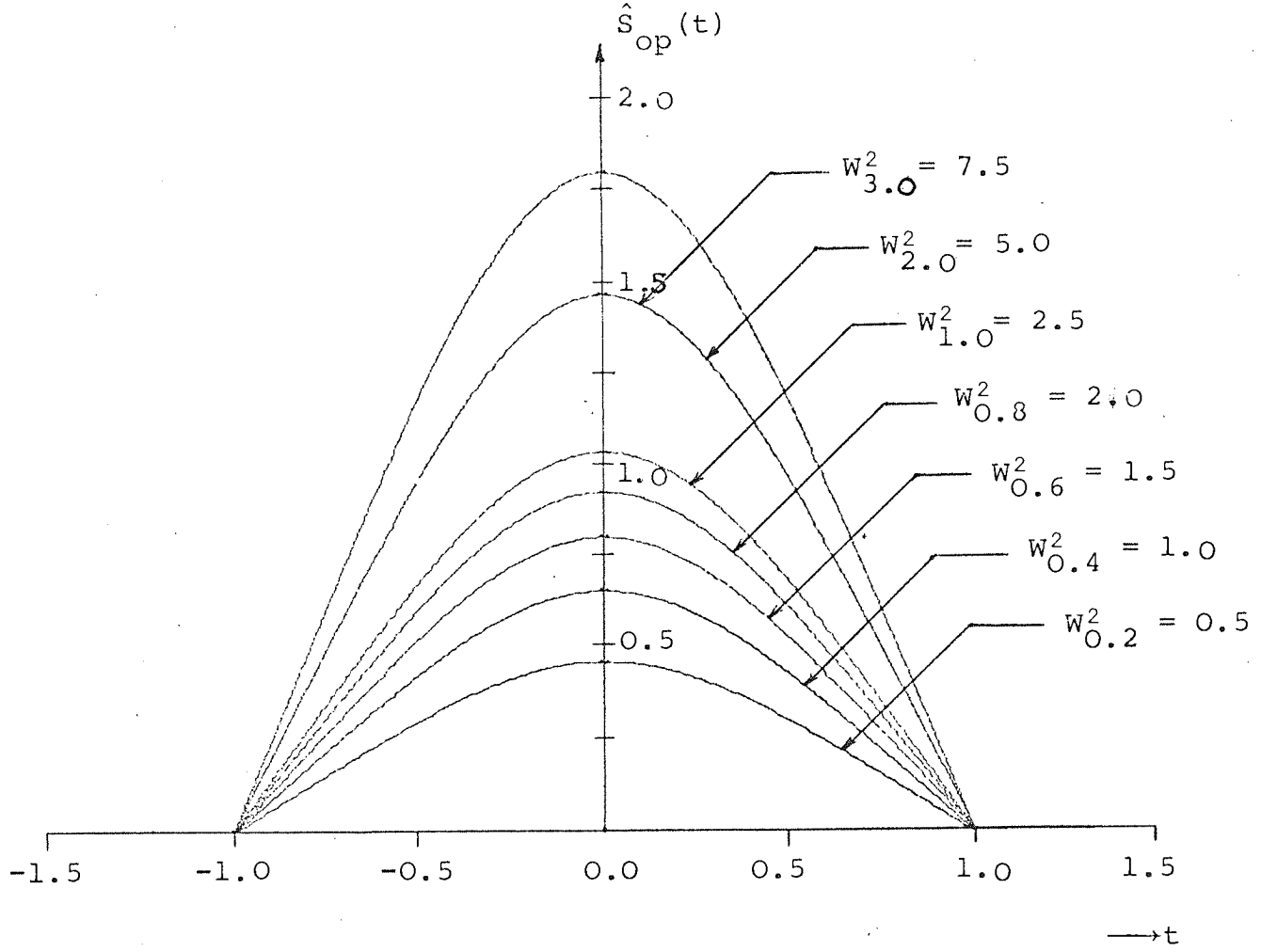

Fig.6.8 Optimal signals of equal duration
T = 2.0 X 10^{-2} secs

the requirement of periodicity.

It should be noted that the convergence of (6.38) will not be uniform in t for all t unless ω is exact, although it may be uniform in $\tau=\omega t$ for all τ.

Using (6.44), (6.45) and (4.46) in (6.38) and using the two integral constraints (6.22) and (6.23) the optimal signal for given signal energy, signal duration and given mean-square bandwidth can be computed. For given energy E, mean-square bandwidth W and the signal duration T, the optimal signal is unique. Some typical optimal signals with equal energy, equal bandwidth and equal duration are shown in Figs. 6.6,6.7,6.8 respectively. The relation between the signal energy E and signal duration for given bandwidth is shown in Fig. 6.9. Another property of the optimal signal $\hat{S}_{op}(t)$, which is useful in the calculations of system performance, is that

$$F = g(T)E^2 \tag{6.48}$$

where F is defined by

$$F = \int_{-T/2}^{T/2} \hat{S}_{op}^4(t)dt \tag{6.49}$$

and g(T) is a function of T. Fig. 6.10 shows the straight line plots of F/E vs. E for various values of T.

6.4 DISCUSSION

In this chapter a special case of the generalised hyperbolic distribution has been applied to the detection of known signals in the presence of noise to determine the optimal-receiver

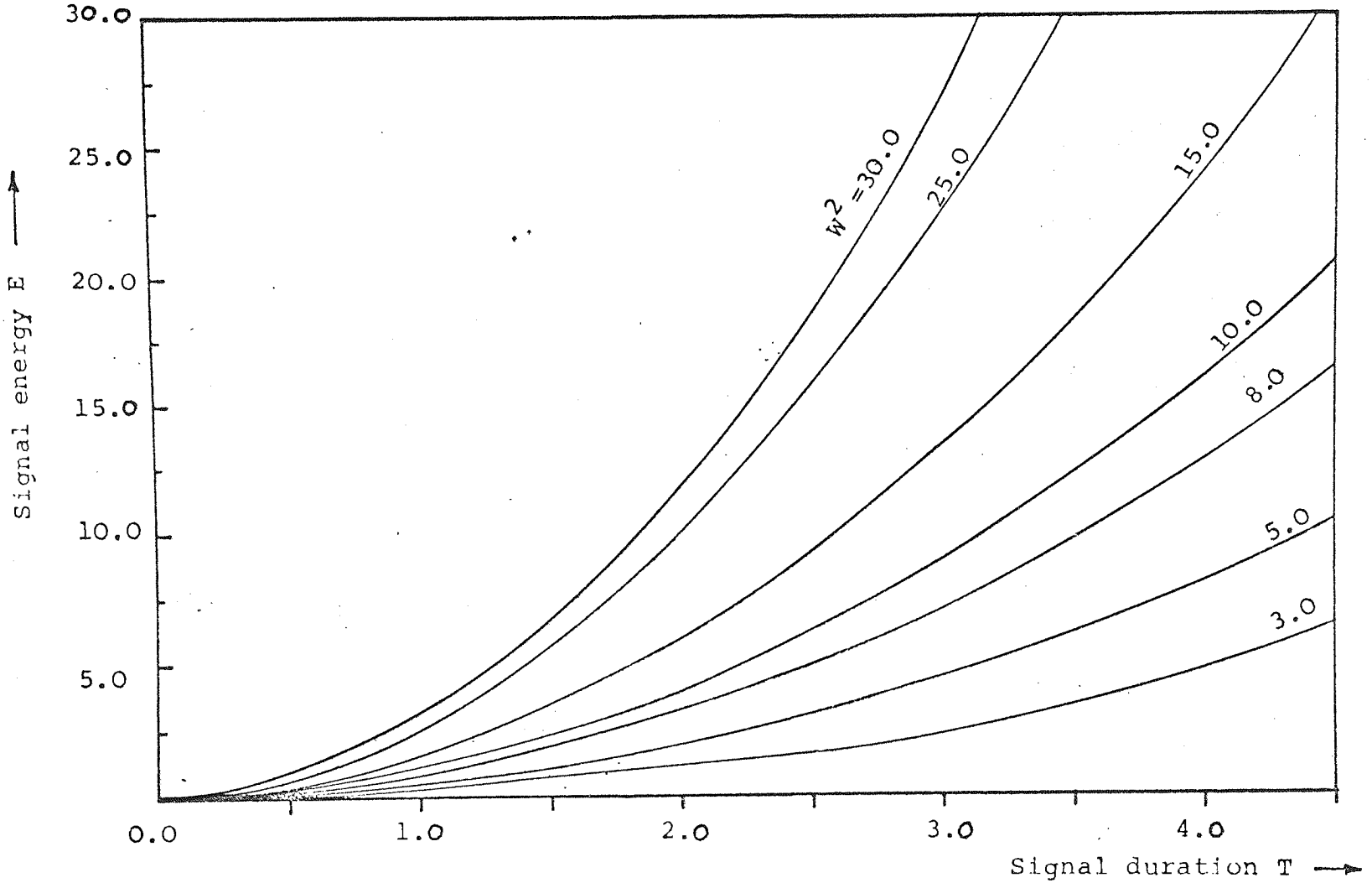

Fig. 6.9 Energy-duration curves for optimal signals for various mean-square bandwidths W^2.

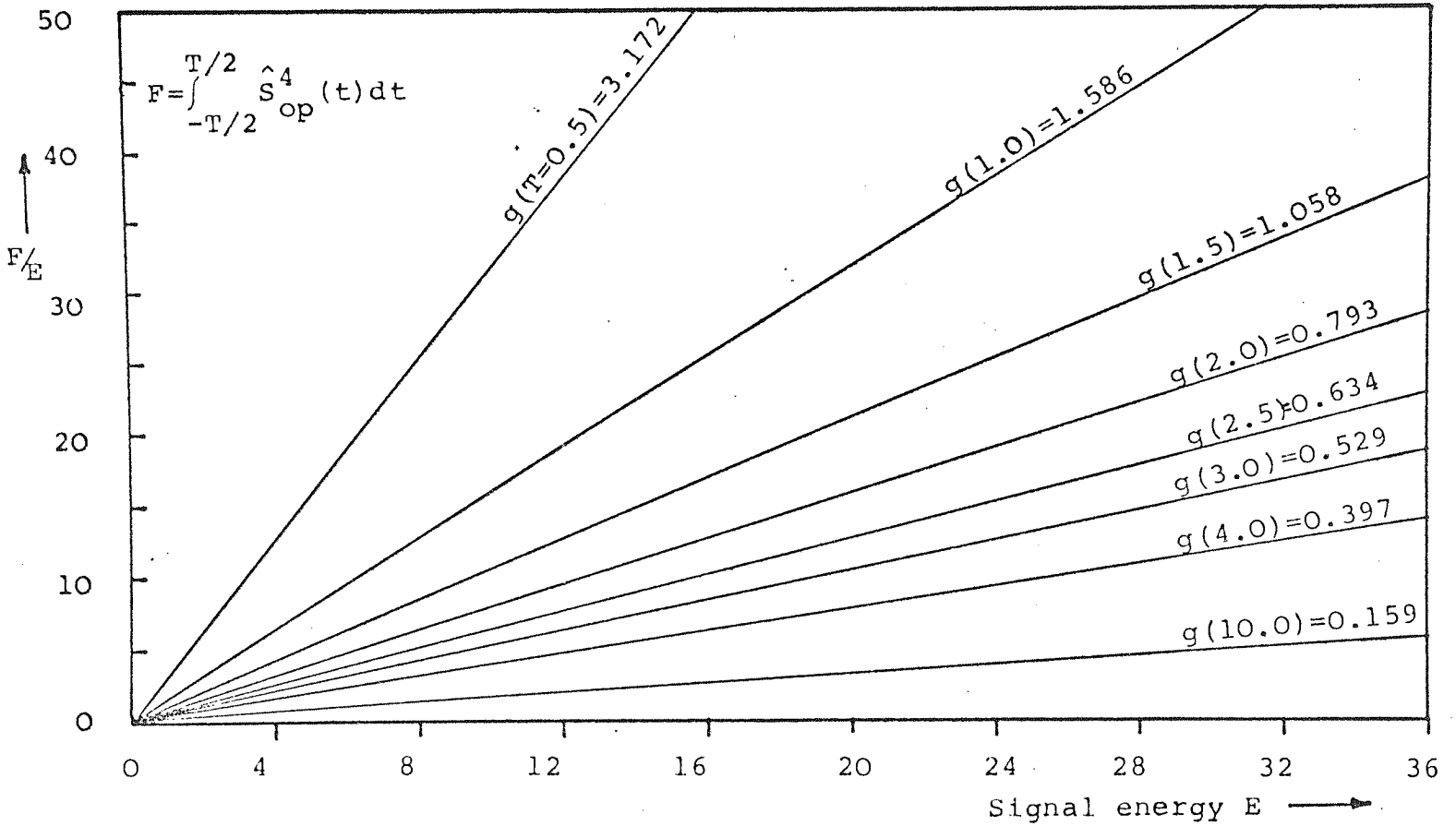

Fig. 6.10 F/E vs. E curves for various values of signal duration T.

structure. The important result suggested by the model is that the performance of an optimal receiver in the presence of non-Gaussian interference is sensitive to the signal shape. We have developed a signal design only for the case of small SNRs. This is justified since the optimality is usually no longer the primary concern at stronger SNRs. It is also observed that the optimum receiver performance in the presence of IN is significantly superior to the performance of an optimal matched-filter receiver in the presence of additive Gaussian noise with the same average noise power.

CHAPTER 7

LIKELIHOOD DETECTION OF SMALL SIGNALS IN NOISE

In this chapter, the problem of threshold detection where the intensity of the accompanying noise is comparable to, or even much greater than that of the signal, is considered. Using the criterion of asymptotic relative efficiency (ARE), the performance of the optimum (and suboptimum) detector is compared with that of the corresponding detector which is optimum for Gaussian noise. Both broad and narrow-band communication systems are considered.

7.1 INTRODUCTION

Recent investigations [41]-[45] have shown that, for the problem of detecting deterministic signals, the incorporation of a light limiter* structure into the usual optimal Gaussian detector structure results in robust detectors for broad classes of heavy-tailed non-Gaussian noise densities.

In this chapter, we look at the optimum detectors when the signals are very weak compared to the arbitrary noise added by the channel. Let R(t) denote a stochastic process $\{R(t): 0<t<T\}$ and R_ℓ ($\ell=1,.....M$) a finite sequence of random variables. We assume, as in the previous chapters, that the random variables are mutually independent, and that $\{R(t)\}$ is stationary, then $R_1,.....R_M$ is a set of independent and identically distributed random variables. The pdf of R_ℓ will be denoted by $p_R(r)$ and will comprise a complete statistical description of R(t). In order to obtain a broad family of pdfs we take the noise pdf $p_N(x)$ to be of the form

* The light limiter is described by (7.17)

$$p_N(x) = (1-\varepsilon)p_G(x) + \varepsilon p_X(x), \qquad 0<\varepsilon<1 \qquad (7.1)$$

where $p_G(x)$ is the Gaussian pdf and $p_X(x)$ is the generalised hyperbolic pdf. Density functions of the mixture form (7.1) have proven useful in modelling some non-Gaussian densities occurring in practice [115]-[117].

The detection problem involves the testing of the hypothesis H_o that the observed process R(t) is noise alone, versus the alternative H_1 that the process R(t) consists of signal plus noise. The decision rule is based on samples R_ℓ which belong to the noise distribution or to the distribution of a mixture of signal and noise. We shall compare the resulting non-linear detector performance on the basis of a decision rule with the aid of the so-called coefficient of asymptotic relative efficiency (ARE), proposed by Pitman [118].

An exact definition of ARE is given in Appendix D. The reference detector considered is the linear detector which is optimum for Gaussian noise.

Since ARE is used to compare the resulting nonlinear detectors with the linear detectors, this chapter is largely concerned with large sample detector performance.

7.2 BASE-BAND SYSTEM

According to the Neyman-Pearson lemma [119], the likelihood ratio for an ON-OFF keying system {see (6.6)}

$$\Lambda(\vec{r}) = \exp\Big[\sum_{\ell=1}^{M} \log p_R(r_\ell - S_\ell) - \sum_{\ell=1}^{M} \log p_R(r_\ell)\Big]$$

is calculated for the input data $\vec{R}$ and is compared to a threshold L_o. If $\Lambda(\vec{r})<L_o$, then we accept H_o 'noise only'. If $\Lambda(\vec{r})\geq L_o$,

then we accept H_1, 'signal and noise'. Using the Taylor series expansion around r_ℓ for the first summation on the right hand side of the above equation yields [43]

$$\Lambda(\vec{r}) = \exp\Big[\sum_{k=1}^{\infty} \frac{(-1)^k}{k!} \sum_{\ell=1}^{M} S_\ell^k \frac{d^k}{dr_\ell^k} \log p_R(r_\ell)\Big]. \qquad (7.2)$$

For weak signals, neglecting second and higher order terms in S_ℓ the above equation reduces to

$$\Lambda(\vec{r}) = \exp\Big\{\sum_{\ell=1}^{M} S_\ell g_{opt}[r_\ell]\Big\} \qquad (7.3)$$

where

$$g_{opt}[r] = -\frac{d}{dr} \log p_R(r) = -\frac{\dot{p}_R(r)}{p_R(r)} \quad , \qquad (7.4)$$

and $\dot{p}_R(r)$ is the first derivative of pdf $p_R(r)$ with respect to r. The detector structure (for small signal case) is therefore a nonlinear lagless section followed by a matched filter shown in Fig. 7.1.

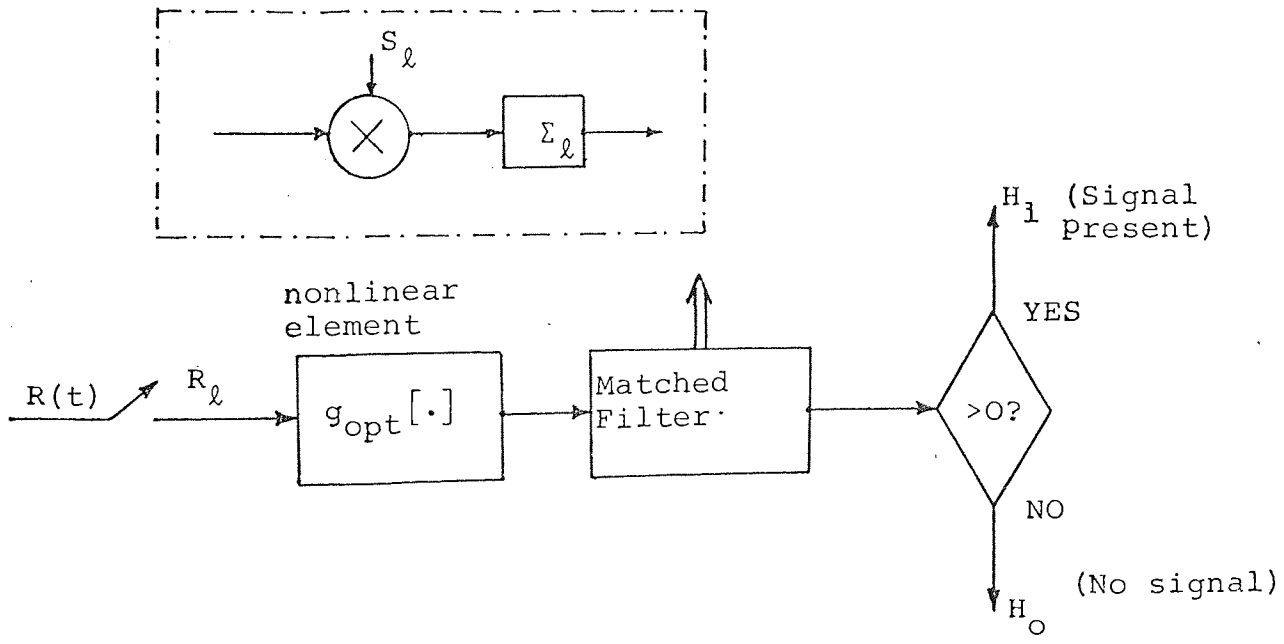

Fig. 7.1 Optimum detector structure for non-Gaussian noise.

The optimum character of the combination of the nonlinear element and the matched filter creates the impression that the nonlinear element transforms the input heavy-tailed noise into Gaussian statistics. A check based on several examples, however, shows that the nonlinear transformation device is not a normalizing link. For example, for logarithmically normal noise whose pdf is

$$p_N(x) = \frac{1}{x\sqrt{2\pi}\sigma_n} \exp\left[\frac{-\log^2 x}{2\sigma_n} \right]$$

the characteristic $g_{opt}[x]$ has the form {using (7.4)}

$$g_{opt}[x] = \frac{1}{x} \{1 + \frac{\log x}{\sigma_n} \} ,$$

while the normalization transformation is log x. It is seen that $g_{opt}[x] \neq \log x$ and consequently the nonlinear element does not normalize the input process.

When the nonlinear detector is used, the general expression of ARE when the reference detector is the linear filter was given recently by Miller et al [67] and Antonov et al [44]. A similar calculation partially based on the work done by Rudnick [120] also appears in Helstrom [121]. The expression is given by

$$\text{ARE} = \frac{\sigma_N^2 \langle \dot{g}[x] \rangle^2}{\langle g^2[x] \rangle - \langle g[x] \rangle^2} \qquad (7.5)$$

where σ_N^2 is the noise variance ($0 < \sigma_N^2 < \infty$) and $\dot{g}[x] = dg[x]/dx$. The maximum value of ARE, denoted by μ, is obtained by using (7.4) in (7.5) as

$$\mu = \max(\text{ARE}) = \sigma_N^2 \int_{-\infty}^{\infty} \frac{\dot{p}_R^2(x)}{p_R(x)}\, dx \qquad (7.6)$$

where we have assumed that $p_R(x)$ is an even function in x under hypothesis H_o.

7.3 NARROW-BAND SYSTEM

In this section we are interested in ARE_{NB} of the system shown in Fig. 7.2, which consists of a series connection of a nonlinear section and a matched filter.

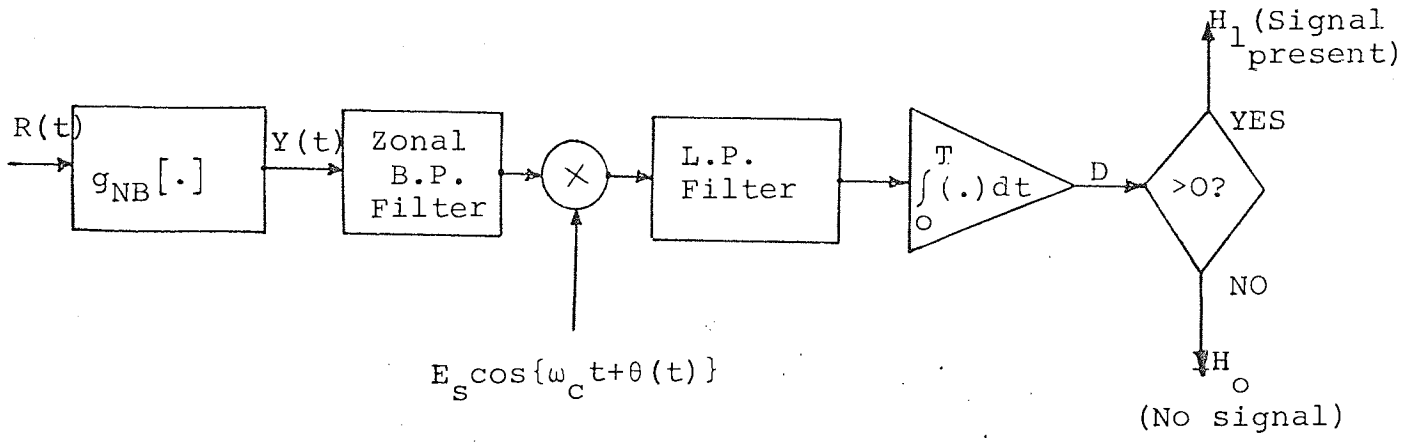

Fig. 7.2 Nonlinear detector under investigation

The input to the system consists of a narrow-band signal and additive narrow-band non-Gaussian noise and can be written as

$$R(t) = E_s(t)\cos\{\omega_c t+\theta(t)\}+E_n(t)\cos\{\omega_c t+\phi(t)\} \qquad (7.7)$$

where $E_s(t)$, $E_n(t)$ and $\theta(t)$, $\phi(t)$ are the envelopes and phases of the signal and noise respectively. We assume that the signal and noise, both of which are amplitude and/or phase modulated and centred on the same carrier frequency ω_c, are uncorrelated. The phases θ and ϕ are independent of the envelopes E_s and E_n respectively. We can express (7.7) as

$$R(t) = e(t)\cos\psi(t) \tag{7.8}$$

where

$$\psi(t) = \omega_c t + \alpha(t),$$

$$e(t) = \left[E_s^2(t) + E_n^2(t) + 2E_s(t)E_n(t)\cos\{\phi(t)-\theta(t)\}\right]^{\frac{1}{2}}$$

and

$$\alpha(t) = \tan^{-1}\left[\frac{E_s(t)\sin\theta(t) + E_n(t)\sin\phi(t)}{E_s(t)\cos\theta(t) + E_n(t)\cos\phi(t)}\right] . \tag{7.9}$$

We assume that $e(t)$ and $\alpha(t)$ of the process (7.8) change slowly in comparison with $\cos\omega_c t$. This assumption is justified for most practical cases.

The output of the nonlinear element is given by

$$Y(t) = g_{NB}[R(t)]. \tag{7.10}$$

Expanding $g_{NB}[R(t)]$ into a Fourier series as a periodic function of the argument $\psi(t)$ the above equation can be expressed as

$$Y(t) = \sum_{\ell=1}^{\infty} K_\ell[e(t)]\cos\ell\psi(t). \tag{7.11}$$

To find the constants $K_\ell[e(t)]$, we multiply through by $\cos\ell\psi(t)$ and integrate over $[-\pi,\pi]$. All terms on the R.H.S. vanish except the $K_\ell[e(t)]$ term, since

$$\int_{-\pi}^{\pi} \cos i\psi(t)\cos k\psi(t)\,d\psi(t) = 0 \text{ for } i\neq k.$$

Using (7.8), (7.10) and (7.11) this gives us

$$K_{\ell}[e(t)] = \frac{1}{\pi}\int_{-\pi}^{\pi} g_{NB}[e(t)\cos\psi(t)]\cos\ell\psi(t)\,d\psi(t)$$

$$\ell=1,2..... \qquad (7.12)$$

From (7.11), the output of the zonal band-pass filter is (neglecting higher frequency terms)

$$Y_B(t) = K_1[e(t)]\cos\psi(t) \qquad (7.13)$$

where $K_1[e(t)]$ is defined by (7.12){ whenℓ =1} . Multiplying (7.13) by $E_s(t)\cos\{\omega_c t+\theta(t)\}$ and integrating with respect to t between O and T yields the decision variable

$$D = \int_0^T E_s(t)K_1[e(t)]\cos\{\alpha(t)-\theta(t)\}dt \qquad (7.14)$$

where we have neglected all higher frequency terms. Assuming the integrand of the above equation has a bounded spectrum, the above equation can be written in a discrete form as [122]

$$D = \sum_{\ell=1}^{M} E_s(\frac{\ell}{2B})K_1[e(\frac{\ell}{2B})]\cos\{\alpha(\frac{\ell}{2B})-\theta(\frac{\ell}{2B})\} \qquad (7.14a)$$

or

$$D = \Delta t \sum_{\ell=1}^{M} E_{s\ell}K_1[e_{\ell}]\cos\{\alpha_{\ell}-\theta_{\ell}\} \qquad (7.14b)$$

where $E_{s\ell}=E_s(t_{\ell})$ is the ℓ^{th} sample, B is the bandwidth, $\Delta t=1/2B$ is the interval between the readings and $M=T/\Delta t$ is the number of samples taken (M is assumed to be large). The crucial point in the sampling method is as follows: in (7.14a) let $M\to\infty$ and $B\to\infty$ simultaneously, so that $M=2BT$ remains valid. Then the sum in (7.14a), by definition of an integral in the Reimann sense, is equal, in the limit as $M\to\infty$, to (7.14).

As the number of samples M becomes large the pdf of the random variable D approaches Gaussian (central limit theorem). The density is therefore fully characterized by its mean $\langle D \rangle$ (when a signal is present) and the variance $\langle D^2 \rangle$.

When the nonlinear element at the input of the detector is not present, the output SNR is given by $E/(N_o/2)$, where E is the energy of the signal and N_o is the spectral density of the input noise (uniform spectrum due to white noise). The ARE_{NB} for the detector of Fig. 7.2 can then be written as

$$ARE_{NB} = \frac{N_o \langle D \rangle^2}{2E\langle D^2 \rangle} \tag{7.15}$$

where $\langle D \rangle^2 / \langle D^2 \rangle$ is the SNR at the output of the nonlinear detector. Using the results of Appendix E the above equation can be written as

$$ARE_{NB} = \frac{\sigma_N^2 \langle \frac{K_1[e]}{e} + \dot{K}_1[e] \rangle_e^2}{2\langle K_1^2[e] \rangle_e} \quad . \tag{7.16}$$

Note that σ_N^2 is the variance of the low-pass process. For v^{th} law devices i.e.,

$$g_{NB}[e] = \begin{cases} ae^v, & e \geq 0 \\ -a|e|^v, & e \leq 0, \end{cases} \tag{7.17}$$

Using (7.12) in (7.16) the ARE_{NB} reduces to

$$ARE_{NB} = \frac{(v+1)^2 \sigma_N^2 \langle e^{v-1} \rangle_e^2}{2\langle e^{2v} \rangle_e} \quad . \tag{7.18}$$

This agrees with the results obtained by Berglund [123]. For a Rayleigh distributed envelope i.e.,

$$p_\eta(e) = \frac{e}{\sigma^2} \exp(-e^2/2\sigma^2)$$

and $v=0$ in (7.17) {hard limiter}, ARE_{NB} takes the value of $\pi/4$ which is in agreement with the well known result [105]. For the case of strong, unmodulated sine-wave interference (7.16), reduces to

$$ARE_{NB} = 4/(v+1)^2.$$

The maximum degradation due to this type of interference is 6 db, occurring when the nonlinear amplifier is an ideal limiter.

The maximum value of ARE_{NB}, denoted by μ_{NB} is obtained when the nonlinear function $\hat{K}_1[e]$ {which specifies the optimum nonlinearity $g_{NB,opt}[e]$} is chosen as (see Appendix F)

$$\hat{K}_1[e] = - B_c \frac{d}{de} \log\left[\frac{p_\eta(e)}{e}\right] \tag{7.19}$$

where B_c is an arbitrary gain constant. For optimum nonlinearity, using (7.19) in (7.16), μ_{NB} becomes

$$\mu_{NB} = \frac{\sigma_N^2}{2} \langle \{\frac{d}{de} \log[\frac{p_\eta(e)}{e}]\}^2 \rangle \tag{7.20}$$

7.4 NONLINEAR ELEMENT FOR OPTIMUM DETECTORS

7.4.1 BASE-BAND SYSTEM

Using (7.1) in (7.4) and substituting for

$$p_X(x) = K(\alpha,\beta)\sigma_o^{\alpha\beta}\{|x|^\alpha+\sigma_o^\alpha\}^{-(\beta+1/\alpha)} \tag{5.8}$$

and

$$p_G(x) = \frac{1}{(2\pi\sigma_g^2)^{\frac{1}{2}}} \exp\{-x^2/2\sigma_g^2\}, \quad -\infty<x<\infty \tag{7.21}$$

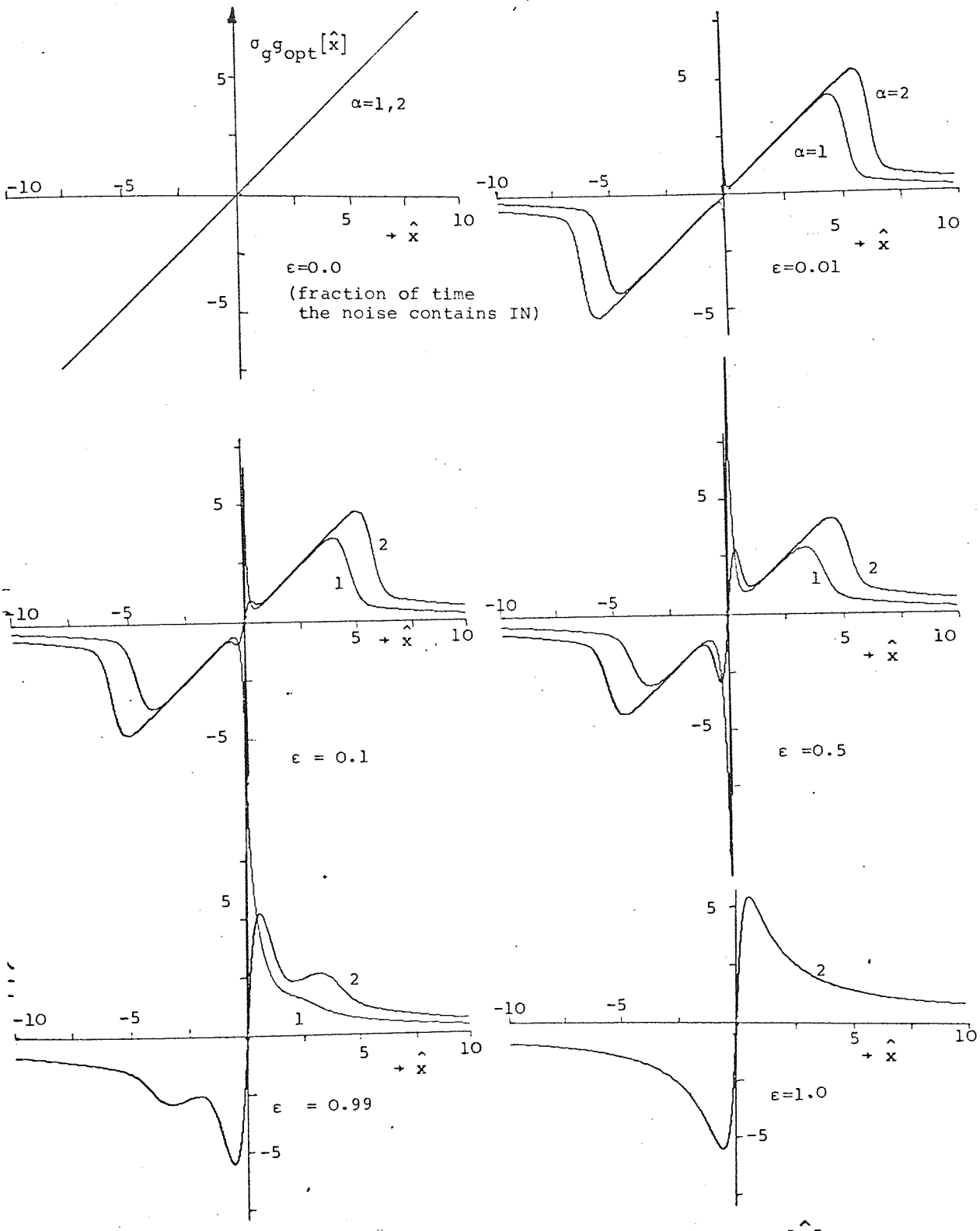

Fig. 7.3 Normalized optimum nonlinearities $\sigma_g g_{opt}[\hat{x}]$ for IN parameters α=1,2 and β=3.0 (IN variance to Gaussian noise variance ratio R=0.1).

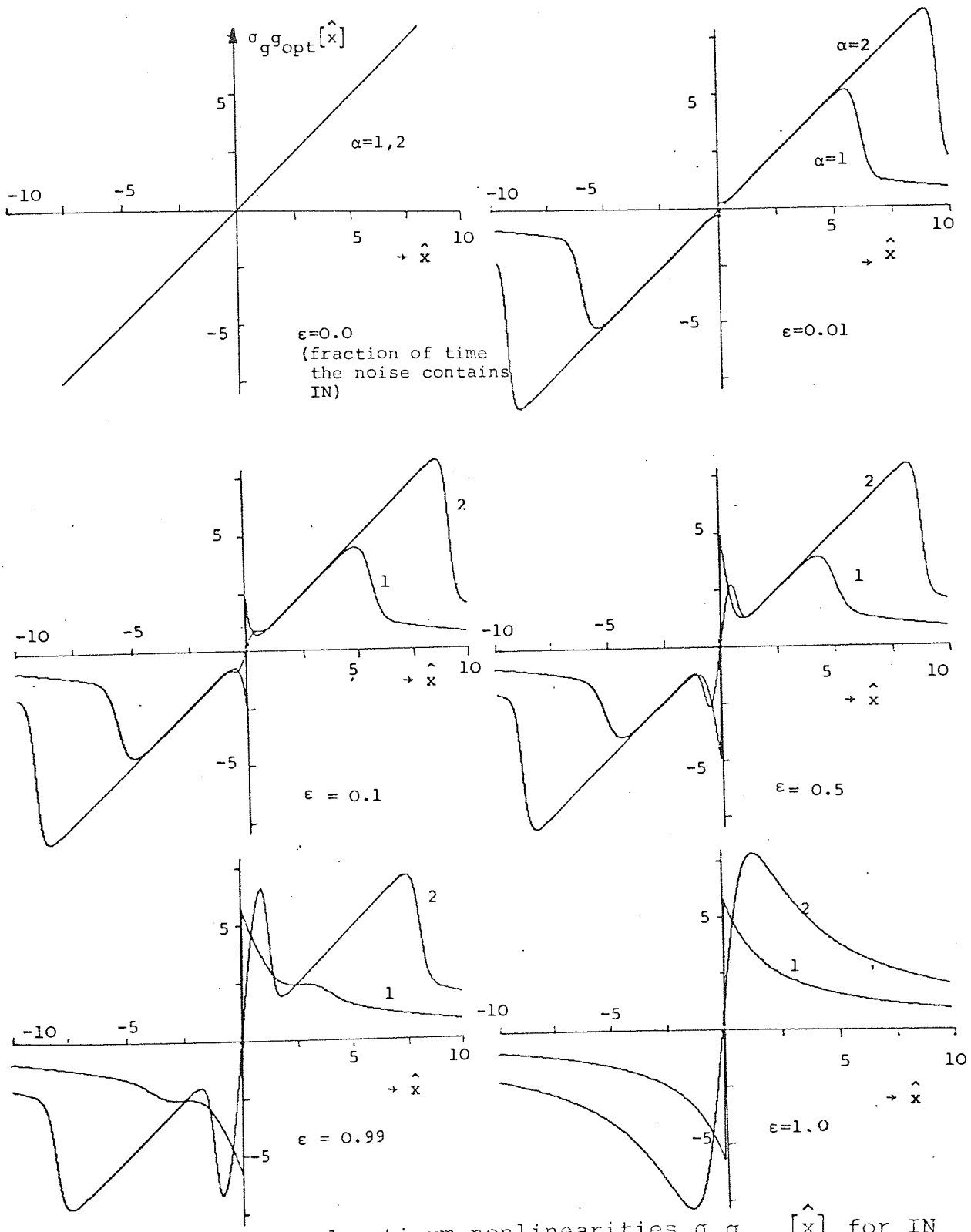

Fig. 7.4 Normalized optimum nonlinearities $\sigma_g g_{opt}[\hat{x}]$ for IN parameters α=1,2 and β=10.0. (IN variance to Gaussian noise variance ratio R=0.1).

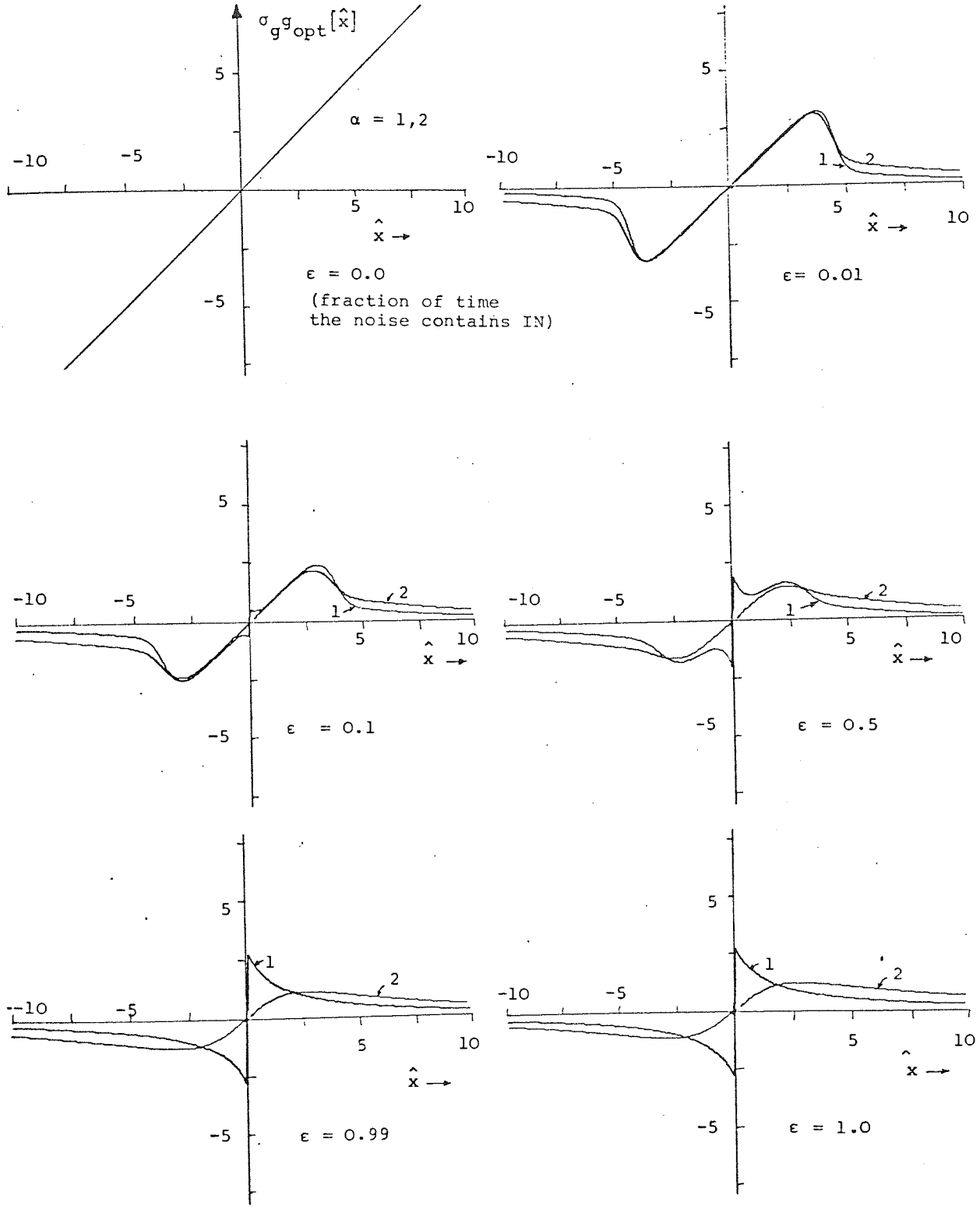

Fig. 7.5 Normalized optimum nonlinearities $\sigma_g g_{opt}[\hat{x}]$ for IN parameters α=1,2 and ρ=3.0 (IN variance to Gaussian noise variance ratio R=2.0).

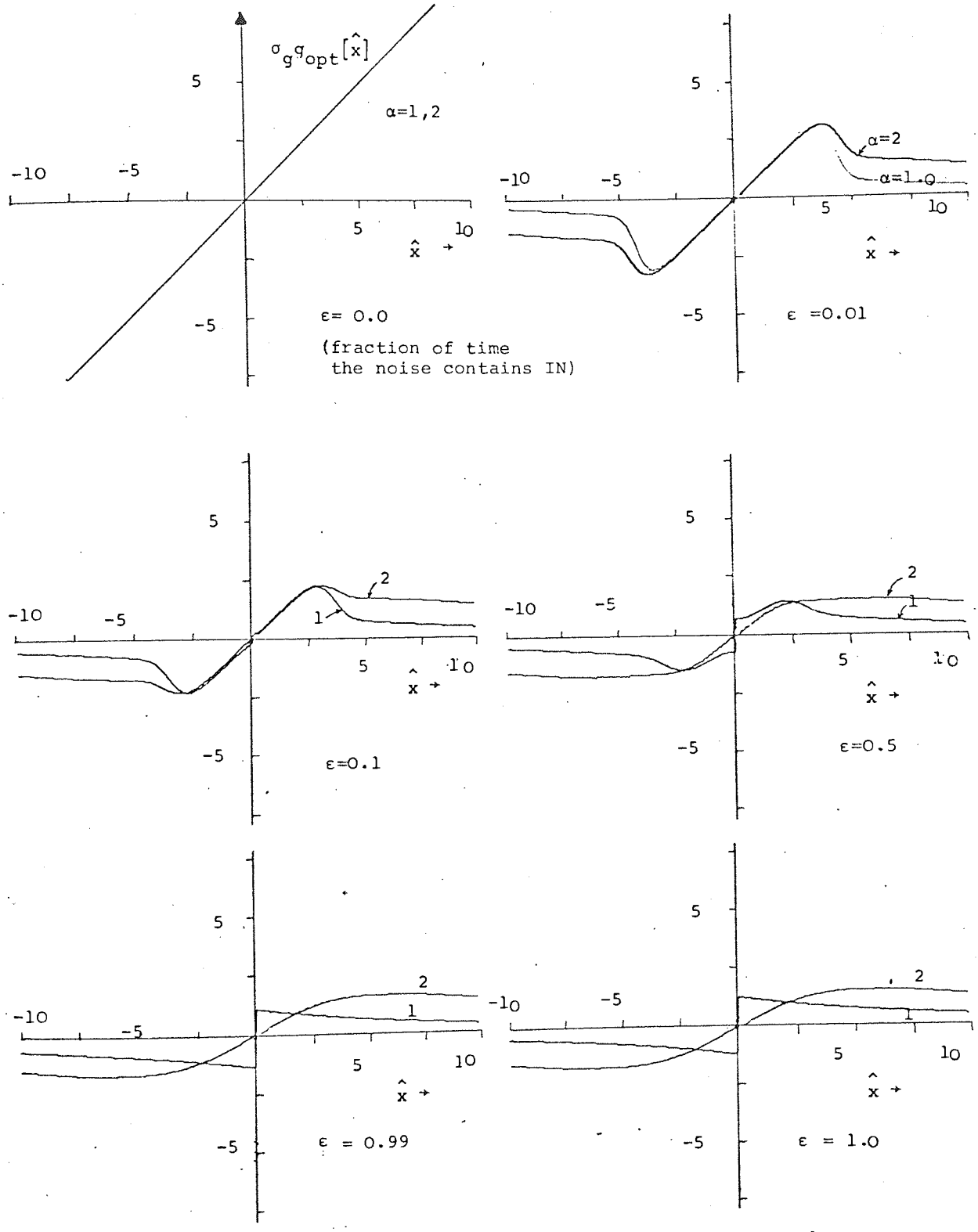

Fig. 7.6 Normalized optimum nonlinearities $\sigma_g q_{opt}[\hat{x}]$ for IN parameters α=1,2 and β=10.0 (IN variance to Gaussian noise variance ratio R=2.0).

the nonlinear element for the mixture noise becomes

$$\sigma_g g_{opt}[\hat{x}] = \frac{NUM1}{DEN1} \tag{7.22}$$

where

$$\begin{aligned}
NUM1 &= (1-\varepsilon)\hat{x}e_{\hat{x}} + \varepsilon K(\alpha,\beta)(\alpha\beta+1)\,\mathrm{sgn}(\hat{x})\,|\hat{x}|^{\alpha-1} f_{\hat{x}}^{-(\beta+1+1/\alpha)} R' \\
DEN1 &= (1-\varepsilon)e_{\hat{x}} + \frac{\varepsilon}{\sqrt{R}} K(\alpha,\beta) f_{\hat{x}}^{-(\beta+1/\alpha)} \\
\hat{x} &= x/\sigma_g \quad \text{(normalized variable)} \\
f_{\hat{x}} &= 1+(\hat{x}/\sqrt{R})^{\alpha} \\
R' &= R^{-(\alpha+1)/2} \\
e_{\hat{x}} &= \frac{1}{\sqrt{2\pi}} \exp\{-\hat{x}^2/2\} \\
R &= \sigma_o^2/\sigma_g^2 \quad \text{(Impulse noise variance to Gaussian noise variance ratio)} \\
K(\alpha,\beta) &\text{ is defined by (5.8)} \\
\mathrm{sgn}(\hat{x}) &= \text{signum function } (=1 \text{ for } \hat{x}\geq 0;\ =-1 \text{ for } \hat{x}\leq 0).
\end{aligned} \tag{7.23}$$

Figs 7.3 - 7.6 give plots of the optimum nonlinearity using (7.22) for values of $R = 0.1, 2.0$. In each of the six figures, plots are given for $\varepsilon = 0.0, 0.01, 0.1, 0.5, 0.99, 1.0$; $\alpha = 1.0, 2.0$, for each $\beta = 3.0, 10.0$.

Note that the degenerate case of $\varepsilon=0$ (Gaussian background noise only), $g_{opt}[\hat{x}]$ is a linear function of $\hat{x}$. Such must be the case, of course. For values of ε strictly between 0 and 1, the mixture is nondegenerate, and $g_{opt}[\hat{x}]$ has the general shape of a piecewise linear function for small $|\hat{x}|$ (with a discontinuity at $\hat{x}=0$) and of a limiter for large $|\hat{x}|$. The larger the values of R, the ratio of non-Gaussian to Gaussian noise variances, the more limiting the structure becomes. This result is also not

very surprising. For $\varepsilon>0.0$, on keeping α and β fixed and $|\hat{x}|\to\infty$, one has

$$g_{opt}[\hat{x}]_{\lim|\hat{x}|\to\infty}\to 0.$$

Thus, whatever the finite, positive values of the parameter α and β in the non-Gaussian density, the corresponding optimum non-linearity approaches zero as $|\hat{x}|$ approaches infinity. The way it approaches this asymptotic value depends, however, on the values of α and β. Substituting the density (7.1) and the expressions for $p_G(x)$ and $p_X(x)$ from (7.21) into the expression for μ of (7.6) gives

$$\mu = 2\{(1+\varepsilon)+\varepsilon\langle x^2\rangle/\sigma_g^2\}\int_0^\infty dy\left(\frac{NUM2}{DEN2}\right) \qquad (7.24)$$

where

$$NUM2 = \frac{(1-\varepsilon)^2}{\sqrt{2\pi}}\, y^2 e_y + 2(1-\varepsilon)y^\alpha e_y \Gamma_1 f_y^{-(\beta+\frac{1}{\alpha}+1)} + \Gamma_1^2 y^{2(\alpha-1)} f_y^{-2(\beta+\frac{1}{\alpha}+1)}$$

$$DEN2 = (1-\varepsilon)e_y + \frac{\varepsilon K(\alpha,\beta)}{\sqrt{R}}\, f_y^{-(\beta+1/\alpha)}$$

$$\Gamma_1 = \varepsilon K(\alpha,\beta)(\alpha\beta+1)/\{R\}^{(\alpha+1)/2}$$

$\langle x^2\rangle$, f_y and e_y are defined by (5.9) and (7.23) respectively. For $\varepsilon=0$ (IN only) a closed form expression of (7.24) can be obtained as

$$\mu = \begin{cases} \dfrac{\Gamma(\beta-\frac{2}{\alpha})\Gamma(\frac{3}{\alpha})\Gamma(\beta+\frac{1}{\alpha})(\alpha\beta+1)^2\Gamma(\beta+\frac{2}{\alpha})\Gamma(2-\frac{1}{\alpha})}{\Gamma^2(\beta)\Gamma^2(\frac{1}{\alpha})\Gamma(\beta+2+\frac{1}{\alpha})}, & \alpha\beta>2 \\ 0, & \alpha\beta\leq 2 \end{cases} \qquad (7.25)$$

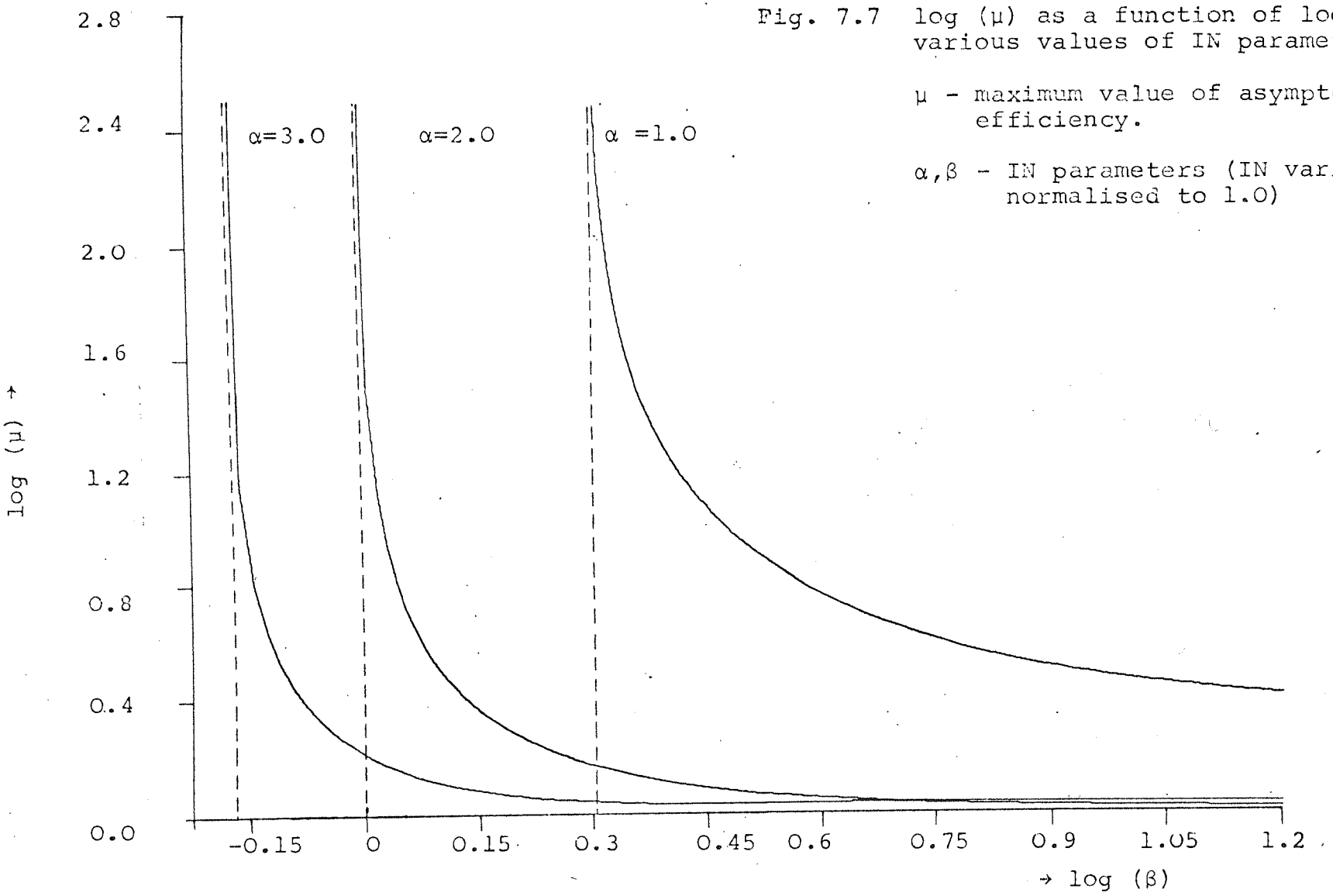

Fig. 7.7 log (μ) as a function of log(β) for various values of IN parameter α

μ - maximum value of asymptotic relative efficiency.

α,β - IN parameters (IN variance is normalised to 1.0)

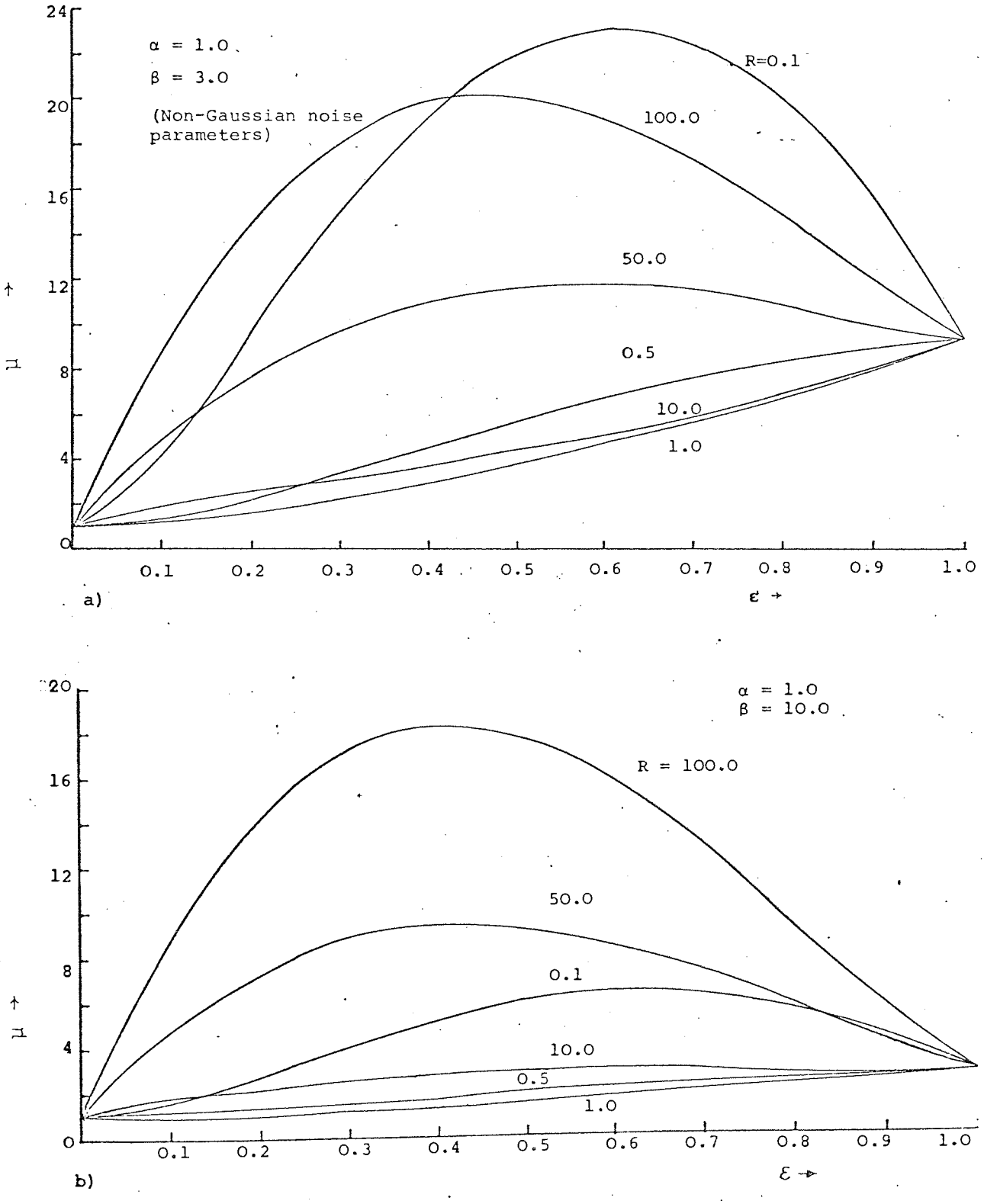

Fig. 7.8 Maximum asymptotic relative efficiency μ vs. the fraction of time the noise contains IN ε (R - IN variance to Gaussian noise variance ratio).

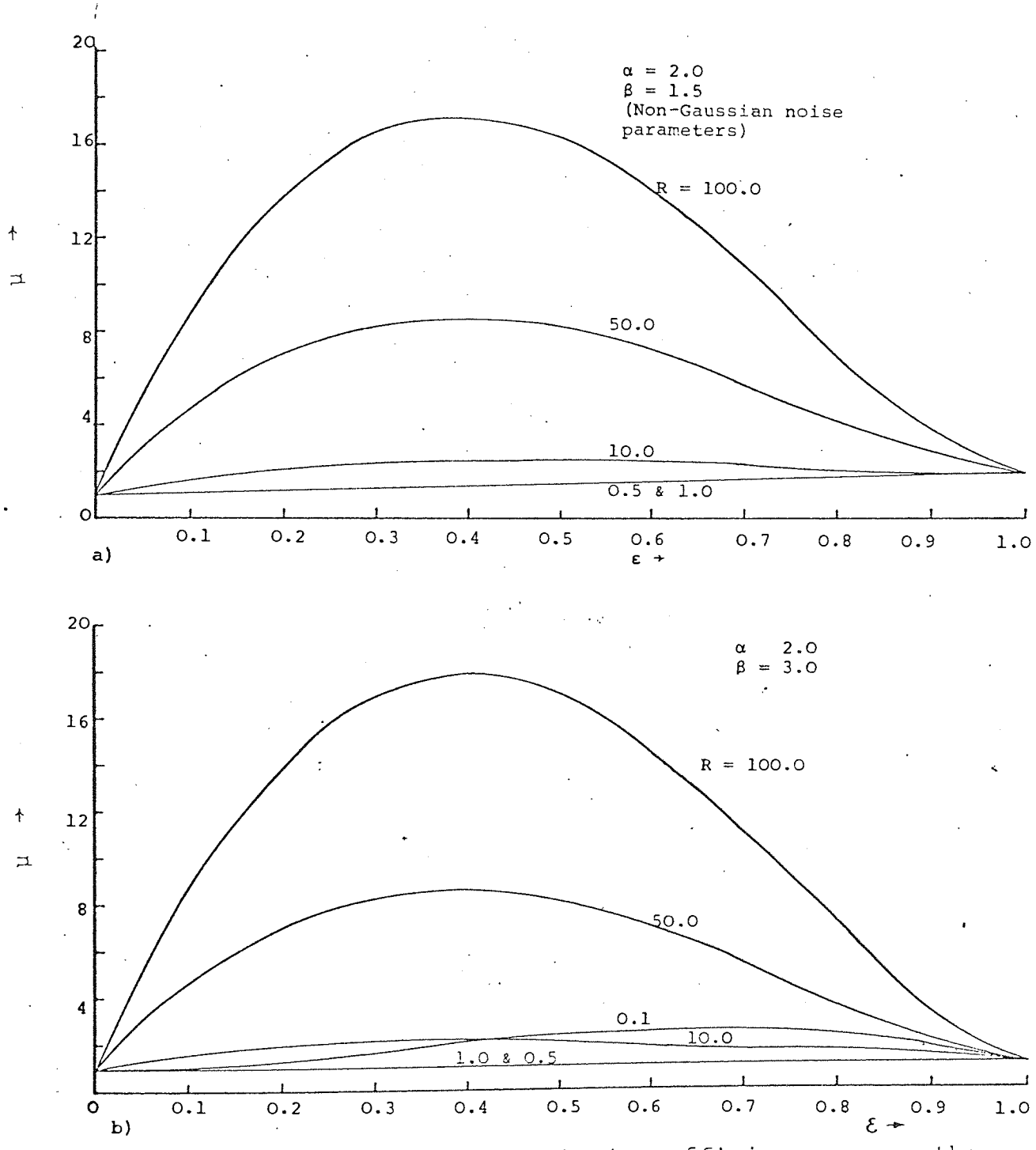

Fig. 7.9 Maximum asymptotic relative efficiency μ vs. the fraction of time the noise contains IN ε (R - IN variance to Gaussian noise variance ratio).

The above equation is plotted against β in Fig. 7.7 for various values of α. From the figure, we see that μ approaches 1 as β (for all α) increases. This must be the case, since as $\beta\to\infty$, the process becomes less impulsive and hence the optimum nonlinearity tends to become linear. The performance of this nonlinearity compared to the matched filter would therefore be the same. For α=1.0,2.0,3.0 μ becomes infinity at β=2.0,1.0 and 0.67 respectively because at these values the variance of the IN process becomes infinity (little limiting in this situation would give a great improvement in performance over the matched filter).

For various combinations of R and ε the R.H.S. of (7.24) was integrated numerically. The results are plotted in Figs. 7.8, 7.9. It is apparent from these curves that for all $\varepsilon[0,1]$, μ is large for both extremely small and extremely large values of R (i.e. R<<1 and R>>1) in comparison to its value for values of R near to unity. It also seems that, for intermediate values of $\varepsilon(\tilde{\approx}0.5)$, arbitrarily large values of μ can be obtained by letting either $R\to 0$ or $R\to\infty$. This situation arises when $\sigma_o\to 0$ or $\sigma_g\to 0$. This can be seen when either σ_o or σ_g=0, although this is not a physically realistic situation. Assuming that the pdf $p_G(x)$ is to have zero mean, the requirement σ_g=0 implies that $p_G(x) = \delta(x)$, that is, the density of the background noise is a Dirac delta function located at the origin. Let A denote the event that the noise is in state ε=0 {background noise with pdf $p_N(x) = \delta(x)$} during at least one of the M sample times. With probability one, no false-alarms or false-dismissals are made if event A occurs. Furthermore, since the M samples are independent, $Pr(A) = 1-\varepsilon^M$ and $Pr(\not A) = \varepsilon^M$. Let $\hat{P}_f$ and $\hat{P}_d$ denote the false-

alarm and detection probabilities, respectively, that would be obtained with only IN having density $p_X(x)\{\ \varepsilon=1$ in (7.1)$\}$. The false-alarm and detection probabilities that are obtained with the mixture of (7.1) are then, in terms of $\hat{P}_f$ and $\hat{P}_d$,

$$P_f = \varepsilon^M \hat{P}_f \quad \text{and} \quad P_d = \varepsilon^M \hat{P}_d + (1-\varepsilon^M)$$

respectively. Since ARE is obtained by letting the signal strength go to zero and the number of samples M approach infinity, let us consider what happens to these detection and false-alarm probabilities as $M\to\infty$. We have for any positive signal strength, any ε strictly less than one, and an optimum nonlinear detector,

$$\lim_{M\to\infty} P_f = 0 \quad \text{and} \quad \lim_{M\to\infty} P_d = 1.$$

This simultaneous false-alarm probability of 0 and detection probability of 1 cannot be obtained for signals of finite energy in additive noise of density

$$p_N(x) = (1-\varepsilon)\delta(x) + \varepsilon p_X(x) \tag{7.26}$$

with any linear detector no matter how many samples are used, unless $\varepsilon=0$. Hence, for noise having the density of (7.26) with $\varepsilon>0$, ARE will equal infinity.

In practice, one would not have $R=0$ or $R=\infty$ but a case of great physical interest is $R>>1$. For example, a value of $R=100$ means that the IN power is 20 db greater than the background noise power, a not unreasonable situation for atmospheric noise. The large values of μ (and ARE for various suboptimum nonlinearities) obtained for $0<\varepsilon<1$ and $R>>1$ thus indicate that

considerable improvement in large sample detector performance in the presence of IN may be achieved by fully exploiting the mixture model of (7.1).

7.4.2 NARROW-BAND SYSTEM

When the noise is narrow-band, the mixture pdf takes the form

$$p_\eta(e) = (1-\varepsilon)\hat{p_E}(e) + \varepsilon p_E(e) \qquad (7.27)$$

where

$$\hat{p_E}(e) = \frac{e}{\sigma_g^2}\exp\left(-e^2/2\sigma_g^2\right) \text{ (Rayleigh distribution)} \qquad (7.28)$$

and

$$p_E(e) = 2\beta\sigma_o^{2\beta}e\{\sigma_o^2 + e^2\}^{-(\beta+1)}, \quad 0\leq e<\infty \qquad (5.17)$$

To obtain the optimum nonlinear element $g_{NB,opt}[e]$, we need to solve the following nonlinear equation {see(f.15)}

$$-B_c\frac{d}{de}\log\left[\frac{p_\eta(e)}{e}\right] = \frac{1}{\pi}\int_{-\pi}^{\pi} g[e\zeta]d\zeta\Big|_{g_{NB,opt}[e]=g[e]} \qquad (7.29)$$

for $g[e]$ where B_c is a constant. In this work we do not try to solve this equation. However, if the optimum nonlinearity is used the max ARE denoted by μ_{NB} can be obtained by using (7.27), (5.17) and (7.28) in (7.20) as

$$\mu_{NB} = \frac{\sigma_N^2}{2}\int_0^\infty \{(1-\varepsilon)\hat{p_E}(e) + \varepsilon p_E(e)\}\,\bullet$$

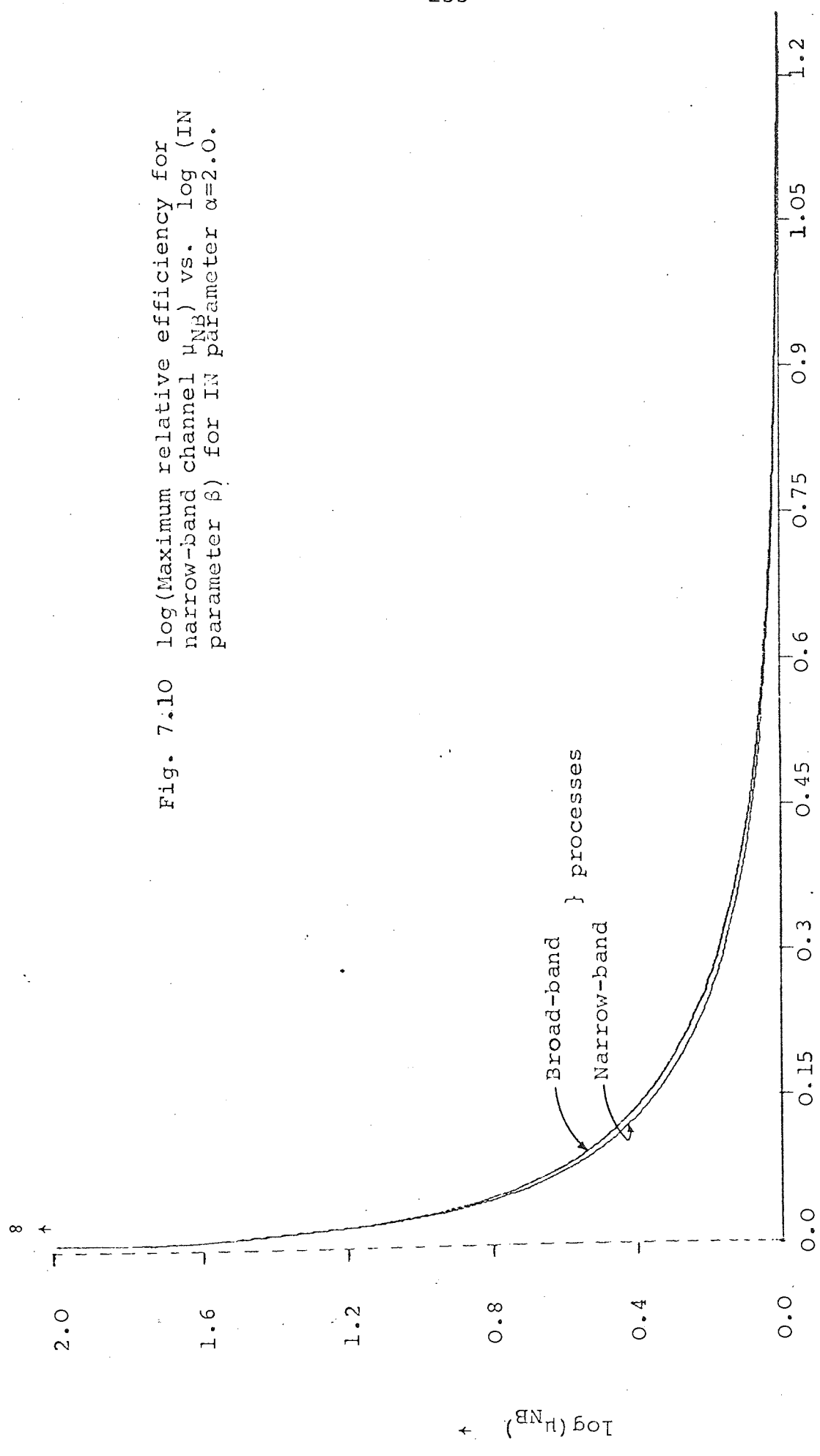

Fig. 7.10 log(Maximum relative efficiency for narrow-band channel μ_{NB}) vs. log (IN parameter β) for IN parameter α=2.0.

$$\cdot\left[\frac{1}{e} - \frac{(1-\varepsilon)\dot{p}_E^{\wedge}(e) + \varepsilon\dot{p}_E(e)}{(1-\varepsilon)p_E^{\wedge}(e) + \varepsilon p_E(e)}\right]^2 de \qquad (7.30)$$

where σ_N^2 is the noise variance $\{=(1-\varepsilon)\sigma_g^2 + \langle x^2\rangle\}$. A closed form can be obtained when $\varepsilon=1.0$. In this case μ_{NB} reduces to

$$\mu_{NB} = 1 + 2/(\beta^2 + \beta - 2), \qquad \beta > 1. \qquad (7.31)$$

The above equation is plotted against β in Fig. 7.10. On the same graph, using (7.25), μ for the low-pass process when $\alpha=2.0$ is also plotted for comparison purposes. The general shape of the two graphs is the same. The reason why μ_{NB} is lower than μ is because we have neglected all higher carrier frequency terms in deriving (7.16).

In view of the complexity of equipment associated with the use of the 'optimum' nonlinearities $g_{opt}[\cdot]$ and $g_{NB,opt}[\cdot]$ in an operational system, we look, in the next section, at the nonlinearities that retain the key qualitative features and performance of $g_{opt}[\cdot]$ or $g_{NB,opt}[\cdot]$, but which would be simpler to implement operationally.

7.5 SUBOPTIMUM DETECTORS

7.5.1 BASE-BAND SYSTEMS

The four suboptimum nonlinearities illustrated in Fig. 7.11 will now be considered in order of increasing complexity. These four nonlinearities were chosen in a more or less ad hoc fashion as being progressively better approximations to the optimum nonlinearities of Figs. 7.3 - 7.6 . All the nonlinearities considered in this section can easily be realised

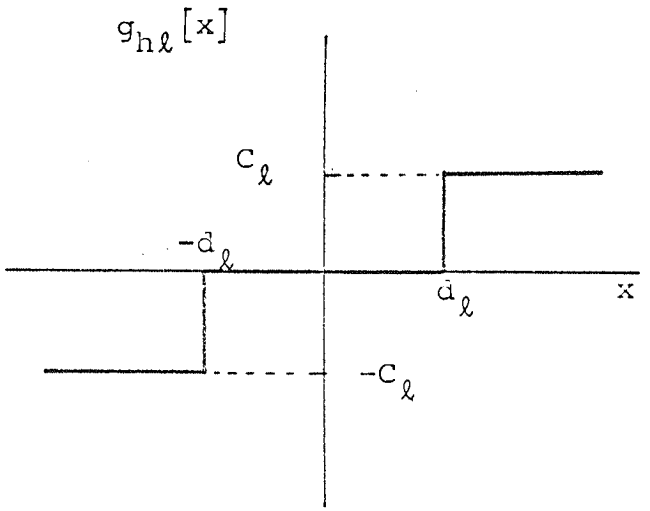

a) Hard-limiter with dead zone

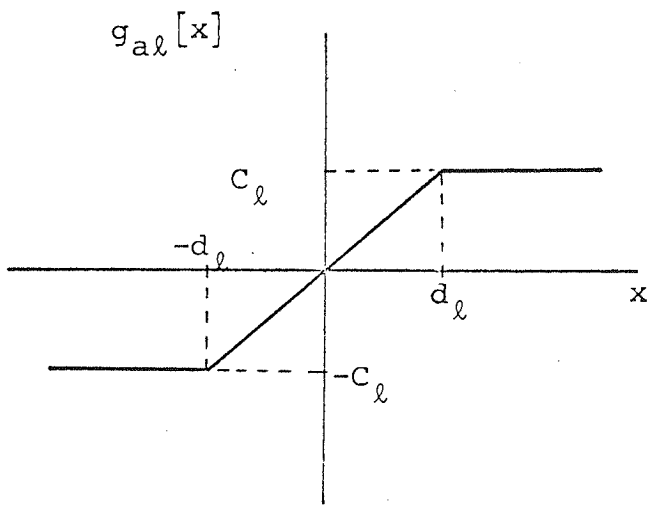

b) Amplifier-limiter

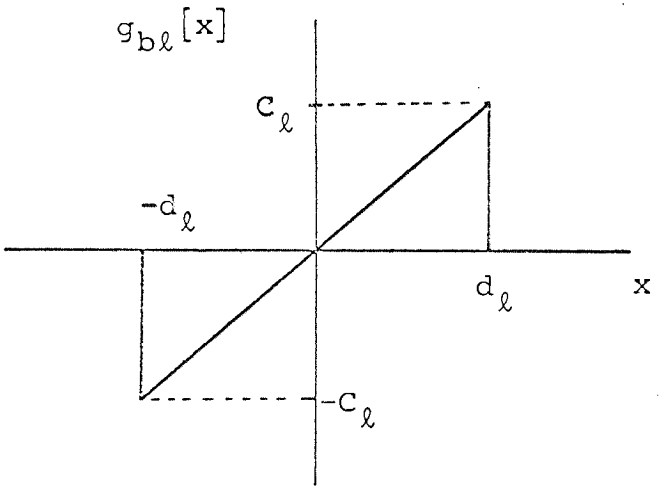

c) Blanker (hole puncher)

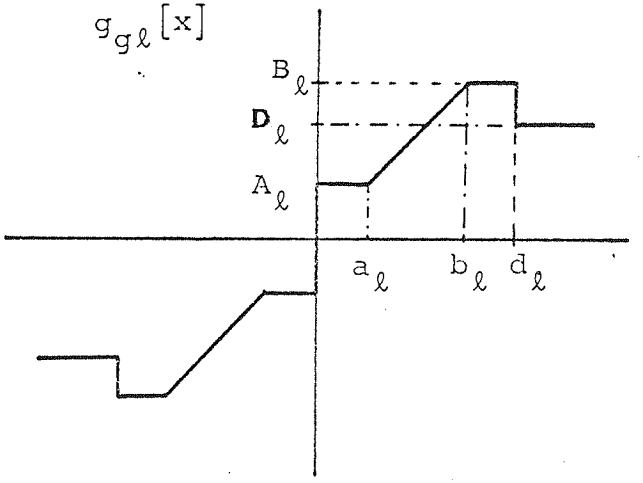

d) General nonlinearity

Fig. 7.11 Suboptimum nonlinearities analysed

in practice.

The simplest nonlinearity is the hard-limiter with dead-zone as shown in Fig. 7.11a. It has the characteristic

$$g_{h\ell}[x] = \begin{cases} C_\ell, & x>d_\ell \\ -C_\ell, & x<-d_\ell \end{cases} \qquad (7.32)$$

Using (7.1), (5.8), (7.21) and (7.32) in the expression for ARE of (7.5) gives

$$ARE_{h\ell} = \frac{2\left[(1-\varepsilon)+\frac{\varepsilon}{\sigma_g^2}\langle x^2\rangle\right]\left[(1-\varepsilon)e_{\hat{d}}+\frac{\varepsilon K(\alpha,\beta)}{\sqrt{R}}f_{\hat{d}}^{-(\beta+1/\alpha)}\right]^2}{(1-\varepsilon)\{1-\mathrm{erf}(\hat{d})\}+\frac{\varepsilon K(\alpha,\beta)}{\alpha}\{B(\beta,\frac{1}{\alpha}|\frac{1}{f_{\hat{d}}})\}} \qquad (7.33)$$

where

$\hat{d} = d_\ell/\sigma_g$ (normalized dead zone),

f_d and e_d are defined by (7.23).

For $\varepsilon=0$ and $\hat{d}=0$ we obtain the desired values of $ARE_{h\ell}$ of $2/\pi$. For values of ε between 0 and 1, it is clear that $ARE_{h\ell}\to\infty$ as $R\to\infty$. This behaviour is due to the same reason given in section (7.4.1). For $\alpha=2.0$; $\beta=1.5$, 3.0 and $\varepsilon=0.05$, 0.1, $ARE_{h\ell}$ is plotted for different values of $\hat{d}$ and R as a parameter. This is illustrated in Fig. 7.12. The maximum value of $ARE_{h\ell}$ occurs at $\hat{d}=0.5$. Using this value of $\hat{d}$ for which $ARE_{h\ell}$ is a maximum, (7.33) is plotted in Fig. 7.13 for various values of ε, where it can be compared with the maximum value of ARE($=\mu$)

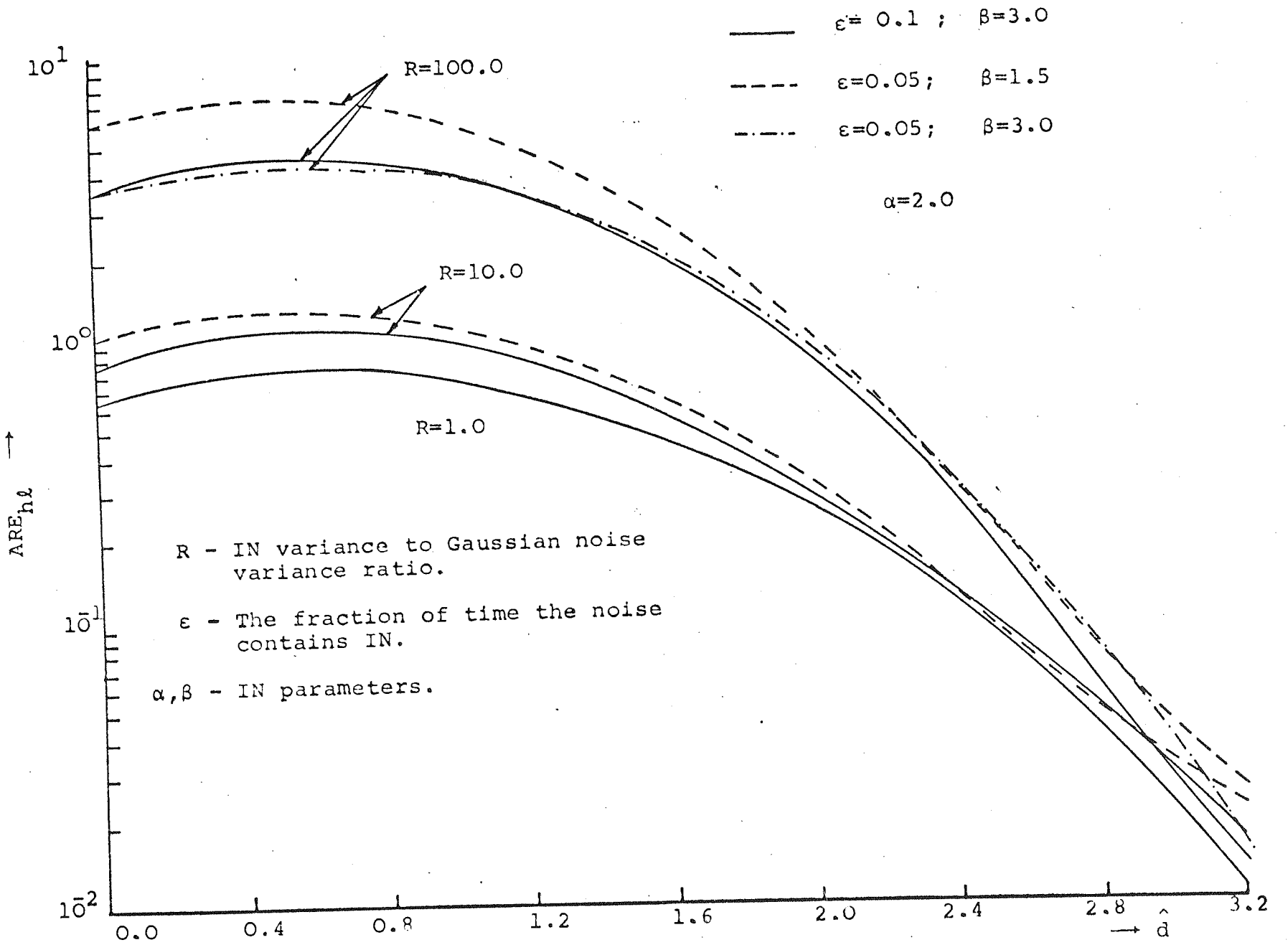

Fig. 7.12 Asymptotic relative efficiency vs. the normalized dead zone for hard limiter nonlinearity (Fig. 7.11a)

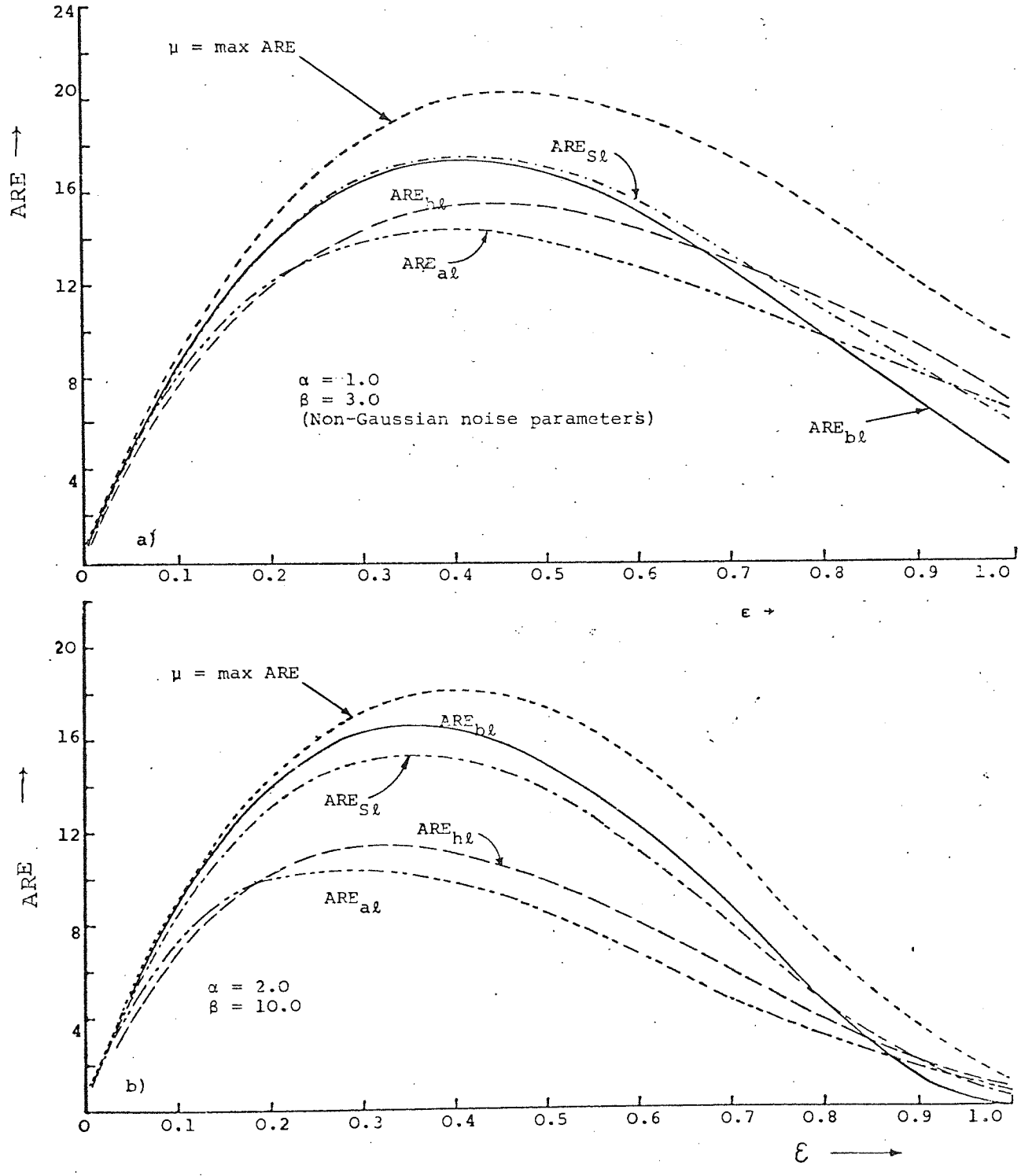

Fig. 7.13. Asymptotic relative efficiency (ARE) vs. the fraction of time the noise contains IN (ε) for optimum and various sub-optimum nonlinearities (IN variance to Gaussian noise variance ratio R=100).

which is also plotted on the same graph using (7.24).

The next simplest nonlinearity that might prove effective for the mixture noise model is the amplifier-limiter nonlinearity which we denote by $g_{a\ell}[x]$ and is illustrated in Fig. 7.11b. It has the characteristic

$$g_{a\ell}[x] = \begin{cases} x, & 0<x<d_\ell \\ C_\ell, & x>d_\ell \\ -x, & -d_\ell<x<0 \\ -C_\ell, & x<-d_\ell . \end{cases} \tag{7.34}$$

Martin and Schwartz [116] showed that a detector using this nonlinearity will have a guaranteed minimum level of performance when used to detect sufficiently large signals in mixtures (7.1) of Gaussian noise having density $p_G(x)$ with small amounts, ($\varepsilon<<1$), of other noise having any arbitrary density $p_X(x)$. After substituting the nonlinearity of (7.34) and the mixture noise model of (7.1), (5.8) and (7.21) into the expression of (7.5) for ARE, one finds that

$$ARE_{a\ell} = \frac{NUM3}{DEN3} \tag{7.35}$$

where

$$NUM3 = \frac{1}{\hat{d}^2}\left[(1-\varepsilon)\{erf(\hat{d})-0.5\}+ \frac{\varepsilon}{2} - \frac{\varepsilon K(\alpha,\beta)}{\alpha} B(\beta,\frac{1}{\alpha}|\frac{1}{f_{\hat{d}}})\right]^2$$

and

$$DEN3 = (1-\varepsilon)\{1-erf(\hat{d})\}+ \frac{\varepsilon K(\alpha,\beta)}{\alpha}\{B(\beta,\frac{1}{\alpha}|\frac{1}{f_{\hat{d}}}\}+$$

$$+ \frac{\varepsilon K(\alpha,\beta) R}{\alpha \hat{d}^2}\left[\frac{\Gamma(\beta-\frac{2}{\alpha})\Gamma(\frac{3}{\alpha})}{\Gamma(\beta+\frac{1}{\alpha})} - B(\beta-\frac{2}{\alpha},\frac{3}{\alpha}|\frac{1}{f_{\hat{d}}})\right] +$$

$$+ \frac{1-\varepsilon}{\hat{d}^2} \{\text{erf}(\hat{d}) - 0.5 - \hat{d}e_{\hat{d}}\}.$$

e_d, f_d, $K(\alpha,\beta)$ are defined by (7.23). The above equation, which is independent of parameter C_ℓ, is plotted in Fig. 7.14 against the normalized limiter breakpoint $\hat{d}$ for α=2.0, β=1.5, ε=0.05, 0.15 and R as a parameter. The limiter breakpoint that maximizes the value of $ARE_{a\ell}$ for values of ε=0.05, 0.15 and R=100.0 is approximately 1.5. Using this value of $\hat{d}$, $ARE_{a\ell}$ vs. ε is plotted in Fig. 7.13 for various values of α,β along with similar curves for the other nonlinearities considered.

The next nonlinearity to be considered is

$$g_{b\ell}[x] = \begin{cases} x, & 0<x<d_\ell \\ 0, & |x|>d_\ell \\ -x, & -d_\ell<x<0 \end{cases} \qquad (7.36)$$

which is shown in Fig. 7.11c. This nonlinearity, which has often been proposed to combat IN interference, starting with the original paper by Lamb [124], is known as the noise blanker. Using(7.36),(7.1),(5.8) and (7.21) one can show from (7.5) that

$$ARE_{b\ell} = \frac{NUM4}{DEN4} \qquad (7.37)$$

where

$$NUM4 = 2\Big[(1-\varepsilon) + \frac{\varepsilon R\Gamma(\beta-\frac{2}{\alpha})\Gamma(\frac{3}{\alpha})}{\Gamma(\beta)\Gamma(\frac{1}{\alpha})}\Big]\Big[(1-\varepsilon)\{\text{erf}(\hat{d})-0.5\} +$$

$$+ \frac{\varepsilon K(\alpha,\beta)}{\alpha}\{\frac{\Gamma(\beta)\Gamma(\frac{1}{\alpha})}{\Gamma(\beta+\frac{1}{\alpha})} - B(\beta,\frac{1}{\alpha}\,|\,\frac{1}{f_{\hat{d}}})\} -$$

$$- \hat{d}\{(1-\varepsilon)e_{\hat{d}} + \frac{\varepsilon K(\alpha,\beta)}{\sqrt{R}} f_{\hat{d}}^{-(\beta+1/\alpha)}\}\Big]^2,$$

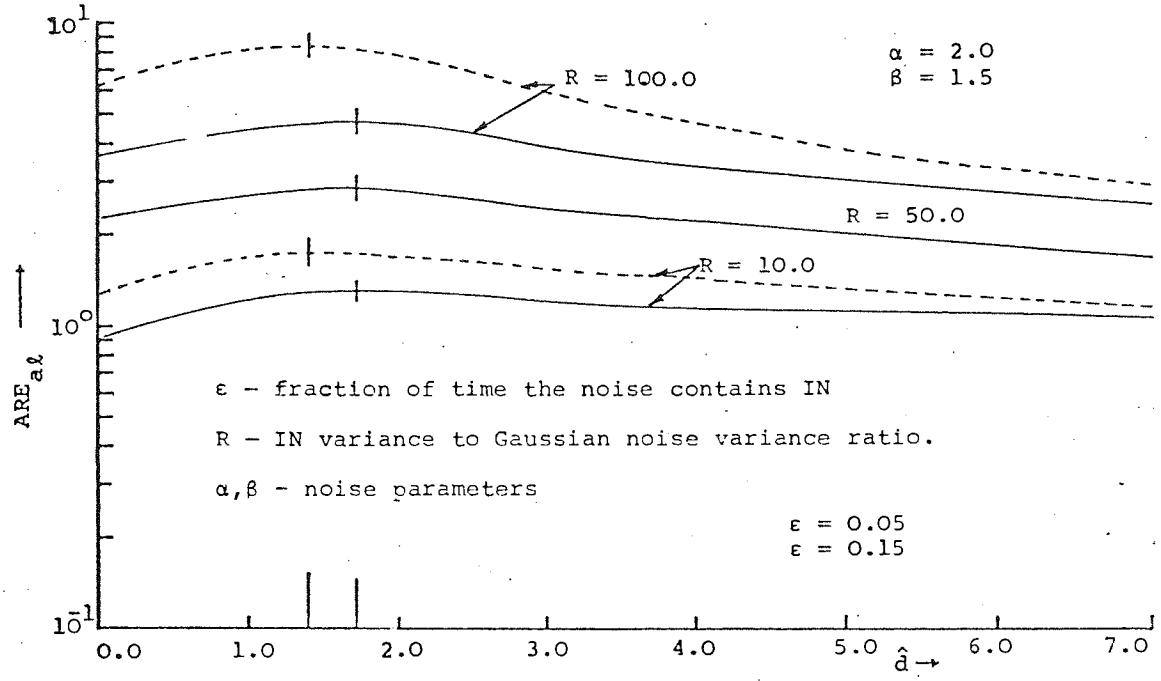

Fig.7.14 Asymptotic relative efficiency vs. the normalized break point for amplifier limiter (Fig. 7.11b)

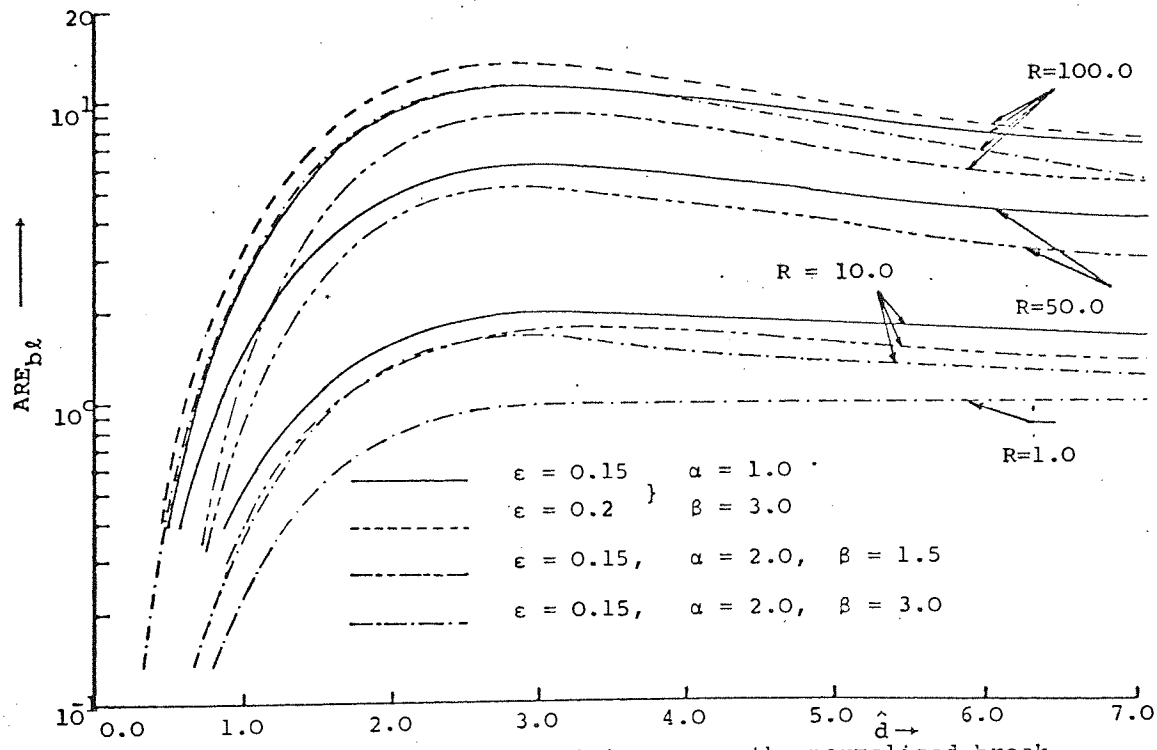

Fig. 7.15 Asymptotic relative efficiency vs. the normalized break point for blanker limiter (Fig. 7.11c)

$$DEN4 = (1-\varepsilon)\{\text{erf}(\hat{d}) - \hat{d}e_{\hat{d}} - 0.5\} + \frac{R\varepsilon K(\alpha,\beta)}{\alpha}\left[\frac{\Gamma(\beta-\frac{2}{\alpha})\Gamma(\frac{3}{\alpha})}{\Gamma(\beta+\frac{1}{\alpha})} - B(\beta-\frac{2}{\alpha}, \frac{3}{\alpha}; \frac{1}{f_{\hat{d}}})\right].$$

$e_{\hat{d}}$, $K(\alpha,\beta)$, R, $f_{\hat{d}}$ and $\hat{d}$ are defined by (7.23). Curves of $ARE_{b\ell}$ vs. the normalized blanking level $\hat{d}$ using (7.37) are given in Fig. 7.15 for α=2.0, β=3.0, 1.5, α=1.0, β=3.0, ε=0.15, 0.2 and R=10, 50, 100. The optimum normalized blanking level $\hat{d}$ is again essentially independent of R and is about 2.8, a result in accordance with the value of three Gaussian noise standard deviations above the signal level found by Ziemer and Fluchel [45] in their error probability simulation for a similar detection problem. Using $\hat{d}$=2.8, (7.37) is plotted against ε in Fig.7.13, along with similar curves for the other nonlinearities considered.

The final suboptimal nonlinearity considered is denoted by $g_{g\ell}[x]$ and is shown in Fig. 7.11d. This nonlinearity is specified mathematically as

$$g_{g_\ell}[x] = \begin{cases} A_\ell, & 0<x<a_\ell \\ \left(\frac{B_\ell - A_\ell}{b_\ell - a_\ell}\right)x + \frac{A_\ell b_\ell - a_\ell B_\ell}{b_\ell - a_\ell}, & a_\ell<x<b_\ell \\ B_\ell, & b_\ell<x<d_\ell \\ D_\ell, & x>d_\ell \end{cases} \tag{7.38}$$

Using (7.38) for $g_{g\ell}[x]$ and (7.1), (5.8) and (7.21) for $p_N(x)$ in (7.5) for ARE yields

$$ARE_{g\ell} = \frac{NUM5}{DEN5} \tag{7.39}$$

where

$$NUM5 = 2\left[(1-\varepsilon)+\frac{\varepsilon R\Gamma(\beta-\frac{2}{\alpha})\Gamma(\frac{3}{\alpha})}{\Gamma(\beta)\Gamma(\frac{1}{\alpha})}\right]+\left[\hat{A}(I_1)+(\hat{D}-\hat{B})(I_2)+\hat{\delta}(I_3)\right]^2,$$

$$DEN5 = \hat{A}^2(I_4)+\hat{B}^2(I_5)+\hat{D}^2(I_6)+\hat{\delta}^2(I_7)+2\hat{\delta}\hat{\zeta}(I_8)+\hat{\zeta}^2(I_9),$$

$$\hat{\delta} = \frac{\hat{B}-\hat{A}}{\hat{b}-\hat{a}}, \quad \hat{\zeta} = \frac{\hat{A}\hat{b}-\hat{a}\hat{B}}{\hat{b}-\hat{a}},$$

$$I_1 = \frac{1-\varepsilon}{\sqrt{2\pi}} + \frac{\varepsilon K(\alpha,\beta)}{\sqrt{R}},$$

$$I_2 = (1-\varepsilon)e_{\hat{d}} + \frac{\varepsilon K(\alpha,\beta)}{\sqrt{R}} f_{\hat{d}}^{-(\beta+1/\alpha)},$$

$$I_3 = (1-\varepsilon)\{\mathrm{erf}(\hat{b})-\mathrm{erf}(\hat{a})\}+\frac{\varepsilon K(\alpha,\beta)}{\alpha}\{B(\beta,\tfrac{1}{\alpha}\,|\,\tfrac{1}{f_{\hat{a}}})-B(\beta,\tfrac{1}{\alpha}|\,\tfrac{1}{f_{\hat{b}}})\},$$

$$I_4 = (1-\varepsilon)\{\mathrm{erf}(\hat{a})-\tfrac{1}{2}\}+\frac{\varepsilon K(\alpha,\beta)}{\alpha}\left[\frac{\Gamma(\beta)\Gamma(\frac{1}{\alpha})}{\Gamma(\beta+\frac{1}{\alpha})}-B(\beta,\tfrac{1}{\alpha}|\,\tfrac{1}{f_{\hat{d}}})\right],$$

$$I_5 = (1-\varepsilon)\{\mathrm{erf}(\hat{d})-\mathrm{erf}(\hat{b})\}-\frac{\varepsilon K(\alpha,\beta)}{\alpha}\{B(\beta,\tfrac{1}{\alpha}\,|\,\tfrac{1}{f_{\hat{b}}})-B(\beta,\tfrac{1}{\alpha}|\tfrac{1}{f_{\hat{d}}})\},$$

$$I_6 = (1-\varepsilon)\{1-\mathrm{erf}(\hat{d})\}+\frac{\varepsilon K(\alpha,\beta)}{\alpha}\{B(\beta,\tfrac{1}{\alpha}\,\tfrac{1}{f_{\hat{d}}})\},$$

$$I_7 = (1-\varepsilon)\{\hat{a}e_{\hat{a}}-\hat{b}e_{\hat{b}}+\mathrm{erf}(\hat{b})-\mathrm{erf}(\hat{a})\}+$$

$$+\frac{\varepsilon K(\alpha,\beta)}{\alpha}R\left[B(\beta-\tfrac{2}{\alpha},\tfrac{3}{\alpha}|\,\tfrac{1}{f_{\hat{a}}})-B(\beta-\tfrac{2}{\alpha},\tfrac{3}{\alpha}|\,\tfrac{1}{f_{\hat{b}}})\right],$$

$$I_8 = (1-\varepsilon)\{e_{\hat{a}}-e_{\hat{b}}\}+\frac{\sqrt{R}\varepsilon K(\alpha,\beta)}{\alpha}\left[B(\beta-\tfrac{1}{\alpha},\tfrac{2}{\alpha}|\tfrac{1}{f_{\hat{a}}})-B(\beta-\tfrac{1}{\alpha},\tfrac{2}{\alpha}\,\tfrac{1}{f_{\hat{b}}})\right],$$

$$I_9 = (1-\varepsilon)\{\mathrm{erf}(\hat{b})-\mathrm{erf}(\hat{a})\}+\frac{\varepsilon K(\alpha,\beta)}{\alpha}\{B(\beta,\tfrac{1}{\alpha})\tfrac{1}{f_{\hat{a}}})-B(\beta,\tfrac{1}{\alpha}|\,\tfrac{1}{f_{\hat{b}}})\}$$

and $f_{\hat{a}}$, $e_{\hat{a}}$, $K(\alpha,\beta)$, R, $\hat{x}$ are defined by (7.23).

Note: for $\hat{A}=\hat{a}=0$, $\hat{B}=\hat{D}$ and $\hat{b}=\hat{d}$ yields $ARE_{a\ell}$ of (7.35) while for $\hat{A}=\hat{a}=0$, $\hat{D}=0$ and $\hat{b}=\hat{d}$ yields $ARE_{b\ell}$ of (7.37).

Instead of computing $ARE_{g\ell}$ specified by (7.39) for various

values of $\hat{A}$, $\hat{B}$, $\hat{D}$, $\hat{a}$, $\hat{b}$, and $\hat{d}$, which cannot be easily calculated without substantial computation, we shall investigate the nonlinearity given in Fig. 7.16 which is a special case of (7.38). The semi-optimum nonlinearity of Fig. 7.16 is obtained by adding a hard - limiting charactersitic for large $|x|$ to the noise blanker to avoid the problem of the nonlinearity disappearing as its blanking level goes to zero. This non-linearity has been used by many authors in the past [60] for combating IN.

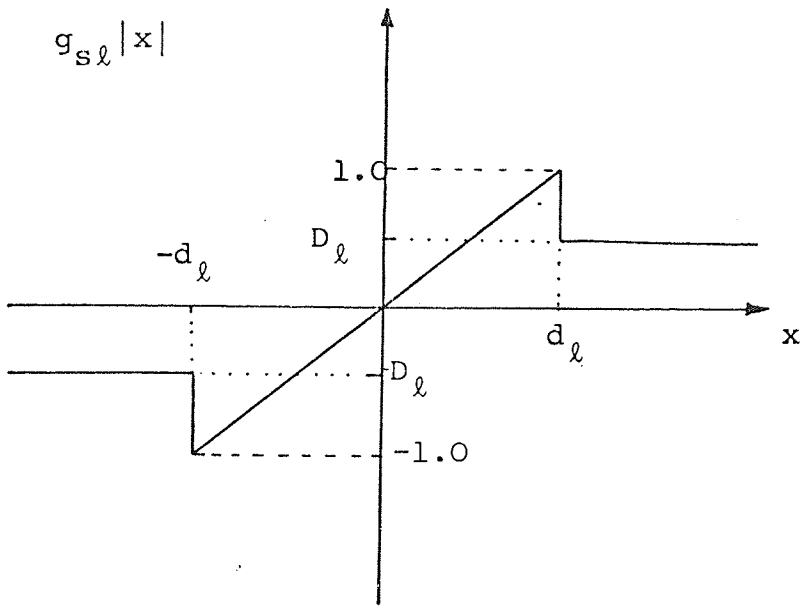

Fig. 7.16 Semi-optimum nonlinearity.

The $ARE_{s\ell}$ due to this semi-optimum nonlinearity can easily be obtained by substituting $\hat{A}=0, \hat{a}=0, \hat{b}=\hat{d}$ in (7.39). The $ARE_{s\ell}$ vs. the normalized break-point $\hat{d}$ for values of $\varepsilon=0.015$, 0.15 and hard limiting values of $\hat{D}$ =0.2, 0.8 times the maximum value of the linear portion of the characteristic is plotted in Fig. 7.17. The $ARE_{s\ell}$ is also plotted in Fig. 7.13 for various values of ε. The nonlinear parameters used for this plot are $\hat{D}$= 0.2, $\hat{d}$=3.0, R=100. Note that the value of $\hat{d}$=3.0 is that which maximizes $ARE_{s\ell}$ for $\hat{D}$=0.2 (see Fig. 7.17a). Values of $\hat{d}$ which

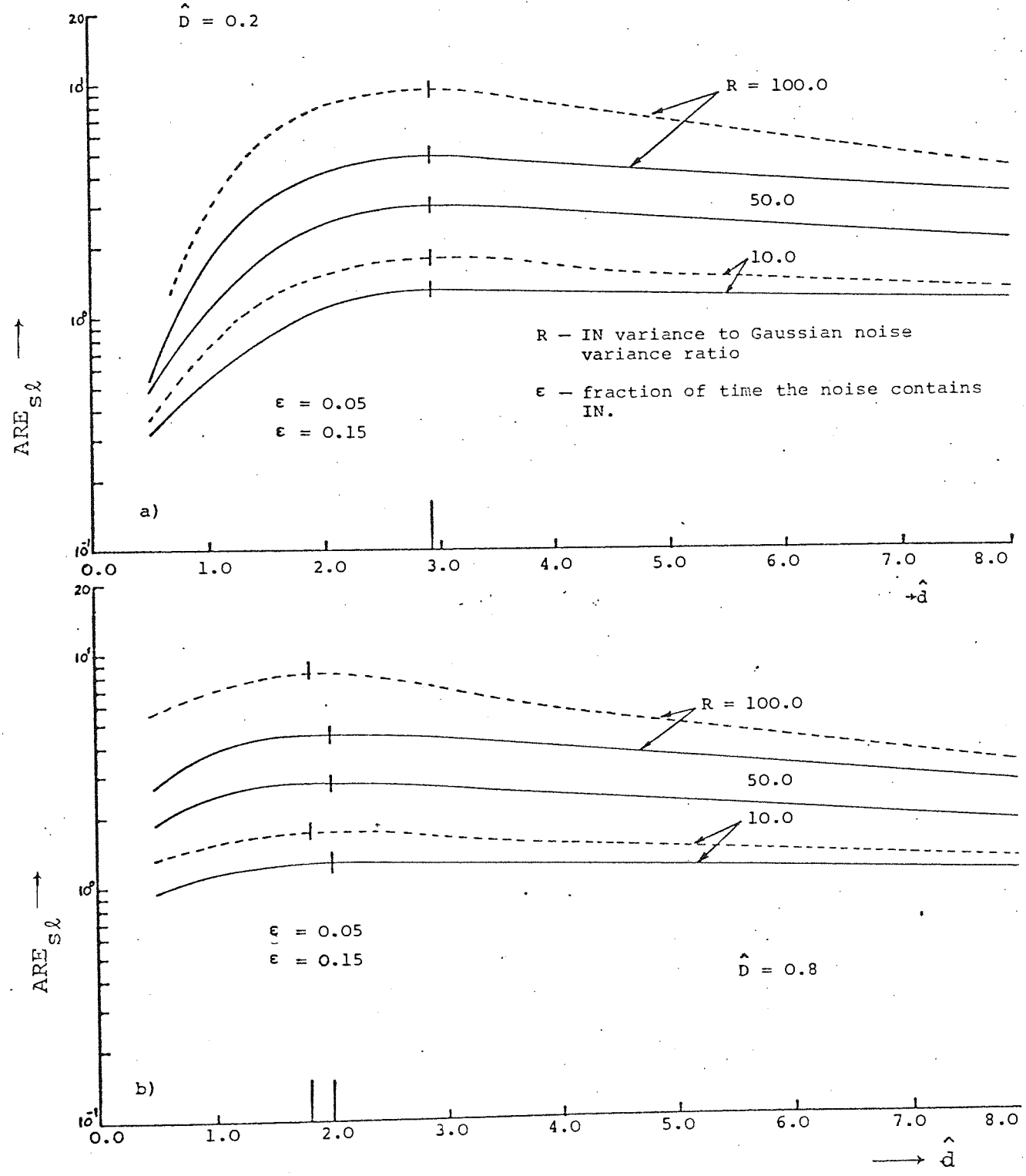

Fig. 7.17 Asymptotic relative efficiency for semi-optimum nonlinearity (ARE$_{s\ell}$) vs. the normalized break point ($\hat{d}$) {Fig. 7.16} (IN parameters α=2.0, β=1.5).

minimize $ARE_{s\ell}$ vary with $\hat{D}$ as expected. Usually the higher the values of $\hat{D}$ the lower values are for $\hat{d}$. This can be seen from Fig. 7.17.

7.5.2 NARROW-BAND SYSTEMS

The nonlinearity shown in Fig. 7.11a (hard limiter with dead zone) will now be considered for the narrowband system. Changing the variable $e\cos\psi=\S$ in (7.12) for $K_1[e]$ and using (7.32) for $g_{h\ell}[e]$ yields

$$K_1[e] = \frac{2C_\ell}{\pi e}\int_{d_\ell}^{e}\frac{\S}{(e^2-\S^2)^{\frac{1}{2}}}d\S = \frac{2C_\ell}{\pi e}(e^2-d_\ell^2)^{\frac{1}{2}} \qquad (7.40)$$

Substituting for

$$\dot{K}_1[e] = \frac{d}{de}K_1[e] = \frac{2C_\ell}{\pi e^2}\frac{d_\ell^2}{(e^2-d^2)^{\frac{1}{2}}}$$

and using (7.27), (7.28), (5.17) and (7.40) in (7.16) for $ARE_{h\ell,NB}$ yields

$$ARE_{h\ell,NB} = \frac{NUM6}{DEN6} \qquad (7.41)$$

$$NUM6 = \frac{\sigma_N^2}{4\sigma_g^2}\Big[\Big(\frac{2}{\pi}\Big)^{\frac{1}{2}}(1-\varepsilon)\exp(-\hat{d}^2/2)+\frac{\varepsilon(\beta'-1)}{\sqrt{\pi R}}\frac{\Gamma(\beta'/2)}{\Gamma(\frac{\beta'+1}{2})}\Big\{\frac{\hat{d}^2}{R}+1\Big\}^{-\beta'/2}\Big]^2,$$

$$DEN6 = \frac{2}{\pi^2}\Big[(1-\varepsilon)\Big\{\exp(-\hat{d}^2/2)-\frac{\hat{d}^2}{2}\,Ei(\hat{d}^2/2)\Big\}+$$

$$+\varepsilon\Big\{\Big(1+\frac{\hat{d}^2}{R}\Big)^{-(\frac{\beta'-1}{2})}-\frac{\hat{d}^2(\beta'-1)}{R}\int_{\frac{\hat{d}}{\sqrt{R}}}^{\infty}\frac{d\S}{\S(1+\S^2)^{(\beta'+1)/2}}\Big\}\Big]$$

where $B' = 2\beta+1$ and

$Ei(x) = \int_x^\infty \exp(-\zeta)d\zeta/\zeta$ (Integral exponential function) [85].

The above equation is plotted against $\hat{d}$ for $\alpha=2.0, \beta=3.0$ and

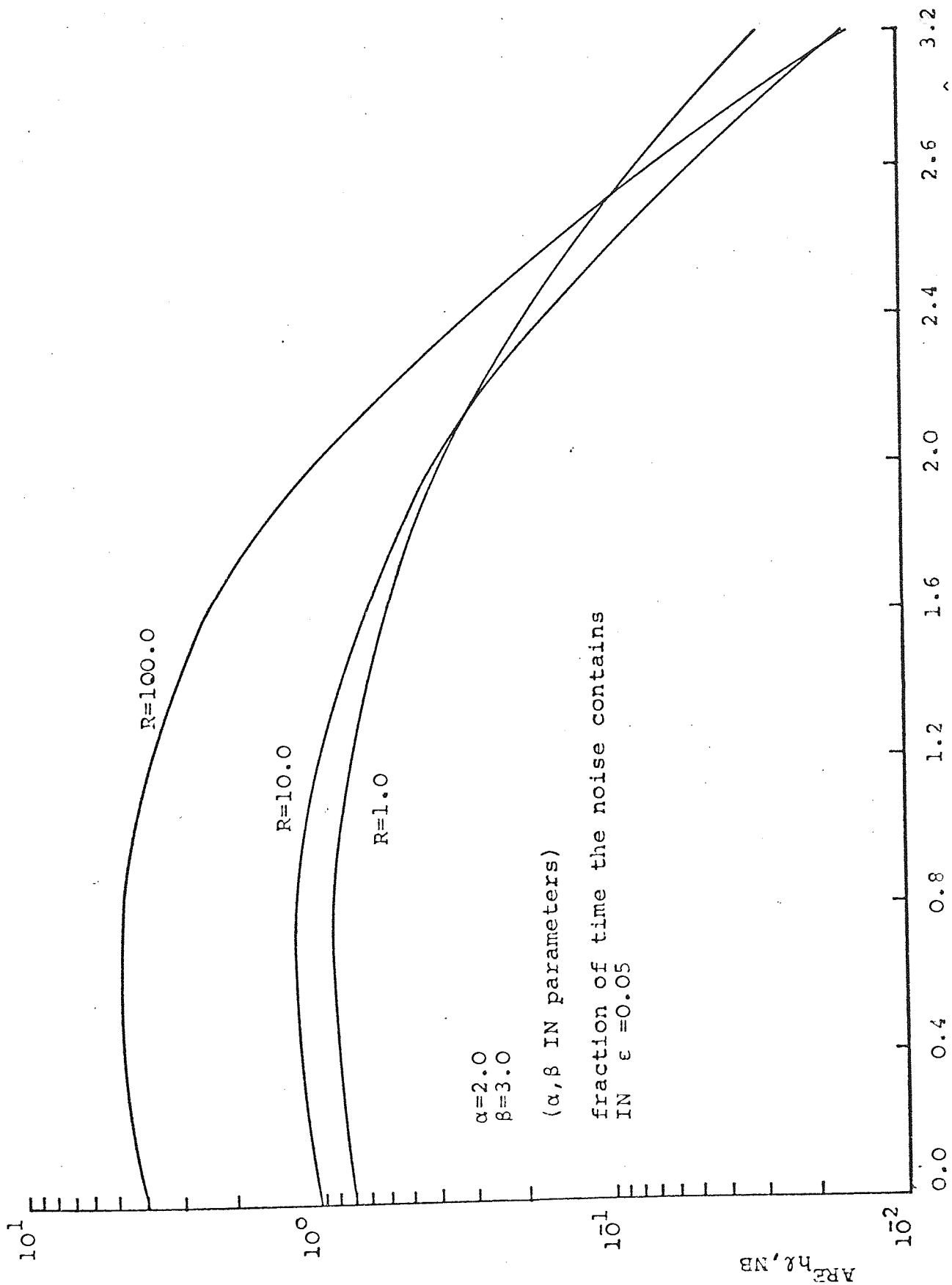

Fig. 7.18 Asymptotic relative efficiency (narrow-band ARE_{NB}) as a function of normalized breakpoint ($\hat{d}$) for hard-limiter with dead zone (Fig. 7.11a).

R=1.0, 10.0, 100.0 in Fig. 7.18. The optimum break point $\hat{d}$ is again essentially independent of R and is about 0.7. It will be recalled that for the equivalent low-pass process the optimum break point $\hat{d}$ was equal to 0.5 and was independent of R.

Similarly the other nonlinearities of Fig. 7.11 can be considered, but these will not be investigated here.

7.6 DISCUSSION

In this chapter, for the case of binary signals, the optimal performance is obtained with a detector consisting of a nonlinear lagless (no-memory) element followed by a matched filter. Since the derivation of an 'optimum' nonlinearity is complex and critically dependent upon the model assumed for the noise process (Figs. 7.3 - 7.6), it is shown that a fairly simple, realisable, sub-optimality (Fig. 7.11) can give good large-sample performance while at the same time not being over sensitive to measurement on parameter errors (Fig. 7.13).

Such a receiver structure can also be developed on the intuitive notion that since the isolated high-amplitude impulses contain much of the energy in noise, a simple clipping circuit in the receiver can remove most of these pulses and thereby reduce the energy in the noise considerably without significantly reducing the signal energy. Experiments with the various nonlinearities (hard-limiter, amplifier-limiter, blanker) have indicated that the amplifier-limiter is effective and practical [49]-[51]. Within experimental accuracy, the amplifier-limiter has performed as well as more accurate approximations to an optimal nonlinearity. Unlike the 'optimum' nonlinearity or 'hole puncher' (blanker), the amplifier-limiter performance

is not sensitive to threshold settings. By dynamically adjusting the threshold to clip a fixed percentage of time (≃50%), near optimal results have been obtained [49]-[51]. This performance has been typically between 1 to 2 db better than the hard limiter (d_ℓ=0 in Fig. 7.11a). It is also shown that the blanker affords no more than 1 to 2 db improvement in system performance over that achievable with the amplifier-limiter. These results agree remarkably well with the results plotted in Fig. 7.13, when the fraction of time IN is present, ε is small. For large values of ε the hard-limiter is expected to perform much better than the amplifier-limiter or the blanker. One final remark about the performance of the amplifier-limiter from Fig. 7.14 is that one clearly loses less by setting the break point d_ℓ too low (which is equivalent to estimating the background noise standard deviation σ_g to be lower than it really is) than by setting it too high (estimating σ_g too high). The reason is that with the mixture noise distribution it is preferable to make an error in the direction of a hard-limiter (d_ℓ=0) than in the direction of a linear detector (d_ℓ=∞).

To have a simple nonlinearity which would perform better for all values of ε ($0<\varepsilon<1$) a semi-optimal nonlinearity of Fig. 7.16 is suggested. This new nonlinearity is obtained by adding a hard-limiting characteristic for large $|x|$ to the noise blanker to avoid the problem of the nonlinearity disappearing as its blanking level goes to zero. Since the semi-optimal nonlinearity becomes an amplifier-limiter when D_ℓ=1.0 and a noise blanker when D_ℓ=0, one can obviously achieve any desired tradeoff between the performance of the amplifier-limiter and the blanker by proper choice of D_ℓ (see Fig. 7.13).

The effect of a nonlinear device on the SNR has been used

here as the criterion of improvement or degradation, and only long-term averages have been considered. A question arises about the validity of ARE as a measure of system performance for a small sample M where alternative and hypothesis are not necessarily close. Relatively little work appears to have been published along these lines. However, studies involving both computer simulation and actual implementation [65] indicate that the ARE converges rather rapidly for the detector considered here with IN whose pdf $p_N(x)$ is given by a generalised Gaussian density (5.2).

CHAPTER 8

AN ADAPTIVE SYSTEM : ESTIMATION OF PARAMETERS

This chapter is devoted to some basic aspects concerning the estimation of states and parameters for an adaptive communication system. A simple procedure is presented and evaluated for estimating the occurrence of an impulse. In estimating the unknown parameters of generalised hyperbolic pdf, maximum likelihood estimators are used.

8.1 INTRODUCTION

Throughout the discussion in the preceeding chapters we have assumed that the noise process is stationary. In practice, it frequently happens that the non-Gaussian noise is non-stationary; the noise statistics vary according to locations and times of day [15]. Under these circumstances it seems reasonable to build a system to operate efficiently in an unknown or changing environment. By allowing the system to measure the noise parameters (e. g β, σ_o^2 in the generalised hyperbolic noise density) and then utilising these measurements to adjust its decision structure, the performance can be improved over that of a fixed system. Such a system would consist of an estimator and a detector.

The chapter is divided into two sections. The problem in the first section can be stated very briefly as, given k (k=1,2,.....) samples from the observation time T_o, we want to decide which noise {either IN with pdf $p_X(x)$ or Gaussian noise with pdf $p_G(x)$} is active in that interval. In the second section an effective algorithm for computing maximum likelihood (ML) estimates of the parameters in the IN model is derived.

8.2 ESTIMATING AN ACTIVE NOISE IN THE BIT INTERVAL

In this section we find the optimum threshold for selecting the IN pdf if, out of k samples, k_o samples cross the given threshold L_k. Before looking at this general case we find the optimum threshold for selecting the IN pdf if we take one sample from the observation interval T_o and test if it is greater then the threshold level L_1 (this method would be quite effective in the very IN case i.e. for generalised hyperbolic pdf with $\alpha=1$, $\beta=1$).

We assume that under hypothesis H_1 the IN is active with pdf $p_X(x)$ and under H_o the Gaussian noise is active with pdf $p_G(x)$. We obtain one sample from the input waveform within the observation interval T_o. We compare this with the threshold L_1 and from this we have to decide which hypothesis is true, depending upon the amplitude of the sample. Assuming that hypothesis $H_1(H_o)$ is active, the condition for correct decoding would be when the sample is greater (smaller) than the threshold level L_1. Let the apriori probabilities of having H_o be ε_1 and H_1 be $(1-\varepsilon_1)$. Therefore probability of correctly decoding the hypothesis H_o or H_1 would be

$$Pc = \varepsilon_1 \int_{L_1}^{\infty} p_X(x)dx + (1-\varepsilon_1) \int_{-\infty}^{L_1} p_G(x)dx. \qquad (8.1)$$

Since the decoder can only base its decision on the volatge amplitude of the sample taken, it is apparent that the only possible way to adjust Pc or to optimize the system is to vary the threshold level L_1 at which the decision is made. An optimum choice of L_1 corresponds to maximum Pc, according to our criterion. Since Pc is a function of L_1, we simply

$\hat{L}_1 = L_1/\sigma_g$			β	α	ε_1
R → 1.0	10.0	100.0			
3.7754	3.0805	2.8958	3.0	1.0	0.1
3.6605	2.8881	2.9283	10.0		
3.8687	2.7551	2.9716	3.0	2.0	
4.1615	2.7380	2.9959	6.0		
2.854	1.8091	1.8138	3.0	1.0	0.5
2.4746	1.6234	1.9593	10.0		
2.6090	1.5445	2.0877	3.0	2.0	
2.4150	1.5749	2.1268	6.0		

Fig. 8.1 Optimum threshold level for comparing single sample for various values of α, β and R.

$\hat{L}_6 = L_6/\sigma_g$		α
R → 1.0	100.0	
2.6175	1.235	1.0
2.5988	1.287	2.0

ε_1=0.1
β =3.0

Fig. 8.2 Optimum threshold level for comparing k=6 samples. {IN present if 4 samples exceeds the threshold level (k_o=4)}

where R - the ratio of IN variance to Gaussian noise variance

$\hat{L}_\ell$ - the normalized threshold level when ℓ samples are taken in the observation interval.

α, β - impulse noise parameters

ε_1 - a priori probability of have IN.

differentiate with respect to L_1 to find the optimum level. In particular we then have

$$\frac{\partial Pc}{\partial L_1} = 0 = -\varepsilon_1 p_X(L_1) + (1-\varepsilon_1) p_G(L_1) \tag{8.2}$$

by invoking the usual rules of differentiation with respect to integrals. It is thus apparent that the optimum threshold level L_1 (in the sense of maximizing probability of correct decoding) depends on the form of the two conditional density functions, as well as the apriori probability ε_1. Using (5.8) and (7.21) for $p_X(x)$ and $p_G(x)$ respectively in (8.2) yields

$$\frac{(1-\varepsilon_1)}{\sqrt{2\pi}} \exp\left(-\frac{\hat{L}_1^2}{2}\right) = \frac{\varepsilon_1}{\sqrt{R}} K(\alpha,\beta) \left[\left(\frac{\hat{L}_1}{\sqrt{R}}\right)^{\alpha}+1\right]^{-(\beta+1/\alpha)} \tag{8.3}$$

where $\hat{L}_1 = L_1/\sigma_g$, $K(\alpha,\beta)$ and R are defined by (7.23) and (5.8) respectively. The above equation has to be solved for $\hat{L}_1$. $\hat{L}_1$ is computed for various values of IN parameters α,β,R and is shown in Fig. 8.1.

Now consider k samples obtained from the observation time T_o. Each one is compared to a threshold L_k. If $k_o (<k)$ samples are found to be greater then L_k, then we ask for the distribution of the samples which are greater than the threshold and those that are not among the k samples. In particular, what is the probability of obtaining no samples greater than L_k (and hence k samples smaller than L_k), one sample greater than L_k, etc? In this case let the space include all possible combinations of samples greater than L_k and samples less than L_k. For simplicity's sake let the random variable $z_i = \ell, \ell = 0,1,..K$.

Since the samples are independent, the probability of having k samples greater than L_k would be given by

$$Pr(z_i=\ell) = {}^{k}C_{\ell}p^{\ell}(1-p)^{k-\ell} \qquad \text{(Binomial distribution)}$$

where

$${}^{k}C_{\ell} = \left(\frac{k!}{\ell!(k-\ell)!}\right)$$

p = is the probability that an event will happen in any single trial.

The probability that $z_i \leq m$ is then just the sum of the probabilities

$$Pr(z_i \leq m) = \sum_{\ell=0}^{m} {}^{k}C_{\ell}p^{\ell}(1-p)^{k-\ell}.$$

Using the arguments given for k=1, the probability of correctly decoding the hypothesis H_o would be

$$Pc = \varepsilon_1 \sum_{\ell=0}^{k_o-1} {}^{k}C_{\ell}p_1^{\ell}(1-p_1)^{k-\ell} + (1-\varepsilon_1)\sum_{\ell=0}^{k-k_o} {}^{k}C_{\ell}p_2^{\ell}(1-p_2)^{k-\ell} \qquad (8.4)$$

where

$$p_1=\int_{-\infty}^{L_k} p_X(x)\,dx \qquad \text{and} \qquad p_2=\int_{L_k}^{\infty} p_G(x)\,dx. \qquad (8.5)$$

Note: for k=1 and k_o=1, (8.4) becomes (8.1).

An optimum choice of L_k corresponds to maximum Pc. For maximum to occur

$$\frac{\partial Pc}{\partial L_k} = 0. \qquad (8.6)$$

Differentiating (8.4) with respect to L_k yields

$$\varepsilon_1 p_X(L_k)\left[\sum_{\ell=0}^{k_o-1} {}^kC_\ell (\ell-k) p_1^\ell (1-p_1)^{k-\ell-1} + \sum_{\ell=0}^{k_o-1} {}^kC_\ell \ell p_1^{\ell-1}(1-p_1)^{k-\ell}\right] +$$

$$+(1-\varepsilon_1)p_G(L_k)\left[\sum_{\ell=0}^{k-k_o} {}^kC_\ell (k-\ell) p_2^\ell (1-p_2)^{k-\ell-1} + \sum_{\ell=0}^{k-k_o} {}^kC_\ell (-\ell) p_2^{\ell-1}\right.$$

$$\left.(1-p_2)^{k-\ell}\right]. \qquad (8.7)$$

Given α,β,R,k,k_o, and ε_1 we can obtain L_k by using (8.7) in (8.6) and solving (8.6). Consider a special case for k=6; k_o=4. Using (8.7) in (8.6) yields

$$3\varepsilon_1 {}^6C_3 p_X(L_6) p_1^3 (1-p_1)^2 = 4(1-\varepsilon_1) {}^6C_2 p_G(L_6) p_2^2 (1-p_2)^3.$$

Using (5.8) and (7.21) for $p_X(x)$ and $p_G(x)$ respectively and (8.5) for p_1 and p_2, the above equation can be solved to obtain the threshold value L_6. For ε=0.1, β=3.0 and various values of α and R the optimum threshold L_6 is computed. The results are given in Fig. 8.2. Similarly, the result for L_k can be computed for various other values of k,k_o,α,β,R and ε_1.

8.3 PARAMETER ESTIMATION OF GENERALISED HYPERBOLIC DISTRIBUTION

8.3.1 INTRODUCTION

Let $X_1,.....X_m$ be a set of M independent random samples drawn from a given population. The population is characterized by a pdf $p_{\vec{X}}(\vec{x};\vec{\theta})$. $\vec{\theta}$ are the parameters of the population distribution. For independent samples, the likelihood function Λ is defined by the relation

$$\Lambda(\vec{x};\vec{\theta}) = \prod_{\ell=1}^{M} p_X(x_\ell;\vec{\theta}). \tag{8.8}$$

The method of maximum likelihood (ML) is one of selecting an estimate $\hat{\theta}$ for θ which will maximize the likelihood function Λ. Since $\log\Lambda$ is a monotonic function and attains its maximum when Λ is a maximum, (8.8) is usually solved for the estimate $\hat{\theta}$ by considering the simpler expression

$$\frac{\partial}{\partial\vec{\theta}}\log\Lambda = 0 = \frac{\partial}{\partial\vec{\theta}} \sum_{\ell=1}^{M} \log p_X(x_\ell;\vec{\theta}) \tag{8.9}$$

rather than the usual more cumbersome form of

$$\frac{\partial\Lambda}{\partial\vec{\theta}} = 0 = \frac{\partial}{\partial\vec{\theta}} \prod_{\ell=1}^{M} p_X(x_\ell;\vec{\theta}).$$

Any solution $\hat{\theta}$ for θ which satisfies (8.9) and is not identically a constant is called a ML estimate of θ. Equation (8.9) is called the likelihood equation.

The theoretical problems inherent in ML estimates are primarily those concerning the variance properties of the estimates, particularly for small sample sizes. For large sample size, the theory has been fairly well developed, and a

host of theories exist for asymptotic characteristics of the estimates as well as for the variances of estimates. Under reasonable general conditions the following may be proved. The likelihood equation has a solution which converges in probability to the true value, as $M\to\infty$. This solution is an asymptotically normal and asymptotically efficient estimate. Rigorous proof on these lines is given by Cramer [74].

In the general case, where there is not necessarily a set of k sufficient statistics for the k parameters, the joint ML estimators have similar optimum properties, in large samples, to those in the single parameter case. Further, it may be shown that the joint ML estimates tend, under regularity conditions, to a multivariate normal distribution, with dispersion matrix whose inverse is given by [79]

$$|\sigma^{-1}_{k\ell}| = -<\frac{\partial^2 \log\Lambda}{\partial\theta_k \partial\theta_\ell}> \quad . \tag{8.10}$$

These properties all deal with the behaviour of ML estimates for large M. They provide some motivation for using the ML estimate even when an efficient estimate does not exist. We now turn to discussion of the case of estimating the parameters α,β,σ_o^2 in the generalised hyperbolic distribution

$$p_X(x) = K(\alpha,\beta)\sigma_o^{\alpha\beta}\{|x|^\alpha+\sigma_o^\alpha\}^{-(\beta+1/\alpha)}, \quad -\infty<x<\infty. \tag{5.7}$$

8.3.2 LIKELIHOOD EQUATIONS

Using (5.7) the logarithm of the likelihood function becomes

$$\log\Lambda(\vec{x};\alpha,\beta,\sigma_2) = \sum_\ell \Big[\log\alpha+\log\Gamma(\beta+\frac{1}{\alpha})-\log 2-\log\Gamma(\beta)-\log(\frac{1}{\alpha}) +$$

$$+ \frac{\alpha\beta}{2} \log\sigma_2 - (\beta+\frac{1}{\alpha}) \log\{|x_\ell|^\alpha+\sigma_2^{\alpha/2}\}],$$

where $\sigma_2 = \sigma_o^2$. Using the above equation, the three likelihood equations are

$$\frac{\partial}{\partial\alpha}\log\Lambda=0=M\{\frac{1}{\alpha}+\frac{\partial}{\partial\alpha}\log\Gamma(\beta+\frac{1}{\alpha})-\frac{\partial}{\partial\alpha}\log\Gamma(\frac{1}{\alpha})+\frac{\beta}{2}\log\sigma_2\} -$$

$$- \frac{\partial}{\partial\alpha}\Big[(\beta+\frac{1}{\alpha}) \sum_{\ell=1}^{M} \log\{|x_\ell|^\alpha+\sigma_2^{\alpha/2}\}\Big], \qquad (8.11a)$$

$$\frac{\partial}{\partial\beta}\log\Lambda=0=M\{\frac{\partial}{\partial\beta}\log\Gamma(\beta+\frac{1}{\alpha})-\frac{\partial}{\partial\beta}\log\Gamma(\beta)+\frac{\alpha}{2}\log\sigma_2\}-$$

$$- \sum_{\ell=1}^{M} \log\{|x_\ell|^\alpha+\sigma_2^{\alpha/2}\} \qquad (8.11b)$$

and

$$\frac{\partial}{\partial\sigma_2}\log\Lambda=0= \frac{M\alpha\beta}{2\sigma_2} - (\beta+\frac{1}{\alpha}) \sum_{\ell=1}^{M} \frac{\alpha}{2} \sigma_2^{(\alpha-2)/2} \{|x_\ell|^\alpha+\sigma_2^{\alpha/2}\}^{-1}$$

(8.11c)

where $\sigma_2 = \sigma_o^2$. Even though the density function (5.7) depends on three parameters, we may be interested in estimating any number of them from 1 to 3, the others being known. Under regularity conditions, the ML estimators of the parameters concerned will be obtained by selecting an appropriate subset of the three likelihood equations and solving them. By the nature of this process, it is not to be expected that the ML estimator of a particular parameter will be unaffected by knowledge of the other parameters of the distribution. The form of the ML estimator depends on the company it keeps, as is made clear from the following analysis.

Suppose first that we wish to estimate σ_2 alone, the other two parameters α,β being known. We then solve (8.11c)

alone. From (8.11c) we have

$$g_M = 0 = \frac{1}{M} \sum_{\ell=1}^{M} \sigma_2^{\alpha/2} \{ |x_\ell|^\alpha + \sigma_2^{\alpha/2} \}^{-1} - \frac{\alpha\beta}{\alpha\beta+1} \qquad (8.12)$$

which has to be solved for σ_2. Obviously the equation has M solutions, but only one out of M is a positive root. This can be seen by taking the derivative of (8.12) with respect to σ_2. Since $\dot{g}_M$ is positive with probability 1 for all $\sigma_2 \geq 0$, g_M is monotonic in σ_2 and so possesses an inverse. The ML estimator problem becomes that of finding the positive root of (8.12) and then setting the estimated $\sigma_2 = (\hat{\sigma}_2)$ equal to this positive root.

For two unknown parameters β and σ_2 and one known parameter α, two simultaneous equations to be solved are specified by (8.11b) and (8.11c). Using [85]

$$\frac{\partial}{\partial\beta} \log\Gamma(\beta) = \frac{\dot{\Gamma}(\beta)}{\Gamma(\beta)} = \lim_{k\to\infty} \{ \log k - \sum_{i=0}^{k} (\beta+i)^{-1} \} \qquad (8.13)$$

(8.11b) simplifies to

$$\lim_{k\to\infty} \left[\sum_{i=1}^{k} \{ (\beta+i)(\alpha\beta+i\alpha+1) \}^{-1} \right] + \frac{\alpha}{2} \log\sigma_2 -$$

$$- \frac{1}{M} \sum_{\ell=1}^{M} \log\{ |x_\ell|^\alpha + \sigma_2^{\alpha/2} \} = 0. \qquad (8.14)$$

From (8.11c) β is specified in terms of σ_2 as

$$\beta = \zeta \{ \alpha(1-\zeta) \}^{-1} \qquad (8.15)$$

where

$$\zeta = \frac{1}{M} \sum_{\ell=1}^{M} \sigma_2^{\alpha/2} \{ |x_\ell|^\alpha + \sigma_2^{\alpha/2} \}^{-1}.$$

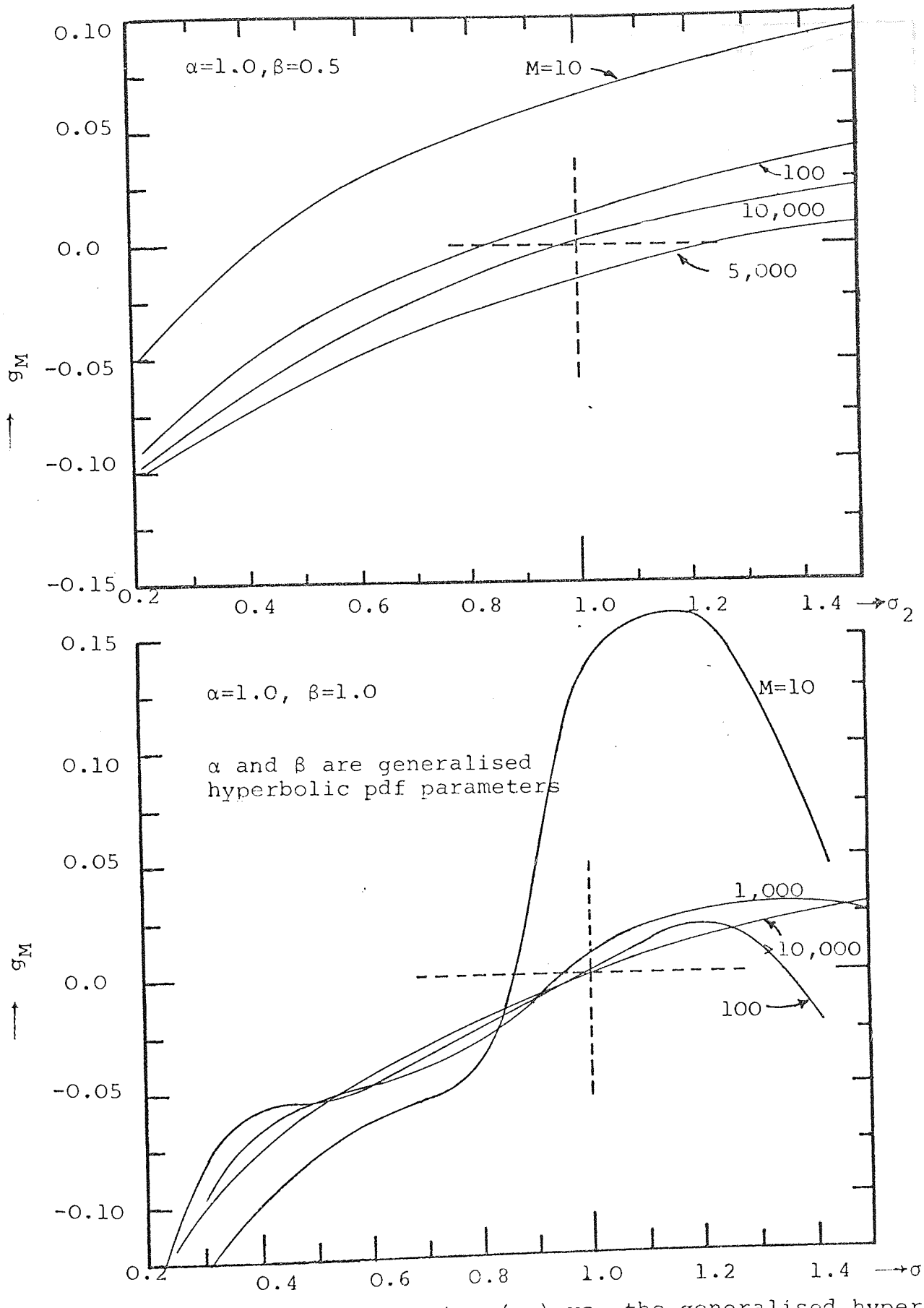

Fig. 8.3 Likelihood function (g_M) vs. the generalised hyperbolic pdf parameter ($\sigma_2=\sigma_o^2$) with the sample size (M) as a variable parameter.

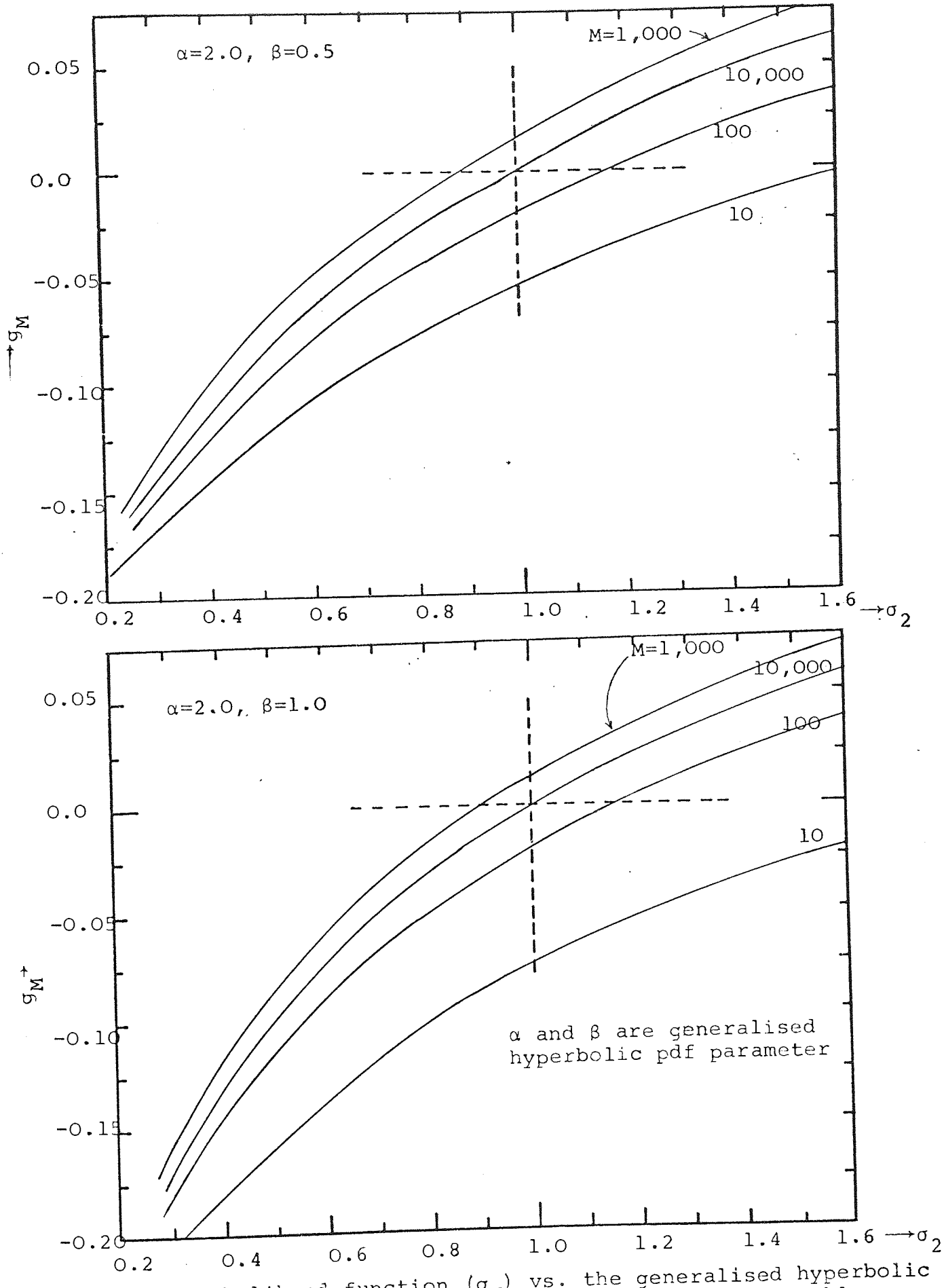

Fig. 8.4 Likelihood function (g_M) vs. the generalised hyperbolic pdf parameter ($\sigma_2=\sigma_o^2$) with the sample size (M) as a variable parameter.

Using (8.15) in (8.14) yields

$$\lim_{k\to\infty}\left[\sum_{i=0}^{k}\alpha(1-\zeta)^2\{(\zeta+i\alpha(1-\zeta))(1+i\alpha(1-\zeta))\}^{-1}\right] +$$

$$+\frac{\alpha}{2}\log\sigma_2-\frac{1}{M}\sum_{\ell=1}^{M}\log\{|x_\ell|^\alpha+\sigma_2^{\alpha/2}\}=0 \qquad (8.16)$$

which has to be solved for σ_2. Once σ_2 is estimated, this value is used in (8.14) to obtain the estimate of β. The analysis can be extended to three unknowns in a similar way but the algebra becomes cumbersome and will not be treated here.

Generating random numbers with given α and β and normalised $\sigma_o=1$, (8.12) is plotted against σ_2 with M as a parameter in Figs. 8.3 and 8.4. From the figures it is noted that a reasonable estimate can be obtained for M≥10,000. Due to the computer time, (8.16) was not solved. However, the method similar to the one used for single unknown parameter can be used in this case also.

8.3.3 ASYMPTOTIC ERROR VARIANCE

SINGLE UNKNOWN : $\sigma_2(=\sigma_o^2)$.

Since the estimate of σ_2 computed here is a ML estimate, it tends to a Gaussian random variable as the number of samples M approaches infinity. From [86]

$$\mathrm{var}\{\hat{\sigma}_2-\sigma_2\}=-\left\langle\frac{\partial^2}{\partial\sigma_2^2}\log p_X(\vec{x})\right\rangle^{-1}. \qquad (8.17)$$

Using (5.7) in (8.17) and performing the differentation and averaging yields

$$\mathrm{var}\{\hat{\sigma}_2-\sigma_2\}=4\sigma_2^2(\alpha\beta+\alpha+1)(M\alpha^2\beta)^{-1} \qquad (8.18)$$

where we have used the fact

$$\sum_{\ell=1}^{M} \frac{\alpha}{2}\,\sigma_2^{(\alpha-2)/2}\{|x_\ell|^\alpha+\sigma_2^{\alpha/2}\}^{-1} = M\alpha\beta\{2\sigma_2(\beta+1/\alpha)\}^{-1}$$

from (8.11c). Use of (8.17) allows an assessment of the value of M for which asymptotic behaviour of $\hat{\sigma}_2$ is approached.

TWO UNKNOWNS : $\sigma_2(=\sigma_o^2)$ and β.

Using (8.10), the dispersion matrix is given by

$$[\sigma_{k\ell}^{-1}] = \begin{bmatrix} -<\frac{\partial^2 \log\Lambda}{\partial\beta^2}> & -<\frac{\partial^2\log\Lambda}{\partial\beta\partial\sigma_2}> \\ -<\frac{\partial^2\log\Lambda}{\partial\beta\partial\sigma_2}> & -<\frac{\partial^2\log\Lambda}{\partial\sigma_2^2}> \end{bmatrix} \qquad (8.19)$$

Using (5.7) in (8.11b) and (8.11c) it can be shown that

$$<\frac{\partial^2\log\Lambda}{\partial\beta^2}> = M\{\frac{\partial^2}{\partial\beta^2}\log\Gamma(\beta+\frac{1}{\alpha}) - \frac{\partial^2}{\partial\beta^2}\log\Gamma(\beta)\},$$

$$<\frac{\partial^2\log\Lambda}{\partial\beta\partial\sigma_2}> = M\alpha\{2\sigma_2(\alpha\beta+1)\}^{-1}$$

and

$$<\frac{\partial^2\log\Lambda}{\partial\sigma_2^2}> = -M\alpha^2\beta\{4\sigma_2^2(\alpha\beta+\alpha+1)\}^{-1}. \qquad (8.20)$$

Using (8.13) and (8.20) in (8.19) and inverting the matrix yields the variances as:

$$\mathrm{var}\{\hat{\beta}-\beta\} = 4\sigma_2^2 g_\Sigma\{M\alpha^2\hat{g}_\Sigma\}^{-1}$$

and

$$\text{var}\{\hat{\sigma}_2-\sigma_2\} = \beta\{M(\alpha\beta+\alpha+1)\hat{g}_\Sigma\}^{-1} \qquad (8.21)$$

where

$$g_\Sigma = \sum_{\ell=0}^{\infty} \alpha\{2(\beta+\ell)+\frac{1}{\alpha}\}\{(\beta+\ell)^2(\alpha\beta+1+\ell\alpha)^2\}^{-1}$$

and

$$\hat{g}_\Sigma = \beta g_\Sigma\{\alpha\beta+\alpha+1\}^{-1} - \{\alpha\beta+1\}^{-2}.$$

8.4 DISCUSSION

In this chapter, a technique for evaluating the occurrence of an impulse by setting a threshold is presented. If the noise sample magnitude exceeds the threshold it is impulsive. The value of the threshold depends on the apriori probability of an occurrence of an impulse and the parameters of the noise pdf.

Means of monitoring the parameters of the generalised hyperbolic density function by means of ML estimators is also presented. The estimators require iteration to yield the value of the estimate. Newton's method for root finding can be used successfully in the case of one unknown parameter. A simulation indicates that the number of independent samples of IN should be greater than 10,000 for satisfactory parameter estimates for a single unknown parameter.

These techniques, used in conjunction with the coherent detection scheme described in Chapter 6, yield a more complete model for the detector in generalised hyperbolic noise.

CHAPTER 9

SUMMARY AND INDICATION OF POSSIBLE FUTURE RESEARCH

This chapter summarizes the major results of the thesis and points out some important subjects for future work.

9.1 SUMMARY

In this thesis two main types of noise processes have been analysed and the summary will be divided accordingly.

9.1.1 PART A

The purpose of the analysis presented in the first part was firstly, to characterize filtered Poisson IN, and secondly, to find the CF of the output of a linear filter excited by IN.

Chapter 2 derived the pdf for the linearly filtered narrow-band Poisson process. Attention was confined to the first-order case only. The approach was canonical in that the results are, in form, independent of the particular emitted waveforms, propagation conditions, source distributions and beam patterns, as long as the interference is narrow-band following the RF stages of a typical receiver.

In Chapter 3 theoretical expressions for the average probability of bit error for binary coherent P.S.K. systems in Poisson IN environments have been obtained for certain limiting cases ($\gamma<<1$, $\gamma>>1$). To check the validity of the assumptions made in deriving the theoretical expressions, experimental measurements of error probability were carried out. The results are shown in Figs.3.6 and 3.7.

Finally, in Chapter 4, a method of modulation is described which gives a particularly good error-rate performance, in comparison to the convention M-ary P.S.K. system, in the presence of Poisson IN. The modulation scheme is a hybrid arrangement of phase and amplitude modulated techniques. Only 8-ary signal sets are considered. Fig. 4.2 shows various hybrid modulation schemes analysed. The theoretical and experimental bit error probabilities are plotted in Fig. 4.4.

9.1.2 PART B

In the second part, Chapter 5 derived and justified a semiempirical, but more analytically tractable IN model. The process was described by the random variable whose pdf was given by a generalised hyperbolic distribution.

The development of detection theory in Chapter 6 results in the structure of optimal detection which, in general, consists of nonlinear elements. The results illustrated that, although we can find the optimum processor, the exact performance may be difficult to calculate. This difficulty motivated the discussion of the upper-bound on the probability of error Pe_{max}. It was observed that the system performance specified by Pe_{max} depended on the SNR, the time-bandwidth product and also the particular signal used. Associated with this fact, the signal design problem was introduced and discussed for the case of weak SNRs. This is justified since the optimality is usually no longer the primary concern at stronger SNRs. The optimal signal shapes were plotted for some particular signal energies, signal bandwidths and signal durations as shown in Figs. 6.5 to 6.7.

In Chapter 7, it was seen that for weak signals the optimum

nonlinear element depended quite critically on the noise density (Figs. 7.3 to 7.6). This dependence led to the question of how much the performance is degraded by small errors in the assumed suboptimal detection. Some specific results relating to this question were discussed. In general it was found that the relatively simple nonlinearities of Fig. 7.11 can give good large-sample performance (Fig. 7.13).

Finally, in Chapter 8 estimates of various unknown parameters in the generalised hyperbolic distribution were derived using maximum likelihood estimators. Also derived was a technique to estimate the location and duration of an impulse based on the knowledge of the parameters of the noise pdf (i.e., α, β, σ_o).

9.2 RECOMMENDATIONS FOR FUTURE RESEARCH

It is well known that the solution of the detection problem in non-Gaussian noise is still in its developing state and thus a great many problems still remain unsolved.

In the first part of the thesis, the analysis was confined to the linear receivers only. No attempt has been made in this investigation to obtain the optimum (maximum likelihood) receiver for IN. Indeed, the general problem of optimum detection in Poisson IN is unsolved and will probably remain so for some time to come. A possible means for finding out more about the structure of the optimum receiver is the use of generalised Hermite polynomial or Jordan series expansions for the pdf of the noise along the line indicated by Stratonovich [108] or Blake [126] respectively. Such investigations might suggest simpler (suboptimum) methods of combating the harmful effects of IN than the one pursued in this study.

The Poisson distribution of noise impulse reoccurrence

times could be modified to some other types of time distribution which would represent the true noise statistics in low-frequency radio channels. An analysis of this might consider a compound Poisson process in which the average repetition rate is statistically amplitude modulated.

In the second part of the thesis, we have obtained analytical solutions of the upper bounds on the probability of error. It might be interesting to know how well the actual system performance is theoretically predicted. For this purpose, the digital data communication system of Fig. 6.2 could be simulated on a digital computer and the experimental probability of error can be determined and compared with the theoretical results.

The development of the optimal detection schemes in this section was based entirely upon binary signals. The analysis could be generalised to take into account an M-ary system.

Finally, some comments should be made on the applicability to a real-world situation of the model that was used here for the received data. First, we did not consider the effect of a restricted receiver bandwidth. With only a limited bandwidth available, the minimum possible sampling rate of the received analogue waveform is in turn fixed. In such a case, the assumption of independent noise samples may be violated and the structure of the optimum detector could differ considerably from those discussed here. Much more work remains to be done in the general area of detection of signals in non-Gaussian noise with dependent samples. The requirement for such work would be, of course, to find additional methods of describing the higher-order statistics of non-Gaussian random variables.

REFERENCES

[1] D. MIDDLETON,"A statistical theory of reverberation and similar first-order scattered fields-Part I:Waveforms and the general processes",IEEE Trans. Inf. Thy., Vol. IT-13, p.372, 1967;"Part II:Moments, Spectra and special distributions",IEEE Trans. Inf. Thy., Vol. IT-13, p.393, 1967;"Part III:Waveforms and fields",IEEE Trans. Inf. Thy., Vol. IT-18, p.35, 1972;"Part IV:Statistical models", IEEE Trans. Inf. Thy., Vol. IT-18, p.68,1972.

[2] F. BONER,"Vehicular Radio frequency interference - Accomplishment and challenge",IEEE Trans.Vehi. Tech., Vol. VT-16, p.58. 1967.

[3] C. EGIDI, E. NANO,"Measurement and Suppression of VHF radio interference caused by motorcycles and motor cars", IRE Trans. Radio Freq. Int., Vol. RFI-3, p.30, 1961.

[4] H. M. HALL,"A new model for "Impulsive" phenomena: application to atmospheric-noise communication channels", Radio-Sci. Lab., Syst. Thoe. Lab., Stanford Electron Labs., Stanford Univ., Stanford Calif. Combined Tech. Reps.3412-8 and 7050-7, 1966.

[5] D. MIDDLETON,"Statistical-physical models of Urban radio-noise environments - Part I and II", Telec. Res. and Eng. Rep., OT/ITS, U.S. Dep. of Commerce, Boulder, Colo., 1974.

[6] R. ESPOSITO,"Research in Characterization and measurement of man-made electromagnetic noise", Raytheon Res., Waltham Mass., Contract DOT-TSC-73, 1st monthly Tech. Rep., 1970.

[7] A. A. GIORDANO, F. HABER,"Modelling of atmospheirc noise", Radio Sci., Vol. 7, p.1011, 1972.

[8] D. MIDDLETON,"Probability Models of received scattered and ambient fields", Proc.,1972, IEEE Int. Conf.,Eng. in the Ocean Environment, New Port, Rhode Isl. Sept. 13-15, 1972.

[9] P. BECKMANN,"Amplitude probability distribution of atmospheric radio noise", Radio Sci., Vol.68, p.723, 1964.

[10] O. IBUKUN,"Structural aspects of atmospheric radio noise in the topics", Proc. IEEE,Vol.54, p.361, 1966.

[11] A. D. WATT, E. L. MAXWELL,"Measured statistical characteristics of VLF atmospheric radio noise", Proc. IRE, Vol.45, p.55, 1957.

[12] C. CLARKE, P. A. BRADLEY, D. E. MORTIMER,"Characteristic of atmospheric radio noise observed at Singapore", Proc. IEE, Vol.112, p.849, 1965.

[13] K. FURUSTU, T. ISINDA,"On the theory of amplitude distribution of impulsive random noise and its application to the atmospheric noise", J. Appl. Phys., Vol.32, p.1206, 1961.

[14] W. Q. CRICHLOW, A. D. SPAULDING, C. J. RONBIQUE, R. T. DISNEY,"Amplitude probability distribution for atmospheric radio noise", NBS. Boulder, Colo., NBS. Mono. 23, 1960.

[15] W. W. PETERSON, T. G. BIRDSALL, W. C. FOX,"World distribution and characteristics of atmospheric radio noise", NBS document submitted to CCIR, 1964.

[16] R. T. DISNEY, A. D. SPAULDING,"Amplitude and time statistics of atmospheric and man-made radio noise", Environment Sci. Services Adm., Tech. Rep. ERL 150-ITS 98, 1970.

[17] "Spectrum engineering the key to progress",A report of Joint Tech. Advi. Committee of the IEEE, Suppliment 9, Unintended Rad., 1968.

[18] R. L. BREWSTER, M. LAWN,"A statistical analysis of telephone line noise", ITT Tech. Rep. STL 1026, 1969.

[19] M. KURLAND, D. A. MOLONY,"Observations on the effects of pulse noise in digital data transmission systems", IEEE Trans. Comm. Tech., Vol. COM-15, p.552, 1967.

[20] J. H. FENNICK,"A report on some characteristics of impulse noise in telephone communications", IEEE Trans. Comm. and Elect., Vol. 83, No. 75, p.700, 1964.

[21] J. H. FENNICK,"Amplitude distribution of telephone channel noise and a model for impulse noise", B.S.T.J., Vol.48, p.3243, 1969.

[22] P. MERTZ,"Impulse noise and error performance in data transmission", Rand memo. RM-4526-PR, DDC AD614416, 1965.

[23] S. M. SUSSMAN,"Analysis of the bursts model for error statistics in telephone circuits", IEEE Trans. Comm. Syst., Vol.11, p. 213, 1963.

[24] H. L. YUDKIN,"Some results in the measurements of impulse noise on several telephone circuits", Proc. Nat. Elec. Conf., 16, Chicago, Ill., p.222, 10-12 Oct. 1960.

[25] J. M. BERGER, B. MANDELBROT,"A new model for error clustering in telephone circuits", IBM J. Res. and Dev., I, p.224, 1963.

[26] B. W. STUCK, B. KLEINER,"A statistical analysis of telephone noise", B. S. T. J. Vol.53, No.7, p.1263, 1974.

[27] A. A. ALEXANDER, R. M. GRYB, D. W. NAST, "Capabilities of the telephone network for data transmission", B.S.T.J., Vol.39, p.431, 1960.

[28] S. M. SUSSMAN,"A matched filter communication system multipath channels", IRE Trans. Inf. Thy., Vol.IT-6, p. 367, 1960.

[29] R. A. WAINWRIGHT,"On the potential advantage of smearing-desmearing filter technique in overcoming impulse-noise problems in data-systems", IRE Trans. Comm. Syst., Vol. CS-9, p.362, 1961.

[30] R. M. LERNER,"Design of signals", in lectures on Comm. Syst. Theo., New York: McGraw-Hill, p.263, 1961.

[31] M. R. WINKLER,"Chirp signals for communications", in 1962 WESCON Tech. papers.

[32] J. C. DUTE, C. A. HINES,"Swept frequency modulation and means of reducing the effects of impulsive noise", Tech. Docu. Rept., No: AST-TDR-62-836, Uni. of Michigan, 1962.

[33] A. W. RIHACZEK, "Principles of high-resolution radar", New York: McGraw-Hill, Chapter 7, 1969.

[34] J. S. ENGEL,"Digital transmission in the presence of impulsive noise", B.S.T.J., Vol.44, p.1699, 1965.

[35] W. J. RICHTER,"Signal design and error rate analysis of a Polar baseband impulse noise communication channel", Ph.D. dissertation, The Cath. Univ. of America, 1971.

[36] R. W. LUCKY, J. SALZ, E. J. WELDON, Jr."Principles of data communicaitons", New York:McGraw-Hill,p.10, 1968.

[37] B. A. BOWEN,"Some analytic techniques for a class of non-Gaussian processes", Queen's Univ., Kingston, Ont., Canada, Res. Rep. 63-3, 1963.

[38] W. L. BLACK,"An impulse noise canceller", IEEE Trans. Comm. Syst., Vol.CS-11, p.506, 1963.

[39] M. BRILLIANT,"An impulse noise canceller", IEEE Trans. Comm. Tech., Vol. COM-12, p.104, 1964.

[40] E. J. BAGHDADY,"Analog modulation systems", in Lectures on Comm. Syst. Theo., E. J. Baghdady,Ed., New York: McGraw-Hill, p.439, 1961.

[41] P. A. BELLO, R. ESPOSITO,"A new method for calculating probabilities of error due to impulsive noise", IEEE Trans. Comm. Tech., COM-17, p.368, 1969.

[42] P. A. BELLO, R. ESPOSITO,"Error probabilities due to impulsive noise in linear and hard-limiter DPSK system", IEEE Trans. Comm. Tech., Vol.COM-19, p.14, 1971.

[43] O. ANTONOV,"Optimal detection of signals in non-Gaussian noise", Radio Eng. and Electro. Phy., Vol.12, p.541, 1967.

[44] O. ANTONOV, S. PONKVOTOV,"Detection of signal in noise by receivers with nonlinear fourpoles at the input", Radio Eng. and Electro. Phy., Vol.13, p.876, 1968.

[45] R. E. ZIEMER, R. B. FIUNCHEL,"Selection of blanking and limiting levels for binary signalling in Gaussian plus impulse noise", Proc. of the 1971 Fall Elec. Conf., Chicago, Ill., p.290, 1971.

[46] R. RICHARD, W. GORE,"A nonlinear filter for non-Gaussian interference", IEEE Trans. Comm. Syst., Vol. CS-11, p.436, 1963.

[47] W. B. SISCO,"Bit and message error rates in atmospheric noise with and without peak limiting", Proc. of the Nat. Elect. Conf., Chicago, Vol.22, p.781, 1966.

[48] W. GOSLING,"Impulsive noise reduction in radio receivers", The Radio and Elec. Eng., Vol.43, No. 5, p.341, 1973.

[49] J. E. EVANS, A.S. GRIFFITS, "Design of a Sanguine noise processor based upon world-wide extremely low frequency

recordings", IEEE Trans. Comm., Vol. COM-22, p.528, 1974.

[50] W. A. DODGE, Jr.,"Proposal for research and experimental in improvement of radio signal-to-noise ratio in the Minuteman ground electronic system", Space Tech. Lab. Doc. No. 6120-J184-TU-000, 1962; See also, "Rept. on hole puncher performance investigation for the radio subsystem of the Minuteman ground electronic system. WS-133B", 1963.

[51] C. O. MALLINCKROAT,"Peak limiter and hole puncher noise suppression capabilities for Minuteman receivers", Space Tech. Lab. Doc. No:6121-7719-RU-000, 1963.

[52] S.S. RAPPAPORT, L. KURZ,"An optimal nonlinear detector for digital data transmission through non-Gaussian channels", IEEE Trans. Comm. Tech., Vol.COM-14, p.266, 1966.

[53] J. W. MODESTINO, "A theoretically optimum ELF receiver structure", Tech. Rep. 494, Lincoln Lab., Mass. Inst. Tech., Lexington, DDC AD-743004, 1972.

[54] D. L. SNYDER,"Optimal detection of known signals in a non-Gaussian noise resembling VLF atmospheric noise", 1968 WESCON Tech. papers, Part IV.

[55] R. G. GALLAGER,"Information theory and reliable communication", New York:Wiley, 1968.

[56] P. A. BELLO,"Error probabilities due to atmospheric noise and flat fading in HF ionospheric communication systems", IEEE Trans. Comm. Tech., Vol. COM-13, p.266, 1965.

[57] P. A. BELLO,"Bounds on the error probability of FSK and PSK receivers due to non-Gaussian noise in fading channels", IEEE Trans. Inf. Thy., Vol. IT-12, p.315, 1966.

[58] R. E. ZIEMER,"Multi-level digital signalling in impulsive noise channels", Ph.D. dissertation, Univ. of Minnesota, U.S.A., 1965.

[59] H. T. HUYNH,"Le bruit impulsionnel et son influence sur la performance des systèmes de communication digitaux incohèrents", D. Sc. dissertation, Univ. Laval, Quèbec, Canada, 1972.

[60] J. D. MOORE,"Characterization of impulse noise and analysis of its effects upon correlation receivers", Ph.D. dissertation, Univ. of Alabama, U.S.A., 1972.

[61] A. BODHARAMIK, J. B. MOORE, R. W. NEWCOME,"Optimum detection and signal design for channels with non-but near-Gaussian additive noise", IEEE Trans. Comm., Vol.COM-20, No.6, p.1087, 1972.

[62] E. CONTE, E. CORTI, R. ESPOSITO, L. PESCATORI,"Error probabilities due to a mixture of impulsive and Gaussian noise in digital communication systems", ALTA Frequenza, Vol.XLI, No.4, p.263, 1972.

[63] J. K. OMURA, P. D. SHAFT,"Modem performance in VLF atmospheric noise", IEEE Trans. Comm. Tech., Vol. COM-19, p.659, 1971.

[64] C. V. TRUCK, S. F. GEORGE,"Detection of targets in non-Gaussian sea clutter", IEEE Trans. Aero. and Elect. Syst., Vol. AES-6, No.5, p.620, 1970.

[65] M. KANEFSKY, J. B. THOMAS,"On polarity detection schemes with non-Gaussian inputs", J. Frank. Inst., Vol.280, p.120, 1965.

[66] V. R. ALGAZI, R. M. LERNER,"Binary detection in white non-Gaussian noise", Lincoln Lab. of M.I.T. Tech. Rep. DS-2138.

[67] J. H. MILLER, J. B. THOMAS,"Detectors for discrete-time signals in non-Gaussian noise", Trans. Inf. Thy., Vol.IT-18, p.241, 1972.

[68] A. CONDA,"The effect of atmospheric noise on the probability of error for a NCFSK system", IEEE Trans. Comm. Tech., Vol. 13, p.280, 1965.

[69] M. KANEFSKY, J. B. THOMAS,"On adaptive nonparameteric detection systems using dependent samples", IEEE Trans. Inf. Thy., Vol. IT-11, p.521, 1965.

[70] S. S. WOLFF, J. L. GASTWIRTH, H. RUBIN,"The effect of auto-regressive dependence on a nonparameteric test", IEEE Trans. Inf. Thy., Vol.IT-13, p.311, 1967.

[71] S. O. RICE,"Mathematical analysis of random noise", B.S.T.J., Vol. 23 and 24, 1944 and 1945.

[72] D. MIDDLETON,"Introduction to statistical communication theory", New York:McGraw-Hill, 1960.

[73] H. L. VAN-TREES,"Optimum signal design and processing for reverberation-limited environments", IEEE Trans. Milt. Electr., Vol. MIL-9, No.3,4, p.212, 1965.

[74] H. CRAMÈR,"Mathematical method of statistics", Prin. Uni. Press., Princeton, N.J., 1971.

[75] R. F. LAMBERT, R. A. JANSSEN,T. I. SMITS,"Response and damage predictions for a linear oscillator under impulsive noise loading", A.F.materials Lab., Tech.Rep.-65-403. AD482281, p.7, 1966.

[76] A. PAPOULIS,"The Fourier integrals and its applications", New York:McGraw-Hill, 1962.

[77] D. MIDDLETON,"On the theory of random noise. Phenomenological models II", J. App. Phys., Vol.22, p.1153, 1951.

[78] J. A. MULLEN, D. MIDDLETON,"The rectification of non-Gaussian noise", Quart. App. Math.,Vol.15, p.395, 1952.

[79] M. G. KENDALL, A. STUART,"The advanced theory of statistics",

Vol.1 and 2, Charles Griffin & Co. Ltd., 1973.

[80] S. P. VOL'FBEIN, N. G. VEKSLER,"Discrete data transmission reliability in the presence of impulsive noise", Elecktrosvyaz, 1966.

[81] S. STEIN, J. JONES,"Modern communication principles with application to digital signalling", New York:McGraw-Hill, 1967.

[82] H. B. DWIGHT,"Tables of integrals and other mathematical data", Macmillan Co., 4th Ed., 1961.

[83] K. PEARSON,"Tables of incomplete Beta-function", Biometeric Office, London, 1934.

[84] H. L. VAN-TREES,"Detection, estimation and modulation theory", Part III, J. Wiley & Sons, New York, 1971.

[85] M. ABRAMOWITZ, I. A. SEGUN,"Handbook of mathematical functions", Dover public., Inc., New York, 1968.

[86] H. L. VAN-TREES,"Detection, estimation and modulation theory", Part I, J. Wiley & Sons, New York. 1971.

[87] E. D. SUNDE,"Communication system engineering theory", Wiley, New York, p.407-414, 1969.

[88] F. E. GLAVE,"Communication over fading dispersive channels with feedback", IEEE Trans. Inf. Thy., Vol.IT-18, p.142, 1972.

[89] C. N. CAMPOPIANO, B. G. GLAZIER,"A coherent digital amplitude and phase modulation scheme", IRE Trans. Comm. Syst., Vol.CS-10, p.90, 1962.

[90] K. KAWAI, S. SHINTANI, H. YANAGIDAIRA ,"Optimum combination of amplitude and phase modulation scheme and its application to data transmission MODEM", Proc. Int. Comm. Conf., p.29.6-29.11, 1972.

[91] C. WEBER,"New solutions to the signal design problem for coherent channels", IEEE Trans. Inf. Thy, Vol.IT-12, p.161, 1966.

[92] R. W. LUCKY, J. C. HANCOCK,"On the optimum performance of N-ary system having two degrees of freedom", IRE Trans. Comm. Syst., Vol.CS-10, p.185, 1962.

[93] J. SALZ, J. R. SHEEHAN, D. J. PARIS,"Data transmission by combined AM and PM", B.S.T.J., Vol.50,p.2399, 1971.

[94] C. M. THOMAS, M. Y. WEIDNER, S. H. DURRANI,"Digital amplitude-phase keying with M-ary alphabets", IEEE Trans. Comm., Vol.COM-22, p.168, 1974.

[95] M. K. SIMON, J. G. SMITH,"Hexagonal multiple phase and amplitude-shift keyed signal sets", IEEE Trans. Comm., Vol.COM-21, p.1108, 1973.

[96] A. V. BALAKRISHNAN,"A contribution to the sphere packing problem of communication theory", J. Math. Anal. Appl., Vol.3, p.485, 1961.

[97] G. J. FOSCHINI, R. D. GITLIN, S. B. WEINSTEIN,"On the selection of a two-dimensional signal constellation in the presence of phase jitter and Gaussian noise", B.S.T.J., Vol.52, p.927, 1973; also "Optimization of two-dimensional signal constellations in the presence of Gaussian noise", IEEE Trans. Comm., Vol.COM-22, p.28, 1974.

[98] E. N. GILBERT,"A comparison of signalling alphabets", B.S.T.J., p.504, 1952.

[99] J. G. SMIT,"A review of multiple amplitude-phase digital signals", Int. Telemetering Conf., p.173, 1973.

[100] C. CHIRATHAMJAREE,"The application of hybrid modulation technique to data transmission", M.Sc. Thesis, Univ. of Aston in Birmingham, 1975.

[101] W. S. BURDIC,"Radar signal analysis", Prentice-Hall Inc. Englewood Cliffs, N. J. p.268, 1968.

[102] B. MANDELBROT,"I/F noises and infrared catastrophe", IEEE Symp. on time varying channels paper, June, 1965.

[103] B. P. LATHI,"Introduction to random signals and communication theory", Scranton, Inter. Text Book, 1968.

[104] M. P. SHINDE, S. N. GUPTA,"Signal detection in the presence of atmospheric noise in tropics", IEEE Trans. Comm., Vol. COM-22. p.655, 1974.

[105] W. D. DAVENPORT, W. L. ROOT,"Random signals and noise", New York:McGraw-Hill, 1958.

[106] H. O. POLLACK, H. J. LANDAU, D. SLEPIAN,"Prolate speroidal wave functions, Fourier analysis, and uncertainty - I,II,III", B.S.T.J., 1961-62.

[107] S. N. GUPTA,"Time characteristics of atmospheric radio noise", Proc. IEEE Conf. Electro. Compat., 1972.

[108] R. L. STRATONOVICH,"Topics in the theory of random noise", Trans. by R. Silverman, Gordon and Breach, New York, 1963.

[109] H. CHERNOFF,"A measure of asymptotic efficiency for tests of a hypothesis based on the sum of observations", Ann. Math. Statist., Vol.23, p.493, 1962.

[110] D. BLACKWELL,"Comparison of experiments", Proc. 2nd Berkely, Symp. Prob. and Stast., Vol.1, Berkely, p.93,1955.

[111] N. ABRAMSON," Bandwidth and spectra of phase-and-frequency modulated noise", IEEE Trans. Comm. Syst., Vol.CS-11, p.407, 1963.

[112] R. P. WEINSTOCK,"Calculus of variation", New York: McGraw-Hill, 1952.

[113] R. A. STRUBLE,"Nonlinear differential equations", New York:McGraw-Hill, 1962.

[114] H. POINCARE,"Les methodes nouvelles de la macanique celeste", Gauthier-Villars, Vol. I,Paris, 1892.

[115] P. J. HUBER,"A robust version of the probability ratio test", Ann. Math. Stat., Vol. 36, p.1753, 1965.

[116] R. D. MARTIN, S. C. SCHWARTZ,"Robust detection of a known signal in nearly Gaussian noise", IEEE Trans. Inf. Thy., Vol. IT-17, 1971.

[117] J. W. MODESTINO, A. H. LEVESQUE,"A mixture model for VLF noise with applications to M-ary spread-spectrum signalling", Proc. of the 5th Amn. Princeton Conf. on Inf. Sci. and Syst., 1971.

[118] J. CAPON,"On the asymptotic efficiency of locally optimum detectors", IRE Trans. Inf. Thy., Vol.IT-7, p.67, 1961.

[119] T. S. FERGUSION,"Mathematical statistics: A decision theoretic approach", New York:Academic Press, 1967.

[120] P. RUDNIK, "A signal-to-noise property of binary decisions", Nature, Vol. 193, p.604, 1962.

[121] C. W. HELSTROM,"Quantum detection theory", Int. Contr., Vol. 10, p.254, 1967.

[122] C. WEBER,"Elements of detection and signal design", New York:McGraw-Hill, 1968.

[123] C. N. BERGLUND,"A note on power-law devices and their effect on signal-to-noise ratio", IEEE Trans. Inf.Thy., p.52, 1964.

[124] T. J. LAMB,"A noise-silencing I.F. circuit for superhet-receivers", QST, 1936.

[125] R. L. STRATONOVICH,"Detection and estimation of signals

in noise when one or both are non-Gaussian", Proc. IEEE, Vol.58, p.670, 1970.

[126] I. F. BLAKE,"A study of some impulsive noise models", Res. Rept., No:64-1, Queen's Univ.,Kingston, Canada, 1964.

[127] J. W. CARYLE,"Nonparametric method in detection theory", in Comm. Theo., A.V. Balakrishnan Ed., New York: McGraw-Hill, Chapter 8, 1968.

[128] R. L. BREWSTER, S. B. PATEL,"Noise in the telephone network and its effect on data transmission", Proc. of Int. Zurich Seminar on dig. comm., p.G4, 12-15 March,1974.

[129] S. B. PATEL, R. L. BREWSTER,"Performance of hybrid modulation system in an impulse noise environment", Under review by IEEE Trans. on Comm..

[130] S. B. PATEL, R. L. BREWSTER,"Optimum detection and signal design for VLF channels", To appear in the Radio and Elec. Eng., 1976.

[131] R. L. BREWSTER, S. B. PATEL,"Data transmission in the presence of noise and channel fading", IEE Conf. on Comm. Equipment and Systems, Brighton, U.K.,8-11 June, 1976.

APPENDIX A

The purpose of this appendix is to outline the derivation of the characteristic function (CF) of the random variable

$$Z = \sum_{i=0}^{N} a_i G(t_i) \cos\psi_i \qquad (a.1)$$

where a_i's, t_i's and ψ_i's are independent random variables. Assuming that N noise impulses have occurred, the conditional CF is given by [72]

$$\Phi_Z(j\xi/N) = \langle \exp\{j\xi \sum_{i=0}^{N} a_i G(t) \cos\psi_i\} \rangle_{t,\psi,a} \qquad (a.2)$$

where the averagings are with respect to t,ψ and a. Since t_i's are uniformly distributed in the observation interval T_O, its density equals $1/T_O$ within the observation interval and zero elsewhere; hence the above equation becomes

$$\Phi_Z(j\xi/N) = \langle \int_{T_O} \frac{dt_i}{T_O} \exp\{ja\xi G(t_i) \cos\psi\} \rangle^N_{a\cos\psi} . \qquad (a.3)$$

The CF is then given by

$$\Phi_Z(j\xi) = \lim_{T_O\to\infty} \sum_{N=0}^{\infty} P_{T_O}(N) \Phi_Z(j\xi/N) . \qquad (a.4)$$

If (2.2) for $P_{T_O}(N)$ is substituted in (a.4) along with (a.2) for $\Phi_Z(j\xi/N)$, and performing the summation yields

$$\Phi_Z(j\xi) = \exp\{-\nu \int_t dt \, (1-\Phi_{a\cos\psi}(j\xi G(t)))\} . \qquad (a.5)$$

By assuming that ψ is independent of a and uniformly

distributed in the range $(0,2\pi)$, $\Phi_{a\cos\psi}(j\xi G(t))$ can be written as

$$\Phi_{a\cos\psi}(j\xi G(t)) = \langle p_{a\cos\psi}(a\cos\psi)\exp(-j\xi a\cos\psi G(t))\rangle_a,$$

$$= \langle \int_0^{2\pi} \frac{d\psi}{2\pi} \exp\ (-j\xi a\cos\psi G(t))\rangle_a.$$

Identifying the integral on ψ as $J_0(a\xi G(t))$ the above equation reduces to

$$\Phi_{a\cos\psi}(j\xi G(t)) = \langle J_0(a\xi G(t))\rangle_a. \qquad (a.6)$$

Substituting (a.6) in (a.5) yields

$$\Phi_Z(j\xi) = \exp\{\nu \int_t dt \langle J_0(\xi a G(t)) - 1\rangle_a\}. \qquad (a.7)$$

$\Phi_Z(j\xi)$ can be identified as the Hankel transform of the resultant envelope of (a.1).

APPENDIX B

This appendix establishes that for $\gamma<<1$ the joint pdf of two-dimensional unfiltered Poisson IN, at the output of the matched filters at time t=T, is approximately radial. The joint pdf of $\hat{X}_i(=X_i/\lambda_2,\ i=1,2..)$, with n(t) constituting Poisson IN defined by (2.1), is impossible to compute in closed form. An approximation can be obtained via the joint CF (as shown in Chapter 2). It is well known [72] that the joint CF of a linearly filtered process is

$$\Phi_{\hat{X}_1,\hat{X}_2}(j\xi_1,j\xi_2)=\exp\left[\frac{\gamma}{T}<\int_o^T dt\{\exp(j\frac{a}{\sigma}\sum_{k=1}^{2}\xi_k h_{Rk}(t))-1\}>_a\right]$$

where $h_{Rk}(t)$, k=1,2 are linear filters (taken here to be matched filters). Using expression for $h_{Rk}(t)(=\Psi_k(T-t)$, k=1,2; $0<t<T)$, and defining polar co-ordinates r,§ by the equation

$$\xi_1=r\cos\S,\ \xi_2=r\sin\S,\ (0<r<\infty, 0<\S<2\pi)$$

one finds that $\Phi_{\hat{X}_1,\hat{X}_2}(r,\S)$ has the form

$$\Phi_{\hat{X}_1,\hat{X}_2}(r,\S)=\exp\left[\gamma<J_o\{ar(\frac{2}{T\lambda_2})^{\frac{1}{2}}\}-1>_a\right]$$

where J_o is a Bessel function of zero-order.

For $\gamma<<1$ (highly IN case), expanding the exponential in the above expression and neglecting higher order terms (in γ), one obtains an approximation for the CF of the form

$$\Phi_{\hat{X}_1,\hat{X}_2}(r,\S)=\exp(-\gamma)\left[1+\gamma<J_o\{ar(\frac{2}{T\lambda_2})^{\frac{1}{2}})\ \}>_a\right].$$

The corresponding joint pdf, using the linear Fourier transformation

$$p_{\hat{X}_1,\hat{X}_2}(r,\S)=(2\pi)^{-1}\int_0^\infty \Phi_{\hat{X}_1,\hat{X}_2}(r,\S)J_o(Rr)dr$$

where R is the radius vector defined by the equation

$$x_1=R\cos\theta, \quad x_2=R\sin\theta \qquad (0<R<\infty, 0<\theta<2\pi),$$

is obtained as

$$p_{\hat{X}_1,\hat{X}_2}(x_1,x_2) = (1-\gamma)\delta(x_1)\delta(x_2)+\frac{\gamma}{\pi}\left[\frac{T\lambda_2}{2(x_1^2+x_2^2)}\right]^{\frac{1}{2}} \cdot \cdot p_A\left[\left(\frac{T\lambda_2}{2}(x_1^2+x_2^2)^{\frac{1}{2}}\right)\right] \qquad (b.1)$$

where we have used the relationship [85]

$$\sqrt{k\hat{k}}\int_0^\infty rJ_o(kr)J_o(\hat{k}r)dr = \delta(k-\hat{k}).$$

APPENDIX C

In this appendix we show that the integral

$$t = \int_0^{S(t)} \frac{d\zeta}{\{1+a\zeta^2+b\zeta^4\}^{\frac{1}{2}}} \qquad (c.1)$$

can be represented in terms of the functions cos t and cosh t or in terms of the Jacobian functions. Specifically, we show that, for b=0, it can be expressed in terms of cos t (sin t) or cosh t (sinh t) and that, for $b \neq 0$, it can be expressed in terms of the Jacobian functions.

If b=0,{which only occurs when the constraints (6.22) and (6.23) are related such that $W^2T^2=\pi^2E$ where W^2 is the mean-square bandwidth, T the signal duration and E the signal energy} and $a \neq 0$, then $1+a\zeta^2$ can be written in the form $1\pm\Omega^2\zeta^2$, where $\Omega>0$. Introducing a new variable $y=\Omega\zeta$, (c.1) becomes

$$t= \frac{1}{\Omega} \int_0^{\Omega S(t)} \frac{dy}{(1\pm y^2)^{\frac{1}{2}}} .$$

From this we have either $S(t)= \frac{1}{\Omega}\cos\Omega t$ or $S(t)= \frac{1}{\Omega}\cosh\Omega t$.

For $b \neq 0$, it is natural to require that the polynomial

$$f(\zeta) = 1 + a\zeta^2 + b\zeta^4$$

in (c.1) shall not be a perfect square, otherwise $\sqrt{f(\zeta)}$ will be of the form $1 + q\zeta^2$, and the integral (c.1) will be expressed either in terms of arc tangent (q>0) or in terms of the logarithm of a linear fractional function (q<0). In each of these cases, examination of the inverse function would yield nothing new. Therefore, in what follows, we shall assume that $a^2 \neq 4b$.

For $b\neq 0$, and $a^2\neq 4b$ we have two cases:

1) $a^2<4b$

This situation does not arise for the problem with which we are concerned; and hence will not be treated here.

2) $a^2>4b$

Here, the roots y_1 and y_2 of the equation $y^2+ay+b=0$ are real and distinct. We have

$$y^2+ay+b = (y-y_1)(y-y_2),$$

or, if we replace y with $1/\zeta^2$,

$$1+a\zeta^2+b\zeta^4 = (1-y_1\zeta^2)(1-y_2\zeta^2).$$

At this point we need to consider three subcases:

a) y_1 and y_2 both positive

b) y_1 and y_2 of opposite sign

c) y_1 and y_2 both negative.

a) We can assume that y_1 and y_2 have the values T^2 and ∇^2, where $T>\nabla>0$. Then,

$$1+a\zeta^2+b\zeta^4= (1-T^2\zeta^2)(1-\nabla^2\zeta^2).$$

Using the above equation in (c.1) and changing the variable $\S=T\zeta$ yields

$$t = \frac{1}{T}\int_0^{\S}\frac{d\S}{\{(1-\S^2)(1-K^2\S^2)\}^{\frac{1}{2}}}, \qquad 0<K^2<1$$

where $K^2 = \nabla^2/T^2$. Thus, in this subcase, using the substitution $\sin\phi = \S$, we obtain [82]

$$t = \frac{1}{T}F(\phi,K) \qquad (c.2)$$

where

$$F(\phi,K) = \int_0^{\phi} \frac{d\phi}{\{1-K^2\sin^2\phi\}^{\frac{1}{2}}} .$$

b) We assume that $y_1=T^2$ and $y_2= -\nabla^2$ where T and ∇ are both positive. We obtain the following factors of $f(\zeta)$:

$$1+a\zeta^2+b\zeta^4= (1-T^2\zeta^2)(1+\nabla^2\zeta^2).$$

Using the above equation in (c.1) and introducing a new variable $\S=(1-T^2\zeta^2)^{\frac{1}{2}}$ yields

$$\hat{K}-(T^2+\nabla^2)^{\frac{1}{2}}t=\int_0^{\S} \frac{d\S}{\{(1-\S^2)(1-K^2\S^2)\}^{\frac{1}{2}}} , \quad 0<K<1$$

where

$$\hat{K}= \int_0^1 \frac{dx}{\{(1-x^2)(1-K^2x^2\}\}^{\frac{1}{2}}} \quad \text{and } K= \frac{\nabla}{\{T^2+\nabla^2\}^{\frac{1}{2}}} .$$

Using the substitution $\phi= \cos^{-1}(\S/\nabla)$, the above equation simplified to

$$t=(T^2+\nabla^2)^{-\frac{1}{2}}\{\hat{K}-F(\phi,K)\} \qquad (c.3)$$

c) When $y_1 = -T^2$ and $y_2 = -\nabla^2$, and assuming $T>\nabla>0$, $f(\zeta)$ can be expressed as

$$1+a\zeta^2+b\zeta^4=(1+T^2\zeta^2)(1+\nabla^2\zeta^2).$$

Using the above equation in (c.1) and introducing a new variable $\S=T\zeta/(1+T^2\zeta^2)^{\frac{1}{2}}$ yields

$$t = \frac{1}{T} \int_0^{\S} \frac{d\S}{\{(1-\S^2)(1-K^2\S^2)\}^{\frac{1}{2}}}, \qquad 0<K<1$$

where $K = \{T^2-\nabla^2\}^{\frac{1}{2}}/T$. From this, using $\phi = \tan^{-1}(\S/\nabla)$ yields

$$t = \frac{1}{T} F(\phi,K). \tag{c.4}$$

In this appendix we have shown that the integral (c.1) with $b \neq 0$ can be expressed in terms of the Jacobian functions with appropriate modulus K and, for $b=0$, in terms of the circular or hyperbolic sine.

APPENDIX D

ASYMPTOTIC RELATIVE EFFICIENCY (ARE)

A detector based on the test statistics L_1 can be compared to the detector based on the test statistics L_2 on the basis of the asymptotic relative efficiency defined as:

$$ARE_{L_1,L_2} = M_2/M_1$$

where M_2 and M_1 are the independent samples required by L_2 and by L_1 respectively, for the detection of the same signal in the same environment and with the same false alarm probability P_f and false dismissed probability P_d.

It should be clear that ARE_{L_1,L_2} is a function of P_f, S (signal strength), M_1 and M_2; and it may be difficult to evaluate for arbitrary P_f, S, M_1 and M_2. It is often simplest to let M_1 and M_2 approach infinity. Since in such a case the probability of detection will approach unity (for consistent tests against fixed alternatives), it is necessary to allow the alternative hypothesis H_1 to approach the hypothesis H_o in such a way that the probability of detection P_d remains constant as M_1 and $M_2 \to \infty$. The ARE of detector L_1 with respect to detector L_2 therefore becomes

$$ARE_{L_1,L_2}\Big|_{\substack{S\to O \\ M_1\to\infty \\ M_2\to\infty}} = \frac{M_2(P_f,P_d,S)}{M_1(P_f,P_d,S)}.$$

A convenient choice for the reference detector is the linear detector in which the signal samples are simply summed and compared to the threshold L_o. The linear detector is about as

simple a detector as one can use for the problem of using H_o versus H_1, and moreover if the noise is Gaussian both the optimum and threshold detectors for this problem are equivalent to it. In this thesis the subscripts attached to the ARE will be dropped and it is assumed that the detector under investigation is compared to the linear detector. However, in cases of ambiguity only the first subscript will be used.

It can also be shown [127] that the ARE is a measure of relative information rate. For the sampling rate $1/\tau_o$ samples per second, the interrogation intervals required by L_2 and L_1 are $T_2=M_2\tau_o$ and $T_1=M_1\tau_o$, respectively. Thus, the maximum rate at which symbols can be transmitted by the source and still maintain false-alarm probability P_f and false dismissal probability P_d when detectors L_2 and L_1 are utlized are $1/M_2\tau_o$ and $1/M_1\tau_o$ symbols per second, respectively.

APPENDIX E

DERIVATION OF ASYMPTOTIC RELATIVE EFFICIENCY FOR THE NARROW-BAND SYSTEMS

In this appendix, we derive the asymptotic relative efficiency for the narrow-band system ARE_{NB} defined by

$$ARE_{NB} = \frac{N_o \langle D \rangle^2}{2E\langle D^2 \rangle} \tag{7.15}$$

where (defined in section 7.3)

$$D = \Delta t \sum_{\ell=1}^{M} E_{s\ell} K_1[e_\ell] \cos(\alpha_\ell - \theta_\ell), \tag{7.14b}$$

$$E = \int_o^T E_s^2(t) \cos^2\{\omega_c t + \theta(t)\} dt = \frac{\Delta t}{2} \sum_{\ell}^{M} E_{s\ell}^2 \tag{e.1}$$

(signal energy)

$$e_\ell = \{E_{s\ell}^2 + E_{n\ell}^2 + 2E_{s\ell}E_{n\ell}\cos\chi_\ell\}^{\frac{1}{2}}, \tag{e.2}$$

$$\alpha_\ell = \phi_\ell + \tan^{-1}\left[\frac{E_{s\ell}\sin\chi_\ell}{E_{n\ell}+E_{s\ell}\cos\chi_\ell}\right] \tag{e.3}$$

$\chi = \phi - \theta$,

ϕ and θ are noise and signal phases,

$K_1[e_\ell]$ is a function of e_ℓ (Fourier coefficient)

$E_{s\ell}$ and $E_{n\ell}$ are the signal and the noise samples respectively at time $t=t_\ell$.

The variance of the random variable D is given by

$$\langle D^2 \rangle = (\Delta t)^2 \langle \{\sum_{\ell=1}^{M} E_{s\ell} K_1[e_\ell] \cos\chi_\ell\}^2 \rangle_{e_\ell, \chi_\ell}$$

where we have used the fact $\alpha - \theta = \chi$ when the signal is absent

(θ_ℓ=0). Assuming that the envelope and the phase of the noise process are independent and the phase is uniformly distributed between 0 and 2π the above equation reduces to

$$\langle D^2\rangle = \frac{(\Delta t)^2}{2} \sum_{\ell=1}^{M} E_{s\ell}^2 \langle K_1^2[e_\ell]\rangle_{e_\ell} \qquad (e.4)$$

where we have also assumed the samples to be independent.

To evaluate the mean of the random variable D we make the following approximations for e_ℓ, α_ℓ, $K_1[e_\ell]$ and $\cos(\alpha_\ell-\theta_\ell)$. (We assume the signal $E_{s\ell}$ is weak).

a) e_ℓ:

Rewritting (e.2) as

$$e_\ell = \left[1+\left(\frac{E_{s\ell}}{E_{n\ell}}\right)^2 + \frac{2E_{s\ell}}{E_{n\ell}}\cos\chi_\ell\right]^{\frac{1}{2}} E_{n\ell}$$

and expanding the square root using Binomial theorem we obtain the required form as

$$e_\ell \tilde{=} \{1+\frac{E_{s\ell}}{E_{n\ell}}\cos\chi_\ell\}E_{n\ell} \qquad (e.5)$$

where we have neglected all the higher order terms in $E_{s\ell}$.

b) α_ℓ:

For weak signal, (e.3) can be written as

$$\alpha_\ell = \phi_\ell + \tan^{-1}\{\frac{E_{s\ell}}{E_{n\ell}}\sin\chi_\ell\} .$$

For small $(E_{s\ell}/E_{n\ell})\sin\chi_\ell$, the above equation reduces to

$$\alpha_\ell = \phi_\ell + \frac{E_{s\ell}}{E_{n\ell}}\sin\chi_\ell . \qquad (e.6)$$

c) $K_1[e_\ell]=K_1[E_{n\ell}+E_{s\ell}\cos\chi_\ell]$ {using (e.5)}

Using Taylor's series the above equation becomes

$$K_1[e\ ]\tilde{\sim} K_1[E_n]+E_s\cos\chi\ \dot{K}_1[E_n]+O(E_s^2). \qquad (e.7)$$

d) $\cos(\alpha-\theta)=\cos(\chi+\frac{E_s}{E_n}\sin\chi)$ {using (e.6) and $\chi=\phi-\theta$ }.

Expanding $\cos(\alpha-\theta)$ and using $\cos(\frac{E_s}{E_n}\sin\chi)\tilde{\sim}1$ for small E_s/E_n and $\sin(\frac{E_s}{E_n}\sin\chi)=\frac{E_s}{E_n}\sin\chi$ the above equation can be written as

$$\cos(\alpha-\theta)\tilde{\sim}\cos\chi+\frac{E_s}{E_n}\sin^2\chi. \qquad (e.8)$$

The mean of the variable D is given by

$$<D>=\Delta t<\sum_{\ell=1}^{M} E_{s\ell}K_1[e_\ell]\cos(\alpha_\ell-\theta_\ell)>_{e_\ell,\chi_\ell}.$$

Using (e.7) and (e.8) in the above equation yields

$$<D>=\Delta t<\sum_{\ell=1}^{M} E_{s\ell}[<K_1[E_{n\ell}]\cos\chi_\ell>_{E_{n\ell}\chi_\ell}+<\frac{K_1[E_{n\ell}]}{E_{n\ell}}E_{s\ell}\sin^2\chi_\ell>_{E_{n\ell},\chi_\ell}+$$

$$+<\dot{K}_1[E_{n\ell}]E_{s\ell}\cos^2\chi_\ell>].$$

Averaging the above equation with respect to $E_{n\ell}$ and χ_ℓ yields

$$<D>=\frac{\Delta t}{2}\sum_{\ell=1}^{M} E_{s\ell}^2<\dot{K}_1[e_\ell]+\frac{K_1[e_\ell]}{e_\ell}>_{e_\ell}. \qquad (e.9)$$

Using (e.1), (e.4) and (e.9) in (7.15) for ARE_{NB} yields

$$ARE_{NB}=\frac{\sigma_N^2}{2}\frac{\left[<\dot{K}_1[e_\ell]+\frac{K_1[e_\ell]}{e_\ell}>_{e_\ell}\right]^2}{<K_1^2[e_\ell]>_{e_\ell}} \qquad (e.10)$$

where $\sigma_N^2 = N_o/\Delta t$ is the variance (power) of the noise process.

APPENDIX F

MAXIMUM ASYMPTOTIC RELATIVE EFFICIENCY FOR THE NARROW-BAND SYSTEMS

For a fixed noise pdf, the larger the value of ARE_{NB}, the better-suited (asymptotically) is the corresponding nonlinear detector for detecting a constant signal in that particular noise. Naturally it is of interest to know if for each noise pdf there is a best (or worst) nonlinearity in the sense of maximizing (or minimizing) the expression for ARE_{NB}. Let the maximum ARE_{NB}, obtained when the optimum detector is used, be denoted by μ_{NB} then

$$ARE_{NB} = \frac{\sigma_N^2 \left\langle \frac{K_1[e]}{e} + \dot{K}_1[e] \right\rangle_e^2}{2\langle K_1^2[e]\rangle_e} \leqslant \mu_{NB} \qquad (7.16)$$

Cross-multiplying and then collecting terms in (7.16) gives the function of $K_1[\cdot]$ of which we seek an extremum as

$$K = \langle K_1^2[e]\rangle_e - \frac{\sigma_N^2}{2\mu_{NB}} \left\langle \frac{K_1[e]}{e} + \dot{K}_1[e] \right\rangle_e^2 \leqslant 0 \qquad (f.1)$$

with equality on the right hand side if and only if we actually have an extremum. To carry out the maximization, using the calculus of variation technique [112], we let

$$K_1[\cdot] = \hat{K}_1[\cdot] + \lambda \Delta K_1[\cdot] \qquad (f.2)$$

where

$\hat{K}_1[\cdot]$ - is the optimum nonlinear function which specifies

the nonlinear element.

λ - is the Lagrange multiplier

and $\Delta K_1[.]$ - is some arbitrary function of $K_1[.]$.

Substituting (f.2) in (f.1) and carrying out

$$\frac{dK}{d\lambda}\Big|_{\lambda=0} = 0$$

yields

$$[\hat{K}_1(e) - B_c\{\frac{1}{e} - \frac{d}{de}\log p_\eta(e)\}]p_\eta(e) = 0 \qquad \text{(f.3)}$$

where B_c is a constant defined by

$$B_c = <\hat{K}_1(e)[\frac{1}{e} + \{-\frac{d}{de}\log p_\eta(e)\}]>_e . \qquad \text{(f.4)}$$

Since $p_\eta(e)$ is not zero, the quantity in the square brackets of (f.3) must be zero i.e.,

$$\hat{K}_1[e] = B_c\{\frac{1}{e} - \frac{d}{de}\log p_\eta(e)\} = -B_c\frac{d}{de}\log\{\frac{p_\eta(e)}{e}\} \qquad \text{(f.5)}$$

Since the nonlinear element $g_{NB}[.]$ is defined in terms of $K_1[e]$ as

$$\hat{K}_1[e] = \frac{1}{\pi}\int_{-\pi}^{\pi} g_{NB}[e\zeta]\zeta d\zeta , \qquad \text{(7.12)}$$

the nonlinearity for the optimum detector can be obtained by solving the following integro-differential equation

$$\hat{K}_1[e] = \frac{1}{\pi}\int_{-\pi}^{\pi} g_{NB}[e\zeta]\zeta d\zeta\Big|_{g_{NB,opt}[x]=g[x]} \qquad \text{(f.6)}$$

for $g_{NB}[x]$. Moreover, on substituting (f.5) in (7.16) one finds the maximum ARE_{NB} as

$$\mu_{NB} = \frac{\sigma_N^2}{2}<\{\frac{d}{de}\log\left[\frac{p_\eta(e)}{e}\right]\}^2>_e . \qquad \text{(f.7)}$$